NASA CR-134763

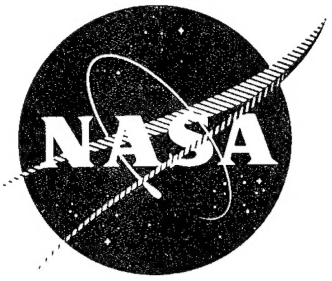

DESIGN, FABRICATION AND TEST OF MULTI-FIBER LAMINATES

by R.A. Pike and R.C. Novak

UNITED AIRCRAFT RESEARCH LABORATORIES

Prepared for

NATIONAL AERONAUTICS AND SPACE ADMINISTRATION

NASA-Lewis Research Center

Contract NAS3-17778

R.F. Lark, Project Manager

DISCLAIMER NOTICE

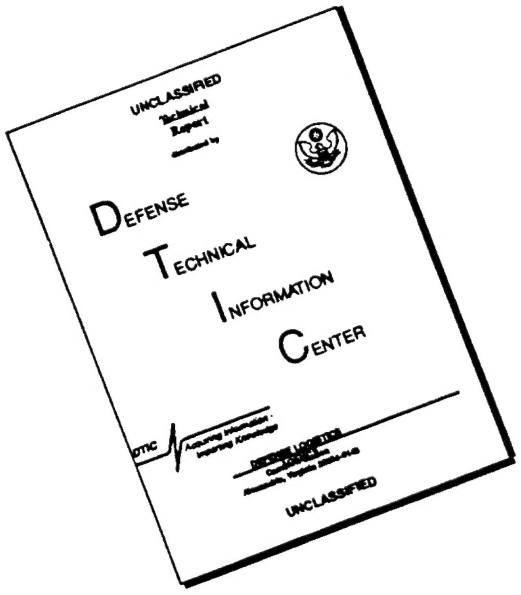

THIS DOCUMENT IS BEST QUALITY AVAILABLE. THE COPY FURNISHED TO DTIC CONTAINED A SIGNIFICANT NUMBER OF PAGES WHICH DO NOT REPRODUCE LEGIBLY.

1. Report No.	2. Government Accession No.	3. Recipient's Catalog No.
NASA CR-134763		

4. Title and Subtitle	5. Report Date
DESIGN, FABRICATION AND TEST OF MULTI-FIBER LAMINATES	January 1975
	6. Performing Organization Code

7. Author(s)	8. Performing Organization Report No.
R. A. Pike and R. C. Novak	R75-911730-15
	10. Work Unit No.

9. Performing Organization Name and Address	11. Contract or Grant No.
United Aircraft Research Laboratories East Hartford, Connecticut	NAS3-17778
	13. Type of Report and Period Covered
12. Sponsoring Agency Name and Address	Contractor Report
National Aeronautics and Space Administration Washington, D.C. 20546	14. Sponsoring Agency Code

15. Supplementary Notes

Project Manager, R. Lark, Materials and Structures Division, NASA Lewis Research Center, Cleveland, Ohio

16. Abstract

The objective of the program is to design, fabricate, and test unidirectional and angleply multi-fiber laminates for improved impact strength and other mechanical properties. The effects of several variables on the mechanical properties of epoxy matrix materials are described. These include fiber type (HMS and AS graphites, glass, and Kevlar 49), ratio of primary to hybridizing fiber and hybrid configuration. It is demonstrated that AS graphite/S-glass in an intraply configuration results in the best combination of static and Charpy impact properties as well as superior ballistic impact resistance. Pendulum impact tests which were conducted on thin specimens are shown to produce different ranking of materials than tests conducted on standard thickness Charpy specimens, and it is shown that the thin specimen results are in better agreement with the ballistic impact data. Additional static test data are reported as a function of temperature for the seven best hybrid configurations having epoxy, polyimide (PMR-15) and polyphenylquinoxaline resins as the matrix.

17. Key Words (Suggested by Author(s))		18. Distribution Statement
Composites	Kevlar 49	Unclassified - unlimited
Hybrids	Mechanical Properties	
Resins	Impact	
Graphite		
Glass		

19. Security Classif. (of this report)	20. Security Classif. (of this page)	21. No. of Pages	22. Price*
Unclassified	Unclassified	188	

* For sale by the National Technical Information Service, Springfield, Virginia 22151

Report R75-911730-15

Design, Fabrication and Test of Multi-Fiber Laminates

TABLE OF CONTENTS

TABLE OF CONTENTS (Cont'd)

TABLE OF CONTENTS (Cont'd)

LIST OF TABLES

LIST OF TABLES (Cont'd)

LIST OF TABLES (Cont'd)

LIST OF ILLUSTRATIONS

LIST OF ILLUSTRATIONS (Cont'd)

LIST OF ILLUSTRATIONS (Cont'd)

LIST OF ILLUSTRATIONS (Cont'd)

LIST OF ILLUSTRATIONS (Cont'd)

I. INTRODUCTION AND SUMMARY

The number of applications being found for high modulus fiber reinforced resin composites is steadily increasing in both aerospace and commercial areas. Their advantages - low density, high stiffness and high strength - are limited, however, by high cost and brittle fracture in potentially large volume use areas such as gas turbine fan blades and helicopter rotor blades. Brittle or catastrophic fracture with drastic loss of dynamic properties, the result of impact by foreign objects, is at present the primary technical problem which must be solved before acceptance in such application areas is achieved. The desirable properties of composites make this a worthwhile goal.

Most studies of composite impact behavior have utilized the Charpy test to examine the effect of material variables and to compare the performance of different composite systems. Work at United Aircraft Research Laboratories (UARL) has shown it is possible to increase the Charpy impact strength of graphite-resin composites through modification of interfacial strength by use of untreated graphite fibers, selection of fibers with high strength, or addition of glass or Kevlar-49 prepreg layers to form graphite epoxy hybrid composites (Ref. 1). Ballistic testing of hybrid composites conducted under NASA sponsorship (Ref. 2) has also demonstrated improved behavior for graphite fiber based composites.

Other investigators have also found merit in the hybrid approach to improving composite impact behavior. Chamis, et al (Ref. 3) related impact resistance to combined fracture modes consisting of fiber breakage, fiber pullout and interply delamination. It was shown that the "hybrid composite", i.e. a composite which consists of two or more different fiber/matrix combinations, takes advantage of two or more of these failure modes to improve impact resistance over the basic graphite-epoxy system.

Simon (Ref. 4), using hybrid composites consisting of 15 percent Kevlar-49 with Modmor II graphite, obtained a 50-60 percent increase in impact resistance compared to an all Modmor IIS epoxy composite but with some sacrifice in interlaminar shear strength.

Because the hybrid fiber approach had demonstrated improvement in composite impact strength, a systematic investigation of graphite, S-glass and Kevlar-49 hybrid reinforced resin composites was initiated at UARL under NASA-Lewis sponsorship. The overall objective of the program was to design, fabricate and test unidirectional and angleply multifiber laminates for improved impact strength and other mechanical properties. Determination of differences in energy absorption characteristics and the relationship between multi-fiber laminate impact

behavior and flexural and shear properties as well as a correlation between ballistic and pendulum impact response were part of the overall objective. In addition, the effect of high temperature matrix resins on these properties was investigated.

This investigation was divided into four basic tasks. The initial phase was devoted to investigating multi-fiber dispersion variables and effects of hybrid fiber ply configurations on epoxy resin composite mechanical properties including shear, flexural and pendulum impact strengths. Task II involved the evaluation of thin angle-ply multi-fiber epoxy resin composites in both pendulum and ballistic impact as well as the effect of composite thickness on pendulum impact strengths. The seven unidirectional hybrid fiber ply configurations which provided the best combination of impact, flexural and shear properties from Tasks I and II were subjected to further room temperature mechanical property characterization in Task III. The same seven laminate configurations were further evaluated at low and elevated temperatures in Task IV using epoxy, polyimide and polyphenylquinoxaline resin matrices. Primary fibers throughout the investigation were AS and HMS graphite while S-glass and Kevlar-49 III were the secondary fibers.

In Task I the hybrid fiber ply constructions investigated included interply, intraply, core-shell and inter-intraply. Particular emphasis was directed toward the intraply hybrid fiber configuration. The study showed that a tow-by-tow ply layup gave superior pendulum impact performance compared to a more dispersed graphite/glass or graphite Kevlar-49 reinforcement when tested in a standard Charpy impact configuration. In general, glass was found to be superior to Kevlar 49 as a hybridizing fiber for strength and impact properties. Core-shell hybrids were characterized by large bending modulus reductions as the percentage of secondary fiber was increased. The interply configuration resulted in the highest moduli for a given hybrid fiber content. The multi-fiber composite shear strength was generally limited by the weakest link. It was also found that additions of Kevlar 49 to HMS graphite did not provide significant improvements in impact (standard Charpy) regardless of ply construction. The best combination of Charpy impact strength and mechanical properties was given by the AS/S-glass intraply (tow-by-tow) system which showed no decrease in flexural strength or modulus, using up to 25 v/o glass, compared with homogeneous AS, with 134 to 150 percent improvement in impact strength. Additional studies in Task I included the effect of specimen thickness on instrumented Charpy impact properties and development of a computer program to facilitate calculation of the flexural modulus of hybrid composites.

Three angle-ply configurations combined with three hybrid fiber constructions were used in Task II to evaluate ballistic vs pendulum impact response and the effect of composite thickness on the latter test. Results showed that at composite thickness levels below 0.508 cm (0.200 in.), the AS/S-glass intraply gave superior performance in pendulum impact.

The ballistic damage parameter (E/V) which relates projectile energy and composite impact affected volume was found to provide correlation with pendulum impact results in that the same ranking order of composites based on data from both tests was obtained.

To provide additional correlation between the ballistic and pendulum impact tests, sixteen unidirectional multi-fiber composites selected on the basis of composite modulus [above 131 GN/m^2 (19 x 10^6 psi)] and having an average thickness of 0.254 cm (0.100 in.) were impacted using the instrumented Charpy test. A different order of composite ranking was obtained compared to the results using standard Charpy specimens. Flexural and shear stress interaction diagrams were constructed to demonstrate the importance of span-to-depth ratio in the pendulum impact test.

Based on the results of Tasks I and II, seven multi-fiber hybrid constructions were selected for further mechanical property characterization in Task III. The epoxy resin unidirectional laminates included three HMS/S-glass (one intraply and two interply), two AS/Kevlar-49 (intraply and interply), and two AS/S-glass (intraply and interply) systems. Tests included longitudinal tension and compression, transverse tension and compression and shear strength at room temperature. The same seven laminates were tested at -65°F, room temperature, 300°F and 600°F for flexure, shear, and thin pendulum impact as well as coefficient of thermal expansion in Task IV. Resin matrices included epoxy, polyimide (PMR-15) and polyphenylquinoxaline.

No unexpected results were obtained in the Task III evaluations. The transverse tensile compressive data reflected the difference between the intraply and interply ply constructions in that with the latter only the fiber layers having the highest transverse strengths are involved in load transfer while in the intraply configuration the combined fiber content is involved. In contrast, the longitudinal properties were found to be relatively insensitive to ply construction. The results from Task IV showed the AS/S-glass/polyimide intraply composite provided the best combination of properties over the temperature range investigated.

II. TASK I - PRELIMINARY COMPOSITE LAMINATE CONFIGURATION SCREENING

The four types of multi-fiber ply construction used throughout the investigation are defined as follows:

Laminate Type No.	Designation	Description
1	Intraply hybrid	A unidirectional composite/ply made from a uniformly distributed mixture of primary and secondary fibers.
2	Inter-intraply (Interspersed) laminate	A laminate made by stacking intraply hybrid with homogeneous primary fiber plys.
3	Interply hybrid laminate	A laminate made by stacking homogeneous primary with homogeneous secondary fiber plys.
4	Selective reinforcement	A laminate made by stacking homogeneous primary and secondary and/or intraply hybrid fiber plys in "shell/core" or "core/shell" configurations.

The laminate design configurations which were tested during Tasks Ia and Ib are shown in Table I.

Hercules Inc. graphite fibers, HMS and AS types, were used throughout the investigation. Both types were coated with a medium sizing (epoxy composites only) by the manufacturer to enhance interfacial bond strength. Union Carbide T-75 graphite was used in two of the inter-intraply type laminates. Ferro Inc. 961 S-glass (20 ends), Owens-Corning S-901 (12 ends), and DuPont Kevlar 49 III roving of 4560 denier were the hybridizing fibers. Kevlar 49 and PRD-49 are used interchangeably to identify this fiber. Dispersed fiber combinations were obtained from Heltra Inc. An air dispersion method was employed for spreading and partially mixing continuous filaments followed by drum winding the spread hybrid fiber tows. The fibers were combined in 8.9 cm (3.5 in.) wide, 0.00381 cm (0.0015 in.) thick tows which were subsequently drum wound in a dry condition for three revolutions of the drum, then coated with resin. This process was continued to produce a twelve ply prepreg tape. The epoxy resin composites were all fabricated using Union Carbide ERLA-4617A with Furan hardener 9245 as matrix resin by the procedure described in the appendix.

Table I

Laminate Design Configurations - Phase I

Composition Type	Laminate Type	Composition	Approx. Vol. %, Secondary Fibers or Intraply Hybrid Plys	Typical Laminate** Cross Section
1	1	AS/S-glass	15	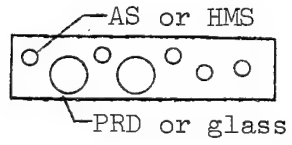
2	1	HMS/S-glass	50, 25, 10	
3	1	AS/PRD-49-III	15	
4	1	HMS/PRD-49-III	50, 10	
5	1	AS/$\frac{\text{S-glass}}{\text{PRD-49-III}}$	20/10 (Composition of the laminate is 70% AS, 20% glass, and 10% PRD)	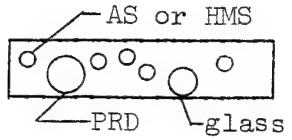
6	1	HMS/$\frac{\text{S-glass}}{\text{PRD-49-III}}$	20/40 (Composition of the laminate is 40% HMS, 20% glass, and 40% PRD)	
7	2	AS/$\frac{\text{AS}}{\text{S-glass}}$	20	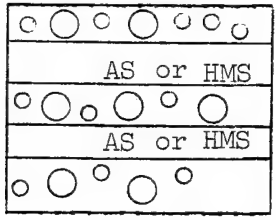
8	2	S-glass/$\frac{\text{T-75}}{\text{S-glass}}$	95, 90	
9	2	HMS/$\frac{\text{HMS}}{\text{S-glass}}$	20	
10	2	S-glass/$\frac{\text{T-75}}{\text{S-glass}}$	85, 80	

Table I (Cont'd)

Composition Type	Laminate Type	Composition		Approx. Vol. %, Secondary Fibers or Intraply Hybrid Plys	Typical Laminate** Cross Section
11	3	AS/S-glass		20, 10	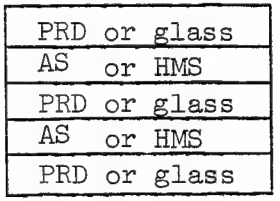
12	3	AS/PRD-49-III		30, 10	
13	3	HMS/S-glass		50, 25, 10	
14	3	HMS/PRD-49-III		50, 10	
		Core	Shell		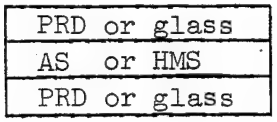
15	4	AS	S-glass	20, 10	
16	4	AS	PRD-49-III	30, 10	
17	4	HMS	S-glass	50, 25, 10	
18	4	HMS	PRD-49-III	50, 10	
19a	4	HMS	AS/S-glass	Percentages of glass in the shell are 20 and 10%. The ratios of primary fibers in core to secondary fibers in shell* are 7.5:1 and 15:1.	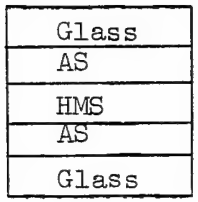
19b	4	HMS	AS/S-glass (Intraply Hybrid)	Same as above (composition 19a)	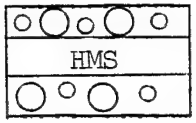

Table I (Cont'd)

Composition Type	Laminate Type	Composition		Approx. Vol. %, Secondary Fibers or Intraply Hybrid Plys	Typical Laminate** Cross Section
		Core	Shell		
20a	4	HMS	HMS/S-glass	Percentages of glass in the shell are 50, 25, and 10%. The ratios of primary fiber in core to secondary fibers in shell* are 3:1, 9:1, and 15:1.	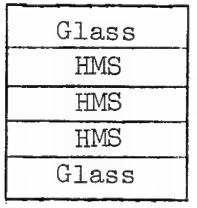
20b	4	HMS	HMS/S-glass (Intraply Hybrid)	Same as above (composition 20a)	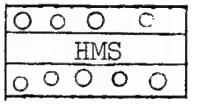

*Two laminates to be fabricated and percentages of components to be selected after completion of testing of Type 1 laminates.

**The typical laminate cross sections are for illustration purposes only and they do not represent the number of plies in the laminate.

The physical properties of all composites fabricated in Task I which includes density, volume percent each fiber, volume percent resin and voids and the ply construction employed are listed in Table II.

2.1 Preliminary Multi-Fiber Dispersion Process Study

To determine the effect of degree of hybrid fiber dispersion on intraply composite properties a series of Type 1 laminates (see Table I) were fabricated using Heltra air dispersed multi-fiber reinforcement and the corresponding tow-by-tow reinforcement made using the same fibers combined by co-winding techniques (see Appendix, section 8.4). Two of the five dispersed fiber combinations were made by mechanical methods at UARL rather than with the Heltra air dispersion system.

The intention of the dispersed fiber approach was to achieve uniform mixing of the primary and secondary filaments. The air dispersion process easily spread the fiber tows employed but resulted in only limited intermixing of the fiber types. Thus, uniform dispersion was not achieved and the effects of total uniform fiber mixing on composite properties remains to be determined.

The flexural, shear and Charpy impact strengths of the intraply hybrid fiber combinations made by dispersion (designated as Heltra) and those using the same fibers combined by co-winding techniques (side-by-side tow - designated UARL) are listed in Table III.

2.1.1 Static Properties

2.1.1.1 Shear Strength

For composites having HMS graphite as the primary fiber, the tow-by-tow S-glass hybrids possessed increased shear strength over that of the primary fiber composite, whereas the dispersed S-glass hybridized composites do not; in fact the shear strengths were degraded. Kevlar 49 hydridization resulted in a slight decrease in composite shear strength regardless of construction, apparently reflecting the lower interfacial bond strength of Kevlar 49 epoxy.

AS graphite primary fiber composites were, in general, much higher in shear strength than the HMS systems. S-glass again was the more effective hybridizing fiber compared to Kevlar 49. Comparison of composites No. 68 and 69, which incorporate both hybridizing fibers in AS graphite, further demonstrates the superiority of the tow-by-tow construction over the dispersed type.

Table II

Physical Properties of Epoxy-Hybrid Fiber Composites

UARL No.	Composition Type	Density g/cc	v/o Total Fiber	v/o Resin	v/o Void	Fiber Ratio v/o (Theory)	Fiber Ratio v/o (Actual)	Ply Construction
NAS-6	11	1.65	AS-53.7 S-6.6	39.7	0	AS-90 S-10	AS-89.1 S-10.9	$AS_{(4)}$-S-$AS_{(4)}$
NAS-8C	11	1.69	AS-49.6 S-12.6	39.0	0	AS-80 S-20	AS-79.8 S-20.2	$AS_{(2)}$-S-$AS_{(4)}$-S-$AS_{(2)}$
NAS-8B	11	1.71	AS-53.5 S-11.9	34.3	0.3	AS-80 S-20	AS-81.7 S-18.3	$AS_{(2)}$-S-$AS_{(4)}$-S-$AS_{(2)}$
NAS-13	12	1.60	AS-59.2 PRD-5.15	35.4	0.25	AS-90 PRD-10	AS-92 PRD-8	$AS_{(4)}$-PRD-$AS_{(4)}$
NAS-14	12	1.54	AS-45.8 PRD-19.9	32.5	1.8	AS-70 PRD-30	AS-69.7 PRD-30.3	AS-PRD-$AS_{(2)}$-PRD-$AS_{(2)}$-PRD-AS
NAS-15	13	1.73	HMS-61 S-7.1	29.3	2.6	HMS-90 S-10	HMS-89.6 S-10.4	$HMS_{(4)}$-S-$HMS_{(4)}$
NAS-15A	13	1.69	HMS-56.8 S-4.1	37.7	1.4	HMS-90 S-10	HMS-93.25 S-6.75	$HMS_{(4)}$-S-$HMS_{(4)}$
NAS-10	13	1.77	HMS-49.6 S-15.4	33.7	1.6	HMS-75 S-25	HMS-76.4 S-23.6	$HMS_{(2)}$-S-$HMS_{(2)}$-S-$HMS_{(2)}$
NAS-9	13	1.83	HMS-34.0 S-28.6	36.7	1.5	HMS-50 S-50	HMS-54.3 S-45.7	HMS-S-HMS-S-HMS-S
NAS-12A	14	1.62	HMS-52.2 PRD-4.2	41.7	1.9	HMS-90 PRD-10	HMS-92.5 PRD-7.5	$HMS_{(4)}$-PRD-$HMS_{(4)}$
NAS-11A	14	1.54	HMS-35.8 PRD-25.6	36.9	3.5	HMS-50 PRD-50	HMS-58.2 PRD-41.8	HMS-PRD-HMS-PRD-HMS-PRD
NAS-20A	15	1.69	AS-55.0 S-9.6	35.0	0.4	AS-90 S-10	AS-85 S-15	$S_{(1/2)}$-$AS_{(8)}$-$S_{(1/2)}$
NAS-17	15	1.74	AS-55.2 S-14.3	30.3	0.2	AS-80 S-20	AS-79.4 S-20.6	S-$AS_{(8)}$-S
NAS-17A	15	1.69	AS-49.7 S-12.2	38.2	0	AS-80 S-20	AS-80.2 S-19.8	S-$AS_{(8)}$-S
NAS-26A	16	1.57	AS-54.1 PRD-5.3	40.2	0.4	AS-90 PRD-10	AS-90.9 PRD-9.1	$PRD_{(1/2)}$-$AS_{(8)}$-$PRD_{(1/2)}$
NAS-23A	16	1.51	AS-38.8 PRD-23.3	35.9	2.0	AS-70 PRD-30	AS-62.5 PRD-37.5	$PRD_{(1-1/2)}$-$AS_{(6)}$-$PRD_{(1-1/2)}$
NAS-24	17	1.74	HMS-57.8 S-8.9	30.8	2.6	HMS-90 S-10	HMS-86.7 S-13.3	$S_{(1/2)}$-$HMS_{(8)}$-$S_{(1/2)}$
NAS-16A	17	1.74	HMS-41.9 S-16.4	40.2	1.50	HMS-75 S-25	HMS-72 S-28	S-$HMS_{(6)}$-S
NAS-18	17	1.83	HMS-30.6 S-32.2	34.5	2.7	HMS-50 S-50	HMS-48.7 S-51.3	$S_{(2)}$-$HMS_{(4)}$-$S_{(2)}$
NAS-28	18	1.63	HMS-55.4 PRD-6.8	36.1	1.7	HMS-90 PRD-10	HMS-89.1 PRD-10.9	$PRD_{(1/2)}$-$HMS_{(8)}$-$PRD_{(1/2)}$
NAS-19	18	1.54	HMS-36.6 PRD-26.6	34.5	2.3	HMS-50 PRD-50	HMS-57.7 PRD-42.3	$PRD_{(2)}$-$HMS_{(4)}$-$PRD_{(2)}$
NAS-34	19a-1	1.64	AS/HMS-55.0 S-4.3	38.7	2.0	S-20 (Shell)		$S_{(1/2)}$-$AS_{(2)}$-$HMS_{(7.5)}$-$AS_{(2)}$-$S_{(1/2)}$

Table II (Cont'd)

UARL No.	Composition Type	Density g/cc	v/o Total Fiber	v/o Resin	v/o Void	Fiber Ratio v/o (Theory)	Fiber Ratio v/o (Actual)	Ply Construction
NAS-35	19a-2	1.65	AS/HMS-57.0 S-3.5	38.0	1.5	S-10 (Shell)		$S_{(1/4)}$-$AS_{(2)}$-$HMS_{(7)}$-$AS_{(2)}$-$S_{(1/4)}$
NAS-55	20a-1	1.68	HM-49 S-8.5	40.3	2.0	S-50 (Shell)	HM-85.2 S-14.8	S-$HMS_{(8)}$-S
NAS-54	20a-2	1.65	HM-55.6 S-1.9	41.2	1.3	S-25 (Shell)	HM-96.8 S-3.2	$S_{(1/2)}$-$HMS_{(12)}$-$S_{(1/2)}$
NAS-36	2-UARL[a]	1.81	HMS-46 S-16.3	37.6	0.1	HMS-75 S-25	HMS-73.5 S-26.5	S/HM (co-wound tow)
NAS-36A	2-UARL	1.81	HMS-14.9 S-36.8	48.0	0.3	HMS-40 S-60	HM-28.8 S-71.2	$S_{(4)}$/HM (co-wound tow)
NAS-36B	2-UARL	1.93	HM-20.4 S-41.2	38.4	0		HM-33.2 S-66.8	S/HM (co-wound tow)
NAS-47	2-Heltra	1.59	HMS-13.9 S-19.7	65.2	1.3	HMS-50 S-50	HMS-41.4 S-58.6	S/HM dispersed tow
NAS-47A	2-Heltra	1.61	HMS-11.5 S-21.2	67.6	0	HMS-50 S-50	HMS-35 S-65	S/HM dispersed tow
NAS-47B	2-Heltra[b]	1.63	HM-15.4 S-22.4	61.2	1.0	HMS-50 S-50	HM-40.7 S-59.3	S/HM dispersed tow
NAS-47C	2-Heltra	1.93	HM-22.1 S-41.9	36	0		HM-34.4 S-65.6	S/HM (dispersed tow)
NAS-47D	2-Heltra	1.84	HM-45.4 S-24.6	30.8	1.3		HM-64 S-36	S/HM (dispersed tow)
NAS-49	4-Heltra[b]	1.44	HMS-15.1 PRD-40.2	44.5	0.3	HMS-50 PRD-50	HMS-27.4 PRD-72.6	HMS/PRD dispersed tow
NAS-49A	4-Heltra[c]	1.43	HMS-20.1 PRD-24.3	54.5	1.1	HMS-50 PRD-50	HM-48.4 PRD-51.6	HMS/PRD dispersed tow
NAS-46	4-UARL[a]	1.46	HMS-25.4 PRD-23.7	48.6	2.4	HMS-50 PRD-50	HMS-56.7 PRD-48.3	HMS/PRD co-wound tow
NAS-64	8	2.00	T-75-4.0 S-57.3	38.7	0	T-75-5 S-95	T-75-6.5 S-93.5	co-wound $tow_{(1/3)}$/S
NAS-66	8	1.98	T-75-5.4 S-54.6	40.0	0	T-75-10 S-90	T-75-9 S-91	2 co-wound $tow_{(1/3)}$/S
NAS-64A	10	1.91	T-75-8.6 S-48.5	42.5	0.4	T-75-15 S-85	T-75-15.1 S-84.9	co-wound $tow_{(1/9)}$/S
NAS-66A	10	1.91	T-75-13.0 S-47.5	39.5	0	T-75-20 S-80	T-75-21.5 S-78.5	2 co-wound $tow_{(1/9)}$/S
NAS-68	5-Heltra	1.59	AS-35.2 S-10.2 PRD-13.8	39.2	1.6	AS-70 S-20 PRD-10	AS-59.4 S-17.2 PRD-23.4	Heltra dispersed tow
NAS-69	5-UARL	1.66	AS-37.0 S-13.7 PRD-14.5	32.8	2.0	AS-70 S-20 PRD-10	AS-56.8 S-21.0 PRD-22.2	co-wound tow
NAS-72	9	1.77	HMS-56 S-12.5	28.6	2.9	HMS-80 S-20	HMS-81.8 S-18.2	co-wound $tow_{(1/1)}$/HM
NAS-74	7	1.68	AS-53.4 S-10.5	35.3	0.8	AS-80 S-20	AS-83.7 S-16.3	co-wound $tow_{(1/1)}$/AS
NAS-76	1	1.76	AS-49.7 S-16.6	33.7	0	AS-85 S-15	AS-75 S-25	co-wound tow (12 end glass)
NAS-78	3	1.60	AS-59.3 PRD-8.6	31.1	1.0	AS-85 PRD-15	AS-87.5 PRD-12.5	co-wound tow (1/4 PRD-49 tow)
NAS-1		1.57	AS-57.7	41.8	0.5	AS-100		
NAS-1a		1.60	AS-59.0	41.2	0	AS-100		
NAS-3a		2.28	S-66	34.0	-	S-100		
NAS-5		1.38	PRD-66.9	31.1	2.0	PRD-100		
NAS-61		1.65	HM-63	36.4	0.6	HM-100		

[a]Prepreg tape made by co-winding alternating tows of fibers

[b]Dispersed tows as received from Heltra Inc.

[c]Dispersed tows made at UARL

Table III

Flexural and Shear Properties of Intraply Epoxy Hybrid Fiber Composites

Composite No.	Intraply Construction[a]	Fiber Ratio, v/o	Short Beam Shear[b]		Flexural Strength[c]		Flexural Modulus[c]	
			MN/m^2	(psi)	GN/m^2	(ksi)	GN/m^2	(psi x 10^6)
47C	2-Heltra	HMS-34.4 S-65.6	45.2	(6560)	1.13	(164.1)	116	(16.8)
47D	2-Heltra	HMS-64 S-36	36.7	(5300)	1.25	(181.5)	158	(22.95)
36	2-UARL	HMS-73.5 S-26.5	56.5	(8200)	1.18	(171)	142	(20.6)
36B	2-UARL	HMS-33.2 S-66.8	68.5	(9950)	1.16	(168.5)	110	(16)
36A	2-UARL	HMS-28.8 S-71.2	71.0	(10,300)	0.87	(126)	82.6	(12)
46	4-UARL	HMS-51.7 Kevlar-48.3	43.5	(6300)	0.61	(88.5)	102	(14.8)
49	4-Heltra	HMS-27.4 Kevlar-72.6	45.6	(6625)	0.716	(104)	86	(12.5)
49A	4-Heltra	HMS-48.4 Kevlar-51.6	45.5	(6600)	0.765	(111)	87.5	(12.7)

Table III (Cont'd)

Composite No.	Intraply Construction[a]	Fiber Ratio, v/o	Short Beam Shear[b] MN/m^2	(psi)	Flexural Strength[c] GN/m^2	(ksi)	Flexural Modulus[c] GN/m^2	(psi x 10^6)
68	5-Heltra	AS-59.4 S-17.2 Kevlar-23.4	64.3	(9320)				
69	5-UARL	AS-56.8 S-21.0 Kevlar-22.2	84.5	(12,270)				
76	1-UARL	AS-75 S-25		(18,250)	1.86	(270.8)	127	(18.5)
78	3-UARL	AS-87.5 Kevlar-12.5		(14,900)	2.02	(293)	126	(18.3)
1	-	AS	124	(17,980)	1.9	(275)	125	(18.1)
3a	-	S-glass	109.2	(15,875)	1.9	(275)	55.9	(8.1)
5	-	Kevlar-49	41.5	(6030)	0.68	(98.4)	75.8	(11)
61	-	HMS	49	(7100)	1.18	(172)	190	(27.5)

[a]UARL = tow-by-tow prepreg; Heltra = dispersed fiber prepreg
[b]Short beam shear, S/D = 4/1
[c]Flexural test - 3 point, S/D = 32/1

2.1.1.2 Flexural Properties

HMS graphite composites hybridized with S-glass show no change in flexural strength compared to the primary fiber system regardless of intraply construction. On the other hand, introduction of Kevlar 49 results in a decrease in flexural strength relative to the HMS composite which is primarily due to the low flexural strength of the Kevlar 49 system. The data indicate that the dispersed construction may be slightly stronger in flexure than the tow-by-tow type.

In the AS graphite composites the excellent flexural strengths of the primary fiber are retained using either hybridizing fiber or construction type. There appears to be little effect of ply construction on modulus when comparison of composites of similar fiber ratios and type are made. However, of particular interest is the equivalent moduli obtained with the tow-by-tow AS/S-glass and AS/Kevlar 49 composites (No. 76 and 78). Based on fiber volume fraction the modulus of the latter composite should be higher (142 GN/m^2). It is hypothesized that the lower than expected modulus of the AS/Kevlar 49 system is due to the contribution of the much lower shear modulus of Kevlar 49 vs S-glass. Shear deflection is not accounted for in the equations used to calculate flexural modulus.

2.1.2 Dynamic Properties

Comparison of the Charpy impact data of the comparable HMS/S-glass fiber ratios shows that the tow-by-tow construction gives composites having higher total impact energy (E_T) than the dispersed fiber system. For example, 36B > 47C and 36 > 47D even though No. 36 contains less S-glass in the composite.

Indication of why the tow-by-tow configuration provides improved impact resistance compared to the dispersed configuration can be seen in Fig. 1 which shows the end fractures of two of the above-listed composites. In the dispersed composites the shear fracture planes are, in general, uninterrupted and straight through the laminate. In the corresponding tow-by-tow composites the shear fracture planes are interrupted and angular in the area of the graphite fiber bundles which apparently requires a greater dissipation of energy in the fracture of the composite. This is also reflected in the load at initial fracture (P_i) and maximum load (P_{max}) attained in the load-time trace of the Charpy impact test as listed in Table IV. As pointed out above the short beam shear strength of the tow-by-tow construction was significantly higher than that of the dispersed fiber construction. On the other hand, the flexural strengths and modulus of the composites of similar fiber ratios are essentially the same. This further demonstrates the importance of shear behavior in the standard Charpy impact test. P_i was determined as being the point at which a change in slope occurred in the initial portion of the load-time curve. It was found that HMS/S-glass dispersed construction is similar in impact response to HMS alone while the tow-by-tow composite shows the influence of added S-glass.

FIG. 1

FRACTURE MODE OF HMS/S GLASS INTRAPLY EPOXY COMPOSITES

NAS–47D
HELTRA–2

NAS–36
UARL–2

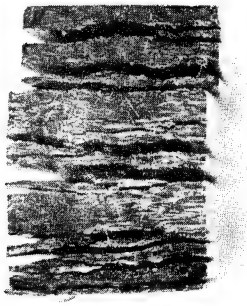

HMS/Kevlar 49 composites did not give as wide a variation in impact strength between the two constructions. However, the tow-by-tow type did result in a higher P_{max} load (Table IV) which was considerably higher than that obtained with either HMS or Kevlar 49 alone. This points out the value of the instrumented test for a complete characterization of a material's response to impact. These results are compatible with data obtained on interply and core/shell laminates which showed that the total Charpy impact strength of a unidirectional HMS/Kevlar 49 composite is essentially the same regardless of the ply construction employed. These data are discussed below.

The AS/S-glass/Kevlar 49 composites had the same load parameters for both types of construction. However, the Charpy impact strengths for the tow-by-tow construction was nearly double that of the dispersed system (Table IV) as was verified by a larger area under the load-time curve. Analysis of the fracture mode showed that, as in the HMS/S-glass laminates, the tow-by-tow construction resulted in angular, out of plane fracture paths. The two AS tow-by-tow laminates hydridized with S-glass (No. 76) and Kevlar 49 (No. 78), which gave nearly the same static properties, were considerably different in impact response. The former system, having the typical out-of-plane shear fracture pattern, had twice the impact strength of the latter.

It is hypothesized that the controlling factor in the Charpy impact behavior of these hybrid composites is the interlaminar shear failure of the weakest layer, generally HMS graphite or Kevlar 49. This results in similar P_i loads for the dispersed intraply and standard HMS composites as listed in Table IV. However, the tow-by-tow intraply composites, because of ply construction, have no continuous layers of graphite; rather the graphite tows effectively line up at an angle to produce a graphite layer out of the plane of the interlaminar shear stress. This presumably requires a higher load to initiate and/or propagate failure.

The standard Charpy test is carried out at a span-to-depth ratio of 4 to 1 ($L/h = 4$). The results described above demonstrate the primary failure mode is shear. It is important to recognize therefore that standard Charpy impact data should be used to determine impact resistance levels only in applications which are to involve loads at low L/h ratios. The effect of using lower L/h ratios will be discussed below.

Based on this evidence it was concluded that the side-by-side tow configuration does provide a greater resistance to impact than the more intimately dispersed fiber reinforcement. Consequently, the remaining intraply composites of Type 1 and 2 laminates were fabricated using side-by-side tows. It should be noted, however, that uniform fiber dispersion should be better than the tow-by-tow configuration in limiting catastrophic crack propagation due to fiber breakage. The Charpy specimens failed in part by delamination and complete fiber uniformity was not achieved, so the principle in actual fact was not tested.

Table IV

Charpy Impact Loads of Composite Types 2, 4 and 5
Intraply

UARL No.	Composition Type	Fiber Ratio v/o (actual)	P_i Newtons	P_i (lbs)	P_{max} Newtons	P_{max} (lbs)	Charpy Impact Strength (experimental) Joules	Charpy Impact Strength (experimental) (ft-lbs)
NAS-47C	2-Heltra	HMS-34.5 S-65.5	2890	(650)	3550	(800)	33.6	(24)
NAS-47D	2-Heltra	HMS-64 S-36	2845	(640)	2940	(660)	28.7	(20.5)
NAS-36	2-UARL	HMS-73.5 S-26.5	4448	(1000)	5350	(1200)	34.4	(24.5)
NAS-36B	2-UARL	HMS-33.2 S-66.8	4050	(910)	4630	(1040)	54.6	(39)
NAS-36A	2-UARL	HMS-28.8 S-71.2	4340	(975)	5780	(1300)	49	(35)
NAS-46	4-UARL	HMS-51.7 PRD-48.3	3550	(800)	6000	(1350)	18.9	(13.5)
NAS-49	4-Heltra	HMS-27.4 PRD-72.6	2845	(640)	4170	(940)	20.3	(14.5)
NAS-49A	4-Heltra	HMS-48.5 PRD-51.6	2760	(700)	3150	(700)	16.8	(11)
NAS-68	5-Heltra	AS-59.4 S-17.2 PRD-23.4	6350	(1430)	6350	(1430)	21	(15)
NAS-69	5-UARL	AS-56.8 S-21.0 PRD-22.2	6450	(1450)	6450	(1450)	39.2	(28)

P_i = load at initial fracture
P_{max} = maximum load attained

2.2 Preliminary Composite Laminate Configuration Screening

The mechanical properties, flexural, shear and impact, of the remainder of the composites fabricated in Task I are listed in Tables V-VIII. The data are presented by fiber types where possible, i.e. HMS/S-glass, HMS/Kevlar 49, AS/S-glass and AS/Kevlar 49 so that a comparison of interply vs core-shell vs intraply vs inter-intraply can be readily made for each fiber combination.

2.2.1 Static Properties

2.2.1.1 Flexural Properties

Flexural properties are one of the major criteria to be used in selecting laminate candidates for Tasks III and IV. A comparison of composite modulus and strength properties as a function of hybrid fiber type and percent hybridizing fiber revealed basic differences between the various laminate types.

The effect on the flexural strength of HMS and AS interply systems hybridized with S-glass is shown in Fig. 2. With the interply configuration there is only a slight increase in flexural strength of the HMS system with increasing glass content with strengths being close to rule-of-mixture predictions. Analysis of the failure mode depicted in Fig. 3 showed that all the HMS/S-glass interply laminates failed in compression in the HMS layer. The compressive crack propagated to the graphite-glass interface; shear failure then resulted. The change in the stress-strain curve was related to the distance the crack traveled. The homogeneous HMS laminate also showed compressive failure. It is apparent that the compressive crack has to propagate a certain critical distance before specimen failure is detected. Observation of the failed HMS specimen showed that this was at least one-half the specimen thickness. Presence of the higher strength glass interply layers blunts the crack propagation prior to reaching the critical crack length and specimen failure was not detected until shear delamination occurred. This happened at higher loads than with homogeneous HMS.

The AS/S-glass interply laminates, in contrast to the HMS system, showed a decrease in flexural strength with increasing glass content, Fig. 2. Analysis of the failure mode shown in Fig. 4 revealed that a progression from tensile f failure in homogeneous AS to tensile/compression failure at 10 v/o glass to compressive failure at 20 v/o glass had occurred. The initial failure occurred in the graphite to the graphite/glass interface where shear failure resulted. The progression from tensile to compressive failure with increasing glass content indicates that addition of glass to the AS graphite in the interply configuration results in a decrease in the compressive strength of the hybrid composite relative to the homogeneous AS laminate. This is reflected in lower flexural strengths for the multi-fiber system.

Table V

Flexural, Shear and Impact Strengths of HMS and T-75/S-Glass Composites

UARL No.	Composition Type	Fiber Ratio v/o (actual)	Short Beam Shear		Flexural[b] Strength		Flexural[b] Modulus		Charpy Impact Specimens		
									Density	Strength (face)	
			MN/m^2	(psi)[a]	GN/m^2	(ksi)	GN/m^2	($psix10^6$)	g/cc	Joules	(ft-lbs)
NAS-9	13	HMS-54.3 S-45.7	54.6	(7940)	1.38	(200.8)	120.5	(17.5)	1.84	28	(20)
NAS-10	13	HM-76.4 S-23.6	55.8	(8100)		(191)	210	(28.7)	1.76	25.2	(18)
NAS-15	13	HM-89.6 S-10.4	45.5	(6600)	1.26	(183)	214	(31)			
NAS-15A	13	HM-93.2 S-6.75	38.2	(5500)	1.30	(183)	190	(27.6)	1.75	16.8	(12)
NAS-18	17	HM-48.7 S-51.3	60.2	(8730)	1.35	(196)	82.8	(12.0)[c] (10.6)	1.86	44.8	(32)
NAS-16A	17	HMS-72 S-28	56.0	(8130)	1.36	(198)	111	(16.1)	1.69	22.4	(16)
NAS-24	17	HMS-86.7 S-13.3	43.6	(6330)	1.26	(183)	157	(22.8)	1.66	12.6	(9)
NAS-36	2-UARL	HMS-73.5 S-26.5	56.5	(8200)	1.18	(171)	142	(20.6)	1.76	34.3	(24.5)
NAS-36A	2-UARL	HMS-28.8 S-71.2		(10,300)	0.87	(126)	82.6	(12)	1.85	54.6	(39)
NAS-36B	2-UARL	HMS-33.2 S-66.8	68.5	(9950)	1.16	(168.5)	110	(16)	1.85	50.5	(36)
NAS-47	2-Heltra	HMS-41.4 S-58.6	55.5	(8050)	0.8	(116)	55.2	(8.0)	1.59	39.2	(28)
NAS-47A	2-Heltra	HMS-35 S-65	53	(7700)	0.78	(114)	60.6	(8.8)			
NAS-47B	2-Heltra	HMS-59.4 S-45.6	56	(8100)	0.8	(116)	71.6	(10.4)	1.67	38.4	(27.5)
NAS-47C	2-Heltra	HMS-34.4 S-65.6	45.2	(6560)	1.13	(164.1)	116	(16.8)	1.92	33.6	(24)
NAS-47D	2-Heltra	HMS-64 S-36	36.7	(5300)	1.25	(181.5)	158	(22.95)	1.80	28.6	(20.5)
NAS-55	20a-1	HMS-85.2 S-14.8	37.4	(5430)	1.18	(171.5)	138	(20.0)	1.70	25.2	(18)
NAS-54	20a-2	HMS-96.8 S-3.2	40.5	(5875)	0.91	(132)	154	(22.3)	1.64	18.2	(13)
NAS-64	8	T-75-6.5 S-93.5	79.6	(12,680)	1.36	(197)	64	(9.3)	1.99	70	(50)
NAS-66	8	T-75-9 S-91	79.6	(12,700)	1.56	(226)	76	(11)	1.90	57.5	(41)
NAS-64A	10	T-75-15.1 S-84.9		(9720)	1.03	(149)	74	(10.7)	1.92	63.6	(45.5)
NAS-66A	10	T-75-21.5 S-78.5		(11,600)	1.22	(178)	82.9	(12)	1.88	51.2	(36.5)
NAS-72	9	HMS-81.8 S-18.2		(5320)	1.30	(189)	174	(25.3)	1.74	22.4	(16)
NAS-61		HM-63	49	(7100)	1.18	(172)	190	(27.5)	1.70	16.8	(12)
NAS-3A		S-66	169.2	(15,870)			55.9	(8.1)	1.91	72.7	(52)

[a]Short beam shear S/D = 4/1
[b]Flexural test - 3 point, S/D = 32/1
[c]Flexural test - 4 point, S/D = 32/1

Table VI

Flexural, Shear and Impact Strengths of HMS-PRD-49-III Composites

UARL No.	Composition Type	Fiber Ratio v/o (Actual)	Short Beam Shear Strength MN/m^2	(psi)[a]	Flexural[b] Strength GN/m^2	(ksi)	Flexural[b] Modulus GN/m^2	($psix10^6$)	Charpy Impact Specimens Density g/cc	Strength (face) Joules	(ft-lbs)
NAS-12A	14	HMS-92.5 PRD-7.5	64.5	(9350)	1.19	(173)	185.5	(26.9)	1.62	15.4	(11)
NAS-11A	14	HMS-58.2 PRD-41.8	38.8	(5640)	1.0	(145)	123	(17.8)	1.49	18.9	(13.5)
NAS-28	18	HMS-89.1 PRD-10.9	52.8	(7640)	1.28	(186)	174	(25.3)	1.59	13.65	(9.75)
NAS-19	18	HMS-57.7 PRD-42.3	39	(5650)	0.895	(130)	86.2	(12.5)	1.48	20	(14.25)
NAS-46	4-UARL	HMS-51.7 PRD-48.3	43.5	(6300)	0.61	(88.5)	102	(14.8)	1.46	18.9	(13.5)
NAS-49	4-Heltra	HMS-27.4 PRD-72.6	45.6	(6625)	0.716	(104)	86	(12.5)	1.42	20.3	(14.5)
NAS-49A	4-Heltra	HMS-48.4 PRD-51.6	45.5	(6600)	0.765	(111)	87.5	(12.7)	1.42	16.8	(12)
NAS-5A		PRD-66.9	41.5	(6030)	0.68	(98.4)	75.8	(11)	1.38	35	(25)

[a]Short beam shear S/D = 4/1
[b]Flexural test 3 point, S/D = 32/1
[c]Average of two tests

Table VII

Flexural, Shear and Impact Strengths of AS S-Glass Composites

UARL No.	Composition Type	Fiber Ratio v/o (Actual)	Short Beam Shear Strength MN/m^2	(psi)[a]	Flexural Strength[b] GN/m^2	(ksi)	Flexural Modulus[b] GN/m^2	($psix10^6$)	UARL No.	Charpy Impact Specimens Density g/cc	Strength (face) Joules	(ft-lbs)[d]
NAS-6	11	AS-89.1 S-10.9	104	(15,125)	1.68	(244)	123	(17.8)	NAS-7	1.71	42	(30)
NAS-8	11					(207)		(17.55)				
NAS-8C	11	AS-79.8 S-20.2	109	(15,800)	1.475	(214)	109	(15.8)	NAS-21	1.75	44.8	(32)
NAS-8B	11	AS-81.7 S-18.3	96	(13,940)	1.47	(213)	123.2	(17.9)[c] (15.8)	NAS-21A	1.72	44.8	(32)
NAS-20A	15	AS-85 S-15	99.5	(14,400)	1.91	(277)	99.5	(14.4)	NAS-38	1.66	30.8	(22)
NAS-17A	15	AS-80.2 S-19.8	98	(14,240)	1.66	(241.5)	82	(11.9)	NAS-22	1.74	46.2	(33)
NAS-35	19a-2	AS/HM-57.0 S-3.5	59.6	(8640)	1.63	(237)	111.8	(16.2)	NAS-53	1.65	17.5	(12.5)
NAS-34	19a-1	AS/HM-55.0 S-4.3	55.8	(8100)	1.5	(218)	109.5	(15.9)	NAS-52	1.66	19.6	(14)
NAS-68	5-Heltra	AS-59.4 S-17.2 PRD-23.4	64.3	(9320)	1.53	(222)	92.5	(13.4)	NAS-70	1.54	21	(15)
NAS-69	5-UARL	AS-56.8 S-21.0 PRD-22.2	84.5	(12,270)	1.68	(242.5)	95	(13.8)	NAS-71	1.57	39.2	(28)
NAS-74	7	AS-83.7 S-16.3		(18,380)		(238)		(15.4)	NAS-75	1.71	37.8	(27)
NAS-76	1-UARL	AS-75 S-25		(18,250)		(270.8)		(18.5)	NAS-77	1.77	51.9	(37.5)
NAS-1		AS-57.7	70.6	(10,250)	0.99	(144)[c]	98	(14.3)[c]	NAS-6C	1.64	24.5	(16.0)
NAS-1a		AS-59	124.0	(17,980)	1.9	(275. ;	125	(18.1)		1.70		
NAS-3A		S-66	109.2	(15,870)			55.9	(8.1)[c]	NAS-62	1.91	73.5	(52.5)

[a]Short beam shear - S/D = 4/1
[b]Flexural test - 3-point, S/D = 32/1
[c]Flexural test - 4-point, S/D = 32/1
[d]Average of two tests

Table VIII

Flexural, Shear and Impact Strengths of AS-PRD-49-III Composites

UARL No.	Composition Type	Fiber Ratio v/o (Actual)	Short Beam Shear Strength MN/m^2	(psi)[a]	Flexural Strength[b] GN/m^2	(ksi)	Flexural Modulus GN/m^2	($psix10^6$)	Charpy Impact Specimens Density g/cc	Strength (face) Joules	(ft-lbs)[d]
NAS-13	12	AS-92 PRD-8	74.5	(10,800)	1.63	(237.5)	125 134.2	(18.2)[c] (19.5)[b]	1.59	29.4	(21)
NAS-14	12	AS-69.7 PRD-30.3	60.5	(8760)	1.475	(214)	121.5 116.0	(17.6)[c] (16.8)[b]	1.56	33.6	(24)
NAS-26A	16	AS-90.9 PRD-9.1	103	(14,900)	1.46	(212)	102	(14.8)[b]	1.61	32.2	(23)
NAS-23A	16	AS-62.5 PRD-37.5	86.2	(12,500)	1.33	(193)	75.8	(11)[b]	1.50	35	(25)
NAS-78	3-UARL	AS-87.3 PRD-12.7		(14,120)		(293)		(18.3)		26.6	(19)
NAS-5A		PRD-66.9	41.5	(6030)	0.68	(98.4)	68.95	(11)[b]	1.38	35	(25)
NAS-1		AS-57.7	70.6	(10,250)	0.99	(144)[c]	125	(14.3)[c]	1.64	22.4	(16)
NAS-1a		AS-59.0	124.0	(17,980)	1.9	(275.5)	55.9	(18.1)	1.70		

[a]Short beam shear - S/D = 4/1
[b]Flexural test - 3-point, S/D = 32/1
[c]Flexural test - 4-point, S/D = 32/1
[d]Average of two tests

FLEXURAL STRENGTH VS V/O HYBRID
AS/S–GLASS AND HMS/S–GLASS INTERPLY COMPOSITES

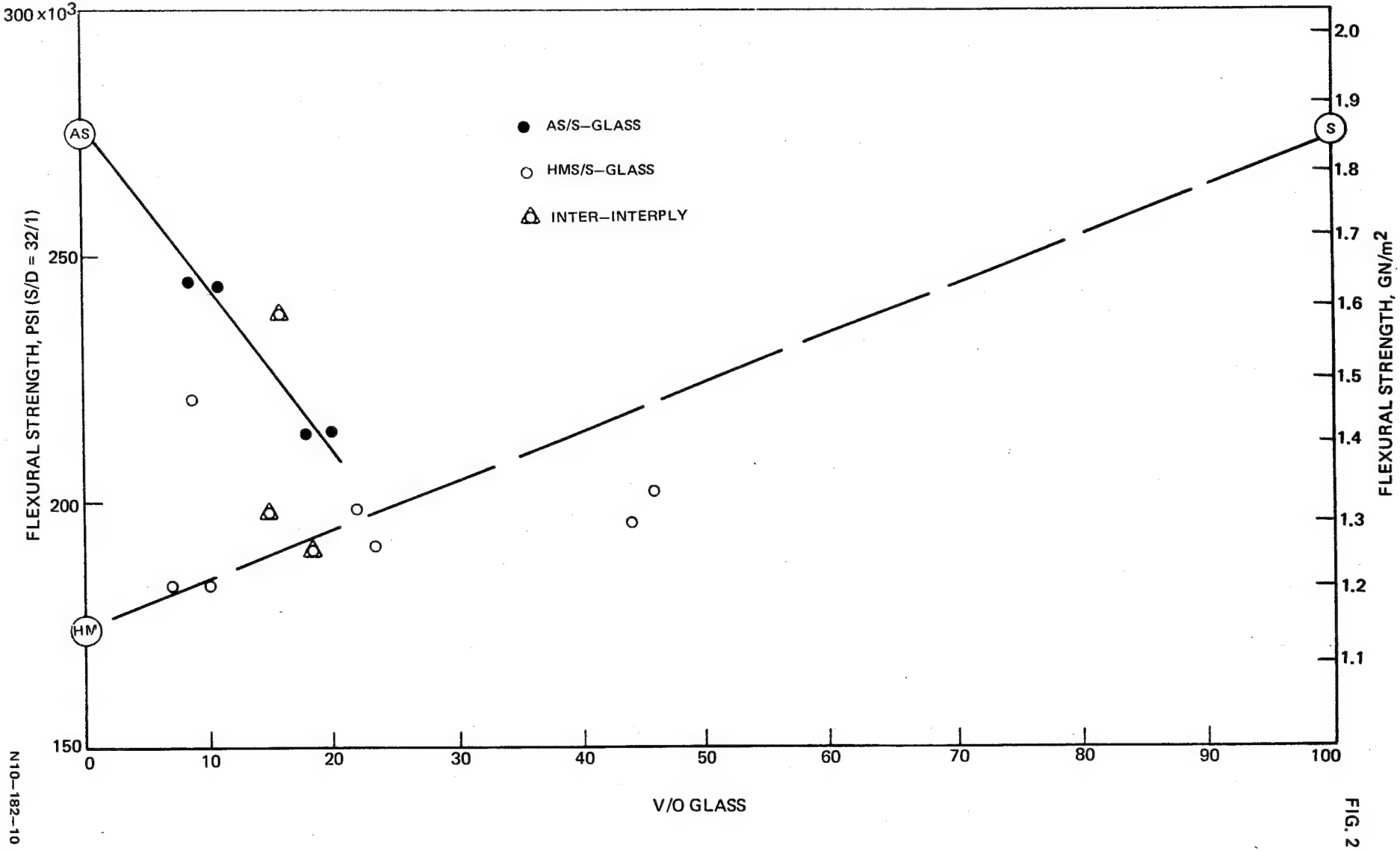

N10–182–10

FIG. 2

FIG. 3

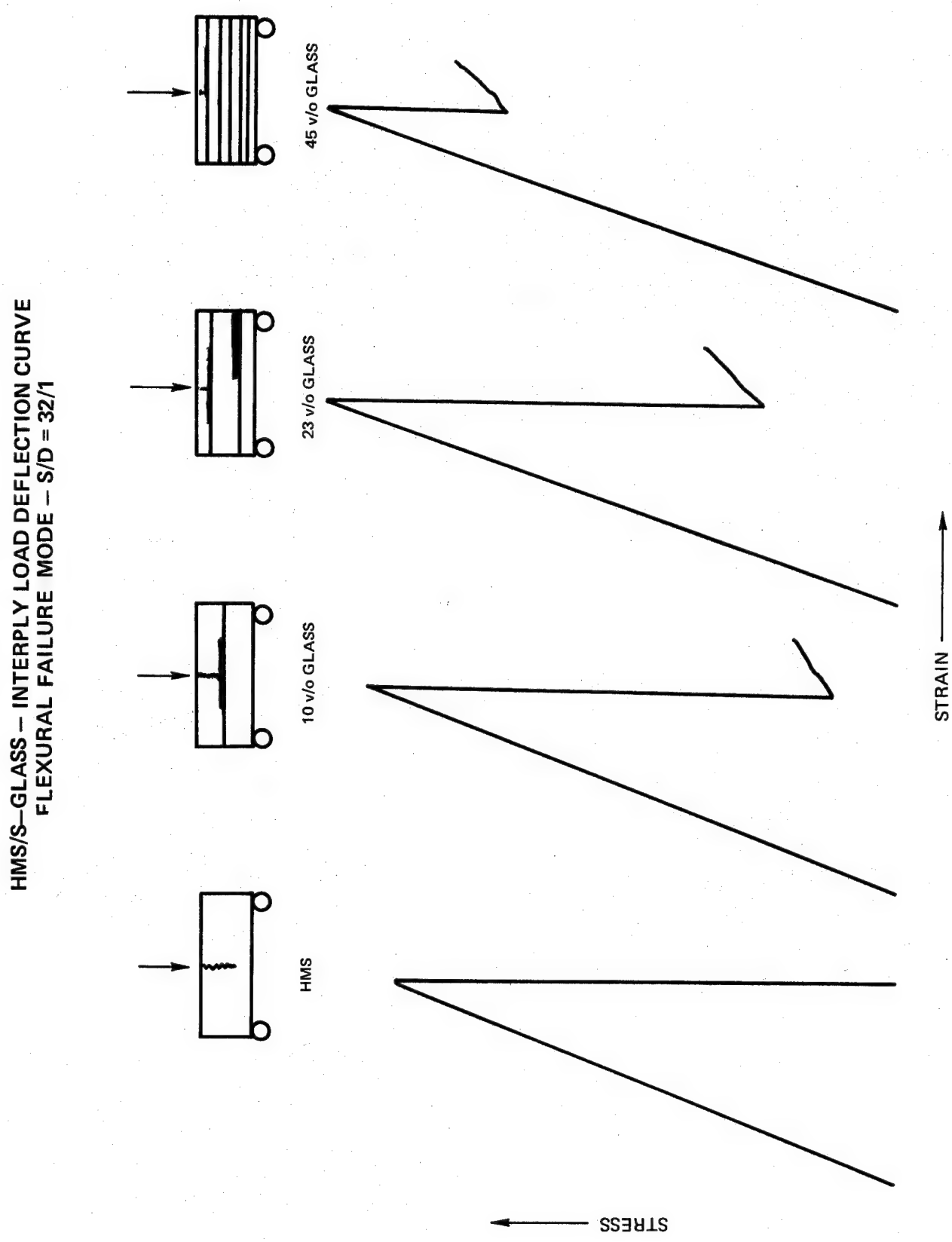
HMS/S–GLASS – INTERPLY LOAD DEFLECTION CURVE
FLEXURAL FAILURE MODE – S/D = 32/1
HMS
10 v/o GLASS
23 v/o GLASS
45 v/o GLASS
STRESS
STRAIN
N10–182–1

FIG. 4

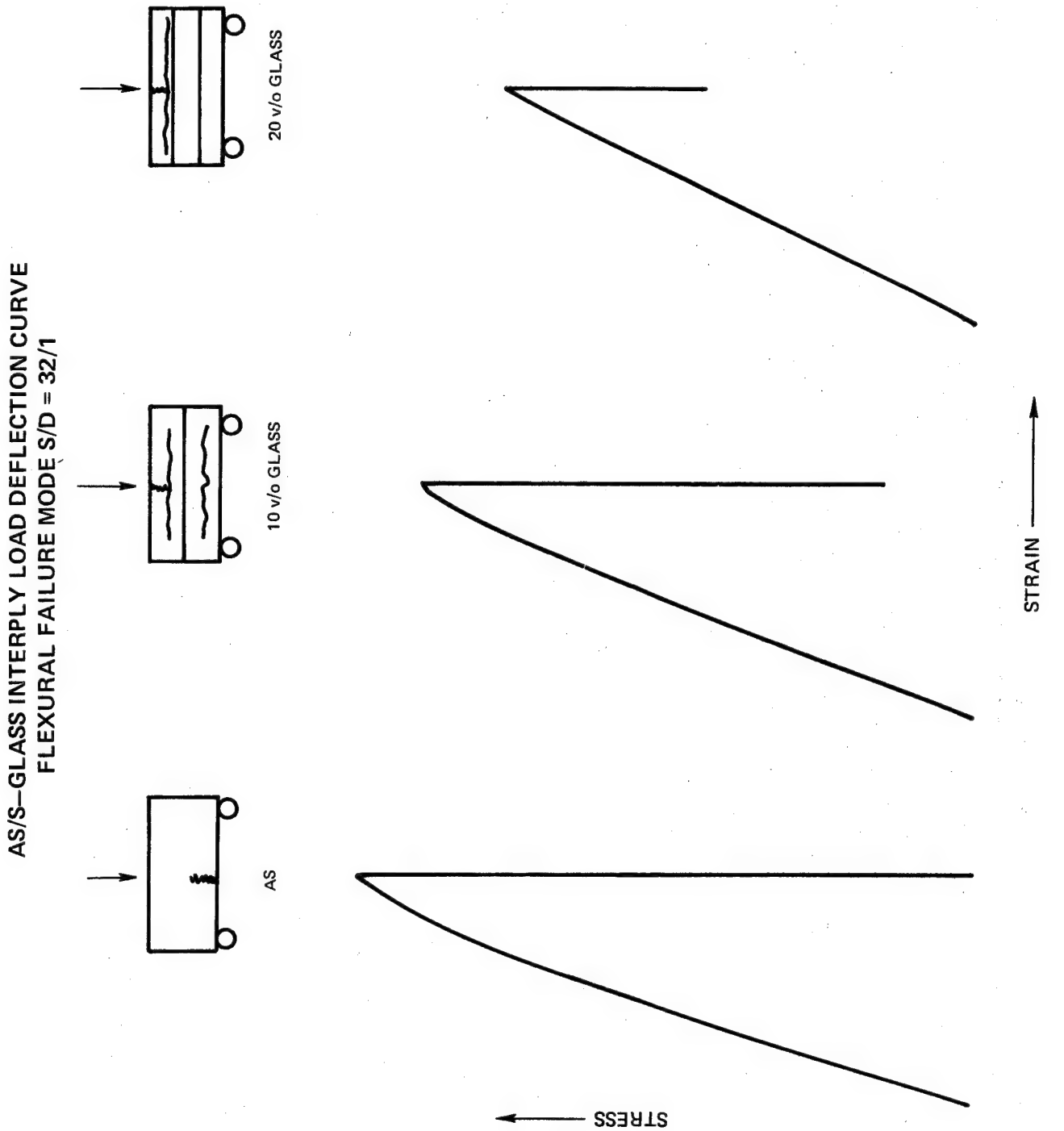

N10–182–2

The decrease in strength with increasing glass content is related to the dilution of graphite filaments with equivalent strength but lower modulus glass filaments in the area of high tensile or compressive stress. Due to the higher modulus of the AS graphite which carries a greater proportion of the load, the lower the graphite fiber content the lower will be the load carrying capability.

The effect of core-shell and intraply construction on flexural strength for the AS and HMS S-glass systems is shown in Fig. 5. As with the interply construction there are minor changes in strength from the rule-of-mixtures prediction in the HMS/S-glass hybrids in either the core-shell or intraply types below 30 v/o glass content. Above this level both types fall below the predicted strength although not below that of homogeneous HMS. Failure in both constructions is compression. The flexural strength of the AS/S-glass core-shell laminates decreases with increasing glass content as did the interply type. However, the intraply flexural strengths did not drop relative to the homogeneous AS laminate. The core-shell composites failed in compression or tension similar to the interply failures, while the intraply exhibited tensile failure in the graphite tows.

The combined inter/intra systems, Types 7 and 9, resulted in composite properties intermediate between the two separate types. No strength advantage was found in using the combined form. However, the ability to tailor specific impact properties at a given level by altering ply construction alone may be of use in design requirements for particular applications.

The flexural strengths of the HMS/Kevlar 49 composites decreased with increased hybrid fiber content irrespective of ply construction as illustrated in Fig. 6. Failures in all cases were of the compressive-shear type. This apparently reflects the poor compressive strength of Kevlar 49 relative to S-glass.

The AS/Kevlar 49 system, Fig. 7, behaved similarly with the exception of the intraply tow-by-tow construction. In this case flexural strengths were essentially equivalent to homogeneous AS as were the intraply AS/S-glass laminates. Failure occurred in tension, compression or both depending upon Kevlar 49 content similar to the glass systems.

Hybrid composite modulus changes with increasing S-glass or Kevlar 49 content were as predicted with one exception. Comparing the HMS hybrids, Figs. 8-10, the data show a decreasing modulus with increasing hybrid content with both S-glass or Kevlar 49 irrespective of ply construction. This would be expected since the moduli of Kevlar 49 and S-glass (20×10^6 psi and 12.5×10^6 psi respectively) are much lower than that of HMS (55×10^6 psi). In general, the core-shell configurations showed the greatest decrease in flexural modulus since the outer shell contained the low modulus hybridizing fiber. If that arrangement was reversed and the shell was reinforced with the high modulus fiber, the composite bending modulus would be much less affected by the addition of hybrid fiber to the inner core. This behavior is in contrast to what would be expected under axial loading where moduli would be relatively insensitive to the position of the fibers within the laminate. The interply and intraply configurations did not differ greatly in their effect on bending modulus.

FLEXURAL STRENGTH VS V/O HYBRID

AS/S–GLASS HMS/S–GLASS CORE–SHELL AND INTRAPLY COMPOSITES

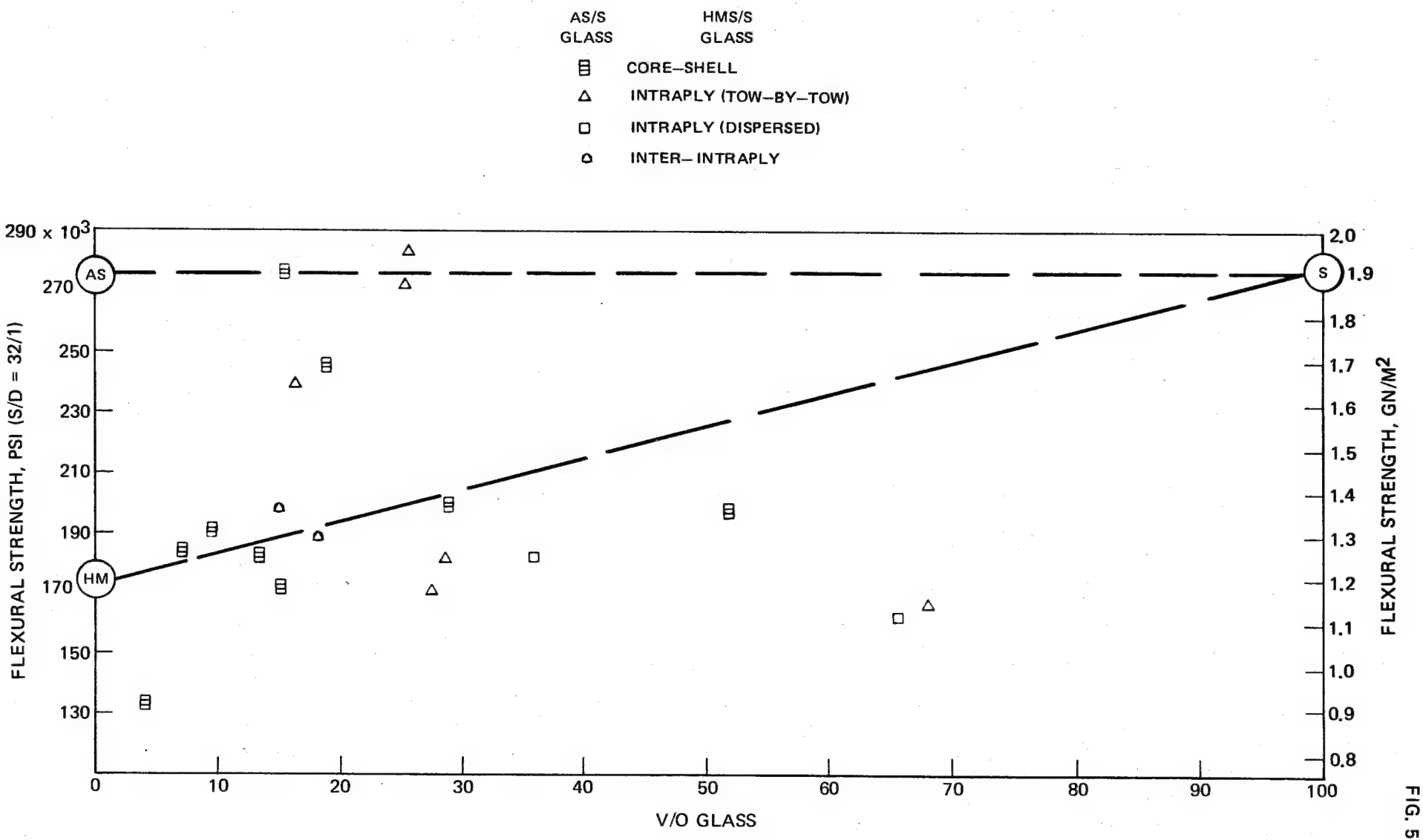

FIG. 5

FLEXURAL STRENGTH VS V/O HYBRID
HMS – KEVLAR 49 COMPOSITES

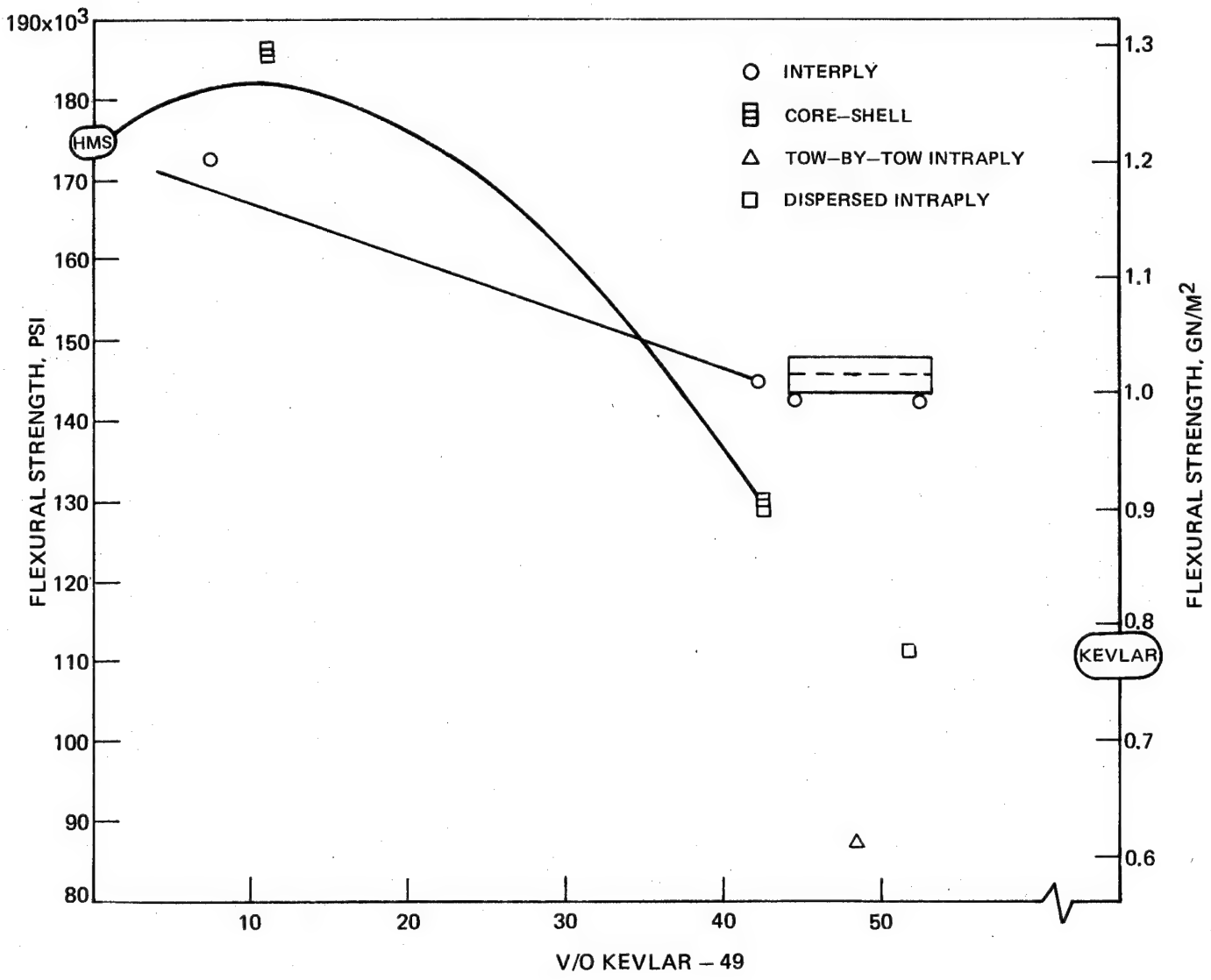

N10–326–10

FIG. 7

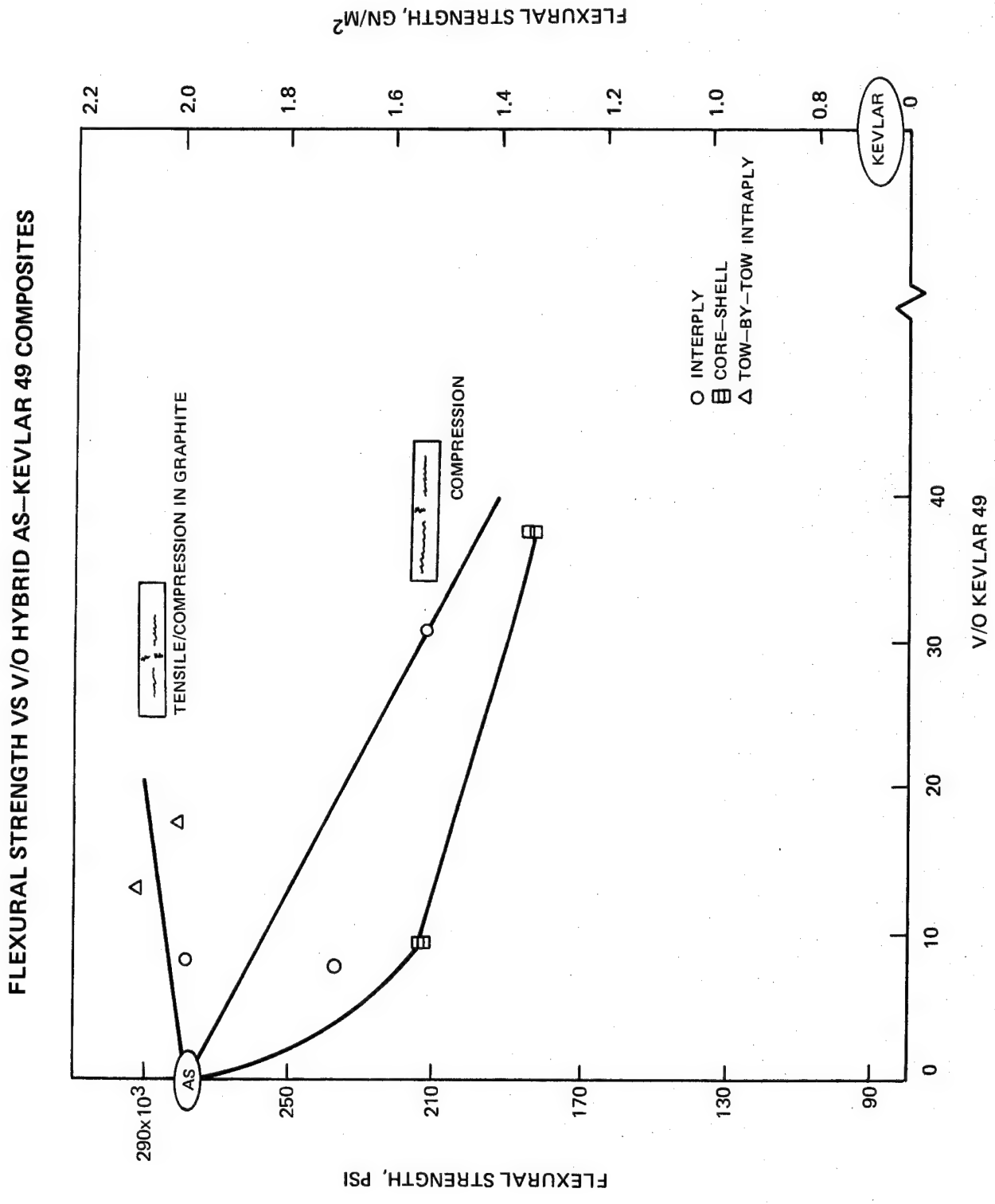
FLEXURAL STRENGTH VS V/O HYBRID AS–KEVLAR 49 COMPOSITES
FLEXURAL STRENGTH, PSI
FLEXURAL STRENGTH, GN/M2
290x10^3
250
210
170
130
90
2.2
2.0
1.8
1.6
1.4
1.2
1.0
0.8
AS
KEVLAR
0
10
20
30
40
V/O KEVLAR 49
TENSILE/COMPRESSION IN GRAPHITE
COMPRESSION
O INTERPLY
CORE–SHELL
Δ TOW–BY–TOW INTRAPLY

N11–8–5

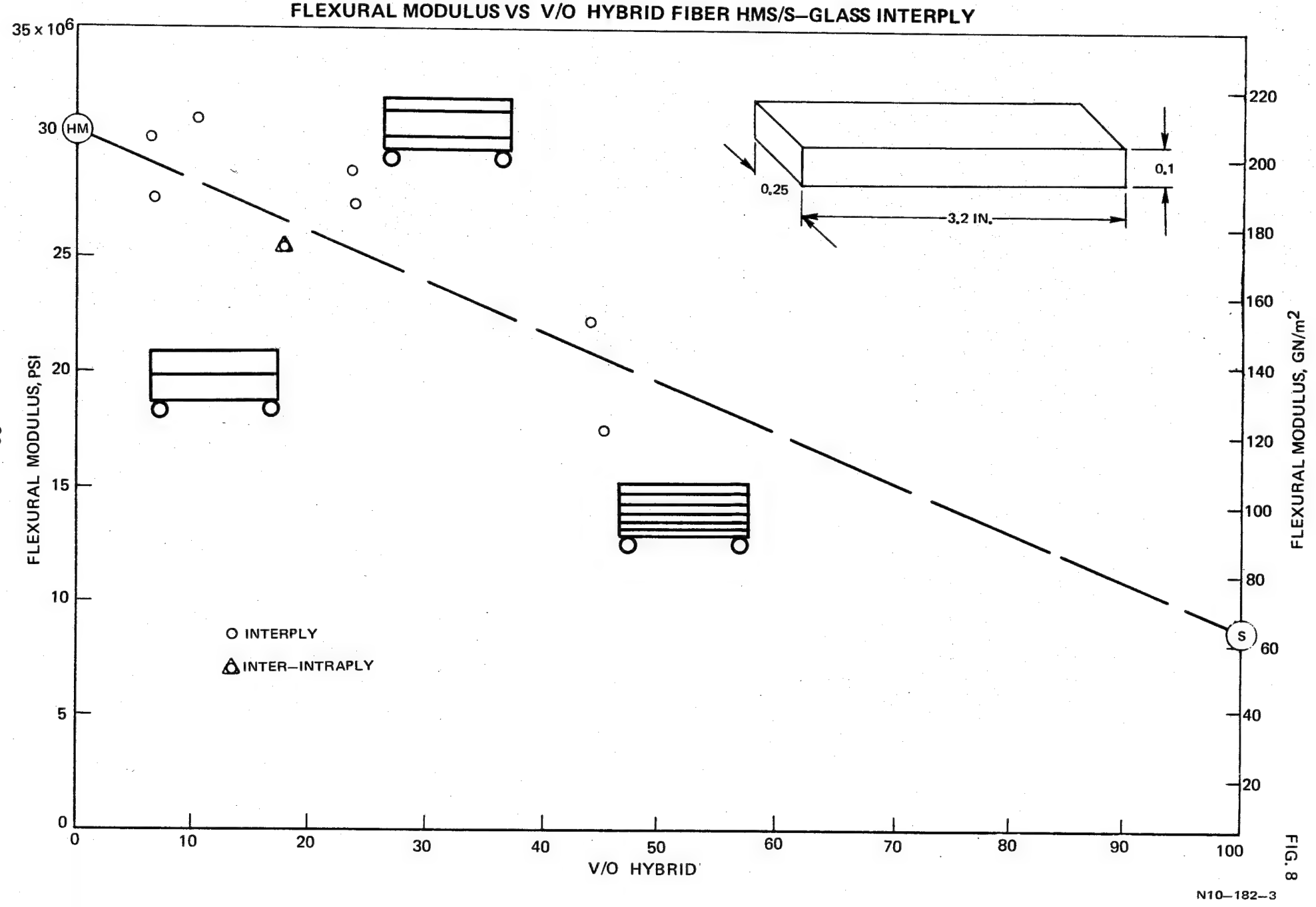
FLEXURAL MODULUS VS V/O HYBRID FIBER HMS/S–GLASS INTERPLY
35 x 10^6
30
25
20
15
10
5
0
HM
S
FLEXURAL MODULUS, PSI
FLEXURAL MODULUS, GN/m^2
220
200
180
160
140
120
100
80
60
40
20
0
10
20
30
40
50
60
70
80
90
100
V/O HYBRID
O INTERPLY
INTER–INTRAPLY
0.25
0.1
3.2 IN.
N10–182–3

FIG. 8

FLEXURAL MODULUS VS V/O HYBRID FIBER HMS/S–GLASS
CORE–SHELL AND INTRAPLY COMPOSITES

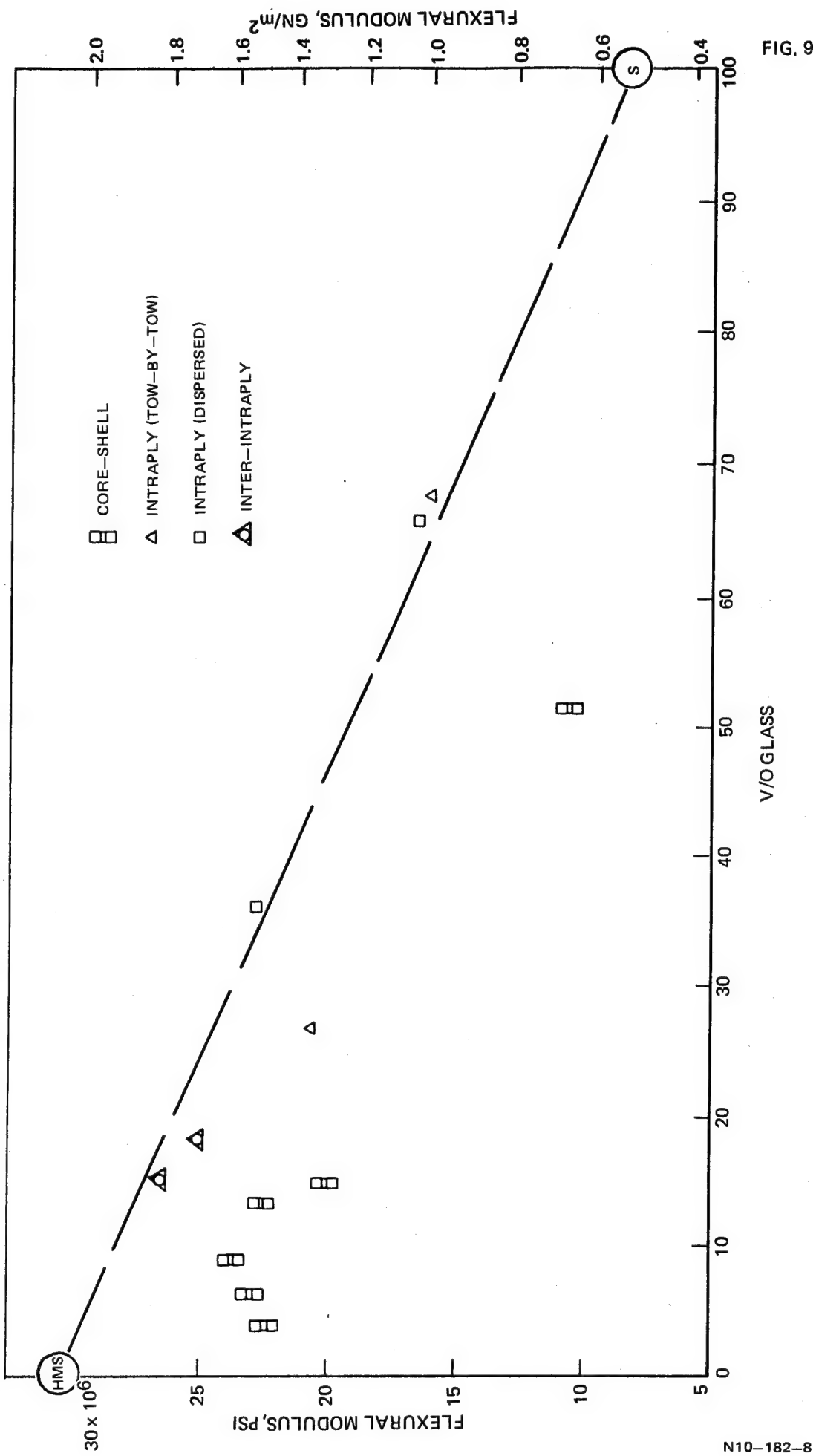

FIG. 9

N10–182–8

FIG. 10

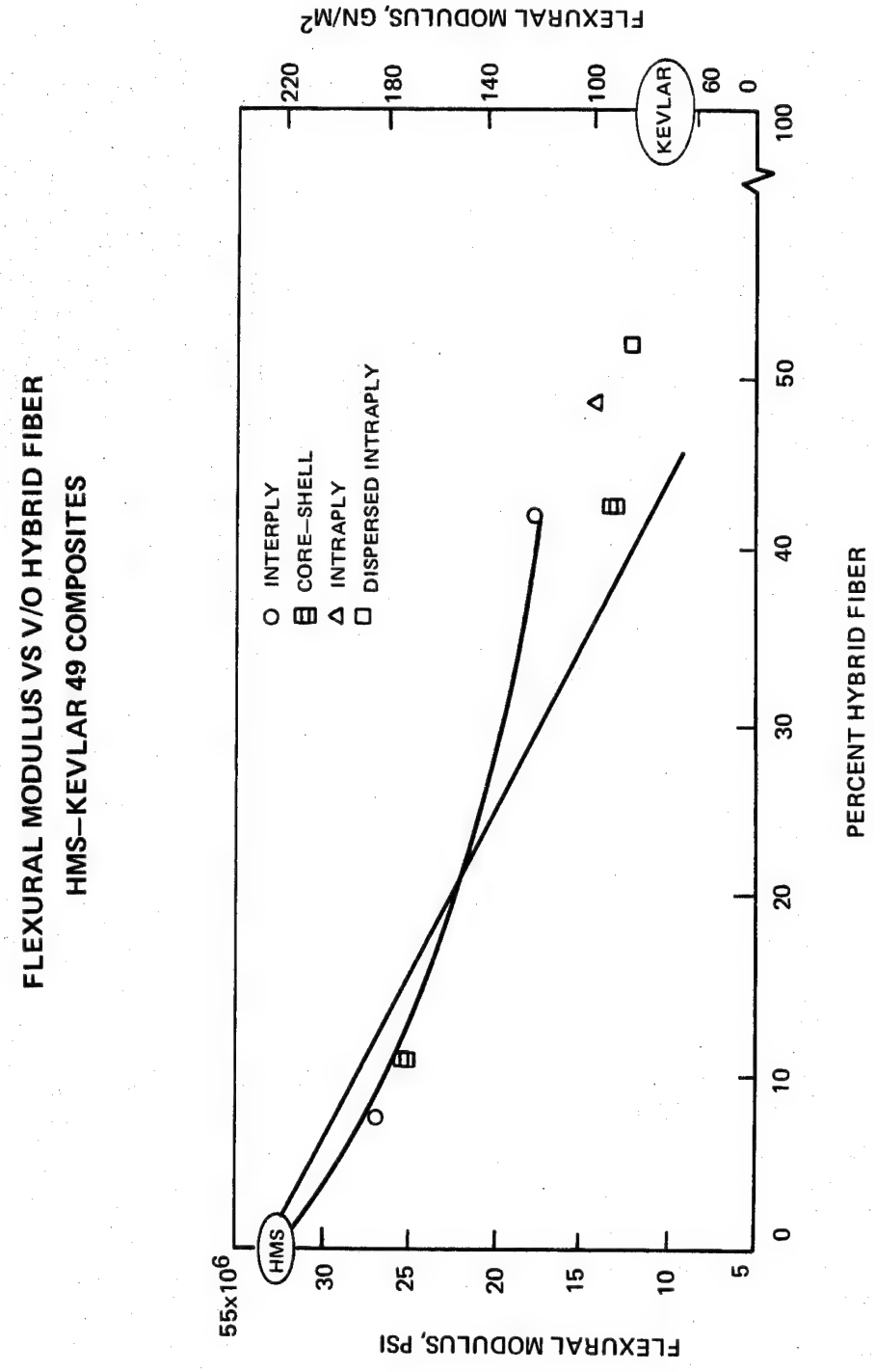
FLEXURAL MODULUS VS V/O HYBRID FIBER
HMS–KEVLAR 49 COMPOSITES
FLEXURAL MODULUS, PSI
55x10^6
30
25
20
15
10
5
HMS
0
10
20
30
40
50
100
KEVLAR
0
60
100
140
180
220
FLEXURAL MODULUS, GN/M^2
PERCENT HYBRID FIBER
INTERPLY
CORE–SHELL
INTRAPLY
DISPERSED INTRAPLY

N11–8–3

The AS hybridized laminate response shown in Figs. 11-13 was somewhat different; modulus again decreased with increasing S-glass or Kevlar 49 content with the exception of the intraply (tow-by-tow) construction. It has also been shown in other government sponsored programs that moduli of AU or T-300 graphite S-glass composites do not drop in the intraply construction up to 25 v/o S-glass. This was true for both secondary fibers. As with the HMS hybrids the core-shell configurations decreased in modulus most rapidly. The interply AS S-glass or Kevlar 49 composites gave little modulus change up to 10 v/o hybrid fiber compared to homogeneous AS. Above this level, rule-of-mixture moduli were obtained.

It is interesting to note that with the AS/S-glass combination whose fiber moduli ratio is approximately 3/1, no change in modulus in the intraply construction was found while the HMS/Kevlar 49 system with a similar moduli ratio shows a rapid decrease in composite modulus in the same configuration.

As expected, because of the high glass contents, none of the T-75/S-glass systems, Types 8 and 10 , Table V, achieved the minimum modulus limit of 131 GN/m^2 (19 x 10^6 psi). It is believed that addition of sufficient T-75 fiber to meet the modulus requirement would undoubtedly result in Charpy impact strengths in the same range or possibly lower than comparable HMS/S-glass systems.

The combined inter/intraply systems, Types 7 and 9, resulted in composite properties intermediate between the two separate types. No strength advantage was found in using the combined form. However, the ability to tailor specific impact properties at a given level by altering ply construction alone may be of use in design requirements for particular applications.

With few exceptions during testing in flexure, shear failure accompanied the tensile of compressive failure in all of the hybrid laminates regardless of ply construction. Interlaminar shear strength tests at a span-to-depth ratio of 4/1 resulted in shear failure in all cases.

With the HMS/S-glass interply laminates no appreciable change in shear strength compared to homogeneous HMS, as seen in Fig. 14, with the possible exception of 10 v/o glass composites were noted. There does appear to be a slight effect on shear related to the position of the glass interply layer relative to the area of high shear stress. This probably accounts for the somewhat lower shear strength in the 10 v/o glass laminates since the glass layer is in the center of the composite. However, the 50 v/o HMS/S-glass laminate which would also have a graphite/glass interface in the center of the composite gave shear values slightly lower than the 25 v/o type, as would be predicted, but higher than the 10 v/o glass systems. The shear strengths of the HMS/S-glass core-shell laminates, Fig. 15, showed a slight increase with increasing glass content.

FLEXURAL MODULUS VS V/O FIBER
AS/S–GLASS – INTERPLY

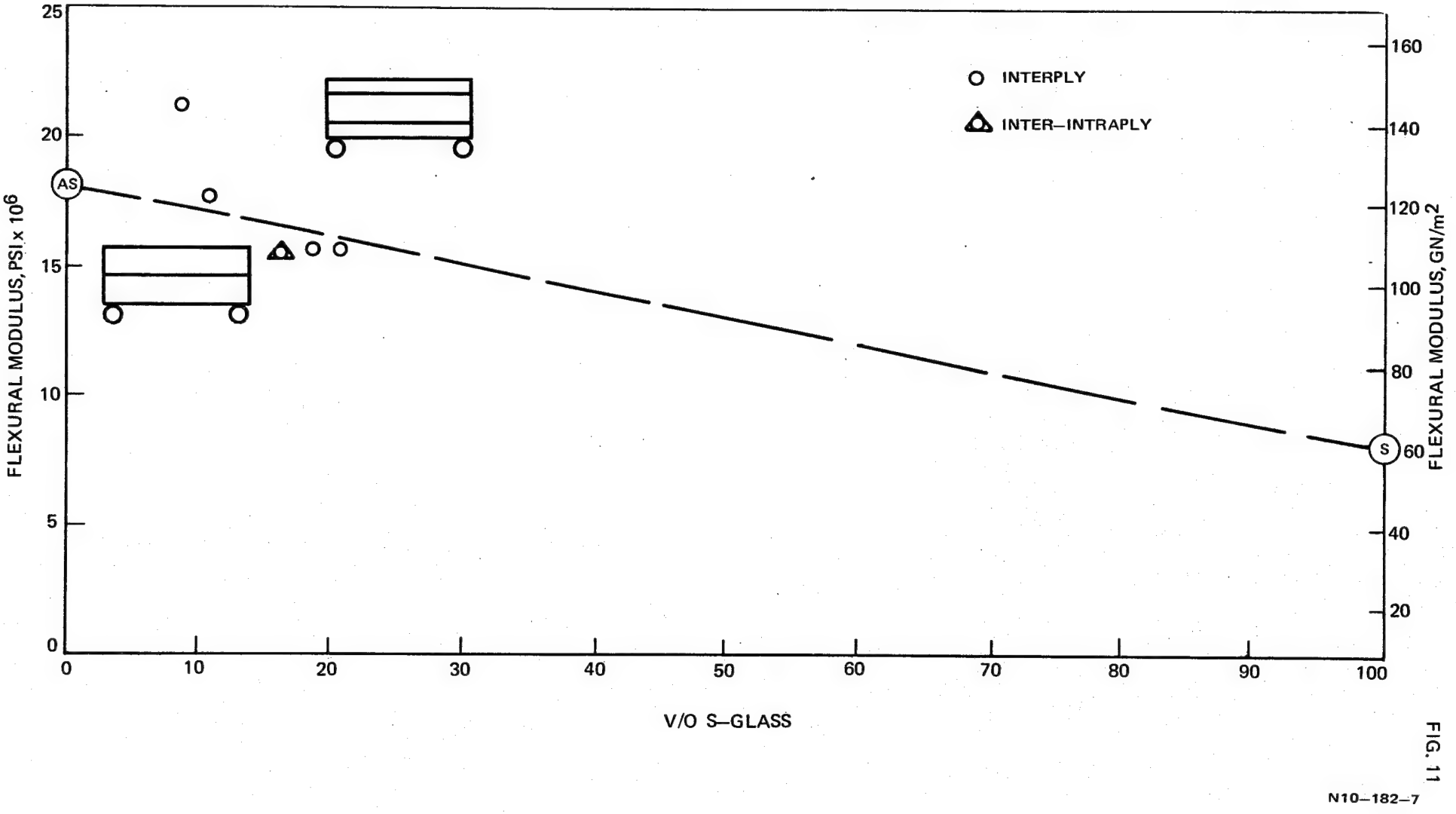

FIG. 11

N10–182–7

FLEXURAL MODULUS VS V/O HYBRID FIBER
AS/S–GLASS CORE–SHELL AND INTRAPLY COMPOSITES

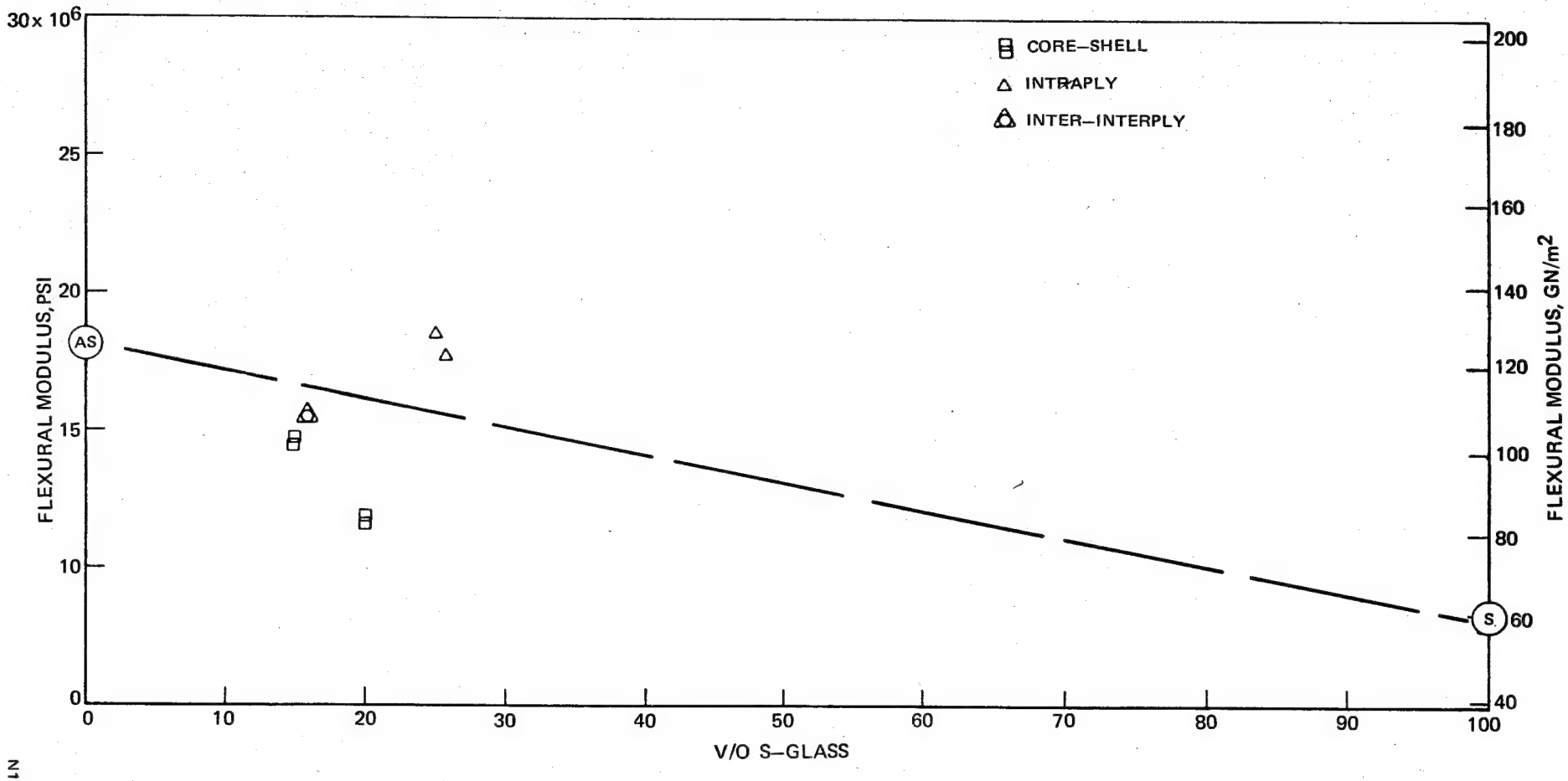

N10–182–4

FIG. 12

FIG. 13

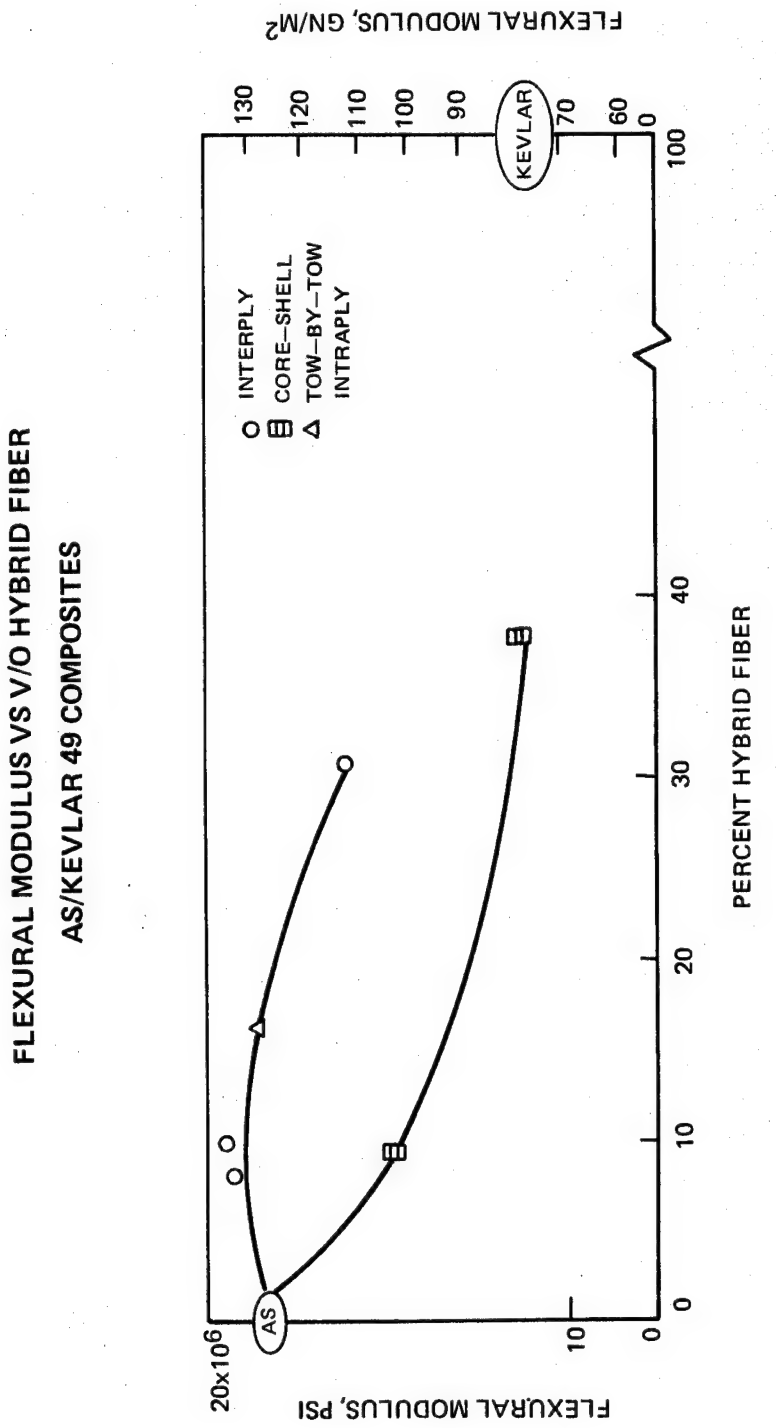
FLEXURAL MODULUS VS V/O HYBRID FIBER
AS/KEVLAR 49 COMPOSITES
FLEXURAL MODULUS, GN/M²
FLEXURAL MODULUS, PSI
PERCENT HYBRID FIBER
INTERPLY
CORE–SHELL
TOW–BY–TOW
INTRAPLY
AS
KEVLAR
20x10⁶
10
0
130
120
110
100
90
70
60
0
100
40
30
20
10
0

N11–8–1

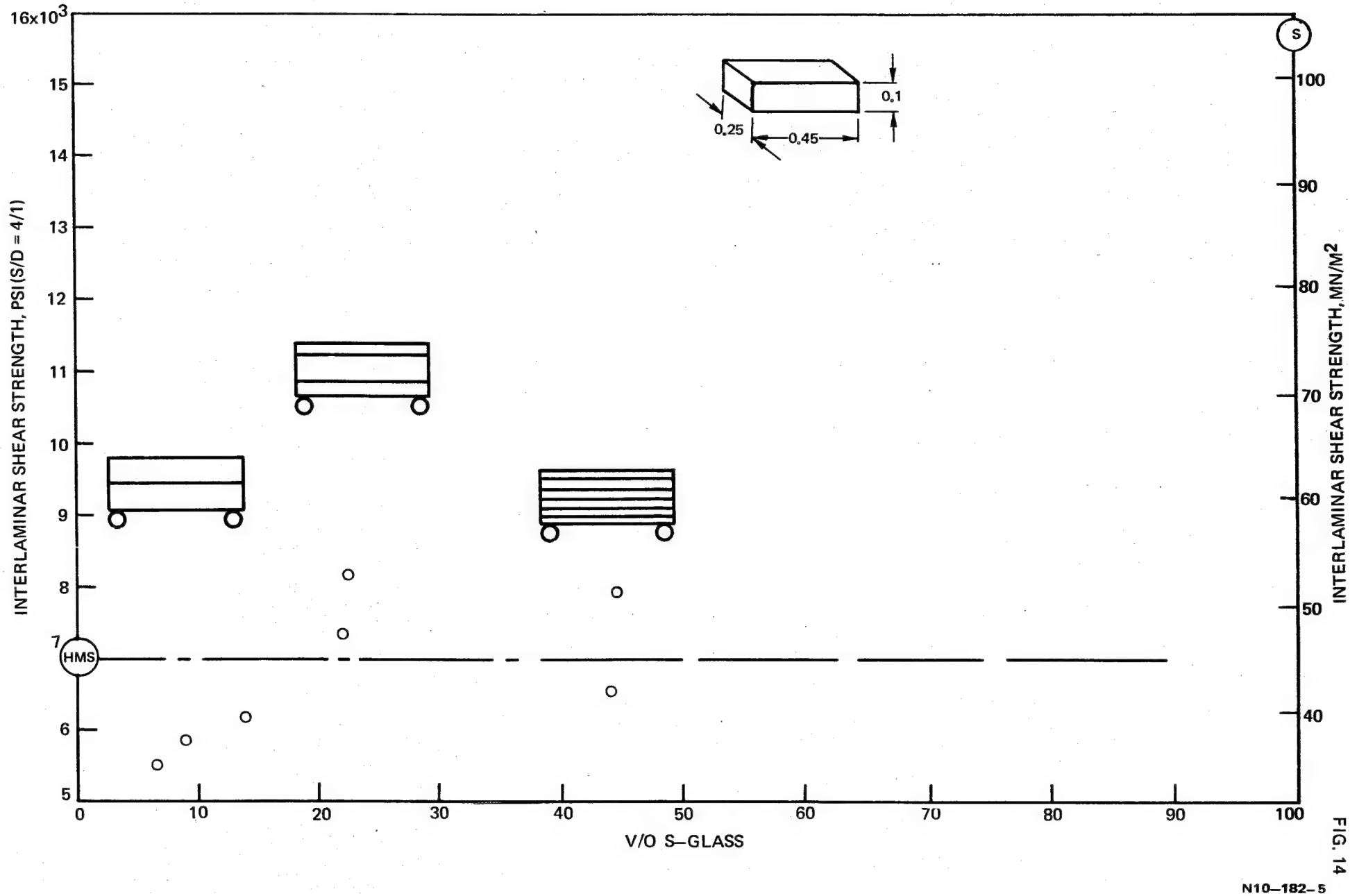
HMS/S–GLASS INTERPLY SHEAR STRENGTH VS V/O FIBER
16x10^3
15
14
13
12
11
10
9
8
7
6
5
HMS
S
100
90
80
70
60
50
40
0.1
0.25
0.45
INTERLAMINAR SHEAR STRENGTH, PSI(S/D = 4/1)
INTERLAMINAR SHEAR STRENGTH, MN/M2
0
10
20
30
40
50
60
70
80
90
100
V/O S–GLASS
N10–182–5

FIG. 14

SHEAR STRENGTH VS V/O HYBRID FIBER
HMS/S–GLASS CORE–SHELL, AND INTRAPLY

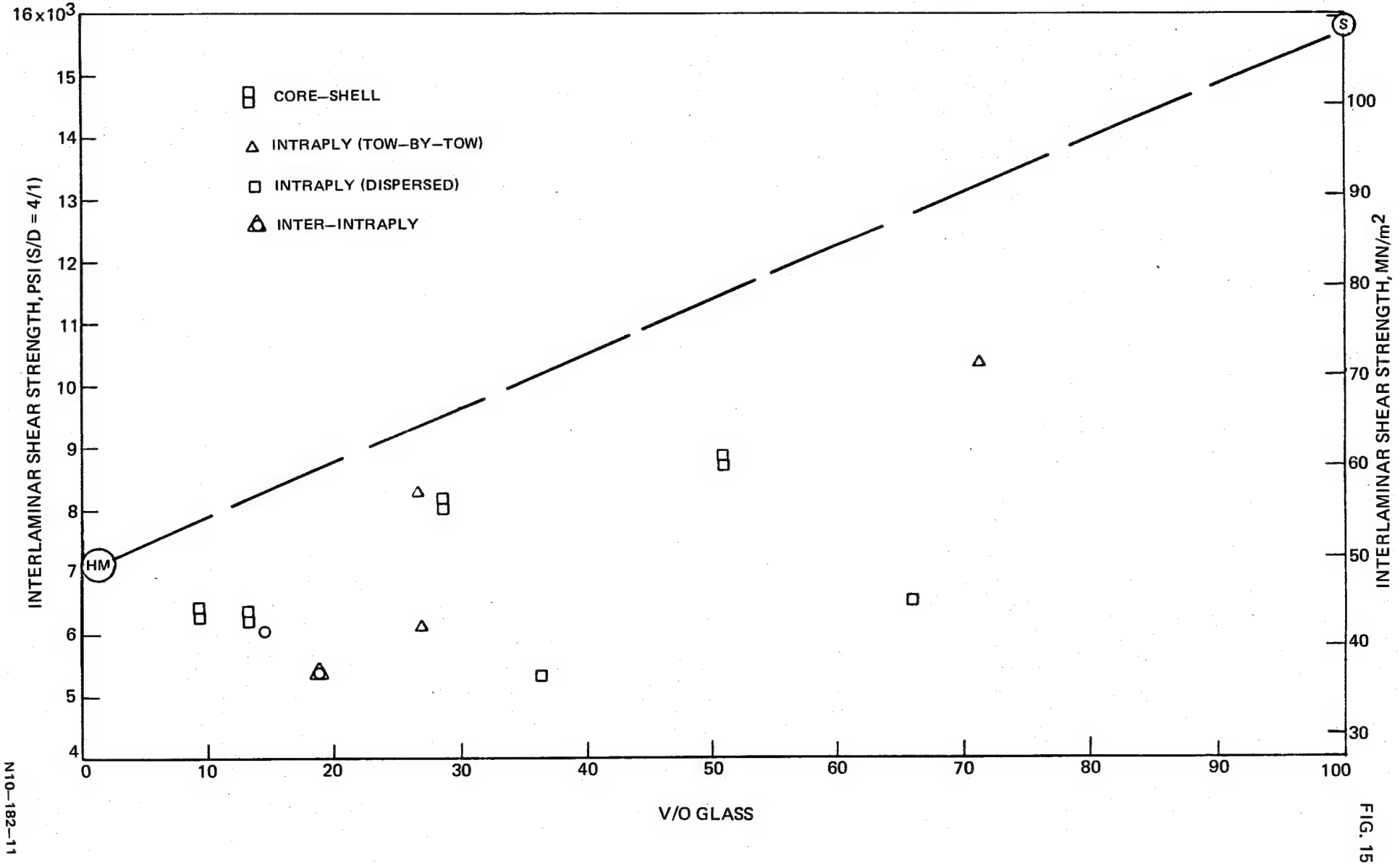

N10–182–11

FIG. 15

All the interply and core-shell AS/S-glass composites gave a decrease in shear strength relative to homogeneous AS with little effect of glass content noted. The core-shell construction had, in general, slightly lower strengths than the corresponding interply type. The intraply (tow-by-tow) composites, however, gave shear strengths equivalent to homogeneous AS as did the inter-intraply laminate, Type 7. Incorporation of HMS graphite or Kevlar 49 into the AS/S-glass system resulted in lower shear strengths relative to the primary AS fiber. These data are shown in Fig. 16.

The low shear strength of homogeneous Kevlar 49 in most instances resulted in shear strengths in all HMS composites somewhere between that of Kevlar 49 and homogeneous HMS irrespective of ply construction. The one exception was the interply laminate containing 7.5 v/o Kevlar 49. Sufficient data are not available at present to determine if such an improvement in shear strength is real.

All shear strengths of AS laminates hybridized with Kevlar 49 were lower than the homogeneous AS composite with the core-shell and intraply (tow-by-tow) type at 9-13 v/o Kevlar 49 concentration providing shear strengths in the 14,000 psi range. Repeat of the interply construction in Task II in this concentration range also resulted in shear strengths of this magnitude. In general, the shear strength of AS/Kevlar 49 laminates decreases with increasing secondary fiber content regardless of construction type.

2.2.2 Dynamic Properties - Analysis of Charpy Impact Data

The application of the instrumented Charpy pendulum impact test has made it possible to more fully characterize composite impact performance. Of particular importance are the loads sustained prior to initial fraction (P_i) and the maximum load prior to failure. For some load controlled applications this parameter could conceivably be more important than total energy absorption considerations. The energy which each multi-fiber type can absorb prior to maximum load or catastrophic failure is an important criterion for ranking of the hybrid composites.

In the following paragraphs the effects of hybrid construction on load capacity, impact absorption energies, the relationship of impact energy to composite flexural modulus as well as the effect of specimen thickness on Charpy impact performance are described.

AS/S–GLASS INTERPLY, INTRAPLY, CORE–SHELL SHEAR STRENGTH VS V/O HYBRID FIBER

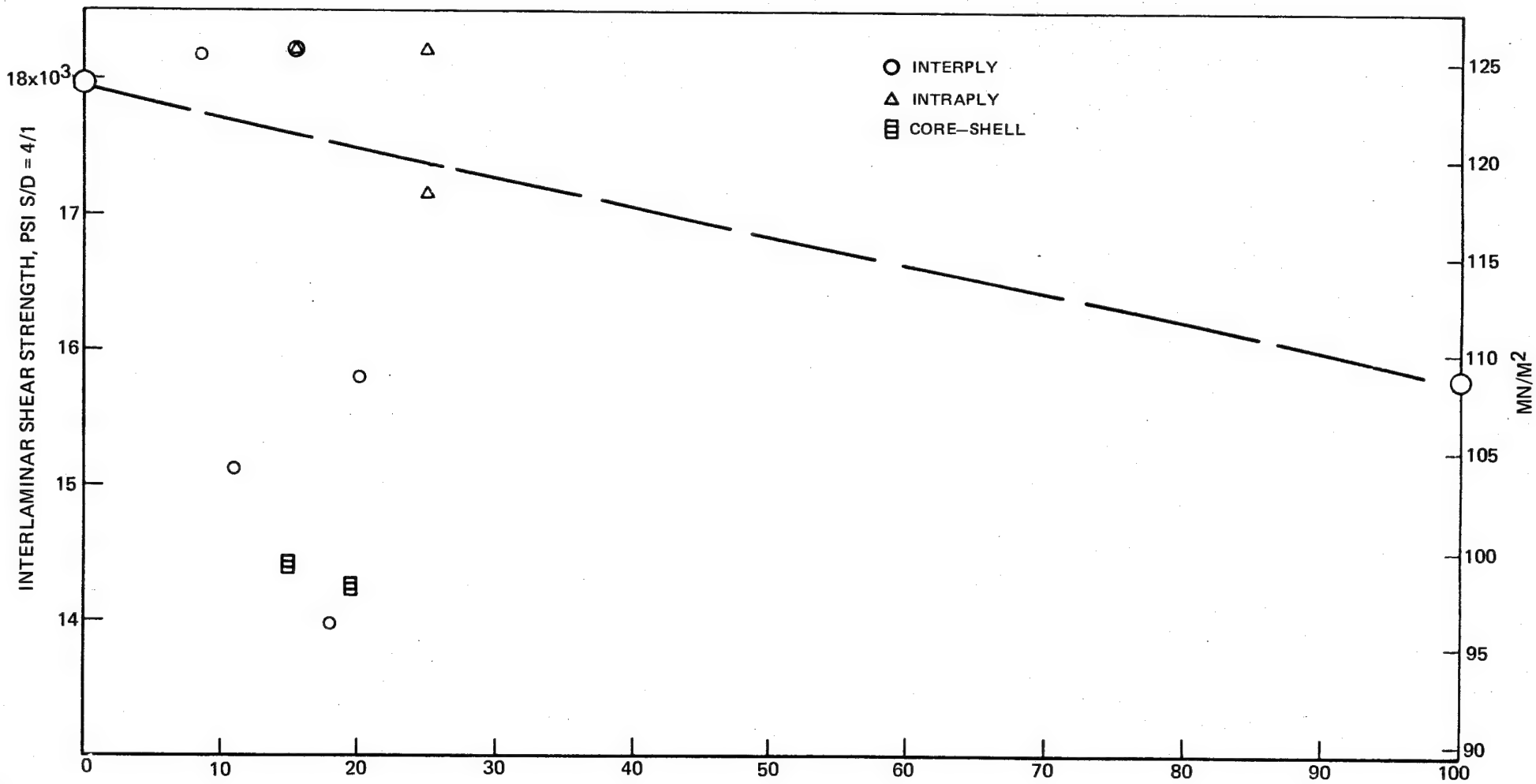

N10–182–12

FIG. 16

2.2.2.1 Load Capabilities

2.2.2.1.1 HMS/S-glass and T-75/S-glass Composites

The load at initial fracture of the intraply composites (Type 2) remains essentially constant for each composition type, even though the percentage of hybrid fiber varies over a large range (Table IV). This same phenomenon is also evident in the interply HMS/S-glass composites (Type 13) but not in the core/shell HMS/S-glass composites (Type 17). In the latter composites, P_i and P_{max} increase with increasing glass content. These data are listed in Table IX. The data for the standard HMS and S-glass composites are shown in Figs. 17 and 18.

It is hypothesized that the controlling factor in impact behavior of these hybrid composites is the interlaminar shear failure of the HMS graphite layers. This results in similar P_i loads for the Heltra intraply, interply, and standard HMS composites as listed in Tables IV and IX. However, the UARL intraply composites, because of ply construction, have no continuous layers of graphite; rather the graphite tows effectively line up at an angle to produce a graphite layer out of the plane of the interlaminar shear stress. This presumably would require a higher load to initiate and propagate failure (Fig. 1).

Identification of the P_i load in the core/shell type is difficult because of nonlinearity in the initial portion of the curves, thus initial fracture may occur at lower P_i's than indicated.

The P_{max} loads of the hybrid composites are apparently related to the thickness and ply construction of the segments formed after the initial delamination has occurred. Thicker sections containing higher percentages of glass are capable of sustaining higher loads. The interply composites (Type 13) appear to give anomalous results in this regard. The Charpy impact strength of the T-75/S-glass (side-by-side tow) composites reflect the high percentages of glass present and as expected with increasing T-75 content the impact strength decreases. There is little effect on P_i or P_{max} below a 20 v/o T-75 content. It is believed that addition of sufficient T-75 fiber to meet the modulus requirement would undoubtedly result in Charpy impact strengths in the same range or possibly lower than comparable HMS/S-glass systems.

No advantage was found in the combined inter/intra type construction (NAS-72, Type 9) over the interply (Type 13) system. This is presumably due to the fact that they both contain continuous HMS graphite layers which would result in similar total impact characteristics.

Table IX

Charpy Impact Loads of HMS/S-Glass and T-75/S-Glass Epoxy Laminates

UARL No. (Impact)	Composition Type	Fiber Ratio v/o (actual)	P_i Newtons	P_i (lbs)	P_{max} Newtons	P_{max} (lbs)	Charpy Impact Strength (experimental) Joules	Charpy Impact Strength (experimental) (ft-lbs)
NAS-15A	13	HMS-89.6 S-10.4	3110	(700)	5780	(1300)	22.4	(16)
NAS-10	13	HMS-76.4 S-23.6	2665	(600)	5560	(1250)	29.4	(21)
NAS-9	13	HMS-54.3 S-45.7	3110	(700)	5780	(1300)	35	(25)
NAS-24	17	HMS-86.7 S-13.3	1775	(400)	3770	(850)	12.6	(9)
NAS-16A	17	HMS-72 S-28	3110	(700)	5340	(1200)	23.8	(17)
NAS-18	17	HMS-48.7 S-51.3	5340	(1200)	11,100	(2500)	51	(36.5)
NAS-72	9	HMS-56 S-12.5	2490	(560)	2490	(560)	22.4	(16)
NAS-64	8	T-75-6.5 S-93.5	5340	(1200)	5780	(1300)	70	(50)
NAS-66	8	T-75-9 S-91	4900	(1100)	5340	(1200)	57.4	(41.0)
NAS-64A	10	T-75-15.1 S-84.9	5300	(1190)	5700	(1280)	63.6	(45.5)
NAS-66A	10	T-75-21.5 S-78.5	3560	(800)	3640	(280)	51.2	(36.5)
NAS-55	20a-1	HMS-85.2 S-14.8	2220	(500)	2440	(550)	25.2	(18)
NAS-54	20a-2	HMS-96.8 S-3.2	2220	(500)	3110	(700)	18.2	(13)
NAS-58	20a-3	HMS- S-	3330	(750)	4000	(900)	15.4	(11)
NAS-63		HMS-63	2890	(600)	3550	(800)	16.8	(12)
NAS-66		S-66	10,000	(2250)	10,450	(2350)	72.7	(52)

P_i = load at point of initial fracture
P_{max} = maximum load attained

INSTRUMENTED CHARPY LOAD–TIME TRACE

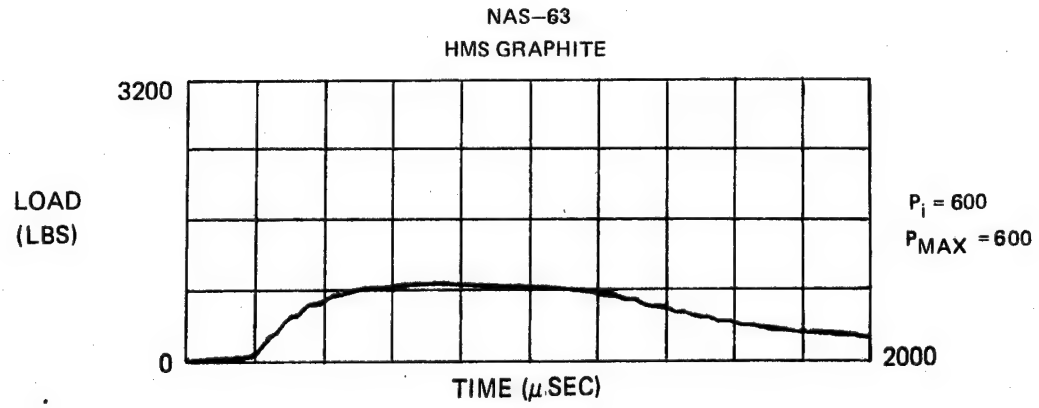

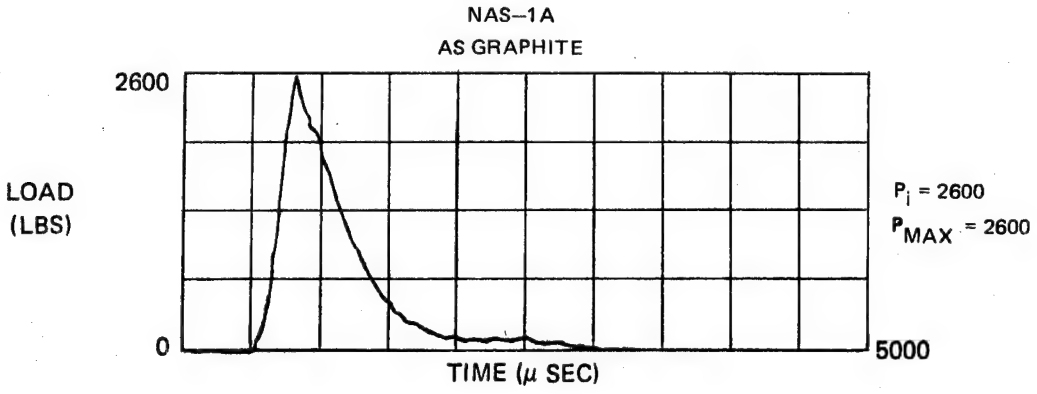

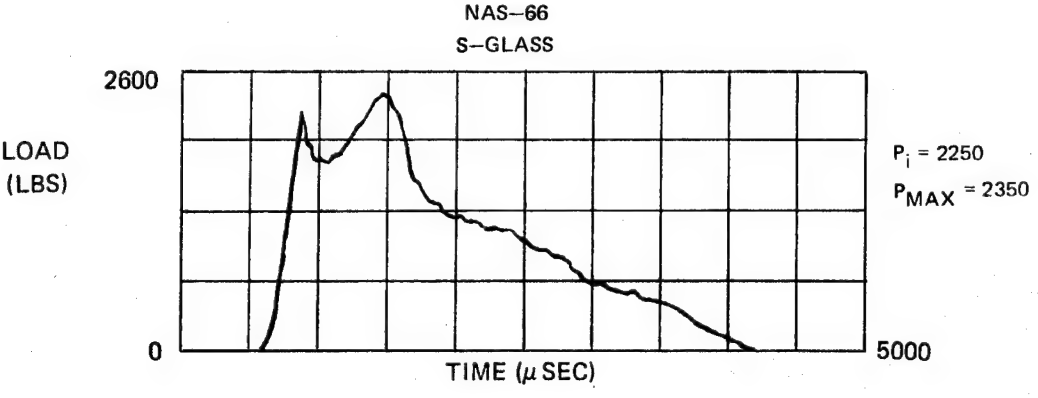

N10–310–6

FIG. 18

IMPACTED COMPOSITE SPECIMENS

NAS–63

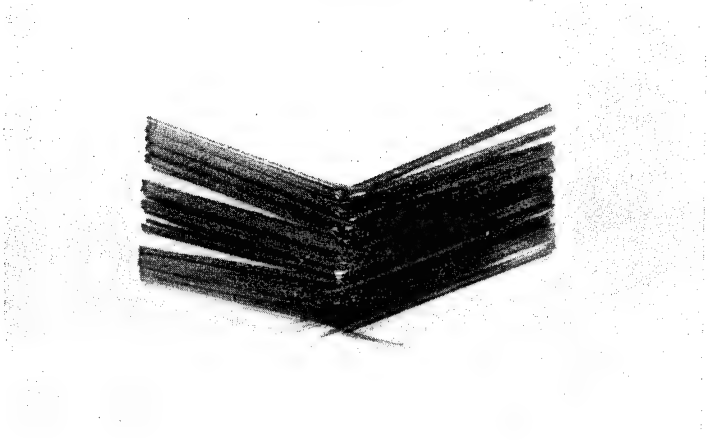

NAS–1A

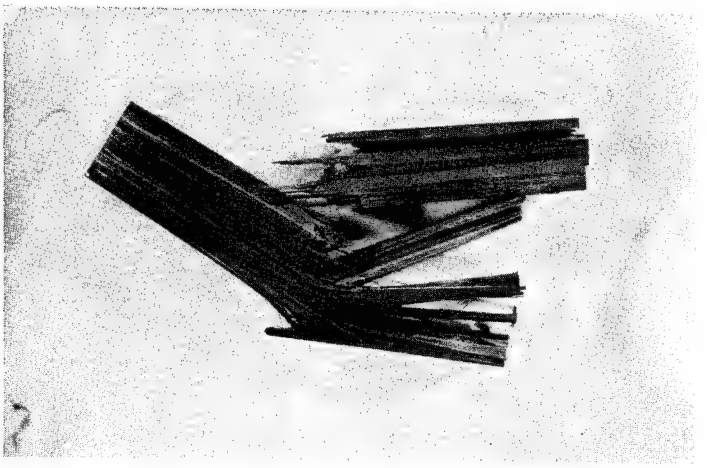

NAS–66

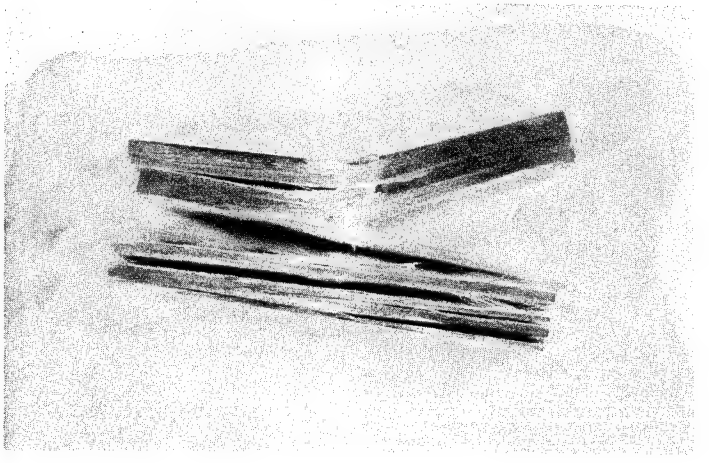

2.2.2.1.2 HMS/Kevlar 49 Composites

As previously discussed in section 2.1.2, the impact strengths and loads of HMS/Kevlar intraply composites show little change with varying secondary fiber content. The interply construction did produce higher P_{max} loads, the same as with the tow-by-tow intraply type with no improvement in total impact, Table X. As with the HMS/S-glass systems the controlling factor in impact behavior of these hybrid composites appears to be the interlaminar shear failure of the HMS graphite layers.

The load-time curve and impact specimen of the Kevlar 49 composite are shown in Figs. 19 and 20.

2.2.2.1.3 AS/S-Glass Composites

A distinct difference in the P_i loads of the interply (Type 11) and core/shell (Type 15) AS/glass systems was found, Table XI. In the former case the P_i load increases with increasing glass content while in the latter, P_i load decreases with increasing glass. This effect appears to be related to the position of the AS/S-glass interface relative to the plane of maximum shear stress through the center of the composite. That is, the nearer the center the lower will be P_i. The interply, 10 v/o glass, system is made by stacking $(AS)_4S(AS)_4$ segments having the interface at the center, while the interply 20 v/o glass composite has an $(AS)_2S(AS)_4S(AS)_2$ sequence with only graphite plys at the center. In the core/shell type the thicker the shell the nearer the interface is to the composite center giving a lower P_i. The 19a type composites having the AS/glass shell and HMS center behave in the same manner as the interply systems, i.e. P_i increasing with glass content and are very similar to NAS-24 and -16A, the core/shell HMS/S composites (Type 17, Table IX), which show increasing P_i and P_{max} with increasing glass content.

The P_{max} of all the systems increases as glass content increases. As with the HMS/S-glass composites this is apparently related to the thickness and ply construction of the segments formed after the initial delamination has occurred. The thicker sections which contain higher glass contents are capable of sustaining higher loads.

The composite properties demonstrated by the intraply (tow-by-tow) Type 1 composite, NAS-76, make this AS/S-glass system a prime candidate for further study if the modulus requirement could be met. The Charpy impact strength and load capability was the highest of any AS/S-glass system. The fracture pattern of the impacted composite had the out-of-plane shear fracture paths typical of the tow-by-tow type construction. The load-time trace and impacted specimen are shown in Figs. 21 and 22.

Table X

Charpy Impact Loads of HMS/PRD-49-III Epoxy Laminates

UARL No.	Composition Type	Fiber Ratio v/o (actual)	P_i Newtons	P_i (lbs)	P_{max} Newtons	P_{max} (lbs)	Charpy Impact Strength (experimental) Joules	Charpy Impact Strength (experimental) (ft-lbs)
NAS-12A	14	HMS-92.5 PRD-7.5	3340	(750)	5780	(1300)	15.4	(11)
NAS-11A	14	HMS-58.2 PRD-41.8	3780	(850)	5780	(1300)	18.9	(13.5)
NAS-28	18	HMS-89.1 PRD-10.9	1780	(400)	3780	(850)	13.65	(9.75)
NAS-18	18	HMS-57.7 PRD-42.3	2220	(500)	2670	(600)	20	(14.25)
NAS-63		HMS	2670	(600)	3560	(800)	16.8	(12)
NAS-5A		PRD-49	3160	(710)	3760	(845)	35	(25)

INSTRUMENTED CHARPY LOAD–TIME TRACE

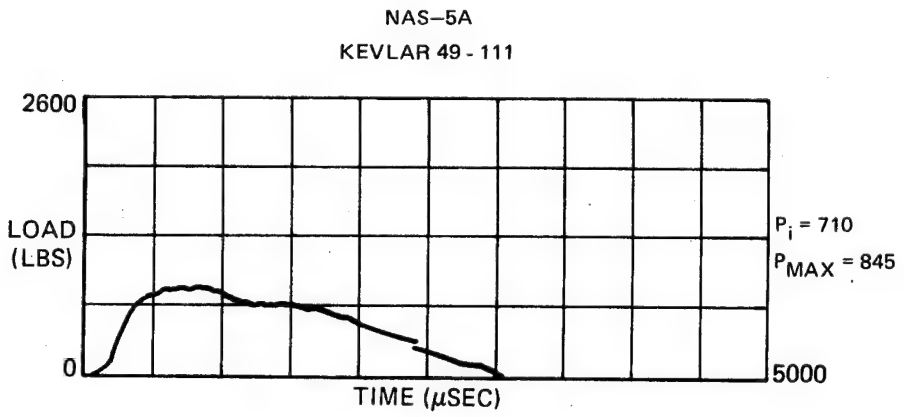

IMPACTED COMPOSITE SPECIMENS

NAS–5A

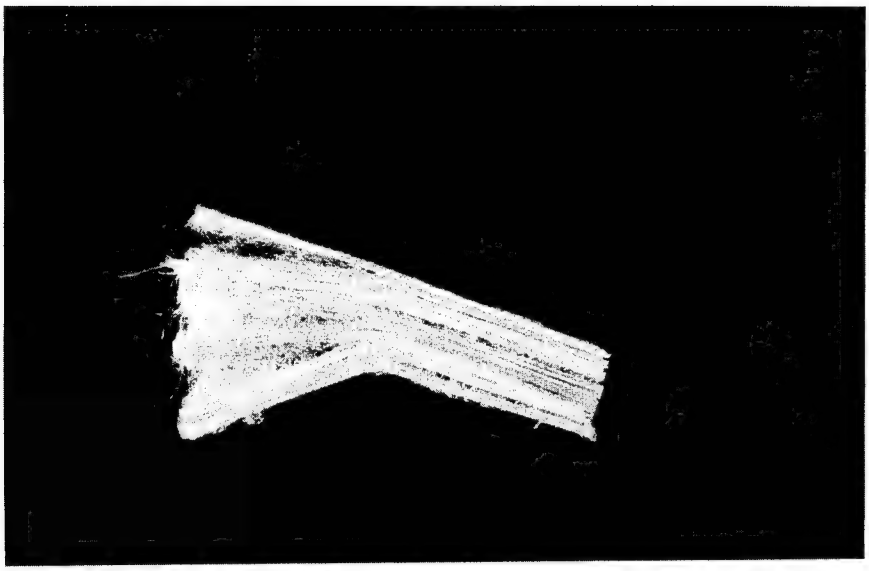

Table XI

Charpy Impact Loads of AS/S-Glass Epoxy Laminates

UARL No.	Composition Type	Fiber Ratio v/o (actual)	P_i Newtons	(P_i lbs)	P_{max} Newtons	(P_{max} lbs)	Charpy Impact Strength (experimental) Joules	(ft-lbs)
NAS-6	11	AS-89.1 S-10.9	5,550	(1250)	10,680	(2400)	42	(30)
NAS-8C	11	AS-79.8 S-20.2	11,110	(2500)	14,240	(3200)	44.8	(32)
NAS-20A	15	AS-85 S-15	3,560	(1450)	8,000	(1800)	30.8	(22)
NAS-17A	15	AS-80.2 S-19.8	3,560	(1600)	10,220	(2300)	46.2	(33)
NAS-35	19a-2	AS/HM-57.0 S-3.5	2,220	(500)	4,120	(925)	17.5	(12.5)
NAS-34	19a-1	AS/HM-55.0 S-4.3	5,120	(1150)	7,120	(1600)	19.6	(14)
NAS-74	7	AS-83.7 S-16.3	12,400	(2800)	12,400	(2800)	37.8	(27)
NAS-76	1-UARL	AS-75 S-25	12,400	(2800)	12,400	(2800)	52.5	(37.5)
NAS-1A		AS	11,580	(2600)	11,580	(2600)	24.5	(17.5)
NAS-3A		S-glass	10,000	(2250)	10,450	(2350)	73.5	(52.5)

INSTRUMENTAL CHARPY LOAD–TIME TRACE

NAS–77

AS/S glass (25) TYPE 1–UARL

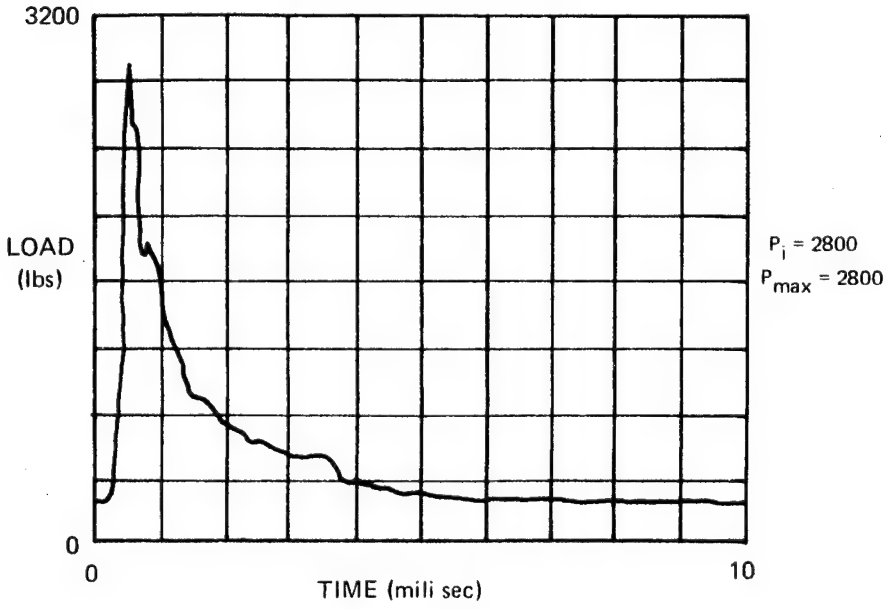

NAS–79

AS/PRD (12.7) TYPE 3–UARL

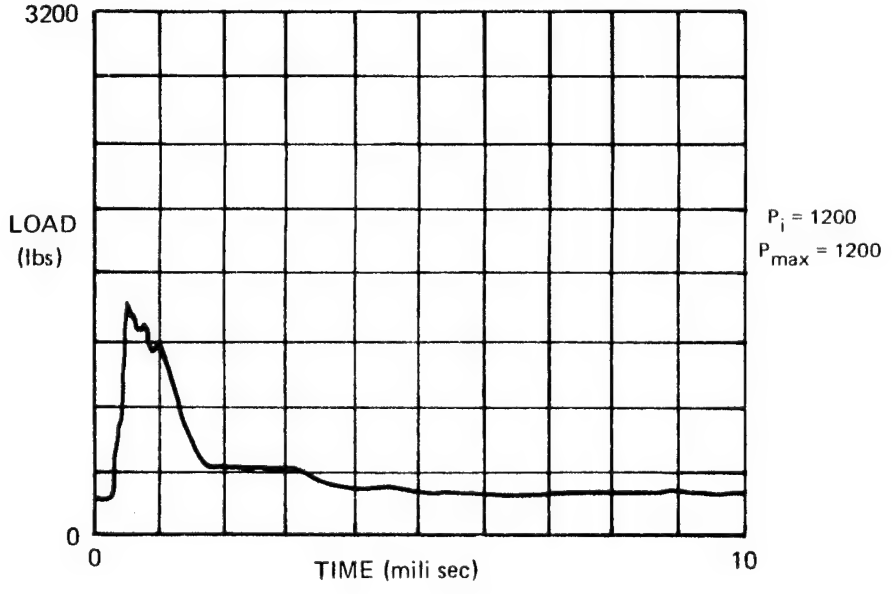

N04–11–2

IMPACTED COMPOSITE SPECIMENS

NAS–77

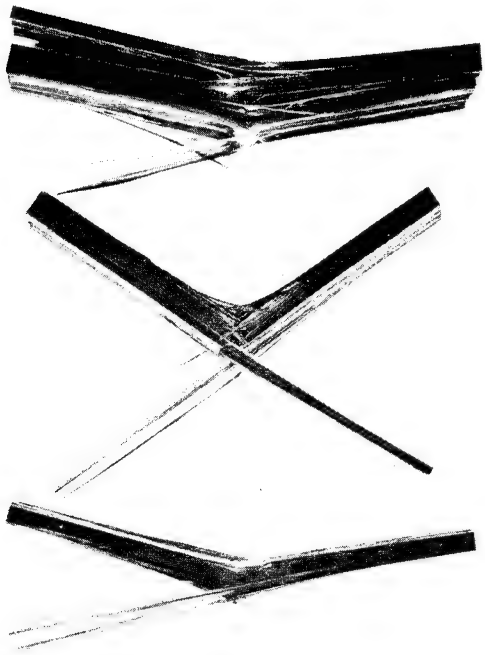

NAS–79

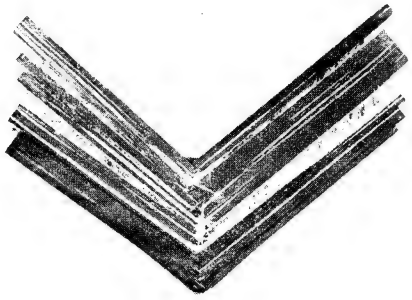

2.2.2.1.4 AS/Kevlar 49 Composites

Unlike the addition of Kevlar 49 to HMS graphite when AS graphite is combined with Kevlar 49, there is a relatively large change which occurs in the P_{max} level, particularly in the interply (Type 12) composites, with little effect on P_i, Table XII. The higher the percentage of Kevlar 49 the lower the P_{max} capability. This would be expected in light of the low P_{max} obtainable with Kevlar 49 alone. This effect is probably related to the poor compressive properties associated with Kevlar 49 systems. This is in contrast to the AS/S-glass interply composites where an increase in glass content resulted in a higher P_{max} load capability. Comparison of the impact properties of the interply, core-shell, and intraply AS/Kevlar 49 systems show little change in total impact characteristics either with Kevlar 49 concentration or ply construction. The P_i and P_{max} loads of the core-shell type are, however, higher than the interply type with the intraply construction being intermediate between the two. The load-time curves and fractured composite for Type 3-UARL are shown in Figs. 21 and 22.

2.2.2.2 Impact Strength vs Hybrid Fiber Composite Modulus

An important consideration in the evaluation of hybrid fiber combinations for structural parts is the relationship of impact strength to composite bending stiffness or modulus. A minimum of 131 GN/m^2 (19×10^6 psi) flexural modulus is one criteria to be used in selecting composites for further evaluation in Tasks III and IV of this study. The correlation of total impact strength with flexural modulus for the hybrid composites tested to date is graphically illustrated in Figs. 23-26 for each hybrid fiber combination. In all cases 3-point moduli were used.

2.2.2.2.1 HMS/S-Glass Composites

With the HMS/S-glass composites, Fig. 23, several combinations provide sufficient moduli with some improvement in impact strength. It is clear, however, the best compromise of impact and mechanical properties is provided by the intraply UARL composite (side-by-side tow) containing 25 v/o S-glass. It is interesting to note that the UARL type intraply systems fall on a line between the pure HMS and S-glass laminates. In contrast the core-shell laminates, although giving a line having a similar slope, are below (left of) that of the nonhybridized systems. This is undoubtedly due to the effect of the lower modulus fiber being on the outside of the laminate where the bending stresses are maximized. The interply and dispersed fiber Heltra intraply do not lie on the same slope as the above two types and it appears initial shear failure in the HMS graphite is the controlling factor in these composites.

Table XII

Charpy Impact Loads of AS/Kevlar 49 III Epoxy Laminates

UARL No.	Composition Type	Fiber Ratio v/o (actual)	P_i Newtons	P_i (lbs)	P_{max} Newtons	P_{max} (lbs)	Charpy Impact Strength (experimental) Joules	Charpy Impact Strength (experimental) (ft-lbs)
NAS-13	12	AS-92 Kevlar-8	3,520	(800)	9,780	(2200)	29.4	(21)
NAS-14	12	AS-69.7 Kevlar-30.3	3,080	(700)	4,448	(1000)	32.2	(24)
NAS-26A	16	AS-90.9 Kevlar-9.1	10,450	(2350)	10,450	(2350)	32.2	(23)
NAS-23A	16	AS-65.5 Kevlar-37.5		(2500)	14,000	(3200)	35	(25)
NAS-78	3-UARL	AS-87.3 Kevlar-12.7	5,350	(1200)	5,350	(1200)	26.6	(19)
NAS-5A		Kevlar	3,120	(710)	3,720	(845)	35	(25)
NAS-1A		AS	11,580	(2600)	11,580	(2600)	24.5	(17.5)

FLEXURAL MODULUS–CHARPY IMPACT STRENGTH HMS–S GLASS COMPOSITES

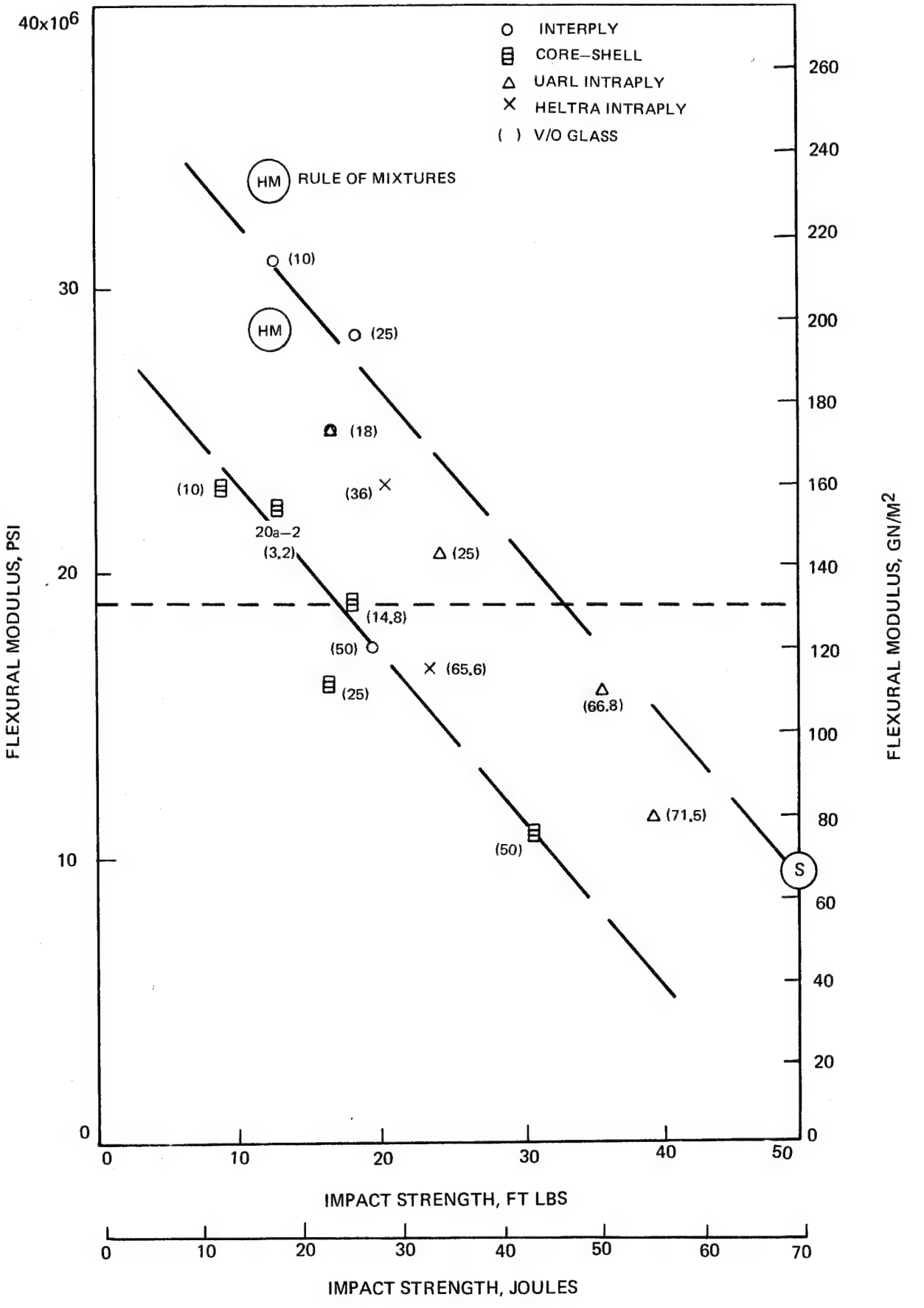

N11–8–6

2.2.2.2.2 HMS/Kevlar 49 Composites

All configurations tested with the HMS/Kevlar 49 fiber combination, Fig. 24, resulted in only slight improvement in impact strength. The modulus of the composites was the only real variable from 10 to 73 v/o Kevlar 49, irrespective of configuration type. The Heltra dispersed fiber composite (50 v/o Kevlar 49), because of lower fiber content, gave the same results as the corresponding core/shell type and both had much lower modulus than the interply composite. Normalized to 60 v/o fiber, the modulus of the Heltra composite would be 17.2×10^6 psi, slightly lower than the corresponding interply laminate. The shear strength of both HMS and Kevlar composites being relatively low and similar, and if shear failure is the primary fracture mode with the thick Charpy type specimen, little effect on impact properties are to be expected.

2.2.2.2.3 AS/S-Glass and AS/Kevlar 49 Composites

The AS S-glass, Fig. 25, laminates all resulted in moduli less than 131 GN/m^2 (19×10^6 psi) but the interply type were at the same level as all AS graphite. The interply configuration while providing no improvement in impact strength particularly at the 20 v/o S-glass level compared to core/shell does result in higher flexural modulus at the two glass fiber contents tested. On this basis, interply configuration would be preferred over core/shell. The large percentage improvement in Charpy impact strength over the pure AS graphite achieved by the intraply system is noteworthy. This is discussed further below.

AS-Kevlar 49 interply combinations, Fig. 26, resulted in composites having moduli at or slightly below 131 GN/m^2 while the core/shell configurations tested are definitely inferior. Impact levels of the 30 v/o Kevlar 49 composites were the same. Clearly, S-glass provides more improvement in impact strength than Kevlar 49 for AS graphite systems with minor changes in modulus.

It is interesting to note that when hybridizing AS graphite with either S-glass or Kevlar 49 the inter and intraply composites give impact/modulus properties which lie above the line connecting the two nonhybridized composites which is contrary to the effect found with HMS graphite. This is presumably related to the higher strain capability of AS compared to HMS which would allow the straining of the hybrid fiber to a greater degree during impact thereby providing a greater energy absorption. The S-glass being capable of straining to a higher degree than Kevlar 49, coupled with a higher flexural strength, would contribute to a higher fracture energy than can be achieved by Kevlar 49. This is illustrated by comparing the percentage improvement in Charpy impact strength for each of the 10 v/o interply type composites as compared to nonhybridized AS or HMS graphite. These data are listed below:

FIG. 24

FLEXURAL MODULUS–CHARPY IMPACT STRENGTH
HMS–PRD 49–III COMPOSITES

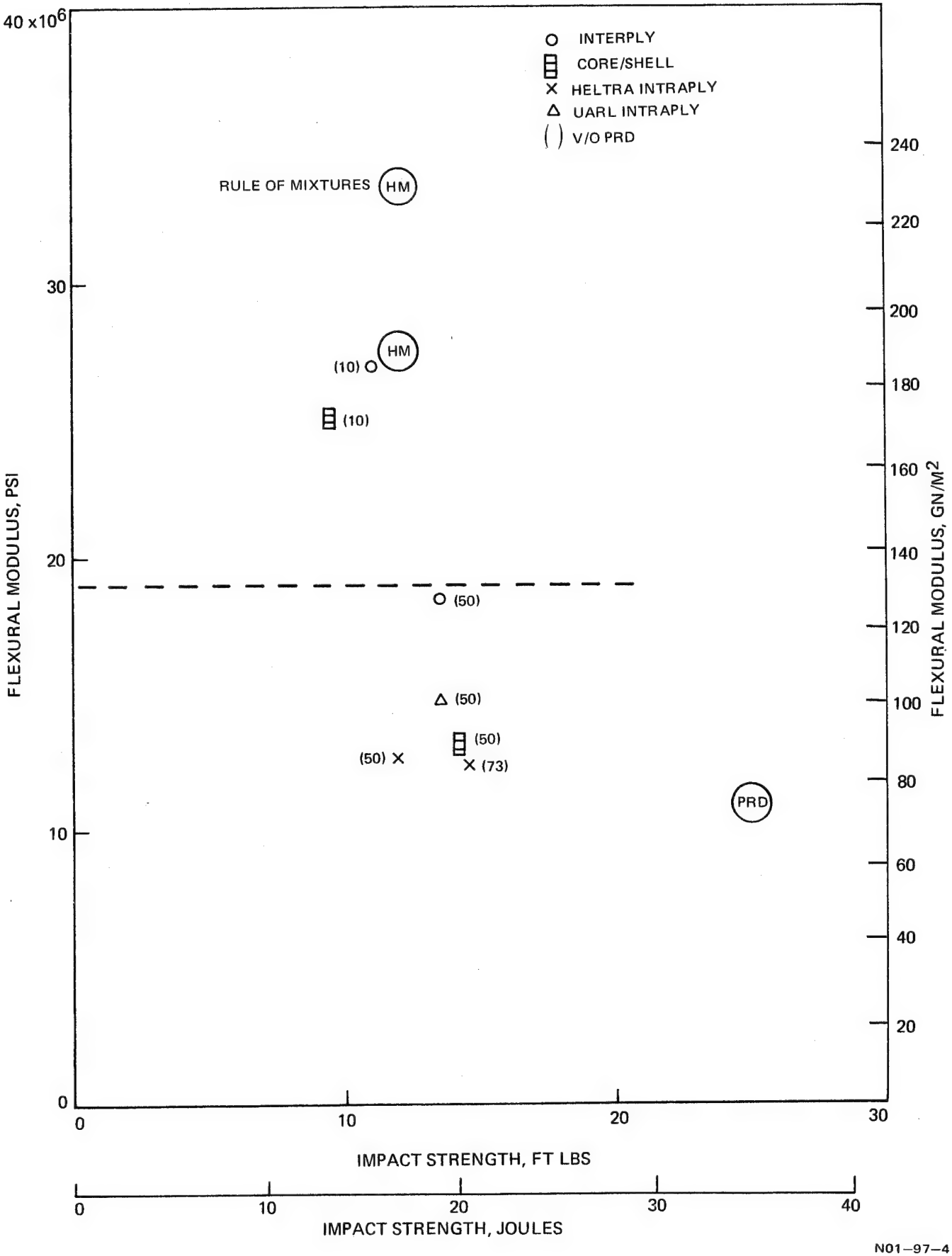

N01–97–4

FIG. 25

FLEXURAL MODULUS–CHARPY IMPACT STRENGTH
AS–S GLASS COMPOSITES

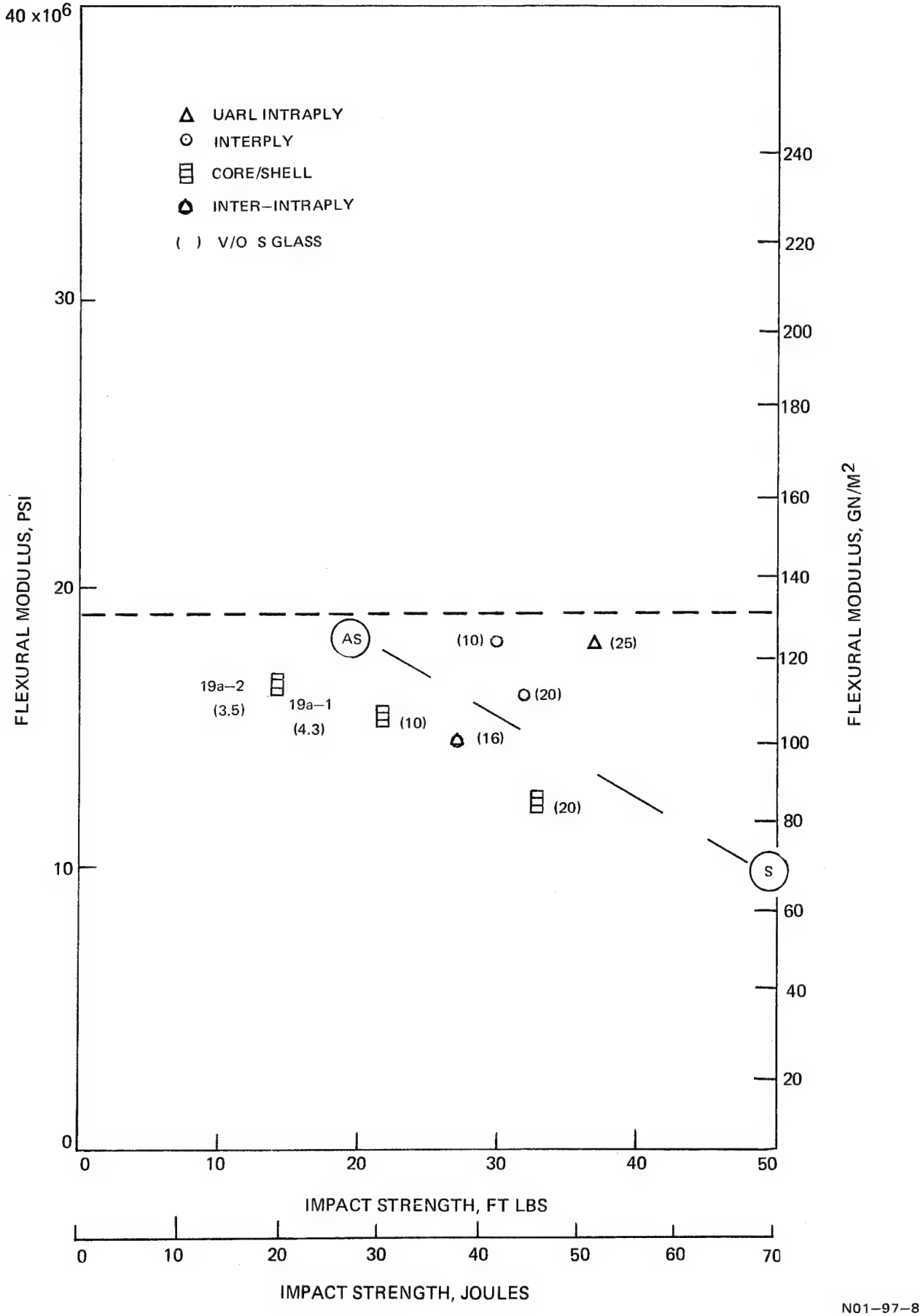

N01–97–8

FIG. 26

FLEXURAL MODULUS–CHARPY IMPACT STRENGTH AS–PRD 49–III COMPOSITES

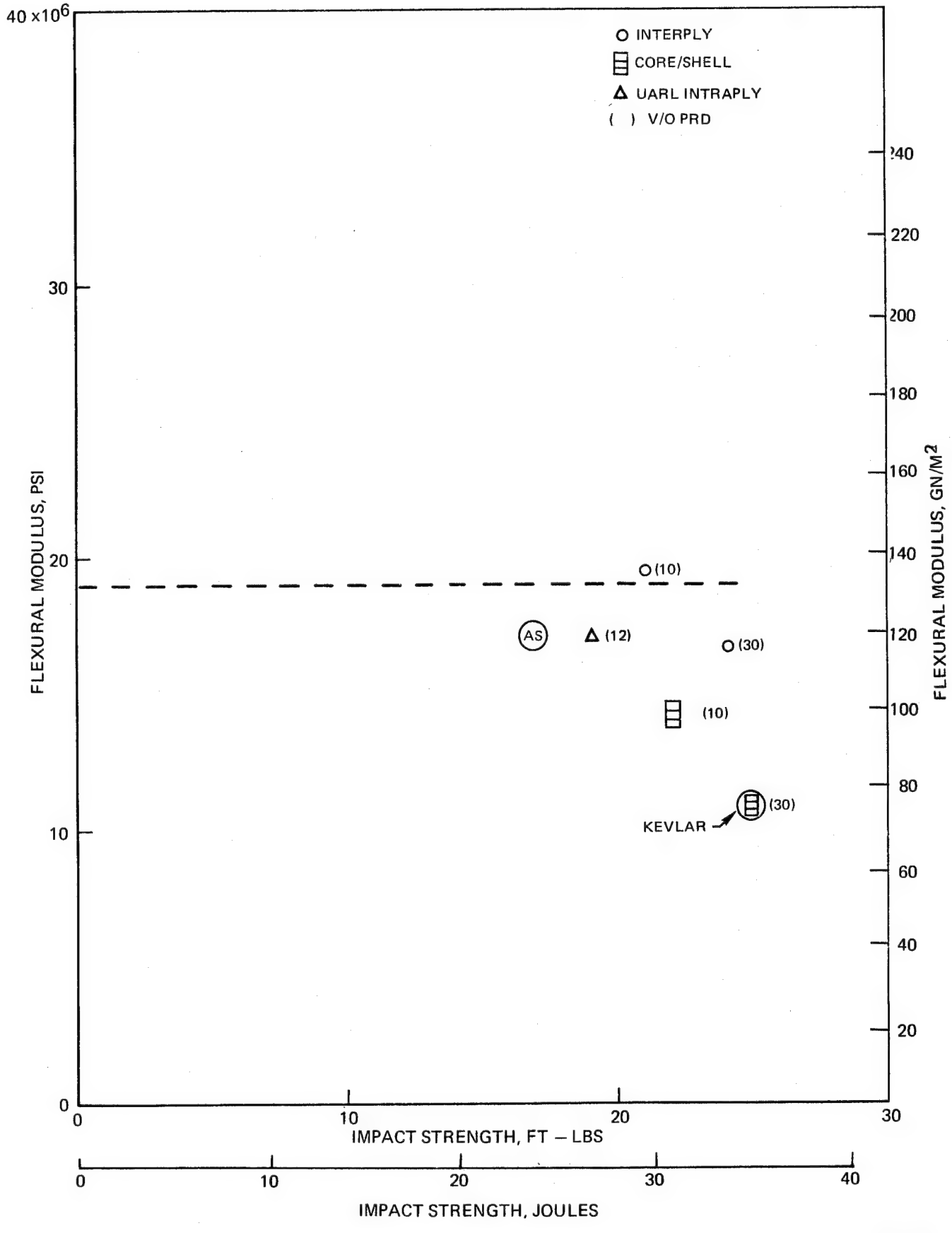

N01–97–7

Composite Type[a]	% Improvement in Charpy Impact Strength over Nonhybridized Graphite
AS/S-glass	112
AS/Kevlar 49	31
HMS/S-glass	0
HMS/Kevlar 49	0

[a]Interply - 10 v/o hybrid fiber

A somewhat modified result is obtained if a similar comparison is made with the interply and intraply composites at the 20-30 v/o hybrid fiber level. These data are tabulated below:

Composite Type (v/o Hybrid Fiber)	% Improvement in Charpy Impact Strength over Nonhybridized Graphite
intraply AS/S-glass (25)	134.0
interply AS/S-glass (20)	100.0
intraply AS/Kevlar 49 (13)	18.7
interply AS/Kevlar 49 (30)	50.0
interply HMS/S-glass (25)	50.0
intraply HMS/S-glass (25)	104.0
interply HMS/Kevlar 49 (50)	12.5
intraply HMS/Kevlar 49 (50)	12.5

The effect of varying amounts of hybrid fiber on the impact capabilities of the high and low modulus graphite fibers is readily apparent. The HMS requires a considerably higher percentage of hybrid fiber to produce any substantial improvements in impact than does the AS graphite with the exception of the S-glass intraply (tow-by-tow) construction.

2.2.2.3 Impact Energies vs Composite Modulus

In addition to the Charpy impact strength and load capabilities of these reinforced composites the energies associated with the fracture mechanism are also of importance in determining the overall impact capabilities of a given system. The following curves illustrated the approach used to calculate the energies from the load-time traces.

The load and energy factors involved are:

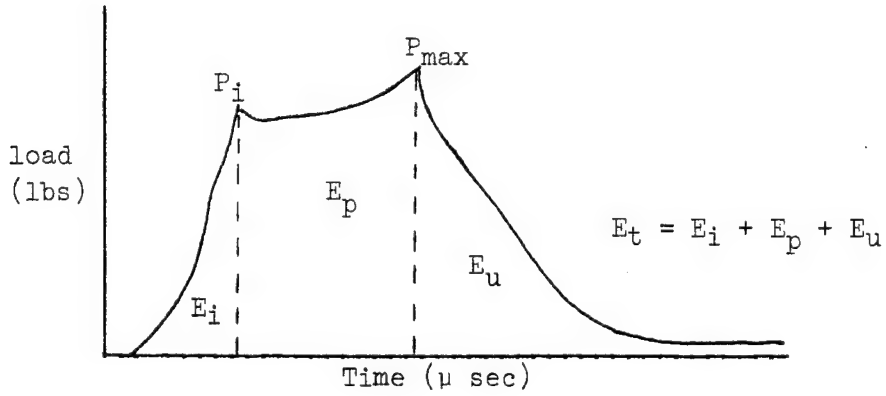

P_i = load required to initiate fracture
P_{max} = maximum load
E_i = energy of fracture initiation
E_p = energy of stable crack propagation
E_u = energy of unstable crack propagation
E_t = total impact energy.

In some cases E_i and E_p will be the same, for example, as in the following curve.

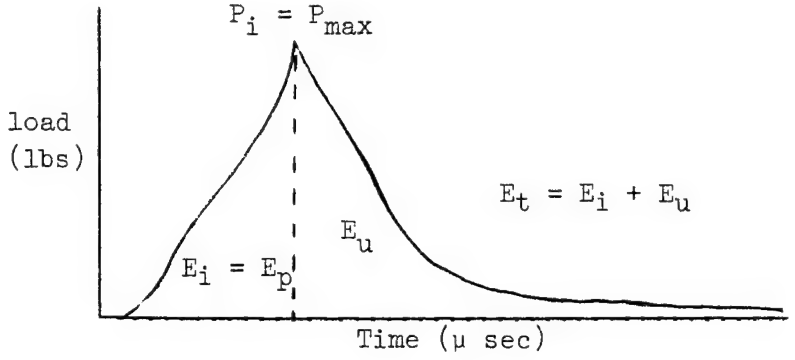

Of particular importance is the energy of stable crack propagation, E_p, which is a reflection of the amount of energy a given specimen can absorb and still retain load carrying capability even though crack initiation may have occurred. In some cases $E_i + E_p$ should be used to predict the energy capability prior to catastrophic failure. Tables XIII-XVI list the calculated energies for each type of reinforcement. The following equation was used in the calculation:

area under load-time curve x load/division x
deflection/division = E, ft-lbs

Table XIII

Impact Energies of HMS/S-Glass Composites

UARL No.	Composition Type	Fiber Ratio v/o (actual)	Charpy Impact Strength (experimental)	E_i	E_p	E_μ	E_T	$E_i + E_p$ (ft-lbs)
			Joules (ft-lbs)					
NAS-9	13	HMS-54.6 S-45.7	28 (20)	0.685 (0.49)	4.56 (3.26)	20.7 (14.8)	25.9 (18.5)	3.8
NAS-10	13	HMS-76.4 S-23.6	25.2 (18)	0.578 (0.413)	7.5 (5.36)	28.3 (20.2)	36.4 (26)	5.8
NAS-15A	13	HMS-89.6 S-10.4	16.8 (12)	0.578 (0.413)	7.5 (5.36)	16.6 (11.9)	24.8 (17.7)	5.8
NAS-18	17	HMS-48.7 S-51.3	44.8 (32)	12.1 (8.64)	26 (18.6)	32.4 (23.2)	70.5 (50.4)	17.2
NAS-16A	17	HMS-72 S-28	22.4 (16)	2.9 (2.07)	5.17 (3.70)	24.2 (17.3)	32.3 (23.1)	5.8
NAS-24	17	HMS-86.7 S-13.3	12.6 (9)	0.91 (0.65)	8.02 (5.73)	11.6 (8.3)	20.6 (14.7)	6.4
NAS-36	2-UARL	HMS-73.5 S-26.5	34.3 (24.5)	3.46 (2.47)	8.64 (6.17)	26.6 (19.0)	38.7 (27.6)	8.6
NAS-36A	2-UARL	HMS-28.8 S-71.2	54.6 (39)	2.83 (2.02)	10.3 (7.33)	41.5 (29.7)	54.5 (39)	9.3

Table XIII (Cont'd)

UARL No.	Composition Type	Fiber Ratio v/o (actual)	Charpy Impact Strength (experimental)	E_i	E_p	E_μ	E_T	$E_i + E_p$ (ft-lbs)
			Joules (ft-lbs)					
NAS-36B	2-UARL	HMS-33.2 S-66.8	(36)	3.29 (2.35)	11.2 (8.0)	33.6 (24)	47.6 (34)	10.4
NAS-47B	2-Heltra	HMS-40 S-60	38.6 (27.5)	7.55 (5.4)	6.16 (4.4)	16.7 (11.9)	30.4 (21.7)	9.8
NAS-47C	2-Heltra	HMS-34.4 S-65.6	(24)	2.34 (1.67)	3.76 (2.69)	25.2 (18)	30.8 (22)	4.4
NAS-47D	2-Heltra	HMS-64 S-36	(20.5)	2.83 (2.02)	2.81 (2.01)	24.1 (17.2)	29.7 (21.2)	4.0
NAS-55	20a-1	HMS-85.2 S-14.8	25.2 (18)	1.4 (1.0)	7.45 (5.33)	4.34 (3.1)	13.2 (9.4)	6.3
NAS-54	20a-2	HMS-96.8 S-3.2	18.2 (13)	0.476 (0.34)	4.67 (3.34)	10.6 (7.6)	15.8 (11.3)	3.7
NAS-58	20a-3	HMS-70 S-30	15.4 (11)	2.31 (0.65)	9.56 (6.84)	11.5 (8.2)	22 (15.7)	7.5
NAS-61		HMS	16.8 (12)	0.686 (0.49)	13.4 (9.6)	6.85 (4.9)	14.1 (10.1)	10.1
NAS-3A		S-glass	73.5 (52.5)	5.16 (3.69)	21.6 (15.4)	46.2 (33)	72.8 (52)	19.1

Table XIV

Impact Energies of HMS/Kevlar 49 III Composites

UARL No.	Composition Type	Fiber Ratio v/o (actual)	Charpy Impact Strength (experimental)	E_i	E_p	E_μ	E_T	$E_i + E_p$ (ft-lbs)
			Joules (ft-lbs)					
NAS-12A	14	HMS-92.5 Kevlar-7.5	15.4 (11)	2.31 (1.65)	2.88 (2.06)	23.10 (16.5)	28.28 (20.2)	3.71
NAS-11A	14	HMS-58.2 Kevlar-41.8	18.9 (13.5)	1.15 (0.825)	7.52 (5.37)	20.72 (14.8)	29.40 (21.0)	6.19
NAS-28	18	HMS-89.1 Kevlar-10.9	13.6 (9.75)	1.61 (1.15)	8.19 (5.85)	9.80 (7.0)	19.60 (14)	7.0
NAS-18	18	HMS-57.7 Kevlar-42.3	20 (14.2)	1.59 (1.14)	7.08 (5.06)	13.72 (9.8)	22.40 (16)	6.2
NAS-46	4-UARL	HMS-51.7 Kevlar-48.3	18.9 (13.5)	2.88 (2.06)	2.89 (2.07)	24.92 (17.8)	30.66 (21.9)	4.13
NAS-49	4-Heltra	HMS-27.4 Kevlar-72.6	20.3 (14.5)	1.72 (1.23)	6.30 (4.5)	16.24 (11.6)	24.22 (17.3)	5.7
NAS-49A	4-Heltra	HMS-48.4 Kevlar-51.6	16.8 (12)	1.93 (1.38)	3.20 (2.29)	6.42 (4.59)	11.56 (8.26)	4.7
NAS-63		HMS	(12)	.686 (0.49)	13.4 (9.6)	6.86 (4.9)	14.14 (10.1)	10.0
NAS-5A		Kevlar	(25)	2.80 (2.0)	7.98 (5.7)	14.56 (10.4)	25.34 (18.1)	7.7

Table XV

Impact Energies of AS/S-Glass Composites

UARL No.	Composition Type	Fiber Ratio v/o (actual)	Charpy Impact Strength (experimental)	E_i	E_p	E_μ	E_T	$E_i + E_F$ (ft-lbs)
			Joules (ft-lbs)					
NAS-6	11	AS-89.1 S-10.9	42.00 (30)	1.14 (0.82)	13.7 (9.8)	39.76 (28.4)	59.60 (39)	10.6
NAS-8C	11	AS-79.8 S-20.2	44.80 (32)	4.57 (3.27)	7.0 (5.0) (11.5)	34.16 (24.4) (12.9)	45.78 (32.7)	8.3 (14.8)
NAS-17A	15	AS-80.2 S-19.8	46.20 (33)	8.85 (0.33)	10.03 (7.17)	26.04 (18.6)	36.54 (26.1)	7.5
NAS-20A	15	AS-85 S-15	30.80 (22)	2.98 (2.13)	2.73 (1.95)	14.84 (10.6)	20.58 (14.7)	4.1
NAS-35	19a-2	AS/HM-57.0 S-3.5	17.50 (12.5)	1.40 (1.0)	3.29 (2.35)	11.06 (7.9)	15.82 (11.3)	3.4
NAS-34	19a-1	AS/HM-55.0 S-4.3	19.60 (14)	2.29 (1.64)	7.0 (5.0)	8.68 (6.2)	22.82 (16.3)	6.6
NAS-76	1-UARL	AS-75 S-25	52.5 (37.5)	4.34 (3.1)	- (0)	36 (25.7)	40.3 (28.8)	3.1
NAS-1A		AS	24.5 (17.5)	6.10 (4.36)	0 (0)	21.00 (15)	26.60 (19)	4.36
NAS-3A		S-glass	73.50 (52.5)	5.16 (3.69)	21.56 (15.4)	46.20 (33)	72.80 (52)	19.1

Table XVI

Impact Energies of AS/Kevlar 49 III Composites

UARL No.	Composition Type	Fiber Ratio v/o (actual)	Charpy Impact Strength (experimental)	E_i	E_p	E_μ	E_T	$E_i + E_p$ (ft-lbs)
			Joules (ft-lbs)					
NAS-13	12	AS-92 Kevlar-8	29.40 (21)	2.50 (1.79)	6.86 (4.90)	15.12 (10.8)	24.50 (17.5)	6.7
NAS-14	12	AS-69.7 Kevlar-30.3	33.60 (24)	.686 (0.49)	16.66 (11.9)	5.46 (3.9)	22.82 (16.3)	12.4
NAS-26A	16	AS-90.9 Kevlar-9.1	14.70 (10.5)	.224 (0.16)	3.43 (2.45)	4.45 (3.18)	8.12 (5.8)	2.6
NAS-23A	16	AS-62.5 Kevlar-37.5	35.00 (25)	6.30 (4.5)	1.82 (1.3)	31.08 (22.2)	39.20 (28)	5.8
NAS-78	3-UARL	AS-87.3 Kevlar-12.7	(19)	(5.4)	0	(6.7)	(12.1)	5.4
NAS-5A		Kevlar	35.00 (25)	2.80 (2.0)	7.98 (5.7)	14.5 (10.4)	25.34 (18.1)	7.7
NAS-1A		AS	22.40 (16)	6.16 (4.4)	0 (0)	21.00 (15)	26.60 (19)	4.4
NAS-70	5-Heltra	AS-59.4 S-17.2 Kevlar-23.4	22.4 (16)	8.06 (5.76)	- (0)	18.4 (13.2)	26.6 (19)	5.76
NAS-71	5-UARL	AS-56.8 S-21.0 Kevlar-22.2	39.2 (28)	8.06 (5.76)	- (0)	49.5 (35.3)	57.4 (41)	5.76

In most instances the total calculated energy, E_T, agreed well with that obtained experimentally, particularly those from the latter part of Task I due to continued refinement of the instrumented Charpy apparatus. E_i, the energy of fracture initiation, however, is somewhat questionable since moduli calculated from the Charpy curves did not agree with statically measured values. The main difficulty arises in the assignment of a point on the load-time trace where fracture actually initiates. In most instances where this is not obvious, a change in slope of the curve was designated as the initiation of fracture.

2.2.2.3.1 HMS/S-Glass Composites

The highest E_p value obtained for the HMS/S-glass systems, Table XIII, which met the minimum modulus requirements, 131 GN/m^2 and had an impact strength greater than 20 ft-lbs was with the side-by-side tow intraply type (NAS-37). In decreasing order, were the interply (NAS-30), core/shell (NAS-43) and the dispersed tow intraply (NAS-48C) configurations. The latter type showed an E_p value only 1/3 that of the NAS-37 intraply. These results, as did the P_{max} values, reflect the importance of shear deflection mechanisms in determining the impact characteristics of a given system.

2.2.2.3.2 HMS/Kevlar 49 Composites

None of the composites in the HMS/Kevlar 49 hybrid fiber combination, Table XIV, meet the minimum Charpy impact strength of 20 ft-lbs (experimental value). It should be noted that in this series the agreement of E_T (calculated) with the measured value is not as consistent as were the glass modified composites. In addition, the E_p values of all the composites were lower than the best HMS/S-glass system which indicates that with HMS graphite S-glass is the preferred hybridizing fiber.

2.2.2.3.3 AS/S-Glass Composites

Applying the same minimum modulus criteria to the AS/S-glass systems, Table XV, would eliminate all composites of this hybrid combination from further consideration. It is felt, however, that because of the high use potential of the low modulus AS type graphite, those composites which maintain the same modulus level as homogeneous AS should be considered for further evaluation. This would allow consideration of the AS/S-glass interply and intraply type composites at the 10 v/o and 25 v/o level respectively of glass fiber. These laminates have demonstrated some of the highest impact strength improvements of the hybrid systems tested to date. If the modulus requirements cannot be met, a possible alternative would be the addition of a thin shell of T-75 or HMS graphite to the AS/glass inter or intraply composites sufficient to increase the modulus to meet the requirements without loss of the desired impact capabilities.

2.2.2.3.4 AS/PRD Composites

Consideration of AS/PRD combinations, Table XVI, is limited to the interply type based on E_p energy calculations. Of the two levels of hybrid fiber tested only the 10 v/o NAS-13 meets the minimum modulus requirements. It should be noted that the E_p of this composite is only half that of the corresponding S-glass composite (NAS-6) and the total impact energy is lower. Results for the intraply type 3-UARL, NAS-78, were lower than expected compared to the improved results obtained with the intraply AS/S-glass combination.

Impact properties were similar to the interply type. It was of interest to correlate initial (E_i) and propagation (E_p) impact energies with flexural modulus to determine if any differences in impact behavior prior to catastrophic failure changed the ranking of the hybrid laminates as compared to total Charpy impact strength. Graphs of ($E_i + E_p$) vs flexural modulus are shown in Figs. 27-30. Although there were some minor shifts in composite behavior, in general, the same relationship of impact energy to flexural modulus was found using the $E_i + E_p$ parameter. This suggests that for the Charpy test using standard size specimens, total impact energy can be used efficiently to correlate impact behavior with other mechanical properties.

2.2.3 Thin Charpy Specimen Tests

Although the instrumented Charpy test using standard size 0.394 in. thick specimens is a valuable screening tool for showing differences in composite impact characteristics, the results from such tests have shown inconsistent correlation at UARL with impact data obtained using ballistic impact tests. Since our results with the standard Charpy specimens are shear limited, laminate types might be selected which would perform unstaisfactorily under ballistic impact. The latter more closely simulates impact in actual use conditions. In addition, it is believed the shear stress to bending stress ratio of the thin Charpy specimen will be in better agreement with those encountered in the ballistic impact test. Because of this fact and previously indicated results using thin Charpy specimens, a series of Charpy tests were run on the intraply type composites made by the Heltra dispersion process and the UARL tow-by-tow construction to determine (1) the effect of specimen thickness on impact failure mode and (2) what correlation, if any, exists between slow bend test data and thin Charpy impact test results. The impact data obtained are listed in Table XVII.

Both shear and bending stresses were calculated from the P_i and P_{max} loads respectively obtained in the Charpy test and compared to static three point flexural test data on the same composites. These results are shown in Table XVIII together with impact data obtained using the corresponding standard Charpy specimens.

FLEXURAL MODULUS – $E_i + E_p$ HMS/S–GLASS

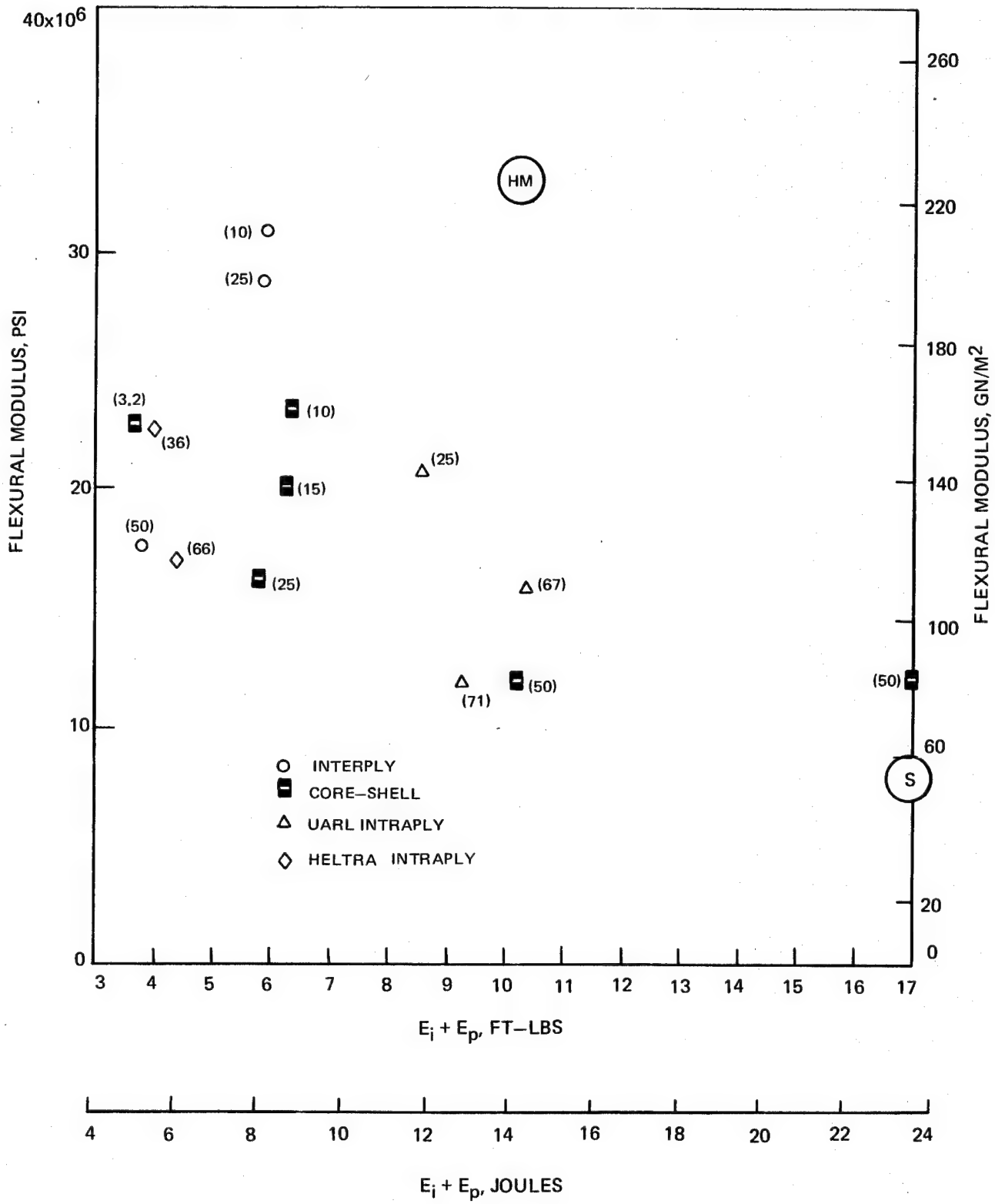

N11–8–7

FLEXURAL MODULUS – $E_i + E_p$
HMS/PRD 49–III

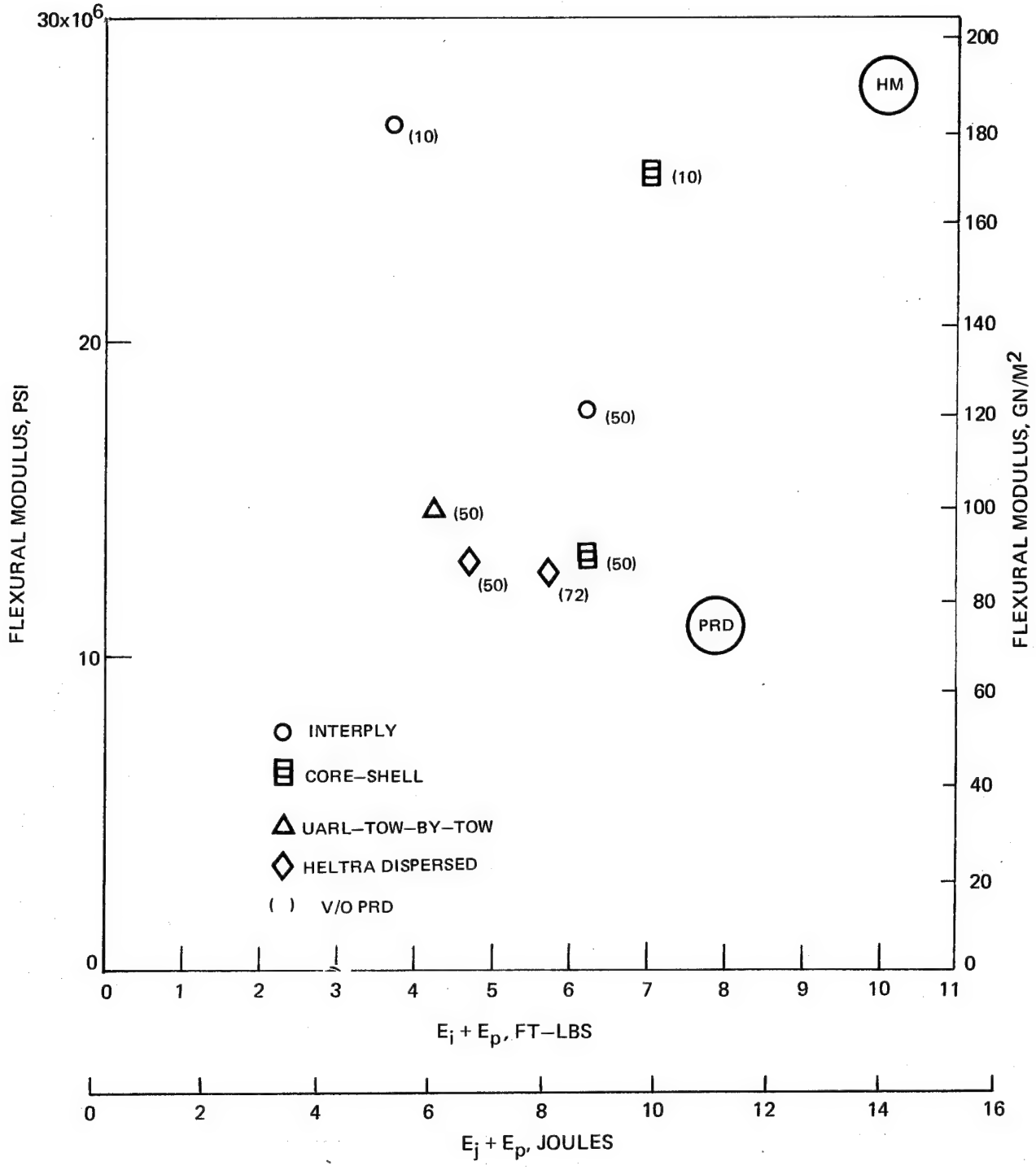

N02–77–2

FIG. 29

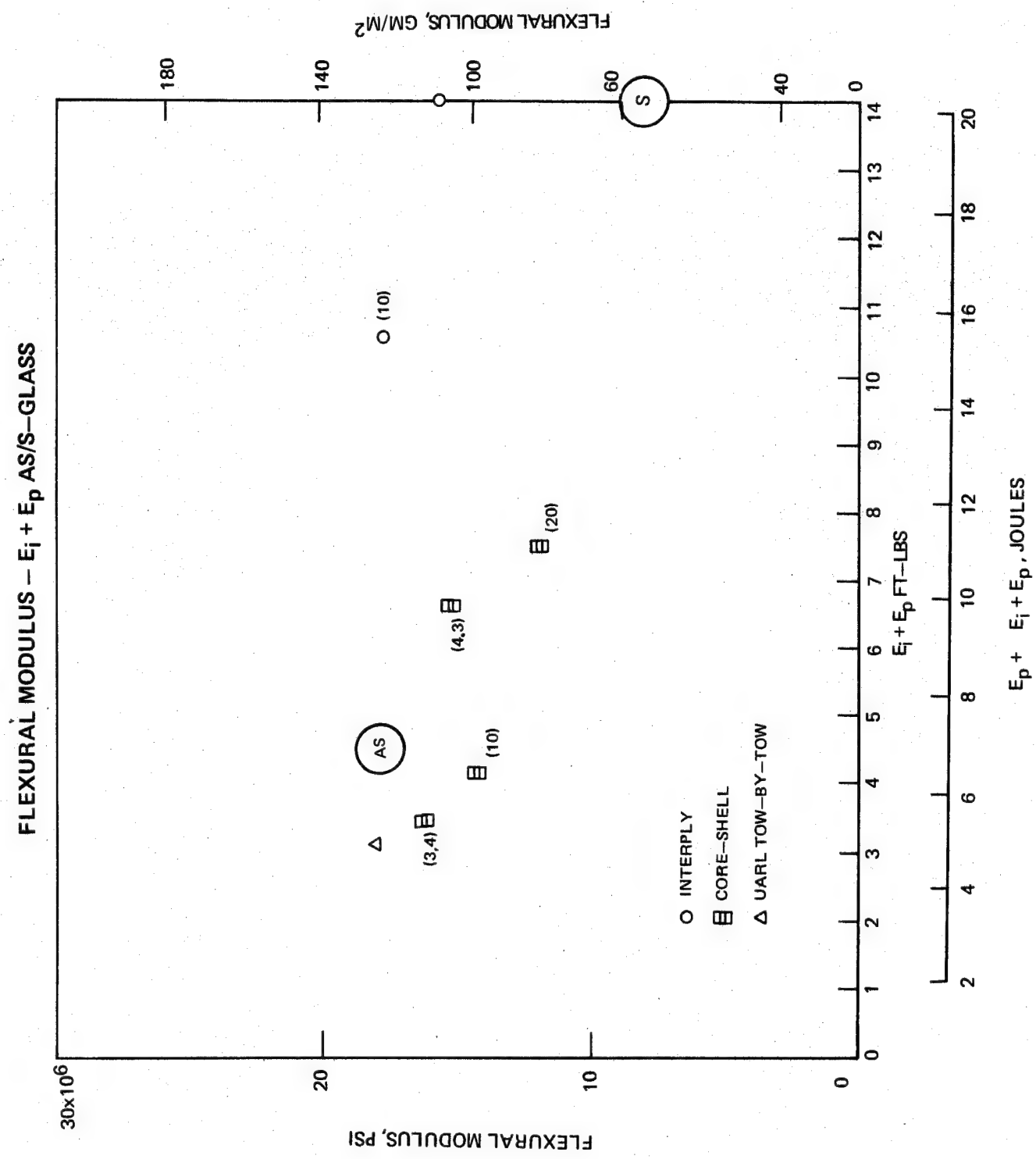
FLEXURAL MODULUS – $E_i + E_p$ AS/S–GLASS
FLEXURAL MODULUS, PSI
FLEXURAL MODULUS, GM/M²
$E_i + E_p$ FT–LBS
$E_p + E_i + E_p$, JOULES
30x10⁶
20
10
0
180
140
100
60
40
0
1
2
3
4
5
6
7
8
9
10
11
12
13
14
2
4
6
8
10
12
14
16
18
20
AS
S
(10)
(3,4)
(10)
(4,3)
(20)
O INTERPLY
CORE–SHELL
Δ UARL TOW–BY–TOW

N11–8–8

FLEXURAL MODULUS – $E_i + E_p$
(AS/PRD 49)

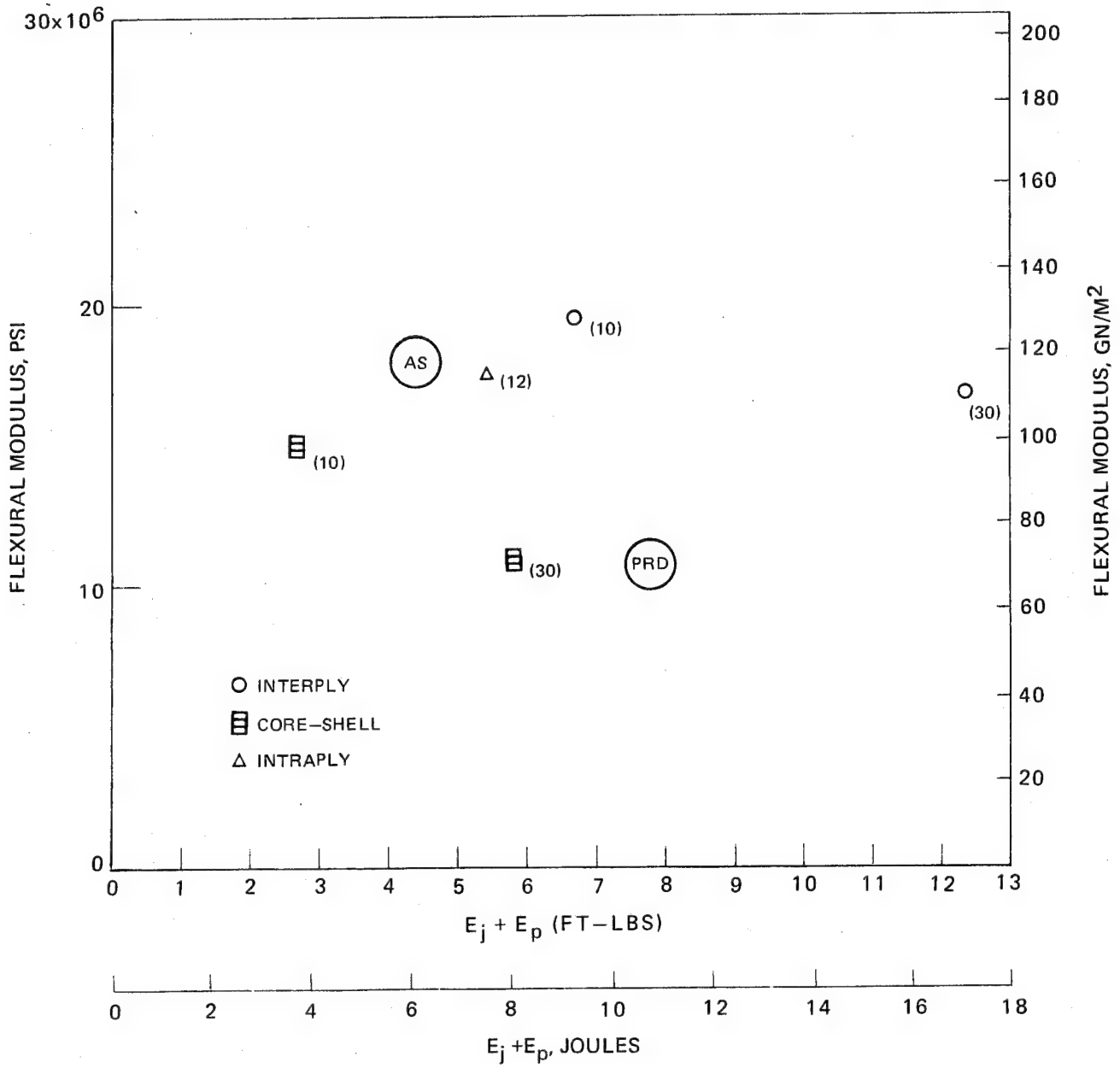

N02–77–1

Table XVII

Charpy Impact of Thin Intraply Epoxy Composites

UARL No.	Type	Fiber v/o (actual)	P_i Newtons	(lbs)	P_{max} Newtons	(lbs)	Charpy Impact Strength Joules	(ft-lbs)
NAS-47C	2-Heltra	HMS-34.4 S-65.6	178	(40)	334	(75)	2.67	(1.91)
NAS-36B	2-UARL	HMS-33.2 S-66.8	507	(114)	507	(114)	5.4	(3.86)
NAS-49A	4-Heltra	HMS-48.4 Kevlar-51.6	133.5	(30)	267	(60)	0.855	(0.61)
NAS-46	4-UARL	HMS-51.7 Kevlar-48.3	625	(140)	625	(140)	1.39	(0.99)
NAS-47D	2-Heltra	HMS-64 S-36	392	(88)	392	(88)	1.3	(0.93)

Table XVIII

Charpy Impact Test Thickness Variations

	Thin Specimen Data				Thick Specimen Data			
	Bending Stress ksi		Shear Stress, psi	Impact Energy/Area			Impact Strength	Impact Energy/Area
UARL No.	Calcd[a]	Exp.	(calcd)[a]	ft-lbs/in.^{2}	P_i(lbs)	P_{max}(lbs)	(ft-lbs)	ft-lbs/in.^{2}
NAS-47C	112	126	2260	76.4	650	800	24	153.6
-36B	119	143	2660	120	910	1040	39	254
-49A	111.8	105.5	2510	34	623	710	12	79
-46	127	98	3980	41.5	800	1350	13.5	88.8
-47D	180.5	159.5	3890	54.5	640	660	20.5	134.5

[a]Standard isotropic homogeneous beam equations used for calculating stresses

Comparison of the total impact strengths obtained with the thin and thick specimens gives the same relative ranking for the composites. However, both the calculated and experimental bending stresses and the calculated shear stress give a different ranking order. The agreement between the experimental and calculated bending stresses, however, is reasonably good. The differences may be due to the fact that some specimens failed in shear rather than tension.

The effect of specimen thickness on Charpy impact strength for these intraply hybrid composites can be seen in Fig. 31 which correlates specimen thickness with Charpy impact energy per unit area. The response of S-glass reinforcement compared to Kevlar 49 with the two different types of intraply construction is readily seen. With Kevlar 49 (PRD) there is only a minor increase in impact strength with increasing thickness with no difference in response for the two types of construction. With S-glass, however, the tow-by-tow system results in considerable increase in impact strength as thickness increases compared to the Heltra type dispersion. Comparison of the slopes of the lines provides an indication of these differences as seen below.

Composite Type	Slope ft-lbs/in.^{3}	Slope Normalized
HMS/S-glass, 2 UARL	470	2.97
HMS/S-glass, 2-Heltra	233	1.48
HMS/Kevlar 49, 4-UARL 4-Heltra	158	1

These differences are undoubtedly related to the different shear-bending stress ratios in the specimens of varying thickness. Further testing was done in Task II using additional hybrid fiber combinations in order to better define the relationship between test specimen geometry and energy absorption.

To gain a better understanding of thickness effects analysis of the data was carried out using the concepts discussed by Mullin and Knoell (Ref. 5). Shear stress and flexural stress interaction diagrams were constructed for unidirectional HMS/Kevlar 49 III intraply composites NAS-46 and 49A. These curves, shown in Figs. 32 and 33, plot the maximum shear and bending stresses, respectively, present in a composite beam as a function of span-to-depth ratio (L/h) based on measured values of shear strength, τ_o, and flexural strength, σ_o. In both cases the inflection point in the curve is the maximum L/h at which failure should occur in interlaminar shear. Beyond that, failure should be controlled by flexural properties. Both curves were calculated from static properties.

EFFECT OF THICKNESS ON TOTAL IMPACT ENERGY PER UNIT AREA

UNNOTCHED CHARPY SPECIMENS

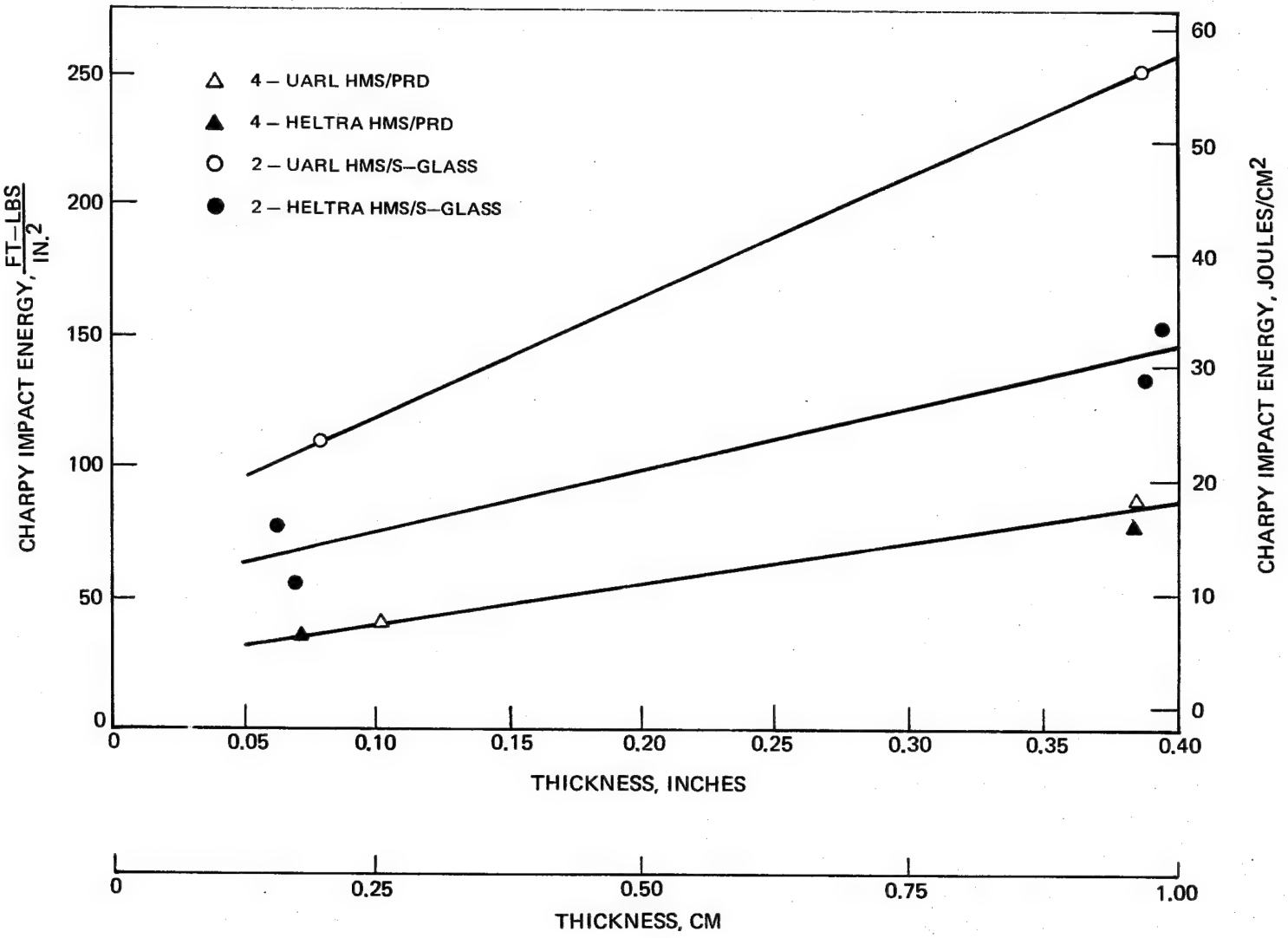

N10–326–3

FIG. 31

FIG. 32

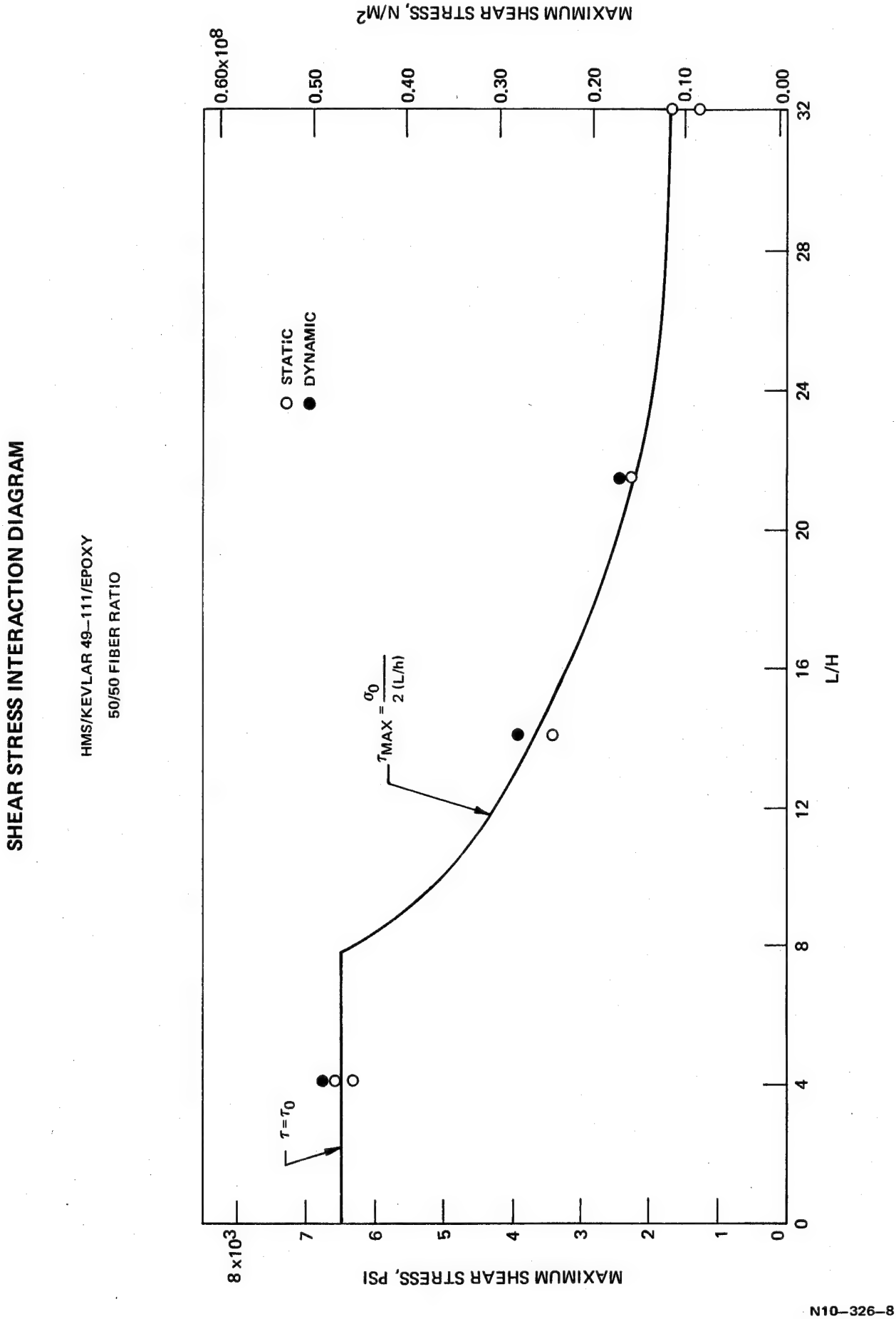

N10–326–8

FLEXURAL STRESS INTERACTION DIAGRAM

HMS/KEVLAR 49–111/EPOXY

50/50 FIBER RATIO

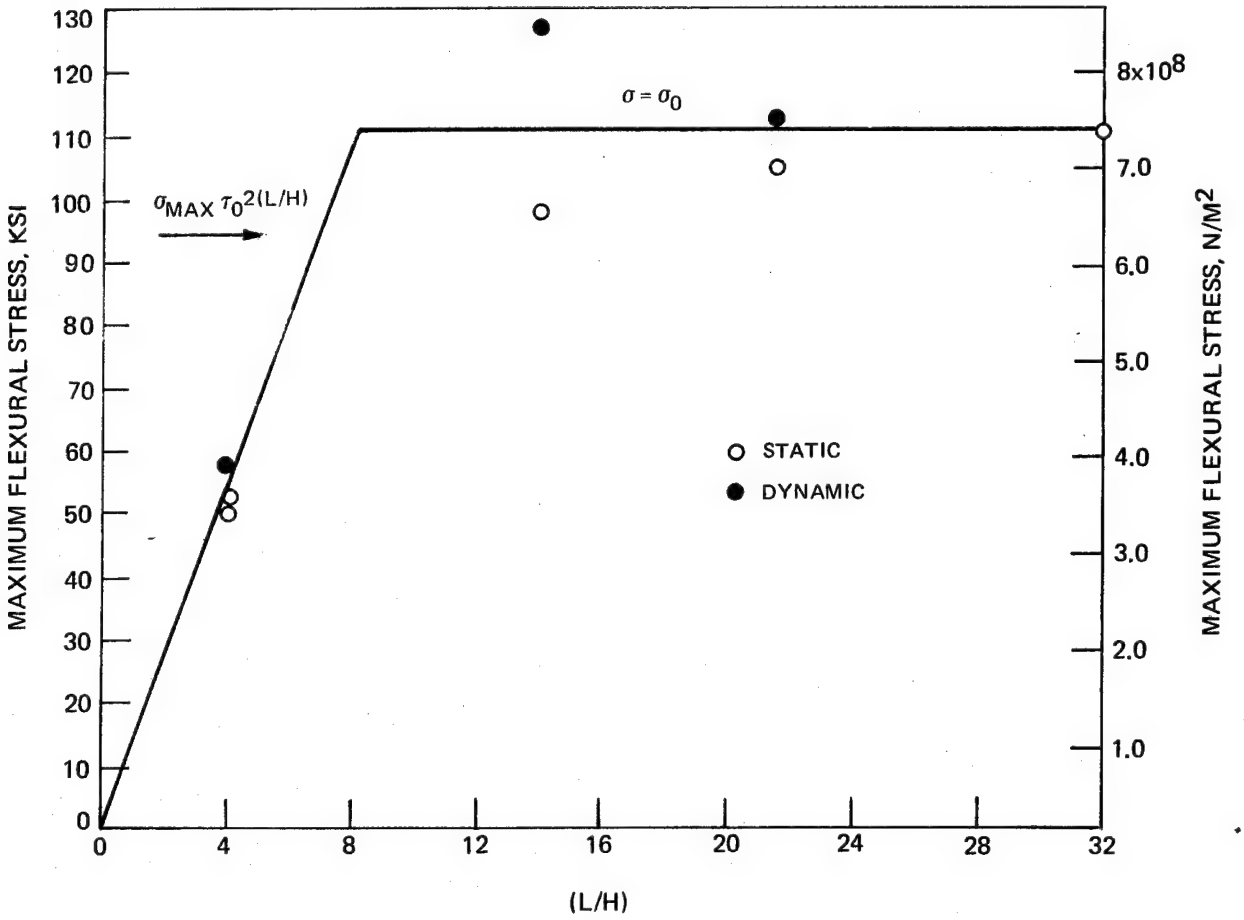

N10–326–6

The shear stress interaction diagram in Fig. 32 indicates that a span-to-depth ratio of 8 is the maximum for shear failure. The data points represent shear stresses calculated from both static and impact tests which were conducted on specimens of various thickness. The shear stresses in the impact tests were calculated from P_i values given in the above-referenced table. The agreement between the curve and the experimental points was excellent over the entire range of L/h investigated. The results also indicate that there was no effect of strain rate since the stress calculated from the static and impact tests were essentially identical.

The flexural stress interaction diagram in Fig. 33 also showed good agreement between the calculated curve and the experimental stresses with the possible exception of the tests conducted at an L/h of 14. With the exception of those tests, the data again indicated a lack of strain rate sensitivity.

Taken together these curves clearly point out the importance of span-to-depth ratio in the pendulum impact test. The standard Charpy test with an L/h = 4 is controlled by shear failure. It has been experimentally shown that at L/h = 14 and higher, behavior is controlled by flexural strength. Calculations indicate that for this material flexural properties will continue to control failure down to L/h = 8. Of course, the response of materials having different τ_o and σ_o would be different.

Similar diagrams have been constructed for the angle-ply composites in Task II. It is believed this analysis points out the danger in using standard Charpy impact data if the intended application is to involve loading at high L/h ratios.

2.2.4 Analytical Calculations

The flexural moduli of the composites tested are in some cases lower than would be predicted on the basis of rule-of-mixtures calculations using fiber tensile moduli. To facilitate calculation of the flexural modulus of hybrid composites a UARL computer program is being applied to calculate bending stiffness for hybrid laminates using individual ply moduli, ply thickness and stacking sequence. Table XIX lists a comparison of the predicted and experimentally measured bending moduli and failure loads for a series of interply and core-shell type hybride laminates. The agreement between predicted and measured moduli was reasonably good. The predicted values generally fell within the experimental scatter of the measurements. Several of the failure loads were not very well predicted however. Furthermore, the predicted failure mode was wrong for several of the composites. In particular, many of the flexural specimens failed partially in shear. Based on the measured short beam shear strengths which were input as failure criteria, the calculations indicated that the maximum shear stresses

Table XIX

Predicted and Experimental Bending Properties

Fibers	Construction	Predicted E (msi)	Measured E (msi)	Predicted Failure Load/Mode	Measured Failure Load/Mode
80-AS/20-glass	interply	16.6	15.8	176/tension	150/tension
90-HM/10-glass	interply	27.5	27.2	120/tension	92/comp., shear
75-HM/25-glass	interply	25.6	28.7	98/tension	144/comp., shear
80-AS/20-glass	core-shell	13.6	12.0	174/tension	177/tension, shear
90-HM/10-glass	core-shell	22.4	23.0	108/tension	113/comp., shear
75-HM/25-glass	core-shell	17.2	16.0	84/tension	127/comp., shear
50-HM/50-glass	core-shell	11.0	10.6	73/tension	103/comp., shear

present in the beams were much too low to cause failure in that mode. As a result of this discrepancy the short beam shear test is currently being analyzed to determine the validity of the calculated shear strengths which were used as failure criteria in the bending analysis.

2.2.5 Hybrid Fiber Content vs Material Costs

Although cost is not a criteria to be used in the current study it was of interest to determine the effect of hybridization on this important parameter of total fiber cost for future reference. These comparisons are illustrated graphically in Figs. 34-37 using flexural modulus as a mechanical property parameter.

In order to analyze these data on the basis of costs it is necessary to establish some design criteria, then compare the costs of the hybrids which meet the requirements. An example of this procedure is illustrated by Table XX which lists all the hybrids which had a flexural modulus of 17.5×10^6 psi or greater along with the fiber types, construction, flexural strength, and fiber cost information. Also listed for comparison are similar properties of AS and HMS composites. Fiber cost per lb was calculated by multiplying the fiber ratio times the fiber cost. Fiber cost per $in.^3$ of composite was obtained by multiplying fiber cost per pound times composite density. The modulus criterion of 17.5×10^6 psi was selected as being a level which could be readily achieved with single component AS graphite-epoxy composites. It is clear that several hybrid systems were capable of producing essentially the same modulus as AS composites with lower overall fiber costs per pound. The AS/25 percent glass intraply composite was 25 percent lower in fiber cost than the AS composite, and had essentially the same flexural strength. The only HMS hybrid which had a lower cost per lb than the AS material was the HMS-55/glass-45 interply which had a lower flexural strength. Thus, the usefulness of that system might depend on whether strength was of critical importance for the particular application. Many of the HMS hybrids which cost more per pound than AS also had higher moduli, and if a structure was stiffness limited it might be possible to achieve a more efficient design or use thinner sections than if AS was the reinforcing fiber.

The advantage of Kevlar 49 (PRD) as a hydridizing fiber is brought out in the column showing fiber costs per cubic inch of composite. Due to the low density of Kevlar 49 versus that of S-glass, it becomes a much more attractive candidate if weight is an important consideration. Another possible advantage for Kevlar 49 in comparing it with S-glass in hybrids is the known degradation of glass by moisture. The manufacturer of Kevlar 49 (DuPont) claims much better moisture resistance compared to glass.

It is interesting to note that none of the core-shell constructions met the modulus requirement, although as mentioned previously, reversing the reinforcing fibers in the core and shell would have changed the situation.

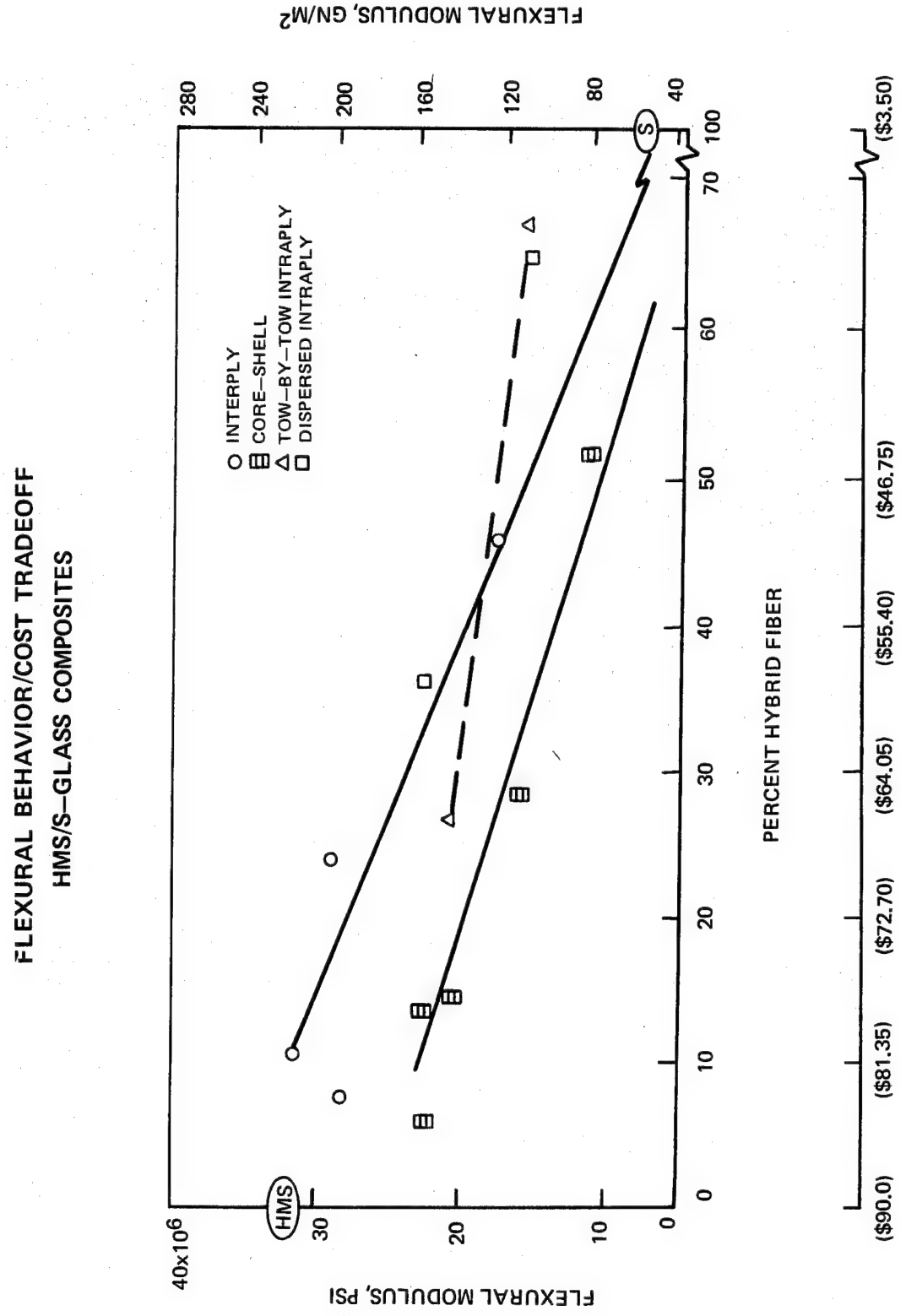
FLEXURAL BEHAVIOR/COST TRADEOFF
HMS/S–GLASS COMPOSITES
FLEXURAL MODULUS, GN/M2
280
240
200
160
120
80
40
INTERPLY
CORE–SHELL
TOW–BY–TOW INTRAPLY
DISPERSED INTRAPLY
S
100
70
60
50
40
30
20
10
0
HMS
40x10^6
30
20
10
0
FLEXURAL MODULUS, PSI
PERCENT HYBRID FIBER
(TOTAL FIBER COST/LB)
($90.0)
($81.35)
($72.70)
($64.05)
($55.40)
($46.75)
($3.50)

FIG. 35

FLEXURAL BEHAVIOR/COST TRADE OFF

HMS–KEVLAR 49 COMPOSITES

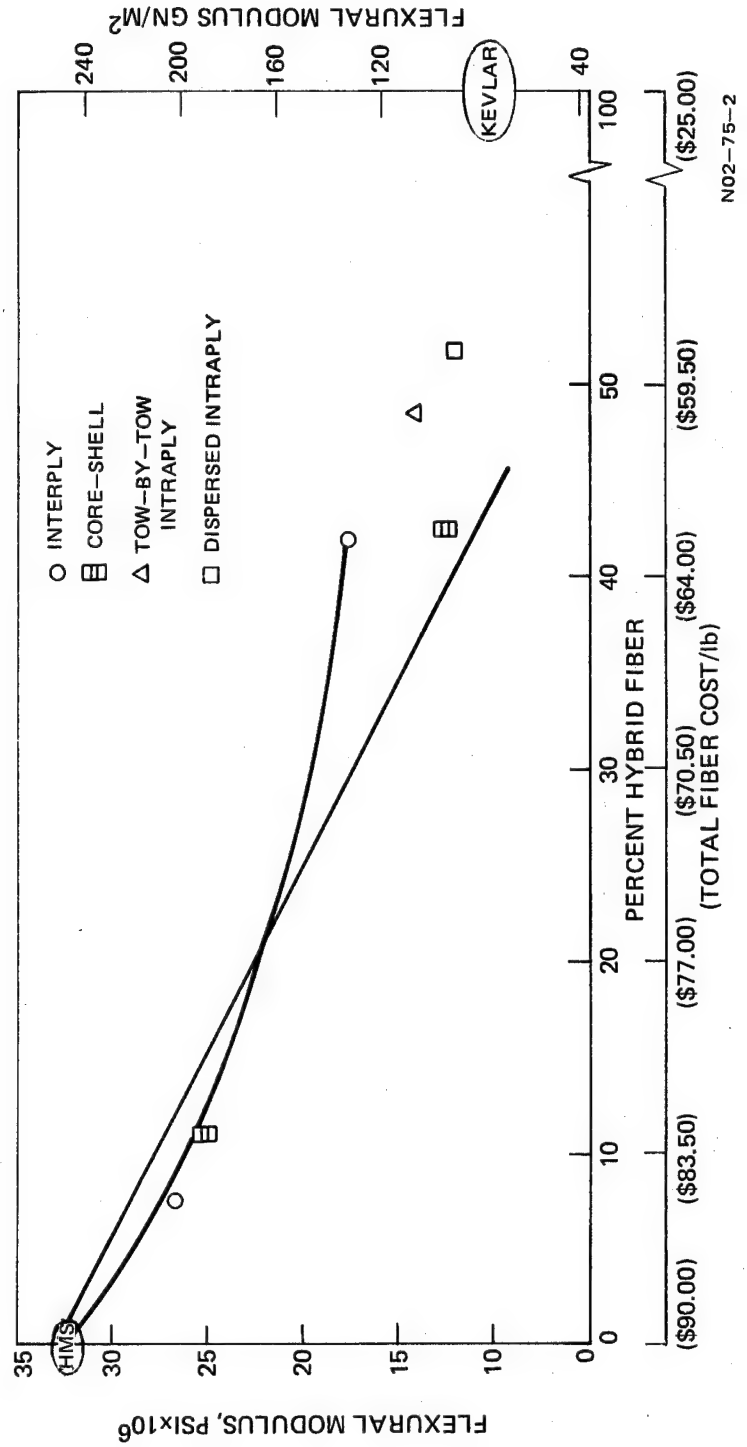

FIG. 36

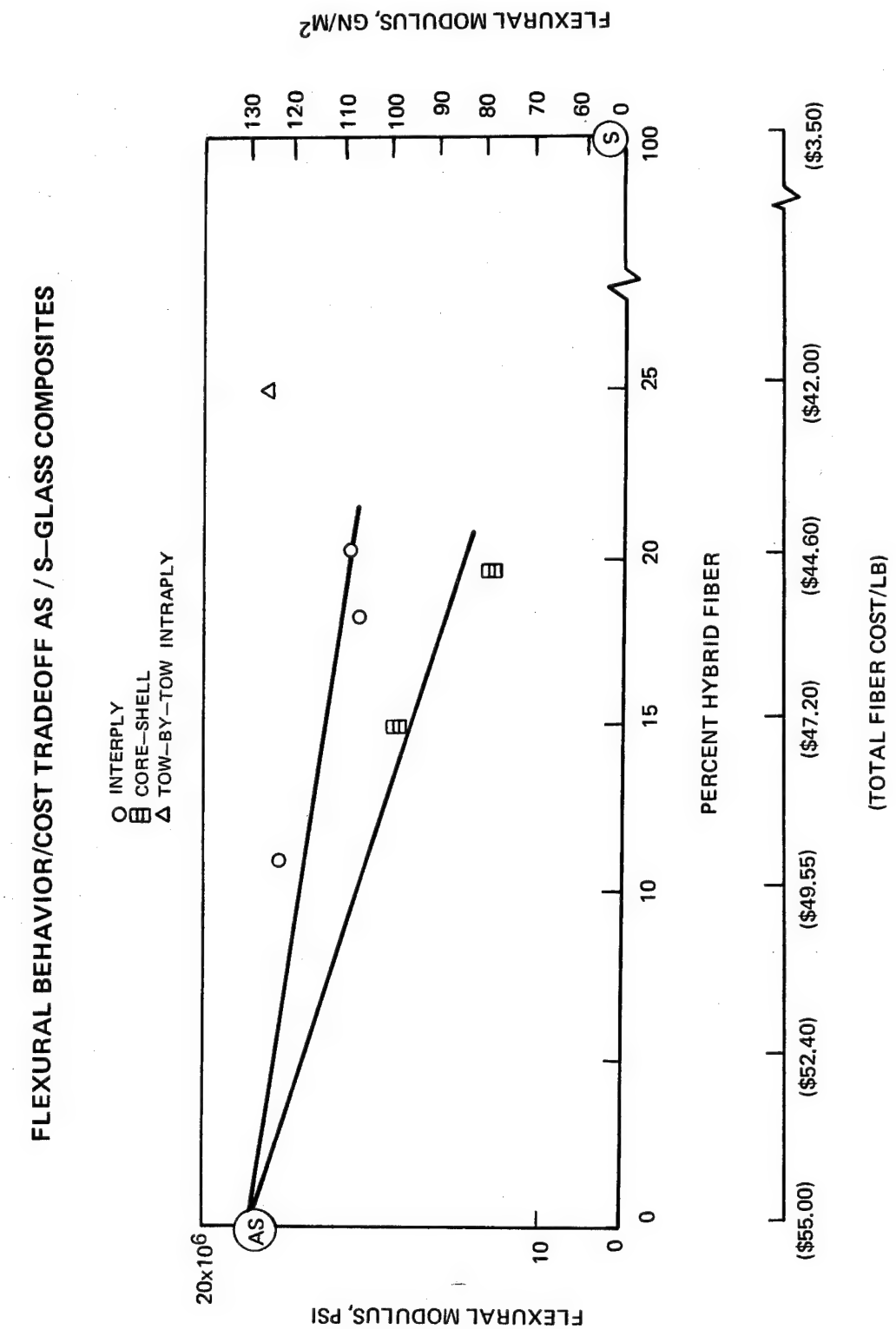
FLEXURAL BEHAVIOR/COST TRADEOFF AS / S–GLASS COMPOSITES
INTERPLY
CORE–SHELL
TOW–BY–TOW INTRAPLY
FLEXURAL MODULUS, PSI
FLEXURAL MODULUS, GN/M2
20x10^6
AS
S
0
10
0
10
15
20
25
0
60
70
80
90
100
110
120
130
PERCENT HYBRID FIBER
($55.00)
($52.40)
($49.55)
($47.20)
($44.60)
($42.00)
($3.50)
(TOTAL FIBER COST/LB)

N11–8–4

FIG. 37

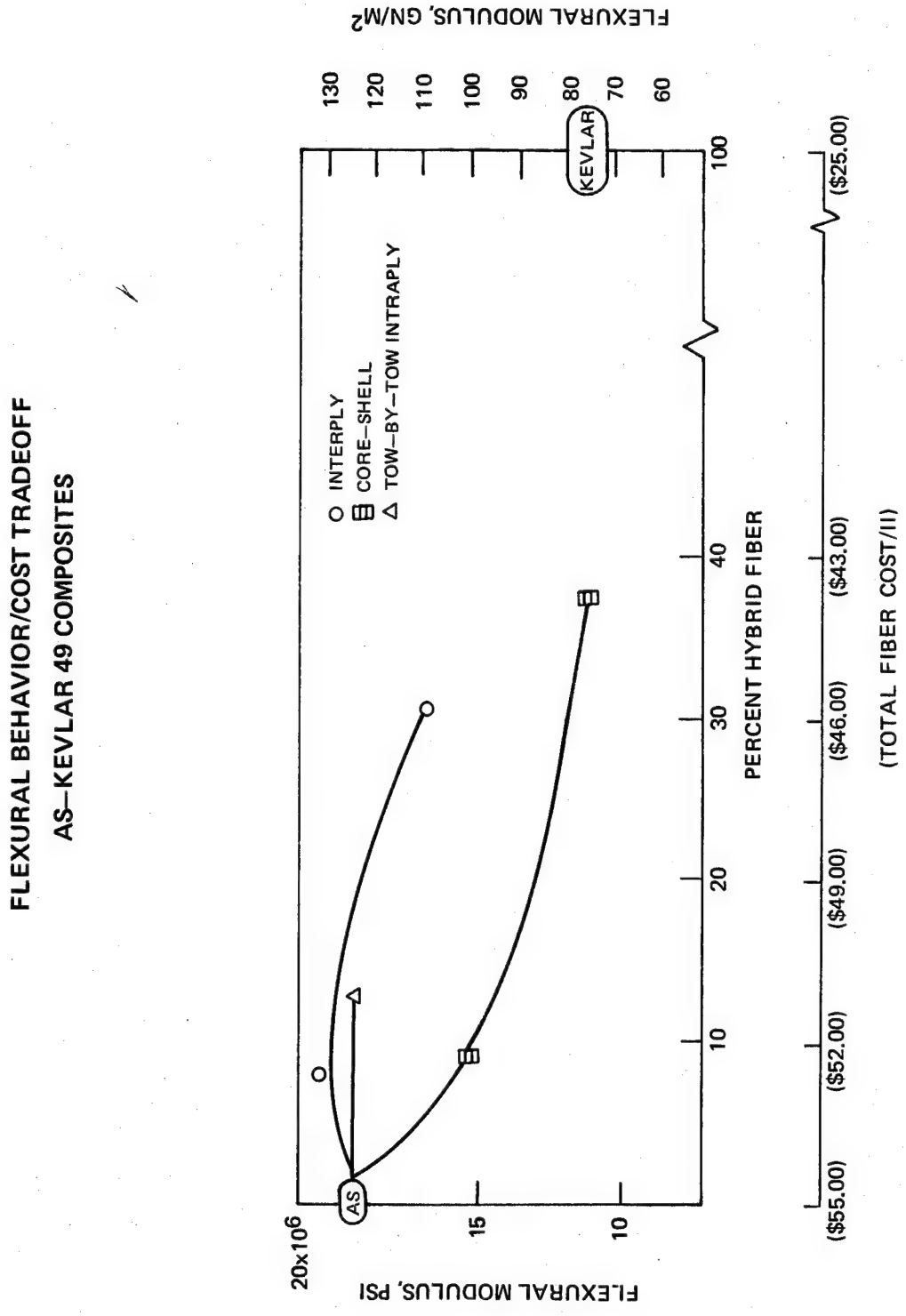

N10–326–4

Table XX

Hybrid Composite Systems Having Greater Than 17.5 x 10^6 psi Flexural Modulus and Costing Less Than $70.00/lb

Fibers (Ratio, v/o)	Construction	Flexural Modulus msi	Flexural Strength ksi	Fiber Cost/lb	Fiber Cost/ $in.^3$ Composite
AS-75 S-glass-25	intraply	18.5	270	$42.00	$2.66
AS-90 S-glass-10	interply	17.8	245	49.55	2.94
HMS-55 S-glass-45	interply	17.5	200	51.08	3.36
AS-85 Kevlar-15	intraply	18.3	290	51.50	2.90
AS-85 Kevlar-15	interply	18.0	225	51.50	2.88
HMS-65 S-glass-35	intraply	22.5	171	59.73	3.94
HMS-60 Kevlar-40	interply	17.8	145	64.00	3.54
HMS-75 S-glass-25	intraply	20.6	171	68.38	4.45
HMS-75 S-glass-25	interply	28.7	190	68.38	4.34
AS	-	18.1	275	55.00	3.16
HMS	-	27.5	175	90.00	5.33

2.2.6 Conclusions from Task I Results

S-glass is, in general, a better reinforcement than Kevlar 49 for strength and pendulum impact properties. Modulus restrictions may limit to some extent AS/S-glass combinations.

With HMS laminates interply hybrids result in the highest moduli for a given hybrid system while in AS laminates intraply hybrids are superior.

Core-shell hybrids, with secondary fibers in the shell, suffer large bending modulus reductions as the amount of hybridizing fiber increases.

Addition of S-glass to HMS graphite causes no loss in flexural strength regardless of ply construction; while with AS graphite flexural strength decreases with increasing glass content except for intraply (tow-by-tow) which gave strengths equivalent to homogeneous AS composites.

Addition of Kevlar 49 to HMS graphite causes large decreases in flexural strength above 10 v/o independent of ply construction. Similar results with AS are obtained except with the intraply tow-by-tow construction which like S-glass resulted in no decrease in flexural strength compared to AS graphite.

Hybrid composite shear strength is generally limited by the weakest link.

In intraply composites the tow-by-tow hybrid configuration is generally superior in pendulum impact behavior to the dispersed fiber type.

Additions of Kevlar 49 to HMS graphite do not provide significant improvements in impact regardless of ply construction.

For pendulum impact tests (Charpy) using standard size specimens total impact energy (E_t) rather than the more difficult to obtain initial fracture energy (E_i) and crack propagation energy (E_p) can be used to correlate impact behavior with other mechanical properties.

The instrumented pendulum impact test provides valuable information for evaluating materials beyond that which can be obtained from standard tests particularly with thin Charpy specimens.

The standard pendulum impact test is shear limited. With thinner specimens the influence of shear on total impact appears to decrease. Bending stresses calculated from P_{max} load obtained in the thin Charpy test correlate well with static three point flexural test results.

In terms of fiber material costs the AS/S-glass (25 v/o) intraply composite was 25 percent lower than homogeneous AS while maintaining the same flexural and shear strengths and flexural modulus with considerably improved impact resistance. These results strongly indicate the need for further investigation of the tow-by-tow AS/S-glass composition to determine (1) the level of hybrid fiber which can be added before a decrease in flexural strength and modulus occurs, (2) the optimum impact strength level which can be reached, and (3) an estimate of the minimum fiber cost which can be obtained.

III. TASK II - IMPACT STRENGTH EVALUATION OF ANGLEPLY AND THIN MULTI-FIBER EPOXY RESIN COMPOSITE LAMINATES

The data analysis of Task I has shown that results with the standard Charpy specimens are shear limited, and if laminate types were selected on this basis alone they might preform unsatisfactorily in ballistic impact tests and, ultimately in component evaluation. In addition, results from Task I indicated that bending stresses calculated from the P_{max} load obtained in thin specimen Charpy tests correlate well with the static three point flexural test results. On the basis of total energy absorption the two tests (thin and thick Charpy) give the same order of ranking for the composites tested. However, on the basis of maximum stresses achieved before failure the rankings were different. In fact the poorest ranking composite in the thick specimen test became the best composite in the thin specimen test. Since the primary objective of the program is to provide multi-fiber composites of maximum impact resistance, it was felt that it was important to gain a better understanding of the correlation between pendulum impact strength testing and the ballistic testing before laminate hybrid types are selected for extensive evaluation.

The primary objective of Task II was to determine the relationship, if any, between pendulum and ballistic impact tests using selected angle-ply hybrid composite types. In addition, the relationship between impact specimen configuration, both angle-ply and unidirectional, with other composite mechanical properties was investigated.

3.1 Thin Angle-Ply Composites

A series of laminates were fabricated using the following angle-ply configurations:

(A) $\pm$40, 0, +10, 0, -10, -10, 0, +10, 0, $\pm$40
(B) $\pm$22, 0, +22, 0, -22, -22, 0, +22, 0, $\pm$22
(C) $\pm$45, 0, +45, 0, -45, -45, 0, +45, 0, $\pm$45

The first angle-ply has been shown by Hanson and Chamis (Ref. 6) to be an effective design for high tip speed compressor blades, the second has been employed by General Electric and the third corresponds to the angle-ply configuration used by Pratt & Whitney Aircraft in a current NASA contract (Ref. 7). Twelve ply laminates were fabricated with each angle-ply configuration using the following fiber combinations and ERLA-4617 epoxy resin:

Type 2-UARL Intraply-HMS(75)/S-glass(25)
Type 1-UARL Intraply-AS(80)/S-glass(20)
Type 12-Interply-AS(90)/Kevlar 49(10)

These composition types were selected on the basis of good overall mechanical properties and variation of hybrid fiber reinforcement and composite construction. In the Type 12 interply laminate Kevlar 49 was used in the outermost 0° plies. The physical properties for each fabricated laminate are listed in Table XXI. Specimens for flexural strength and modulus as well as instrumented thin Charpy tests were cut from a 3.82 cm (1.5 in.) x 12.7 cm (5.0 in.) panel. Fabricating conditions were the same as those described in the Appendix.

The HMS/S-glass Type 2-UARL laminates were fabricated using two different levels of glass content. This was achieved by use of 20 end and 12 end glass roving as indicated. The higher per ply thickness obtained in the interply AS/Kevlar 49 laminates is primarily due to the Kevlar 49. For the ballistic specimens the Kevlar prepreg was spread to help reduce the overall composite thickness. As noted, one composite having $\pm 30°$ instead of $\pm 40°$ plys was inadvertently fabricated.

3.1.1 Static Properties of Thin Angle-Ply Composites

The flexural strength and modulus of the composites made using the three angle-ply configurations and three hybrid fiber combinations are listed in Table XXII. Comparison of the flexural strengths and modulus of the two HMS/S-glass systems (NASX-2 to 4 = 37-38 v/o glass and NASX-11 to 13 = 26 v/o glass) shows that the effect of higher glass content is mainly reflected in the moduli of the two sets of composites, with the lower glass content resulting in greater stiffness, particularly for the $\pm 40,0,10$ and $\pm 22,0$ configurations while the two $\pm 45,0$ laminates gave essentially the same modulus. This latter result is undoubtedly due to the low modulus of the $\pm 45,0$ configuration which resulted in the masking of any hybrid fiber concentration effect. The flexural strengths of the corresponding laminates were nearly the same showing no marked change with varying glass content. It is interesting to note that changing the 40° angle-plies in NASX-2 to 30° (NASX-1) resulted in a modulus 1.5 times greater for the latter angle-ply with only a slight change in flexural strength. Comparison of the flexural strengths of composites NASX-5 through NASX-13 shows that with the intraply composites the strength decreases in the order of $\pm 40,10,0 > \pm 22,0 > \pm 45,0$ type angle-ply. The interply AS/Kevlar 49 laminate (composition 12) is slightly different with $\pm 22,0 > \pm 40,10,0 > \pm 45,0$ angle-ply.

The flexural modulus with all three angle-ply constructions irregardless of composition type or laminate construction decreases in the order of $\pm 22,0 > \pm 40,10,0 > \pm 45,0$ angle-ply. Of particular interest is the equivalent moduli obtained with the 1-UARL (AS/S-glass) and type 12 (AS/Kevlar 49) laminates. Although the former is intraply and the latter interply it would be expected that the modulus of the type 12 composite should be considerably higher. It is hypothesized that the lower than expected modulus of the type 12 system is due to the contribution of the much lower shear modulus of Kevlar 49 vs S-glass. Shear deflection is not accounted for in the equation used to calculate flexural modulus.

Table XXI

Physical Properties of Angle-Ply Hybrid Fiber Epoxy Matrix Composites

UARL No.	Composition Type	Angle-Ply[c]	Thickness mil/ply	Density g/cc	v/o Resin	v/o Fiber	v/o Void	v/o Fiber Ratio
NASX-1	2-UARL[a]	$[\pm 30,0,+10,0,-10]_2$	7.1	1.81	32	HMS-41 S-24.4	2.6	HMS-62.7 S-37.3
-2	"	A	7.5	7.5	41.8	HMS-34.9 S-21.6	1.7	HMS-61.8 S-38.2
-3	"	B	8.2	1.72	45.8	HMS-32.9 S-20	1.3	HMS-62.3 S-37.7
-4	"	C	8.8	1.71	46.3	HMS-33.0 S-19.2	1.5	HMS-63.1 S-36.9
-5	1-UARL[b]	A	6.3	1.71	29	AS-51 S-16.5	3.5	AS-75.7 S-24.3
-6	"	B	6.5	1.74	31.7	AS-50.7 S-16.7	0.8	AS-75.4 S-24.6
-7	"	C	6.7	1.73	30.5	AS-51.4 S-16.4	1.7	AS-76.3 S-23.7
-8	12	A	11.5	1.56	22.5	AS-63.8 Kevlar-7.9	5.8	AS-89.2 Kevlar-10.8
-9	"	B	11.5	1.55	24.5	AS-62.1 Kevlar-7.4	5.9	AS-89.5 Kevlar-10.5
-10	"	C	10.9	1.54	26.8	AS-58.2 Kevlar-9.8	5.2	AS-85.3 Kevlar-14.7

Table XXI (Cont'd)

UARL No.	Composition Type	Angle-Ply	Thickness mil/ply	Density g/cc	v/o Resin	v/o Fiber	v/o Void	v/o Fiber Ratio
NASX-11	2-UARL[b]	A	6.35	1.73	35.7	HMS-44.4 S-16.7	3.2	HMS-72.5 S-27.5
-12	"	B	6.67	1.72	35.5	HMS-43.9 S-16.5	4.1	HMS-72.8 S-27.2
-13	"	C	6.67	1.77	30.1	HMS-48.4 S-17.7	3.8	HMS-73.2 S-26.8

[a]Fabricated tow-by-tow using Ferro S-glass 20 end roving

[b]Fabricated tow-by-tow using Owens-Corning S-glass 12 end roving

[c]A = $\pm$40,0,10; B = $\pm$22,0; C = $\pm$45,0

Table XXII

Flexural Strength and Modulus of Angle-Ply Hybrid Fiber Epoxy Matrix Composites[a]

UARL No.	Composition Type	Angle-Ply[b]	Flexural Strength GN/m^2	(ksi)	Flexural Modulus GN/m^2	($psix10^6$)
NASX-1	2-UARL	-[c]	0.47	(68.7)	69.6	(10.12)
-2	"	A	0.457	(66.3)	46.9	(6.81)
-3	"	B	0.49	(71.05)	87.6	(12.71)
-4	"	C	0.39	(56.6)	46.7	(6.78)
-5	1-UARL	A	0.816	(118.5)	53.5	(7.75)
-6	"	B	0.745	(108)	84.8	(12.3)
-7	"	C	0.58	(84.1)	35.8	(5.19)
-8	12	A	0.398	(57.7)	54.8	(7.95)
-9	"	B	0.43	(62.3)	85.1	(12.35)
-10	"	C	0.30	(43.5)	31.8	(4.4)
-11	2-UARL	A	0.51	(74)	57.5	(8.35)
-12	"	B	0.483	(70)	104	(15.1)
-13	"	C	0.358	(52)	45.6	(6.61)

[a] Tests conducted at room temperature, S/D = 32/1, 3-point loading. Duplicate tests.

[b] A = $\pm$40,0,10; B = $\pm$22,0; C = $\pm$45,0.

[c] Angle-ply $\pm$30,0,+10,0,-10,0; 0,-10,0,+10,0,$\pm$30

3.1.2 Dynamic Properties of Thin Angle-Ply Composites

The Charpy impact loads and strengths for the thin composites are listed in Table XXIII. Data for both composites of each type are listed. For the three composite types tested the ±40,0,10 angle-ply configuration resulted in the highest impact strength (ft-lbs/in.^{2}) with AS/S-glass (1-UARL) > AS/Kevlar 49 (Type 12) > HMS/S-glass (2-UARL). With the first two types the ±22,0 angle-ply was nearly as effective in terms of impact while the latter type (2-UARL) showed a substantial decrease in impact response in both the ±22,0 and ±45,0 configuration compared to the ±40,0,10.

In the HMS/S-glass containing the high glass content (NASX-2,3,4) the ±22,0 configuration was superior and all angle-ply configurations were higher than the comparable lower glass content composites (NASX-11,12,13) as would be predicted.

With two exceptions the P_i and P_{max} loads were identical indicating that the main failure mode was in flexure. Composites NASX-6 (AS/S-glass ±22,0) and NASX-8 (AS/Kevlar 49 ±40,0,10) showed indications of shear failure by a definite P_i prior to reaching P_{max}. These data are shown in Table XXIII. No positive explanation for this occurrence has been found. As mentioned previously, there is some degree of uncertainty associated with identification of P_i. With these angle-ply systems, however, it is clear that P_i and P_{max} for the most part occur at the same load level which is contrary to the standard Charpy thick specimens.

The relationship between static property and impact strength as affected by angle-ply is shown in Fig. 38 which plots flexural modulus vs the average impact energy in ft-lbs/unit area for each composite. In terms of modulus the ±22,0 angle-ply is superior while the ±40,0,10 angle configuration results in the highest impact strengths.

It is interesting to note that there is little variation in either modulus or impact energy between the HMS/S-glass (37 v/o), AS/Kevlar or AS/S-glass composites using the ±22,0 configuration. For every angle-ply, however, the intraply AS/S-glass system appears to offer the best combination of modulus and impact energy.

3.1.3 Varying Thickness Angle-Ply Composites

To gain a better understanding of the effect of thickness on composite impact properties and to aid in the correlation of pendulum impact vs ballistic impact, a series of laminates of each composite type was fabricated using the ±22,0 angle-ply configuration. Specimens of approximately 0.127, 0.254, 0.508, 0.90 and 1.016 cm (0.50, 0.100, 0.200, 0.300 and 0.400 in.) thickness have been made with the AS/S-glass, HMS/S-glass intraply and AS/Kevlar interply types. The

Table XXIII

Impact Data for Thin Angle-Ply Hybrid Fiber Epoxy Composites

UARL No.	Composition Type[a]	Angle-Ply[b]	$P_i = P_{max}$ Newtons	Newtons	(lbs)	(lbs)	Charpy Impact Strength Joules	(ft-lbs)	Impact Strength Per Unit Area Joules/cm^2	(ft-lbs/in^2)
NASX-1	2-UARL	-[c]	334	369	(75)	(83)	-/1.74	(-/1.24)	8.1	(37.4)
-2	"	A	320	426	(72)	(96)	2.35/3.14	(1.68/2.24)	10.38/13.3	(47.8/61.3)
-3	"	B	497	497	(112)	(112)	3.38/3.89	(2.42/2.78)	13.5/15.04	(62.2/69.4)
-4	"	C	426	426	(96)	(96)	2.62/1.75	(1.87/1.25)	9.7/6.48	(44.7/29.9)
-5	1-UARL	A		444	(104)	(100)	3.52/3.16	(2.51/2.26)	18.1/16.1	(83.4/74.2)
-6	"	B	P_i 444	466	(100)	(105)	3.14/2.69	(2.24/1.92)	15.8/13.55	(72.9/62.4)
			P_{max} 534	534	(120)	(120)				
-7	"	C	400	444	(90)	(100)	2.1/2.7	(1.50/1.93)	10.4/12.78	(48/58.8)
-8	12	A	P_i 835	845	(188)	(190)	5.22/5.0	(3.73/3.57)	14.75/13.95	(68/64.3)
			P_{max} 1200	1158	(270)	(260)				
-9	"	B	845	1022	(190)	(230)	4.76/5.14	(3.40/3.67)	13.35/14.3	(61.5/66)
-10	"	C	622	578	(140)	(130)	3.01/3.15	(2.15/2.25)	9.15/9.86	(42.2/45.5)
-11	2-UARL	A	311	311	(70)	(70)	-/1.51	(-/1.08)	-/12.4	(-/57.2)
-12	"	B	267	249	(60)	(56)	1.33/1.37	(0.95/0.98)	6.6/6.9	(30.4/31.8)
-13	"	C	267	327	(60)	(73.5)	-/1.595	(-/1.14)	-/8.06	(-/37.2)

[a]2-UARL = HMS/S-glass; 1-UARL = AS/S-glass; 12 = AS/Kevlar 49

[b]A = $\pm$40,0,10; B = $\pm$22,0; C = $\pm$45,0

[c]Angle-ply $\pm$30,0,+10,0,-10,0,0,-10,0,+10,0,$\pm$30

FIG. 38

FLEXURAL MODULUS – PENDULUM IMPACT ENERGY/UNIT AREA OF ANGLE–PLY COMPOSITES

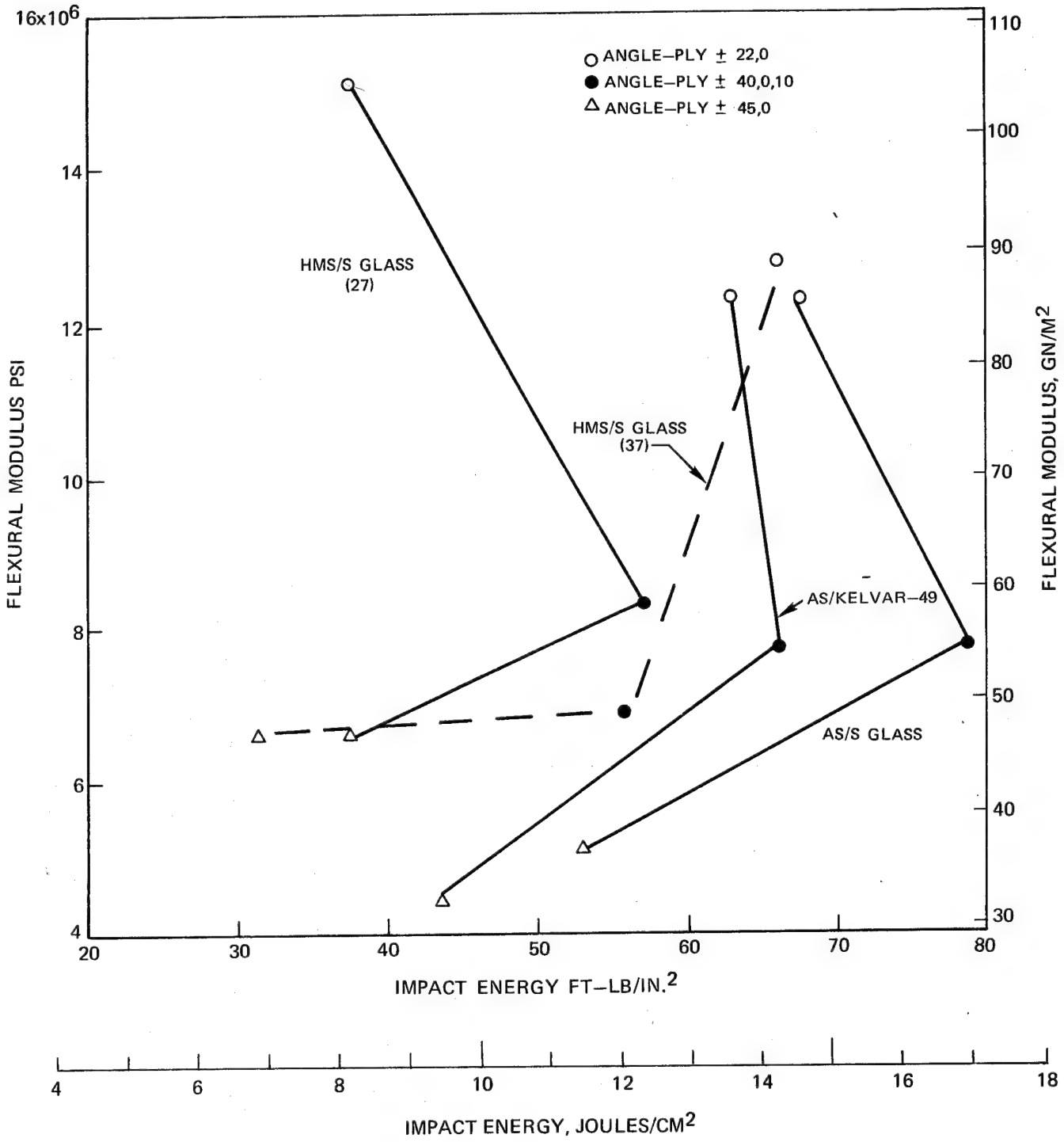

N05–250–5

±22,0 angle-ply was chosen because it produced the highest modulus values. In addition, because of superior impact response, the AS/S-glass intraply type was also fabricated in the same thickness series using the ±40,0,10 angle-ply. Three specimens were cut from a 3.81 cm (1.5 in.) x 6.03 cm (2 3/8 in.) block for each thickness level. Two were tested by instrumented Charpy and one in slow bend. The thickness and density of each thickness level is listed in Table XXIV as is the average Charpy impact energy and energy/unit area.

Figure 39 illustrates graphically the relationship of thickness to Charpy impact strength (ft-lb/sq. in.). The AS/S-glass and HMS/S-glass ±22,0 laminates follow the same general trend of increasing impact strength with increasing thickness. The AS/S-glass in the ±40,0,10 angle-ply however gave no increase in impact energy up to 0.200 in. thickness. Above this thickness level the rise in impact energy was essentially the same as that for the ±22,0 angle-ply. The AS/Kevlar ±22,0 laminates gave an opposite trend with impact energy increasing up to 0.250 in. thickness before leveling off at an energy level below the two AS/S-glass systems. This is probably a reflection of the predominance of the shear failure mode in the thicker laminates coupled with the poor shear capability of Kevlar 49 reinforcement.

With the two angle configurations using the AS/S-glass system, as previously found, Fig. 38, the ±40,0,10 configuration has a higher impact energy than the ±22,0 using specimens up to 0.354 cm (0.140 in.) thick. Beyond this level the latter angle-ply provides a higher impact resistance. This may be due to the higher flexural strength of the ±40,0,10 composite at the 0.254 cm thickness level (see Table XXII) which is reflected by the failure mode being in bending rather than shear which predominates for the standard Charpy specimens.

Comparison of the three ±22,0 angle-ply types indicates, particularly with the HMS/S-glass and AS/Kevlar 49 composites, a definite change in impact energy levels near the 0.508 cm (0.200) thickness range. This may well be the thickness range where the failure mode changes from predominantly bending to shear.

The instrumented Charpy load-time traces of these same composites are shown in Figs. 40-43.

The influence of specimen thickness is clearly seen in each case with a substantial change in the curve shape occurring above the 0.100 in. level in terms of time to reach the maximum load level. Above 0.200 in. thickness the traces with minor exceptions tend to follow the same pattern. These results indicate that a change in fracture mechanism occurs in the vicinity of a span-to-depth ratio of 10-15/1.

Table XXIV

Angle-Ply Hybrid Fiber Composites of Varying Thickness

Composite No.	Type	Fiber	Cross-Ply	Thickness[a] cm	(in.)	Density g/cc[a]	Charpy Impact Energy[b] Joules	(ft-lbs)	Charpy Impact Energy/Unit Area[b] Joules/cm^2	(ft-lbs/in.^{2})
NASX-6	1-UARL	AS/S-glass	±22,0	0.127	(0.050)	1.74	1.68	(1.2)	13.2	(61.0)
				0.279	(0.110)	1.69	4.76	(3.4)	17.2	(78.5)
				0.508	(0.200)	1.70	11.75	(8.4)	23.2	(106.2)
				0.772	(0.304)	1.75	21.2	(15.1)	27.4	(125.0)
				1.05	(0.413)	1.74	39.2	(28.0)	37.4	(176.0)
NASX-9	12	AS/Kevlar	±22,0	0.1245	(0.049)	1.56	1.32	(0.93)	10.6	(48.2)
				0.246	(0.097)	1.56	3.64	(2.6)	14.75	(68.0)
				0.569	(0.224)	1.62	13.3	(9.5)	23.4	(107.6)
				0.748	(0.296)	1.55	15.6	(11.15)	20.9	(95.8)
				1.00	(0.394)	1.56	25.2	(18.0)	25.9	(116.0)
NASX-12	2-UARL	HMS/S-glass	±22,0	0.117	(0.046)	1.79	0.76	(0.54)	6.5	(29.8)
				0.262	(0.103)	1.75	1.85	(1.32)	7.1	(32.6)
				0.503	(0.198)	1.76	6.3	(4.5)	12.5	(57.7)
				0.74	(0.291)	1.76	10.8	(7.7)	14.6	(67.4)
				0.985	(0.388)	1.75	18.2	(13.0)	18.5	(84.6)
NASX-5	1-UARL	AS/S-glass	±40,0,10	0.223	(0.088)	1.755	4.2	(3.0)	18.8	(86.5)
				0.468	(0.184)	1.725	8.8	(6.3)	18.7	(87.0)
				0.721	(0.284)	1.725	16.1	(11.5)	22.3	(103.0)
				0.965	(0.380)	1.71	30.8	(22.0)	32.0	(146.5)

[a]Average of 3 values measured using specimens cut for instrumented Charpy test
[b]Average of 2 tests

CHARPY IMPACT ENERGY VS SPECIMEN THICKNESS (ANGLE–PLY COMPOSITES)

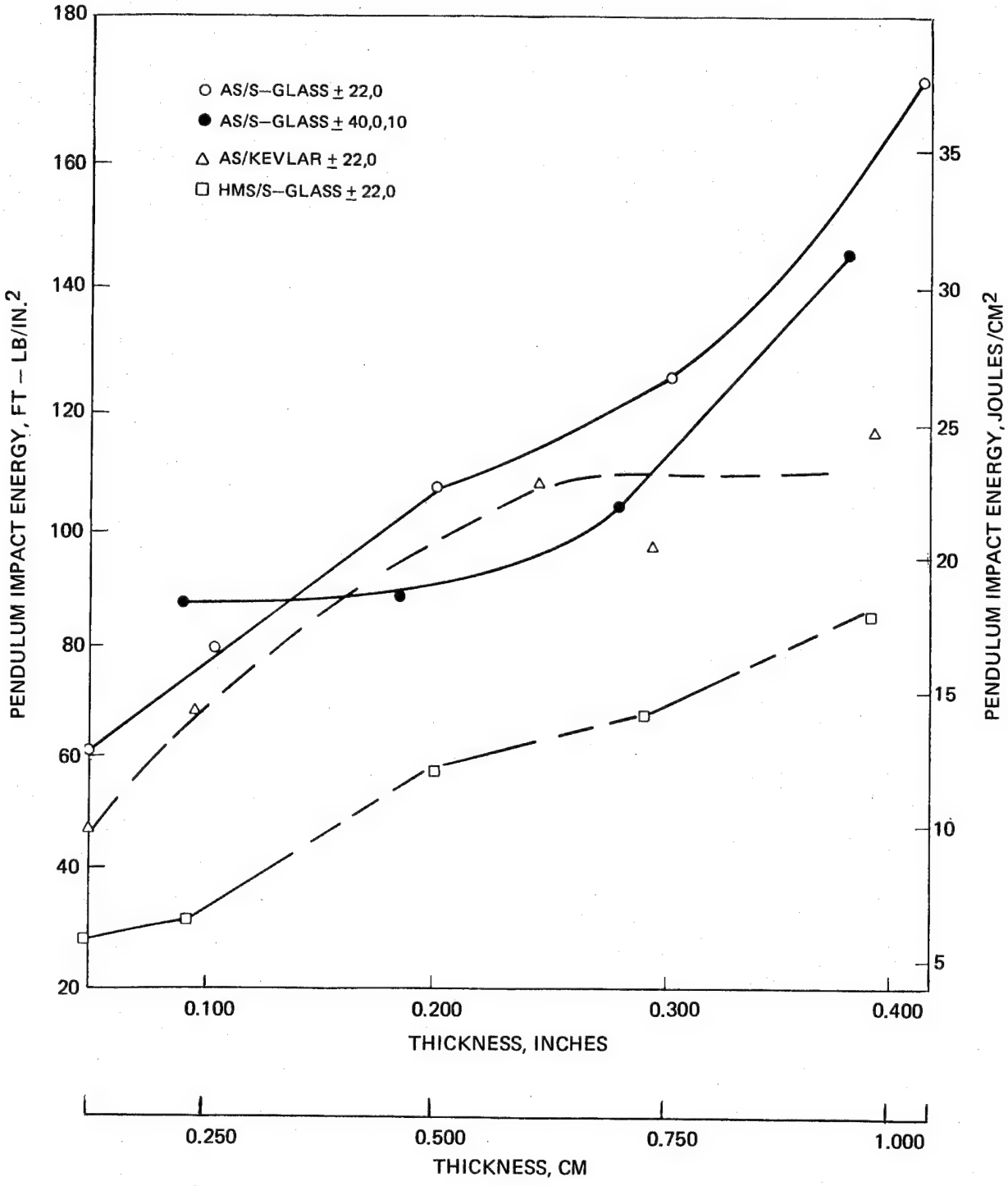

N07–15–2

FIG. 40

CHARPY LOAD–TIME TRACE

AS/S–GLASS NASX–6 $[\pm 22,0,+22,0-22]_S$ ANGLE–PLY
EFFECT OF THICKNESS

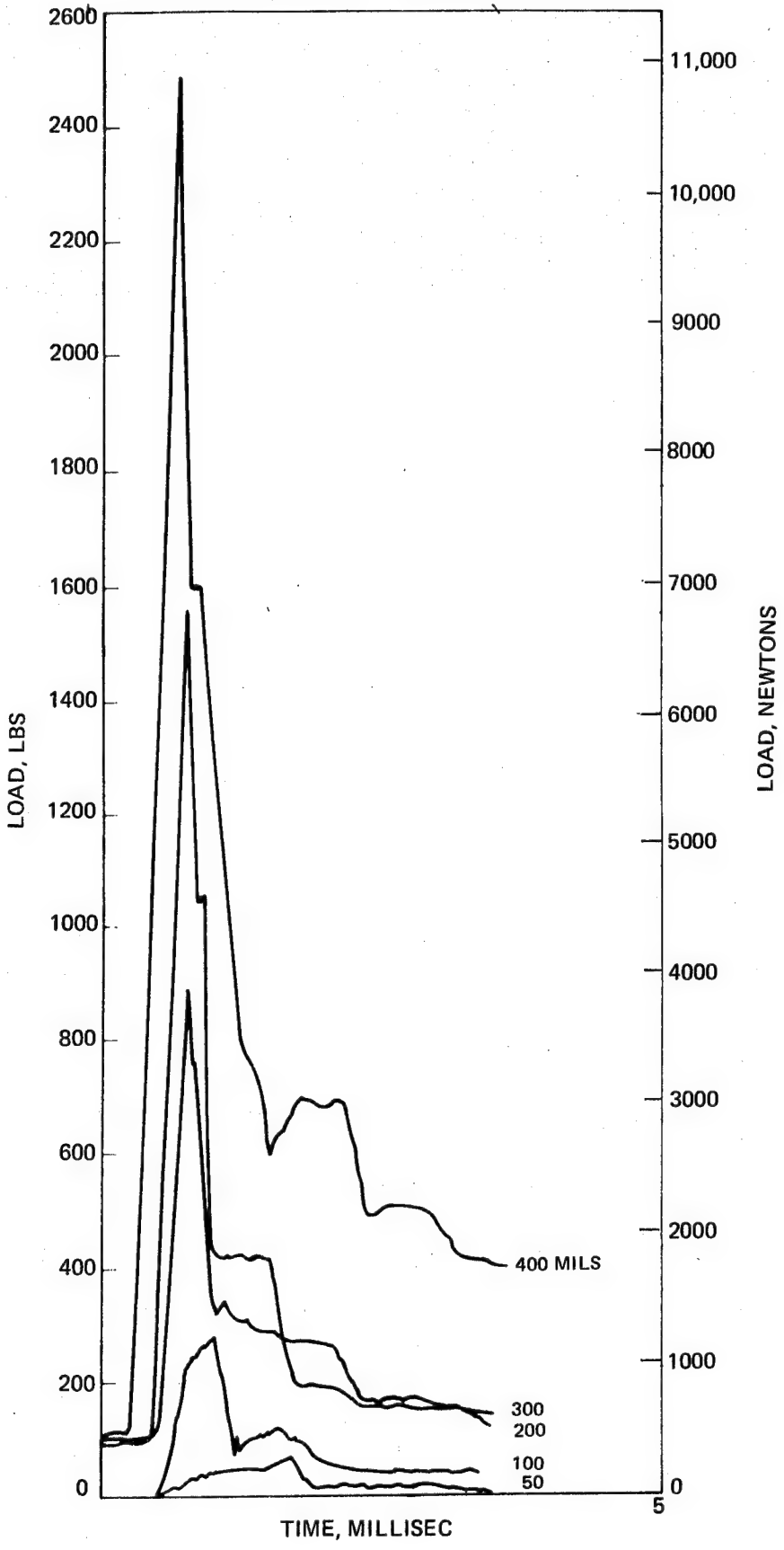

N07–15–1

FIG. 41

CHARPY LOAD–TIME TRACE

AS/S–GLASS NASX–5 $[\pm 40,0, +10,0,-10]_S$ ANGLE–PLY

EFFECT OF THICKNESS

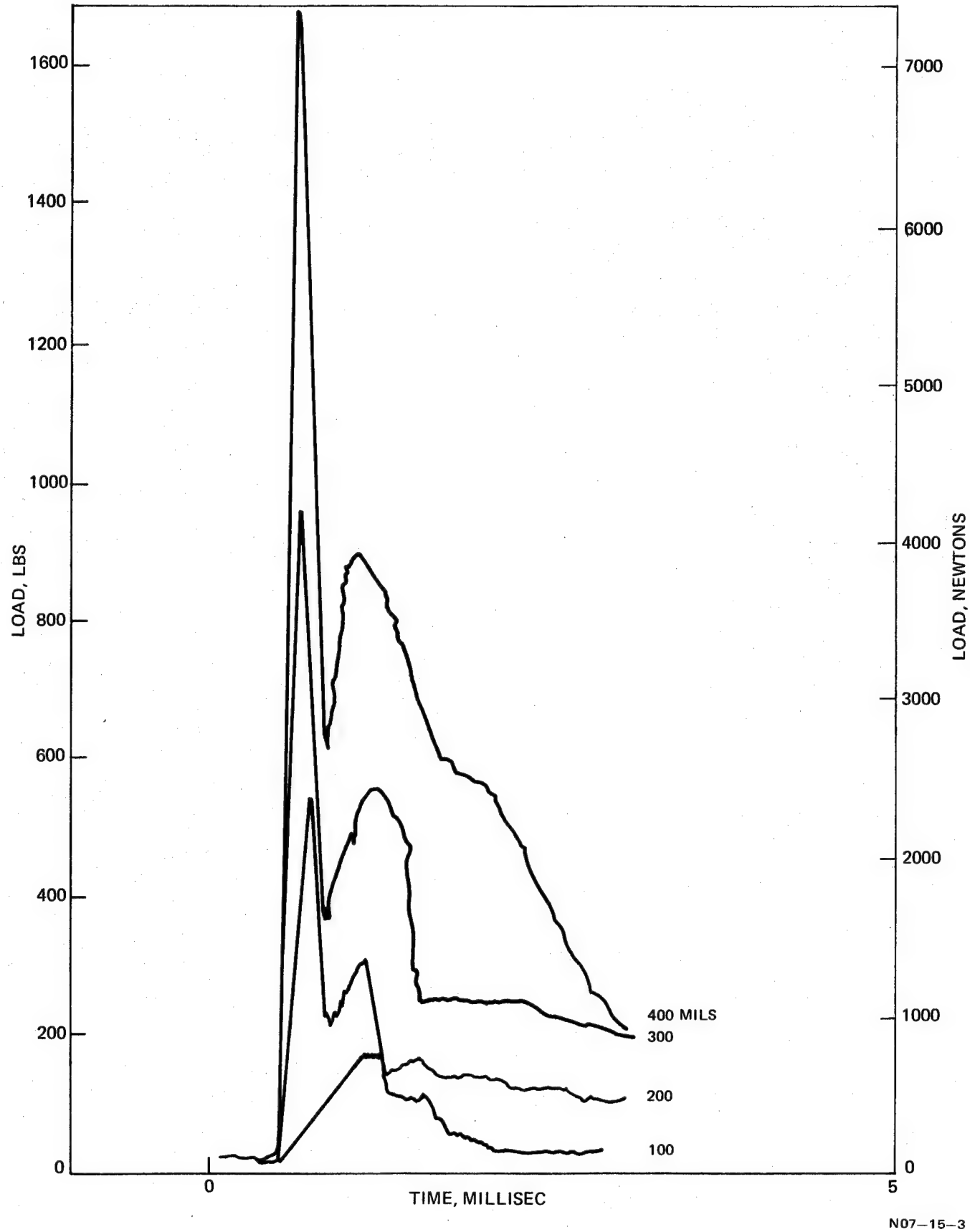

CHARPY LOAD–TIME TRACE

HMS/S–GLASS – NASX–12 $[\pm 22,0 + 22,0–22]_S$ ANGLE–PLY

EFFECT OF SPECIMEN THICKNESS

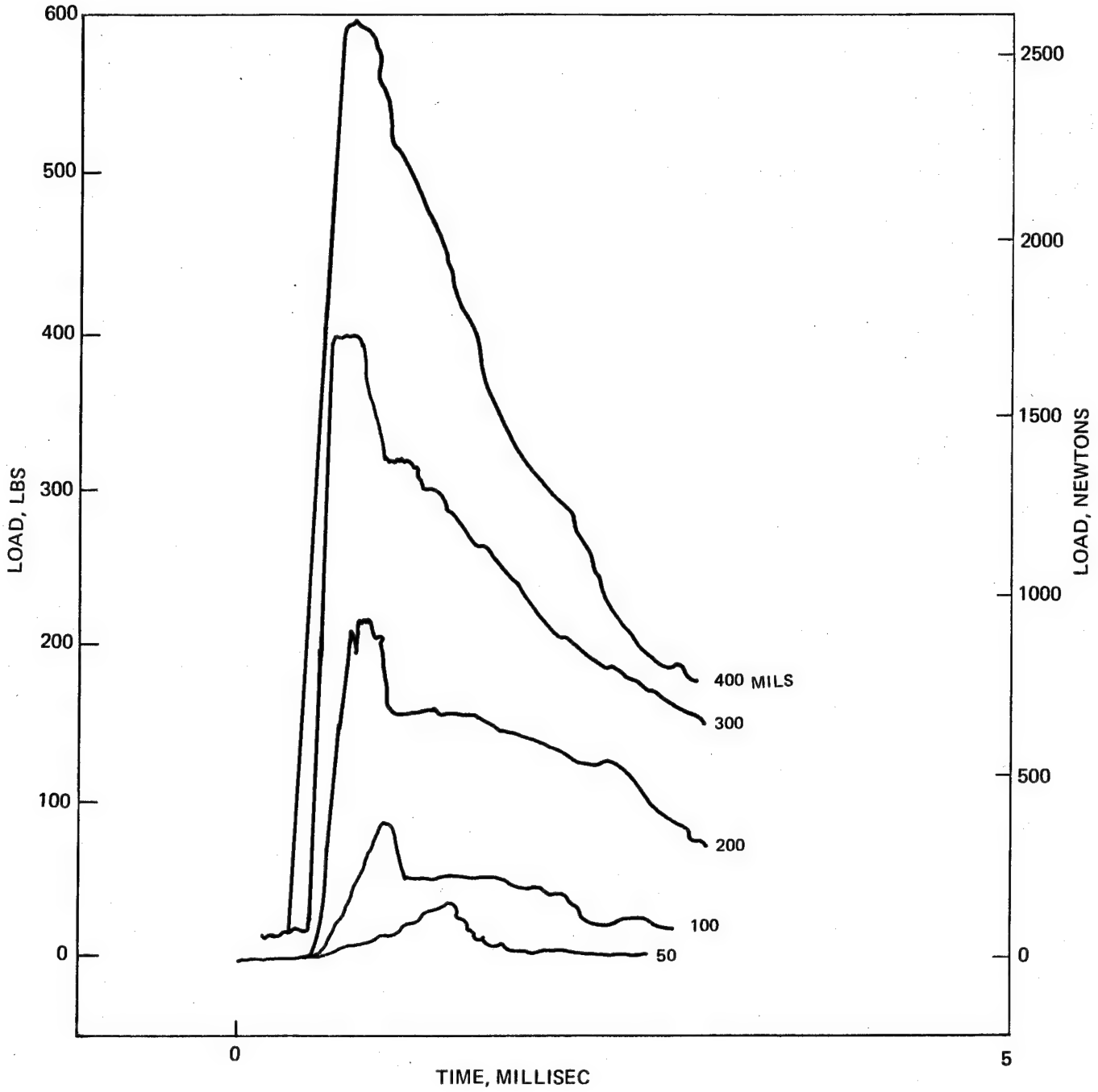

N07–15–4

FIG. 43

CHARPY LOAD–TIME TRACE

AS/KEVLAR 49 – NASX–9 $[\pm 22,0,+22,0-22]_S$ ANGLE–PLY
EFFECT OF SPECIMEN THICKNESS

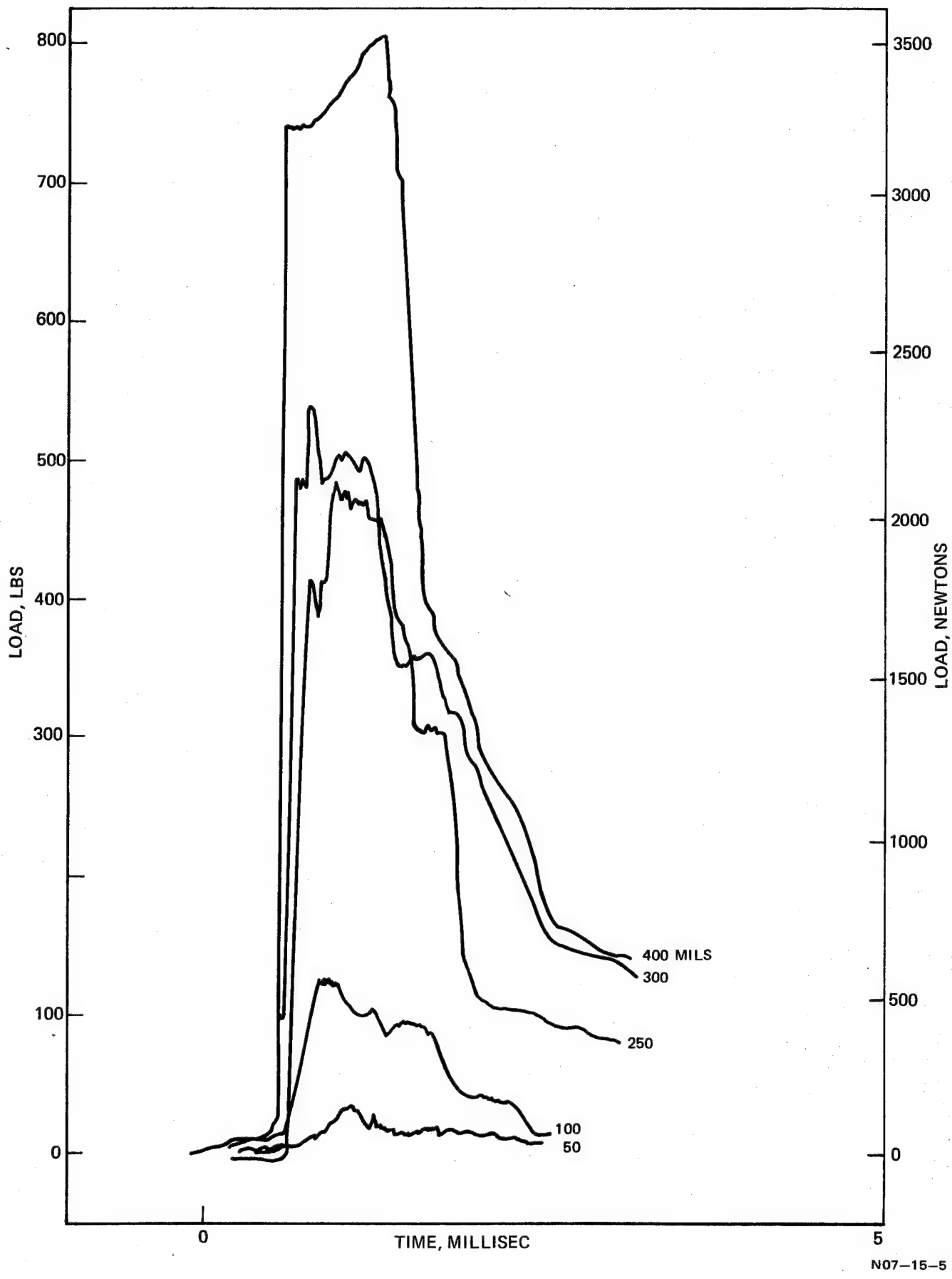

N07–15–5

The P_i and P_{max} of the $\pm$40,0,10 AS/S-glass intraply system at all thicknesses are the same, however, in the $\pm$22,0 angle-plys P_i and P_{max} are different for the 0.050 and 0.100 in. thick composites. The opposite holds true for the AS/Kevlar 49 interply laminates where P_i and P_{max} were the same at the two lower thicknesses but occur at different loads at 0.250 in. thickness and greater. The HMS/S-glass intraply composites P_i and P_{max} appear equivalent with the possible exception of the 0.200 in. thick specimen. These variations again indicate a possible shift in predominant impact fracture mode in the 0.100-0.200 in. thickness range.

Further conformation of the change in failure mode mechanism was obtained by comparison of calculated shear and bending stresses (from P_i and P_{max} respectively) with shear and bending stresses measured in a conventional slow bend test using the same span as in the Charpy impact test. These results are listed in Table XXV.

There is, in general, good correlation between the static and dynamic stress levels particularly where marked changes in stress occur. Although there is some overlap, the 0.100-0.200 in. thickness range appears to be the critical range as indicated above for changes in fracture mode.

3.2 Ballistic Impact Properties of Multi-Fiber Angle-Ply Epoxy Resin Composites

To correlate the pendulum impact properties of the angle-ply composites with ballistic impact characteristics, a series of 36 ballistic impact specimens was fabricated using the three angle-ply configurations and three hybrid constructions previously described in section 3.1. The test specimens were obtained by cutting two 5.08 cm (2 in.) x 22.85 cm (9 in.) specimens from a 11.32 cm (4.5 in.) x 25.4 cm (10 in.) panel. Specimen thicknesses ranged from 0.252 cm (0.095 in.) to 0.343 cm (0.135 in.) depending upon layup design. Torsion and bending moduli were measured before impact for each specimen. Specimens were then ballistically impacted using jelly spheres, 1.27 cm (0.5 in.) diameter, at room temperature. Tests were conducted using four different projectile velocities, 183, 213, 243, and 274 m/sec (600, 700, 800, and 900 ft/sec) to ascertain the threshold and structural damage levels of each angle-ply hybrid fiber combination. The torsion and bending moduli were remeasured on the impacted specimens as a measure of the extent of damage. The results of these measurements are listed in Tables XXVI-XXVIII and illustrated graphically in Figs. 44-46 in terms of shear modulus retention vs projectile velocity for each composite type and angle-ply.

Table XXV

Comparison of Dynamic and Static Shear and Bending Stresses at Varying Composite Thickness

Composite No. (Thickness-in.)	Shear Stress, psi		Bending Stress, ksi	
	Dynamic[a]	Static	Dynamic[a]	Static
NASX-6 AS/S-glass				
(±22,0) -(50)	1830	1540	140.0	161.5
-(100)	3600	4230	130.5	158.0
-(200)	8320	5920	130.0	143.0
-(300)	9620	4340	99.6	45.0
-(400)	10900	4420	83.0	33.4
NASX-5 AS/S-glass				
(±40,0,10) -(100)	3680	3410	132.5	122.0
-(200)	5430	5770	94.4	98.3
-(300)	6470	8000	36.6	89.2
-(400)	7580	8740	36.9	72.3
NASX-9 AS/Kevlar 49				
(±22,0) -(50)	1140	1120	74.8	72.6
-(100)	3060	3460	100.0	113.0
-(200)	3300	4330	46.8	56.2
-(300)	3100	4270	38.3	45.3
-(400)	3820	5280	31.2	30.7
NASX-12 HMS/S-glass				
(±22,0) -(50)	1240	1400	68.8	97.0
-(100)	1670	1880	79.6	74.0
-(200)	2060	3240	34.7	51.4
-(300)	2610	3740	28.0	41.1
-(400)	2810	5130	21.9	30.75

[a]Calculated using conventional beam equations from P_i (shear) and P_{max} (bending)

Table XXVI

Ballistic Impact Data
Ply Configuration and Hybrid Fiber Study
Type UARL-1 AS/S-glass Intraply

Composite No.	Angle-Ply	Projectile Velocity[a] (fps) m/sec	Bending Modulus Retention(%)	Shear Modulus Retention(%)
B-4-R	±40,0,10	(608) 186	100	100
B-4-L		(694) 212	100	100
B-13-R		(805) 246	100	80
B-13-L		(832) 254	97	75
B-5-R	±22,0	(589) 180	98	100
B-5-L		(703) 214	93	100
B-14-R		(830) 253	100	95
B-14-L		(922) 281	100	62
B-6-R	±45,0	(588) 179	100	100
B-15-R		(728) 222	100	100
B-6-L		(808) 247	99	100
B-15-L		(910) 278	100	43

[a]Actual projectile velocity

Table XXVII

Ballistic Impact Data
Ply Configuration and Hybrid Fiber Study
Type 12 - AS/Kevlar 49 Interply

Composite No.	Angle-Ply	Projectile Velocity[a] (fps) m/sec	Bending Modulus Retention(%)	Shear Modulus Retention(%)
B-7-R	±40,0,10	(595) 182	100	100
B-7-L		(698) 213	100	100
B-16-R		(823) 254	100	80
B-16-L		(900) 275	95	73
B-8-R	±22,0	(603) 184	100	100
B-8-L		(700) 214	100	100
B-17-L		(842) 257	100	100
B-17-R		(910) 278	100	65
B-9-R	±45,0	(611) 187	100	100
B-9-L		(707) 216	100	79
B-18-R		(819) 250	92	38
B-18-L		(910) 278	86	24

[a]Actual projectile velocity

Table XXVIII

Ballistic Impact Data
Ply Configuration and Hybrid Fiber Study
Type UARL-2 HMS/S-glass Intraply

Composite No.	Angle-Ply	Projectile Velocity[a] (fps)	m/sec	Bending Modulus Retention(%)	Shear Modulus Retention(%)
B-1-R	±40,0,10	(605)	185	87	70
B-1-L		(702)	214	90	50
B-10-R		(805)	246	89	49
B-10-L		(878)	268	88	38
B-2-R	±22,0	(597)	182	100	88
B-2-L		(721)	220	95	76
B-11-R		(804)	245	75	48
B-11-L		(887)	273	57	34
B-3-R	±45,0	(600)	182	100	76
B-3-L		(695)	212	100	45
B-12-R		(805)	246	79	31
B-12-L		(900)	275	54	21

[a]Actual projectile velocity

SHEAR MODULUS RETENTION VS PROJECTILE VELOCITY HYBRID FIBER COMPOSITES

$[\pm 22,0,+22,0,-22]_S$ ANGLE–PLY

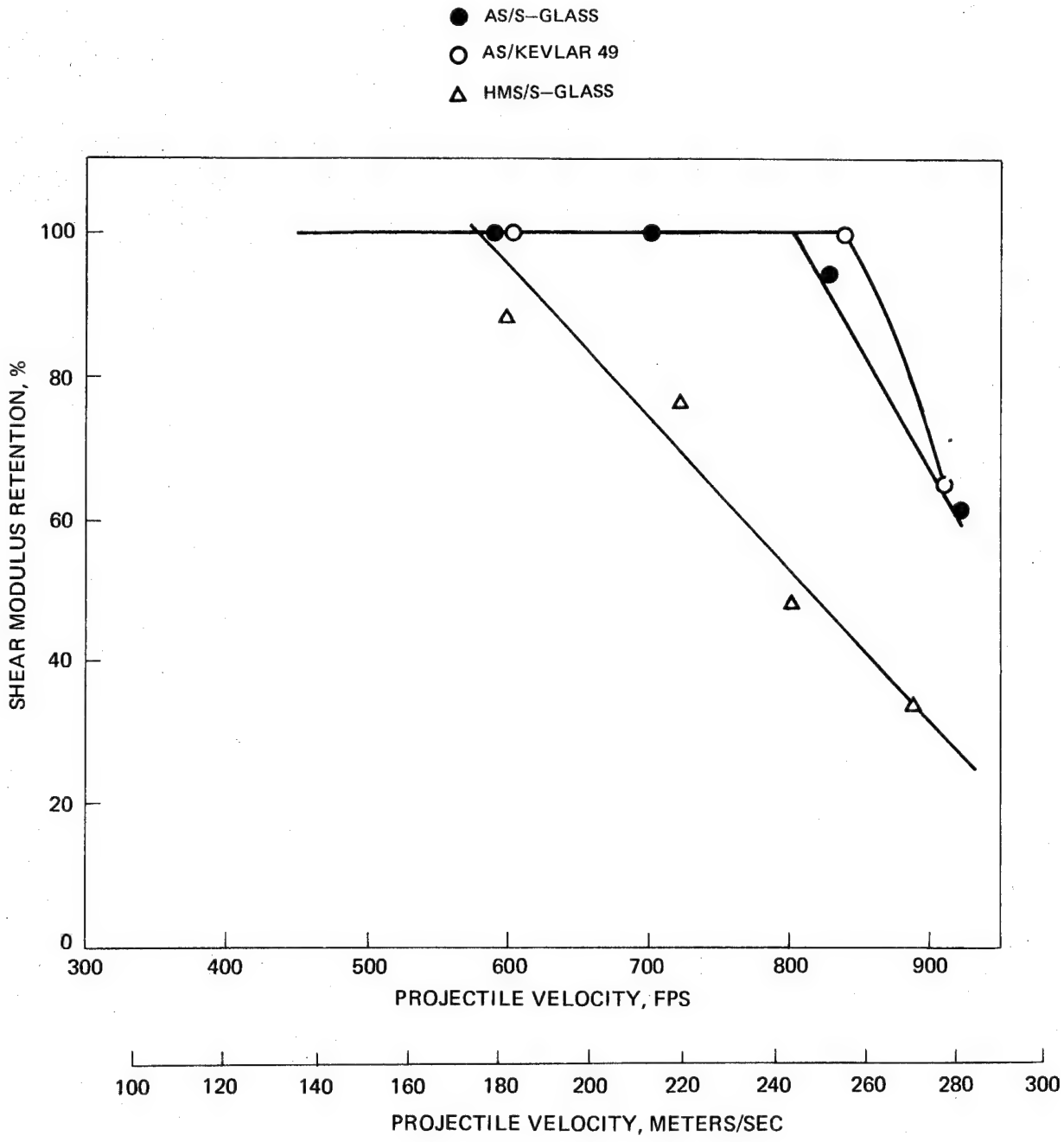

N07–116–1

SHEAR MODULUS RETENTION VS PROJECTILE VELOCITY
HYBRID FIBER COMPOSITES

$[\pm 40, 0, +10, 0, -10]_S$ ANGLE–PLY

● AS/S–GLASS

○ AS/KEVLAR 49

△ HMS/S–GLASS

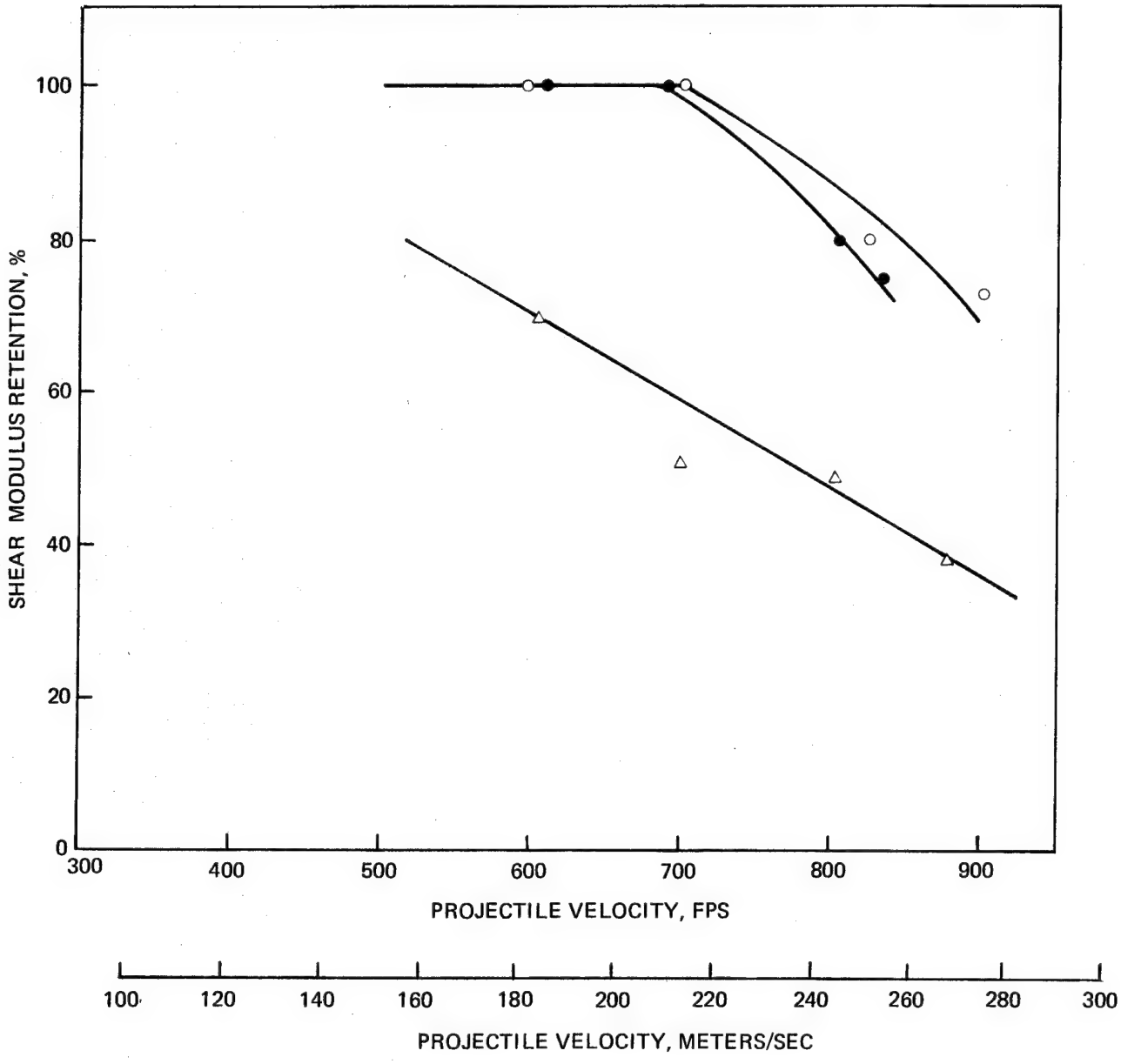

N07–116–2

SHEAR MODULUS RETENTION VS PROJECTILE VELOCITY HYBRID FIBER COMPOSITES

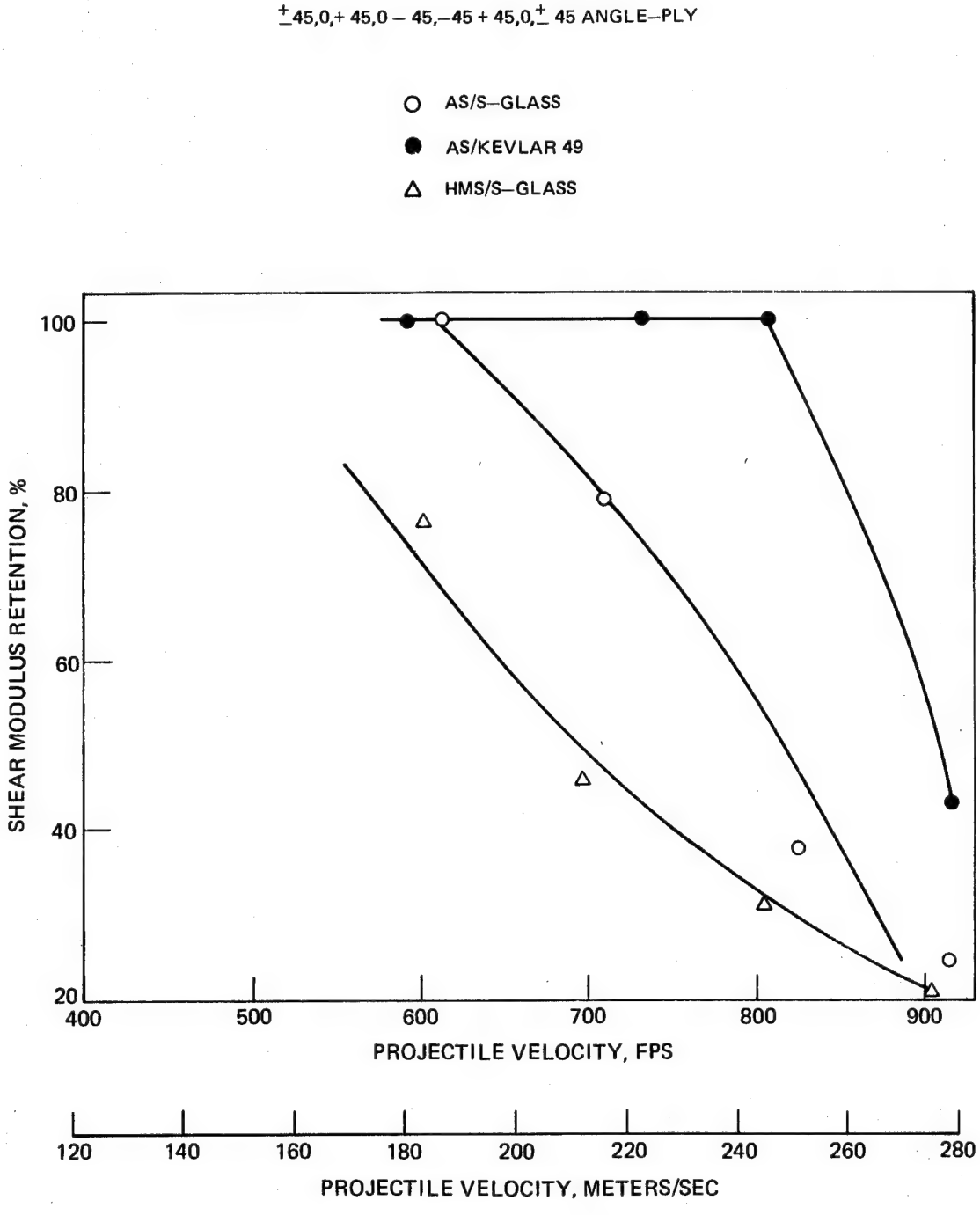

N10–326–2

3.2.1 Correlation of Percent Shear Modulus Retention with Projectile Velocity

It is apparent that shear modulus retention is a more sensitive measure of impact damage than is bending modulus retention. With the exception of the intraply HMS/S-glass system little change in bending modulus was noted even at the 275 m/sec (900 fps) range. As seen in Figs. 44 and 45 the AS/S-glass and AS/Kevlar 49 composites in both the ±22,0 and ±40,0,10 angle-ply configurations are nearly identical in terms of threshold damage levels, 259 m/sec (850 fps) and 214 m/sec (700 fps) respectively for the two angle-plys with the Kevlar 49 hybrids being slightly superior. The ±45,0 angle-ply composites showed a distinct difference between the S-glass and Kevlar 49 hybrid AS laminates, 243 m/sec (800 fps) vs 152 m/sec (500 fps) threshold energy damage. The HMS/S-glass system gave a continuous drop in shear modulus at all velocities and was considerably poorer than the AS systems in all three angle-ply configurations.

Indication of the extent of damage at 275 m/sec (900 fps), somewhat above the threshold damage level for the AS/S-glass intraply ±22,0 composite, is shown in Figs. 47 and 48. The corresponding test specimen for AS/Kevlar 49 interply ±22,0 laminate is shown in Figs. 49 and 50. There appears to be only small amounts of delamination in either case, with no loss of any of the composite by spalling which characterized the HMS/S-glass laminates as shown in Figs. 51 and 52.

Comparison of the Charpy impact results as shown in Fig. 39 for varying thicknesses with the ballistic data showed that at the lower thickness levels, <0.356 cm (0.140 in.), the AS/S-glass and AS/Kevlar 49 composites gave nearly the same pendulum impact energy while the HMS/S-glass was lower. In the pendulum impact test, however, the AS/S-glass ±22,0 system was rated slightly superior to the corresponding Kevlar 49 hybrid which is the reverse of the ballistic data.

3.2.2 Correlation with Total Charpy Impact Energy

An alternative comparison between the two sets of test data is seen in Fig. 53 which relates the ballistic shear modulus retention to the total Charpy impact energy on a specimen thickness basis. It is apparent that in the thin specimen range the data is more compatible between the two tests than for thicknesses above .508 cm (0.200 in.). Again in this correlation the interply Kevlar hybrid is slightly superior to the intraply AS/S-glass system. Thus, it appears on this basis as well as the slow bend stress data that there is reasonable but not total agreement between the ballistic and Charpy impact test data for ranking the composites at thickness levels below 0.508 cm (0.200 in.). It should be pointed out, however, that in the ballistic tests the effect of damping is not accounted for and may be the reason that the Kevlar 49 hybrid appears slightly superior to the S-glass system while the opposite is true for the pendulum impact results. In addition, the S-glass composite was impacted at 922 fps while the Kevlar 49 hybrid was impacted at 910 fps.

BALLISTIC IMPACT TEST

AS/S–GLASS – $[\pm 22,0,+22,0,-22]_S$ AT 922 FPS

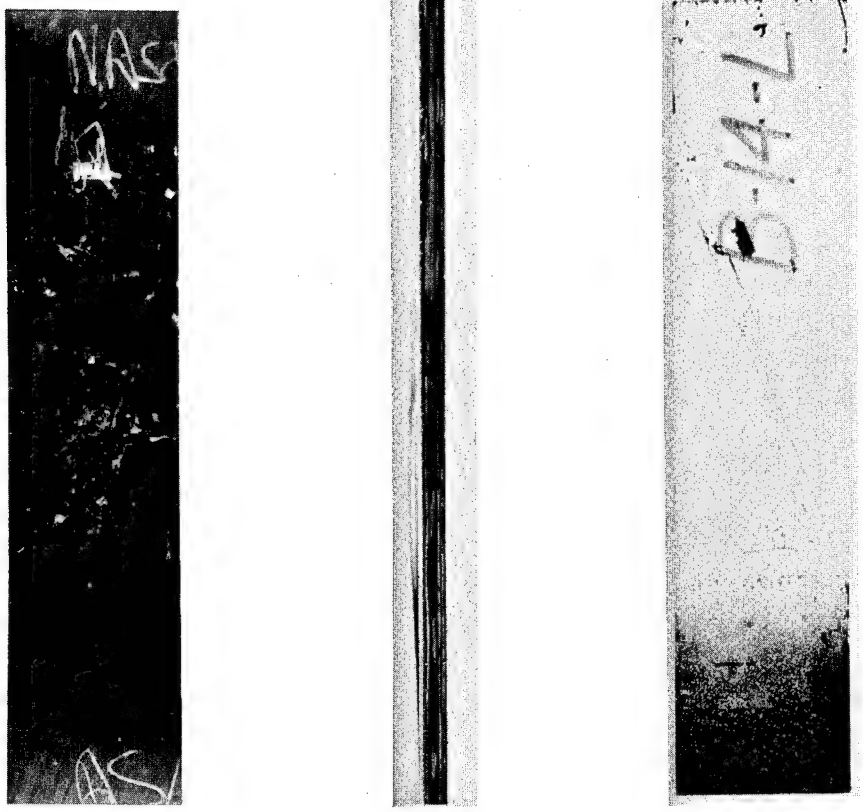

FRONT SIDE BACK

N10–181–7

BALLISTIC IMPACT TEST

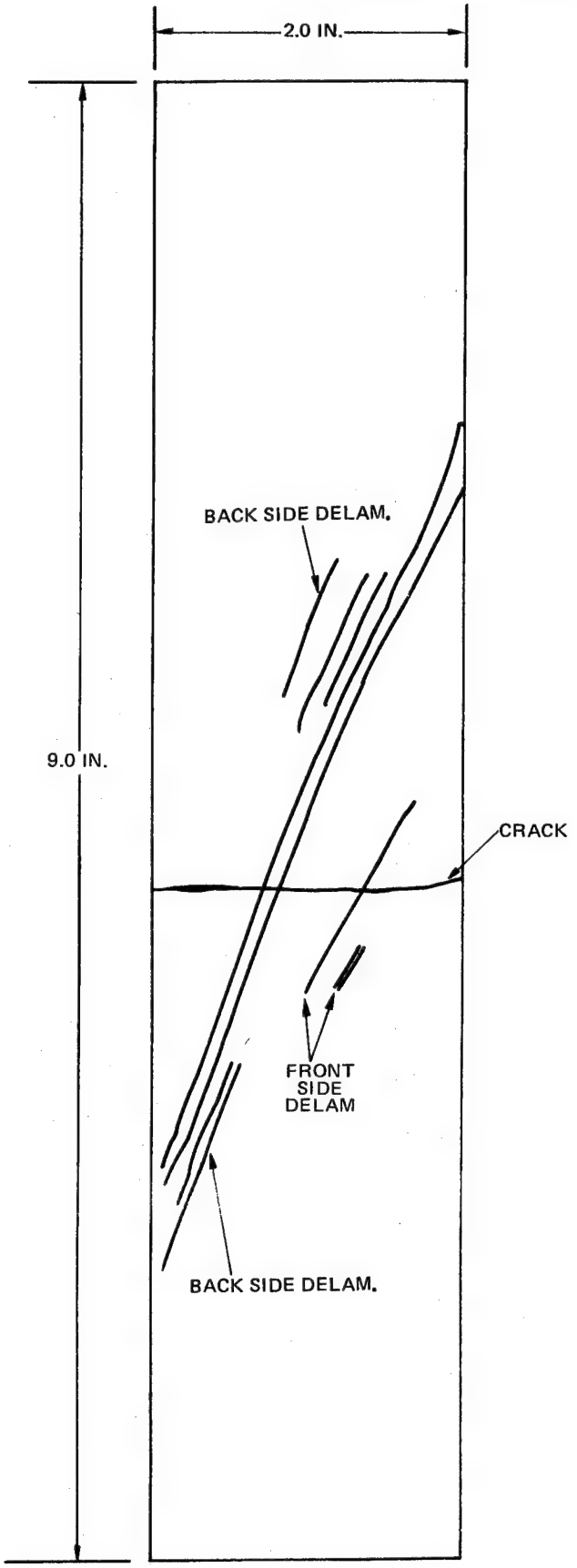

SPECIMEN NO: B–14–L

TYPE: AS/S–GLASS, $[\pm 22,0 + 22,0–22]_S$

PROJECTILE:

1/2 IN. GELATIN BALL

VELOCITY:

ACTUAL 922 FT/SEC

REMARKS:

CRACK APPEARS TO BE ONLY THROUGH 1–2 PLY

N10–181–10

BALLISTIC IMPACT TEST

AS/KEVLAR–49 – $[\pm 22,0, +22,0, -22]_S$ AT 910 FPS

FRONT SIDE BACK

N10–181–5

BALLISTIC IMPACT TEST

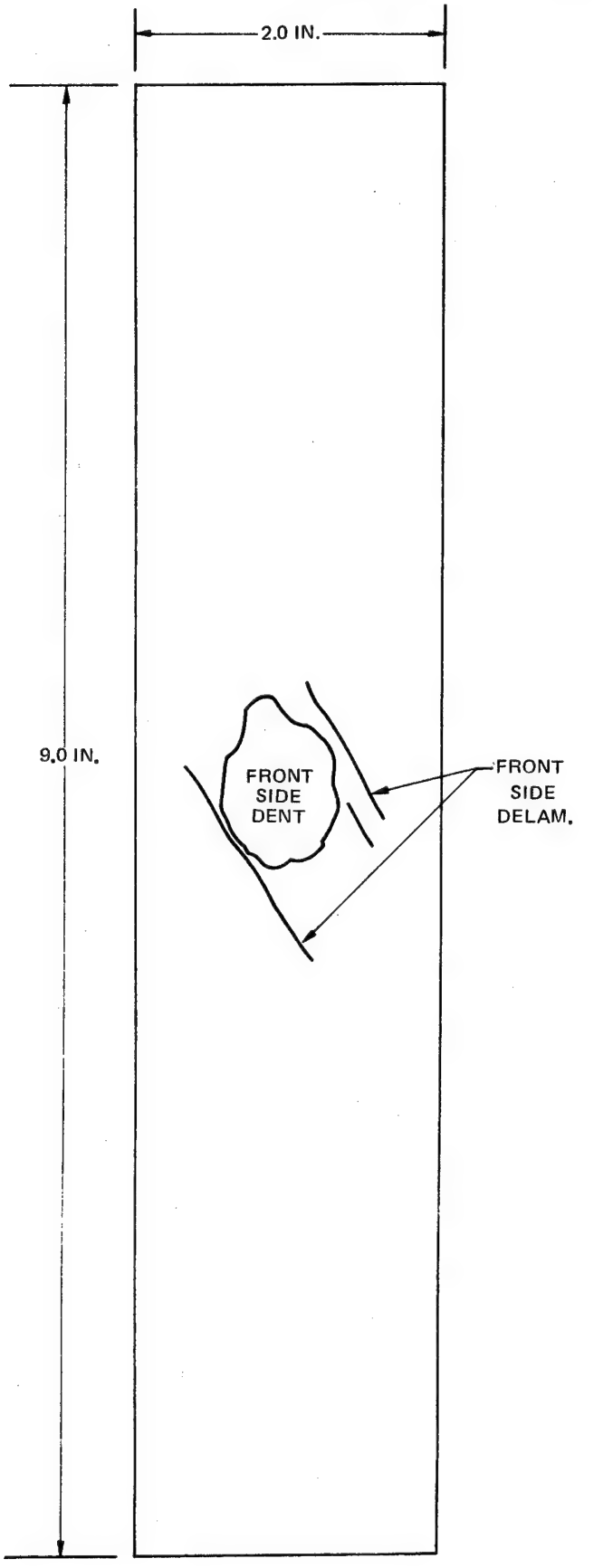

SPECIMEN NO: B–17–R

TYPE AS/KEVLAR 49, $[\pm 22,0,+22,0-22]_S$

PROJECTILE:

1/2 IN. GELATIN BALL

VELOCITY:

ACTUAL 910 FT/SEC

REMARKS:

3 CRACKS ON BACK SIDE AT IMPACT AREA

N10–181–9

BALLISTIC IMPACT TEST

HMS/S–GLASS –[±22,0, + 22,0,–22] $_S$ AT 887 FPS

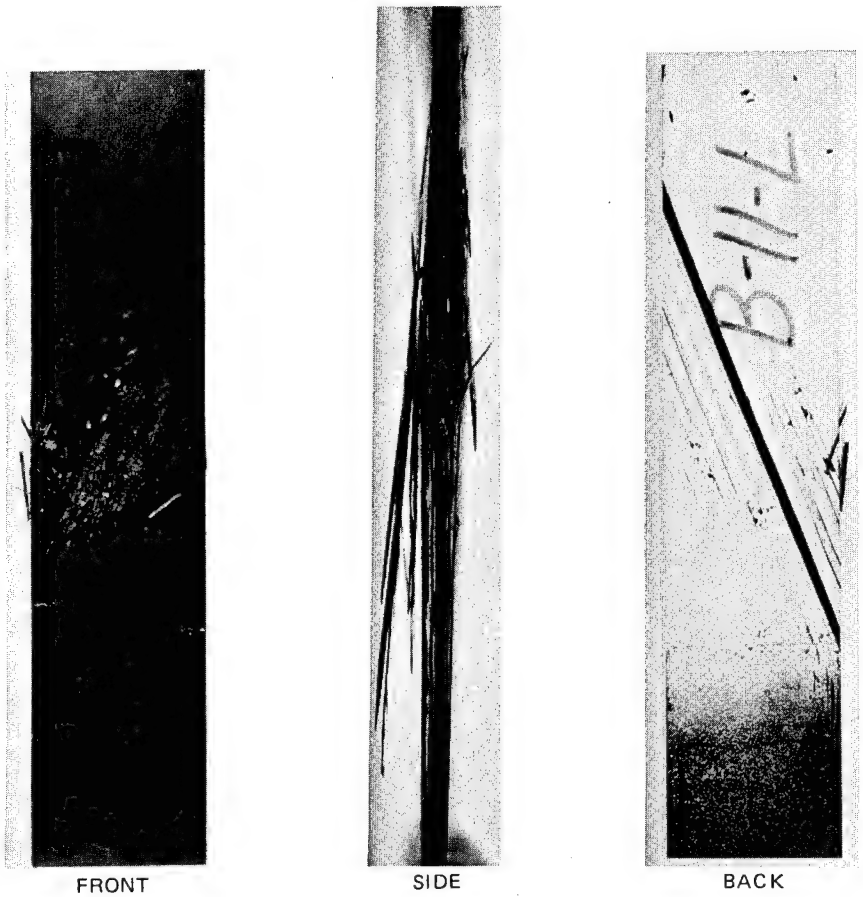

FRONT SIDE BACK

N10–181–6

FIG. 52

BALLISTIC IMPACT TEST

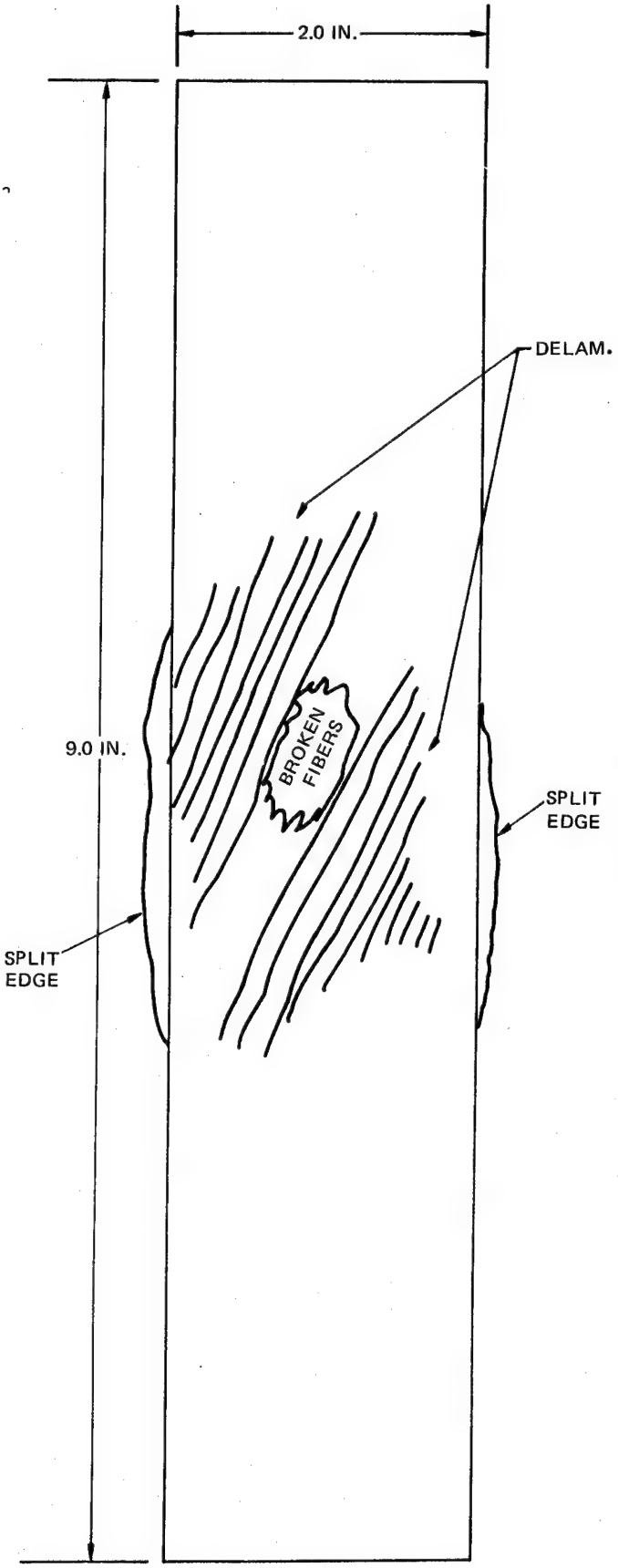

SPECIMEN NO: B–11–L

TYPE: HMS/S–GLASS, $[\pm 22,0,+22,0-22]_S$

PROJECTILE:
1/2 IN. GELATIN BALL

VELOCITY:
ACTUAL 887 FT/SEC

REMARKS:
FRONT SIDE WAS CAVED IN CAUSING MUCH MORE DELAM. & MISSING PLIES THAN ON THE BACK SIDE.

N10–181–8

FIG. 53

RELATIONSHIP OF BALLISTIC TO PENDULUM IMPACT DATA

SHEAR MODULUS RETENTION AT 900 FPS VS TOTAL CHARPY IMPACT ENERGY

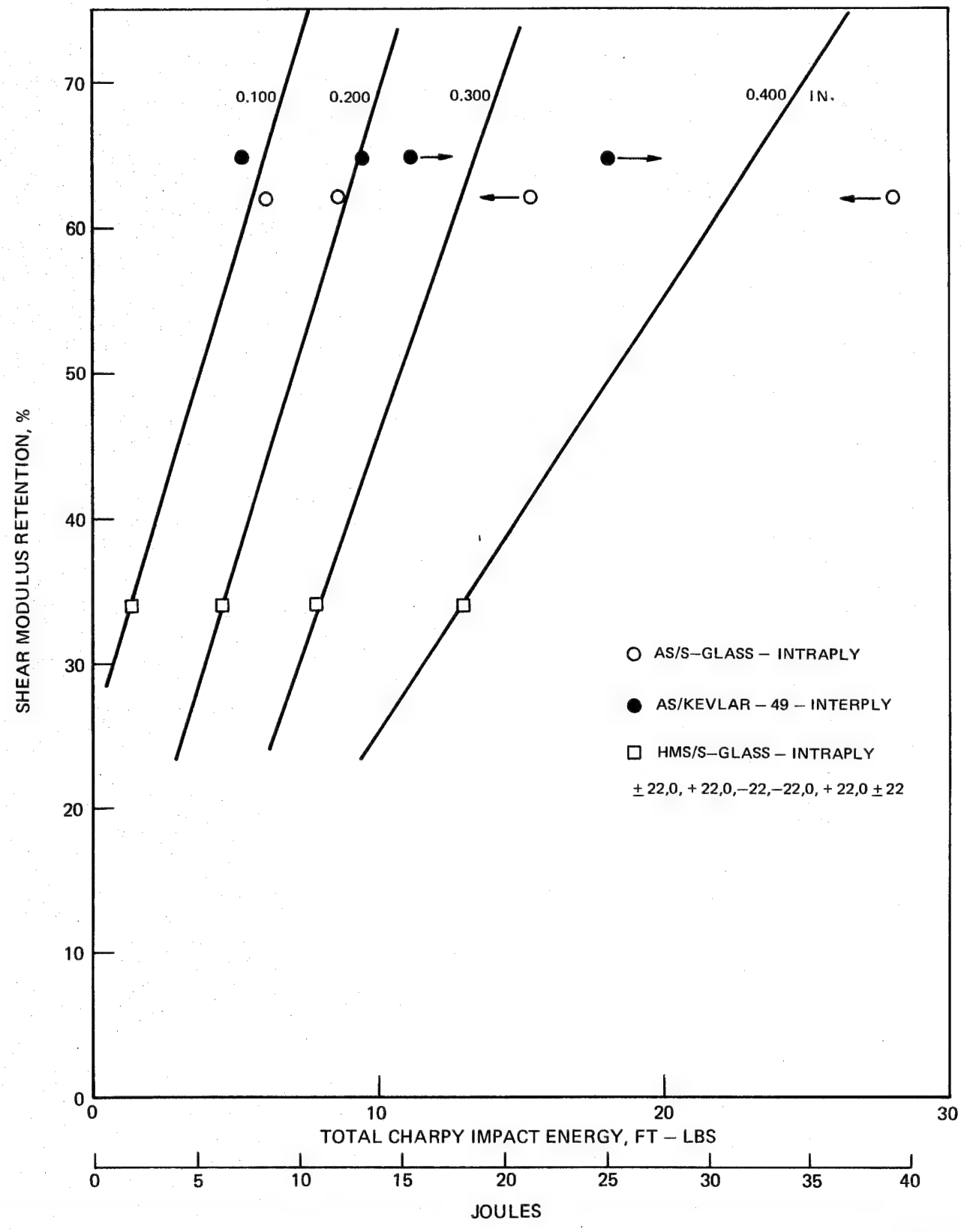

N10–181–4

3.2.3 The E/V Parameter

The chief reason for the slight reversal in performance of the AS/S-glass and AS/Kevlar 49 in the two tests (pendulum vs ballistic) is probably related to the differences in thickness of the laminates involved. Due to ply layup and construction the Kevlar hybrid was 23 percent thicker in the ballistic test than the S-glass hybrid (0.343 cm vs 0.289 cm respectively). Significantly lower damage levels have been found in Modmor II/286 epoxy systems by doubling the thickness during ice ball ballistic impact. As determined by C-scan inspection the extent of delamination was reduced from 30 percent to 4 percent with the increase in thickness (Ref. 8).

To ascertain the effect of thickness on the results of the ballistic data from the present work, percent retention of shear modulus has been related to projectile energy and the impact affected volume of the composite. This is the energy the specimen is capable of absorbing in a given volume under the point of projectile contact. This will be referred to as the E/V parameter.

Thus: $$E/V = \frac{\text{Projectile Energy}}{\text{impact affected volume}} = \frac{1/2 \text{ mass} \times (\text{velocity})^2}{\text{volume}}$$

where: impacted affected volume = (diameter of projectile)^2 x specimen thickness in meters

mass of projectile = grams

velocity = cm/sec

or $$E/V = \frac{1/2 \text{ g}\cdot\text{cm}^2/\text{sec}^2}{\text{meter}^3} = \frac{\text{dyne-cm}}{\text{meter}^3} = \frac{\text{ergs}}{\text{meter}^3} = \frac{\text{Joules} \times 10^{-7}}{\text{meter}^3}$$

English units for the parameter are ft-lbs/in.^{3}.

A recent report describes the use of a similar parameter in analyzing the residual strength of impacted laminates (Ref. 9).

The width and length of the impact affected volume was arbitrarily chosen based on the diameter of the projectile. Any other width or length could be employed and would only result in a shift of the resulting data points as long as the actual specimen thickness was used. The E/V parameter for each composite and angle-ply tested is listed in Tables XXIX to XXXI.

The relationship of percent shear modulus retention to the E/V parameter is shown graphically in Figs. 54 to 56. The results show that with the $\pm$22,0 composites, when thickness is accounted for, the intraply AS/S-glass laminate is better than the interply AS/Kevlar 49 as was indicated by the pendulum impact test, Fig. 39, the intraply HMS/S-glass being considerably poorer. Similarly, using the $\pm$40,0,10 angle-ply configuration, Fig. 55, the intraply AS/S-glass was also found to be superior to the interply AS/Kevlar 49. The difference between

Table XXIX

Ballistic Impact Ply Configuration Study
Correlation of Projectile Velocity and Specimen Thickness
Type UARL-1 AS/S-Glass Intraply

Composite No.	Angle-Ply	Projectile Velocity (fps)	m/sec	Projectile Energy/ Impact Affected Volume (E/V) Joules/$m^3 \times 10^8$
B-4-R	±40,0,10	(608)	186	4.02
B-4-L		(694)	212	4.98
B-13-R		(805)	246	8.12
B-13-L		(832)	254	8.6
B-5-R	±22,0	(589)	180	4.23
B-5-L		(703)	214	5.55
B-14-R		(830)	253	7.78
B-14-L		(922)	281	9.55
B-6-R	±45,0	(588)	179	3.59
B-15-R		(728)	222	5.73
B-6-L		(808)	247	6.31
B-15-L		(910)	278	8.88

Table XXX

Ballistic Impact-Ply Construction Study
Correlation of Projectile Velocity and Specimen Thickness
Type UARL-2 HMS/S-Glass Intraply

Composite No.	Angle-Ply	Projectile Velocity (fps)	Projectile Velocity m/sec	Projectile Energy/ Impact Affected Volume (E/V) Joules/m^3 x 10^8
B-1-R	±40,0,10	(605)	185	5.4
B-1-L		(702)	214	6.94
B-10-R		(805)	246	8.08
B-10-L		(878)	268	9.38
B-2-R	±22,0	(597)	182	4.32
B-2-L		(721)	220	6.46
B-11-R		(804)	245	7.87
B-11-L		(887)	273	9.68
B-3-R	±45,0	(600)	182	4.13
B-3-L		(695)	212	5.62
B-12-R		(805)	246	7.86
B-12-L		(900)	275	9.88

Table XXXI

Ballistic Impact-Ply Construction Study
Correlation of Projectile Velocity and Specimen Thickness
Type 12 AS/Kevlar 49 Interply

Composite No.	Angle-Ply	Projectile Velocity (fps)	Projectile Velocity m/sec	Projectile Energy/ Impact Affected Volume (E/V) Joules/m^3 x 10^8
B-7-R	±40,0,10	(595)	182	3.37
B-7-L		(698)	213	4.32
B-16-R		(823)	254	6.63
B-16-L		(900)	275	7.71
B-8-R	±22,0	(603)	184	3.64
B-8-L		(700)	214	4.95
B-17-L		(842)	257	6.45
B-17-R		(910)	278	7.76
B-9-R	±45,0	(611)	187	3.7
B-9-L		(707)	216	4.86
B-18-R		(819)	250	6.82
B-18-L		(910)	278	8.45

FIG. 54

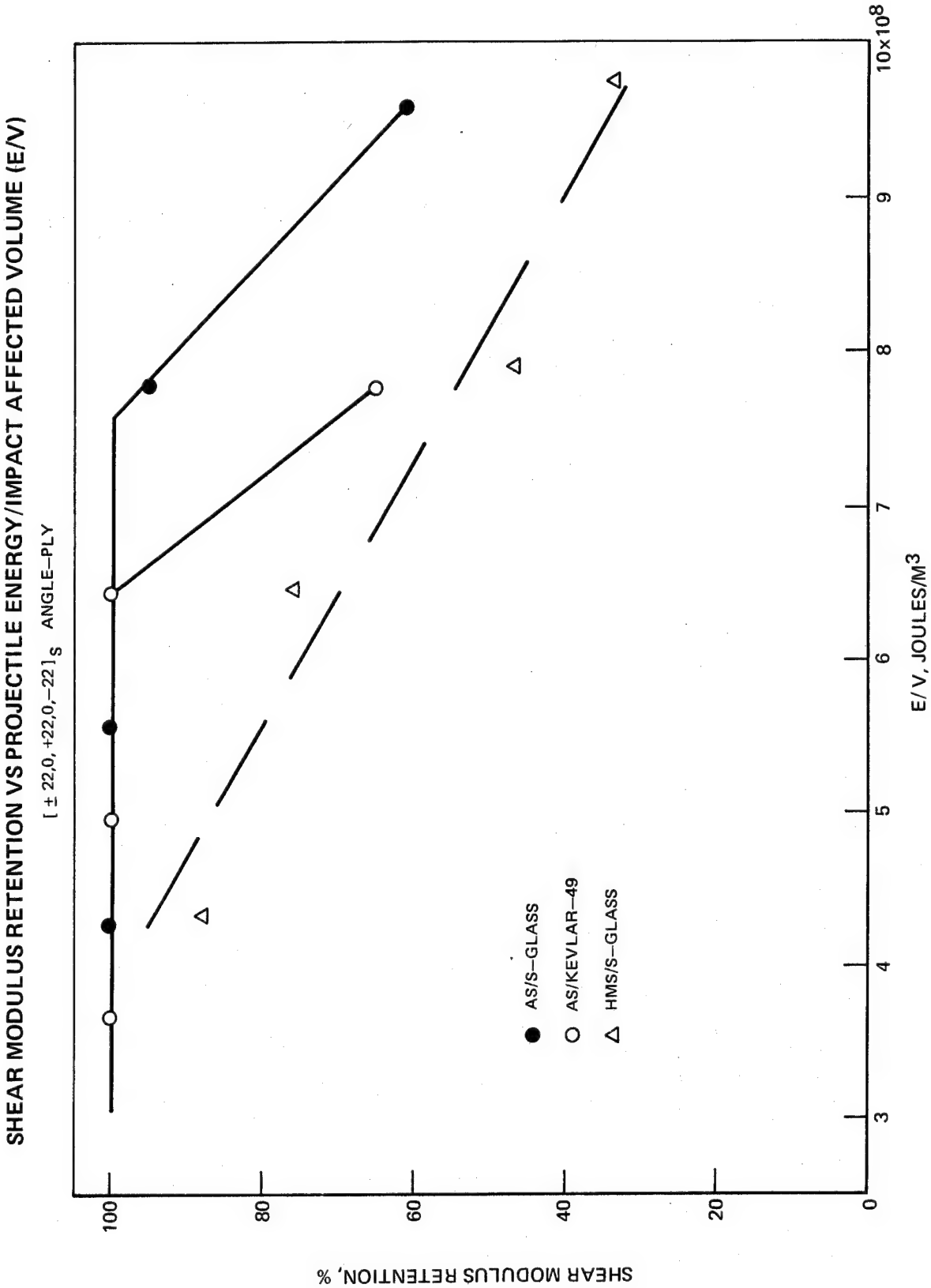

N10−181−2

FIG. 55

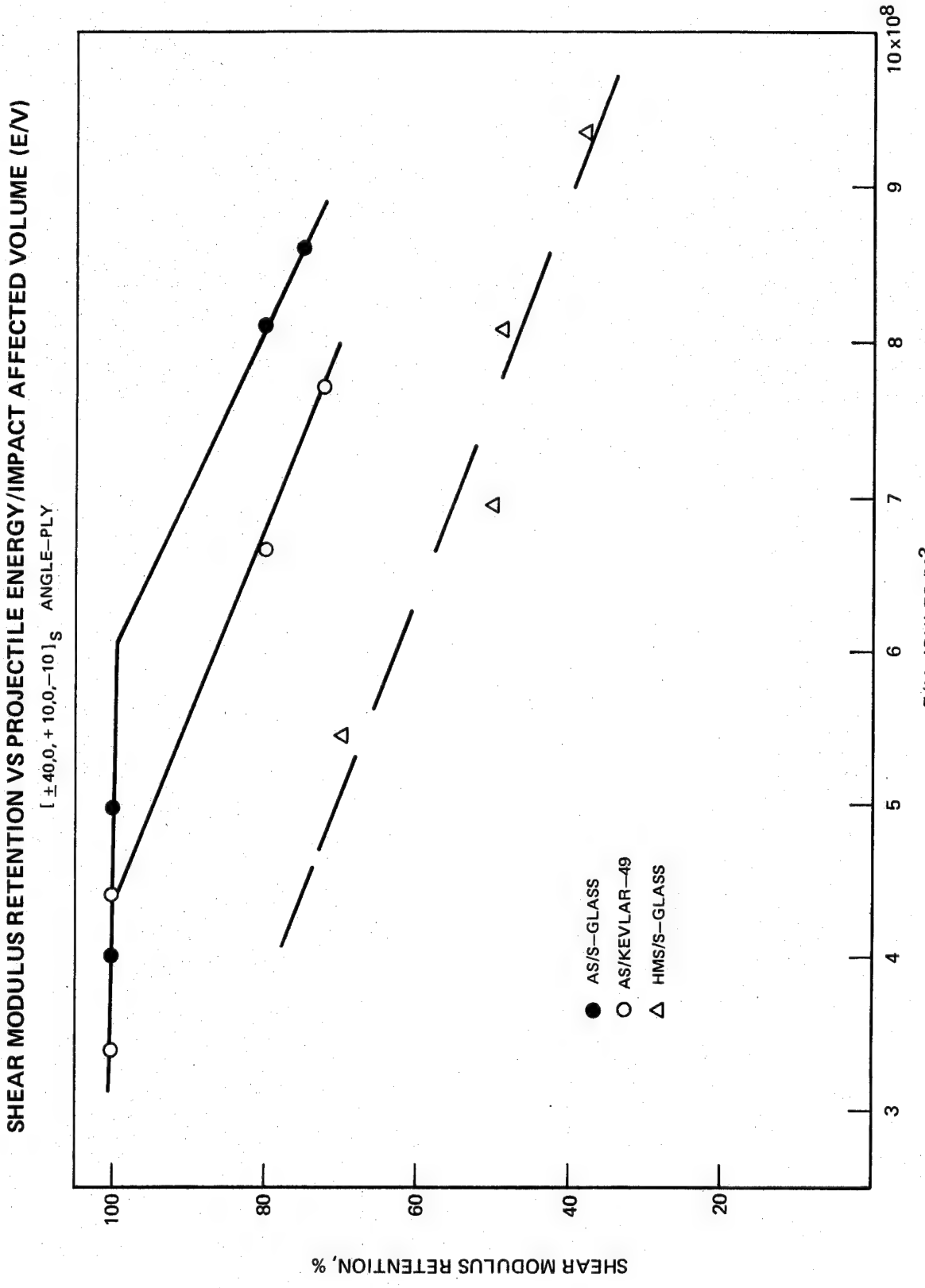

N10–181–1

FIG. 56

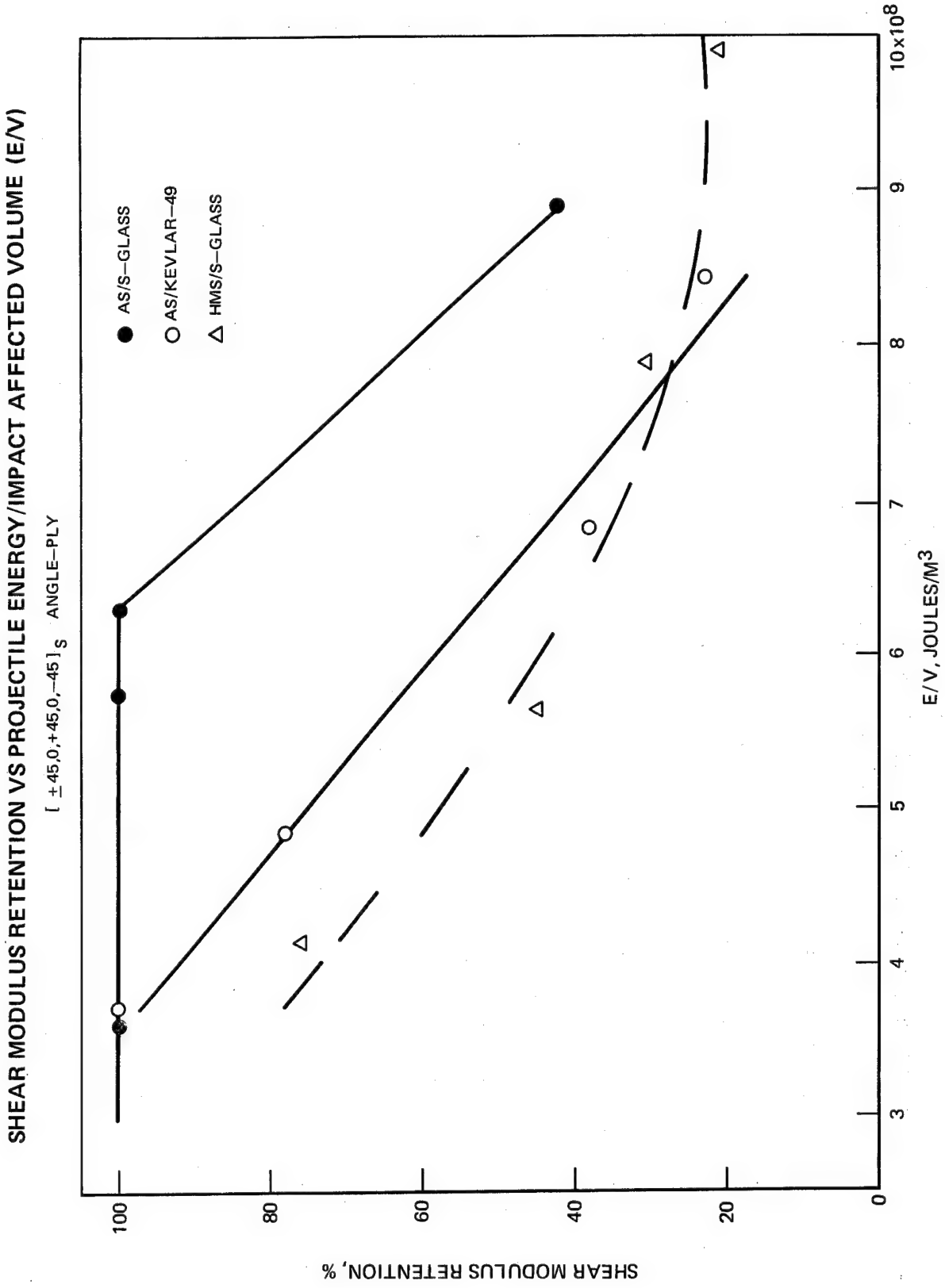

N10-181-3

the three angle-plys is also evident in that $\pm 22,0 > \pm 40,0,10 > \pm 45,0$ with the possible exception of the intraply AS/S-glass $\pm 40,0,10$ and $\pm 45,0$ laminates which gave similar E/V values. Because of the lack of a sufficient number of data points the degree of improvement of the AS/S-glass over the AS/Kevlar 49 cannot be accurately determined. A more definitive study of varying composite thickness, varying angle-ply and additional projectile velocities must be carried out to establish the validity of using the E/V parameter obtained from the ballistic test to correlate with the pendulum impact data using thin impact specimens.

3.2.4 Correlation of E/V Parameter with Charpy Fracture Initiation Load, P_i

An alternative approach to correlation of the two tests is the relationship of the threshold damage E/V parameter to the fracture initiation load, P_i, obtained in the pendulum impact tests. Using the four angle-ply composites which were ballistically impacted, this correlation is shown graphically in Figs. 57 and 58. With the thin specimens, Fig. 59, the three intraply types, AS/S-glass ($\pm 22,0$ and $\pm 40,0,10$) and HMS/S-glass all fall on a line while the interply AS/Kevlar 49 is slightly below. A similar plot using the P_i loads from the standard sized Charpy specimens, Fig. 58, also resulted in the three intraply specimens falling on a straight line with the interply AS/Kevlar 49 composite falling considerably below. Because of the lack of sufficient data positive conclusions concerning this correlation cannot be made. However, it appears that (1) with intraply construction P_i correlates with E/V regardless of ply angle and primary fiber, (2) there is more general correlation between the pendulum and ballistic impact tests using the thin pendulum specimens, i.e. the interply AS/Kevlar 49 is in better agreement with the intraply data.

3.2.5 Correlation of E/V Parameter with Total Pendulum Impact Energy

An E/V value related to total destruction of the ballistic specimens should correlate with the total impact energy measured by the Charpy tests, particularly in the case of thin specimens. Although projectile velocities were not sufficient to cause total destruction of the panels, a correlation of E/V vs total Charpy impact energy is shown in Fig. 59 using the E/V values at 900 fps. In contrast to the P_i relationship, in this instance the three AS graphite hybrid laminates fall on a line irrespective of angle-ply or construction type while the HMS/S-glass laminate falls well below. A similar plot of the same E/V values vs total impact energy obtained using standard size Charpy specimens resulted in complete scatter of the data points with no correlation.

THRESHOLD DAMAGE ENERGY/VOLUME VS Pi

(THIN CHARPY SPECIMENS)

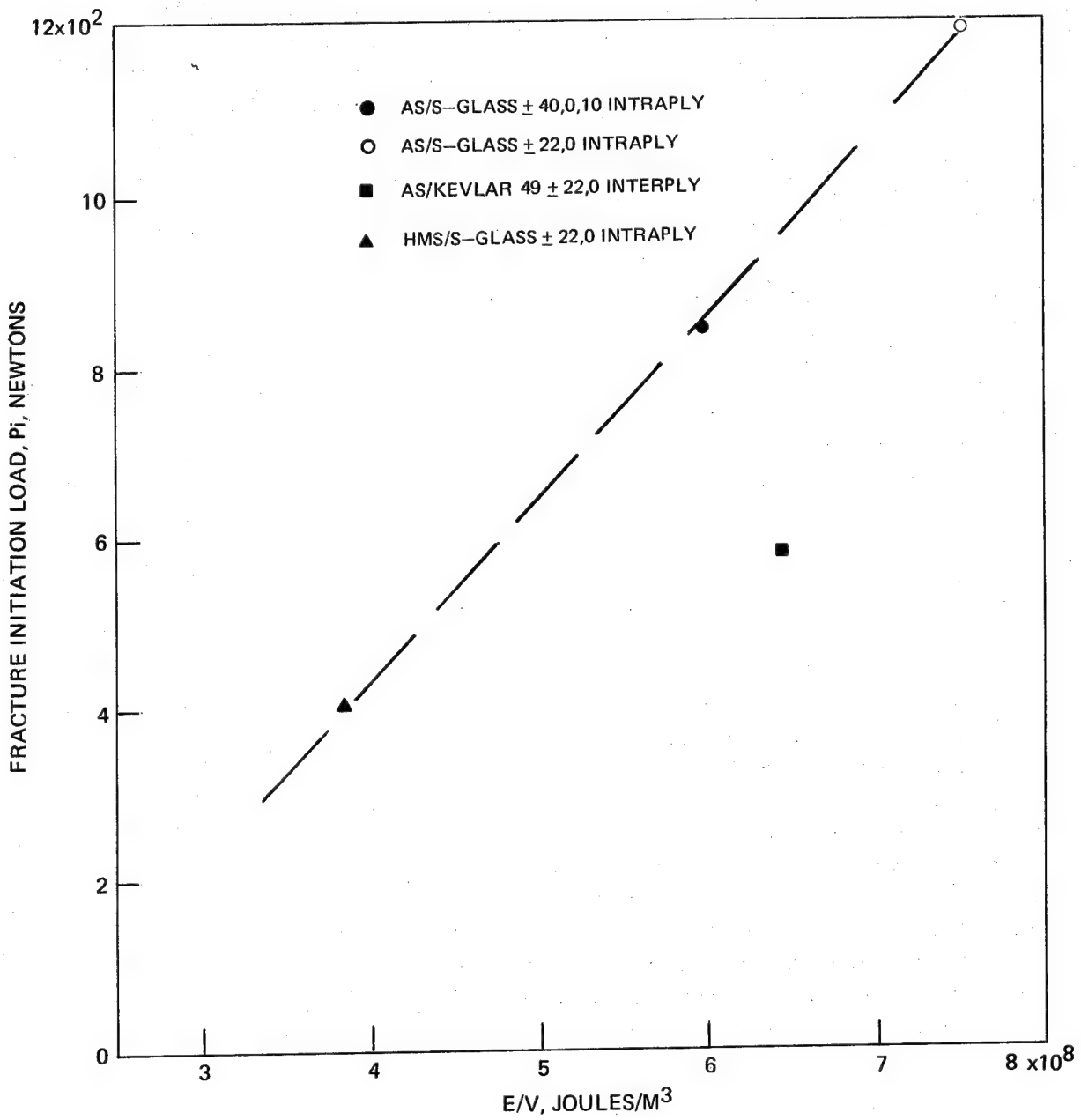

N10–310–3

FIG. 58

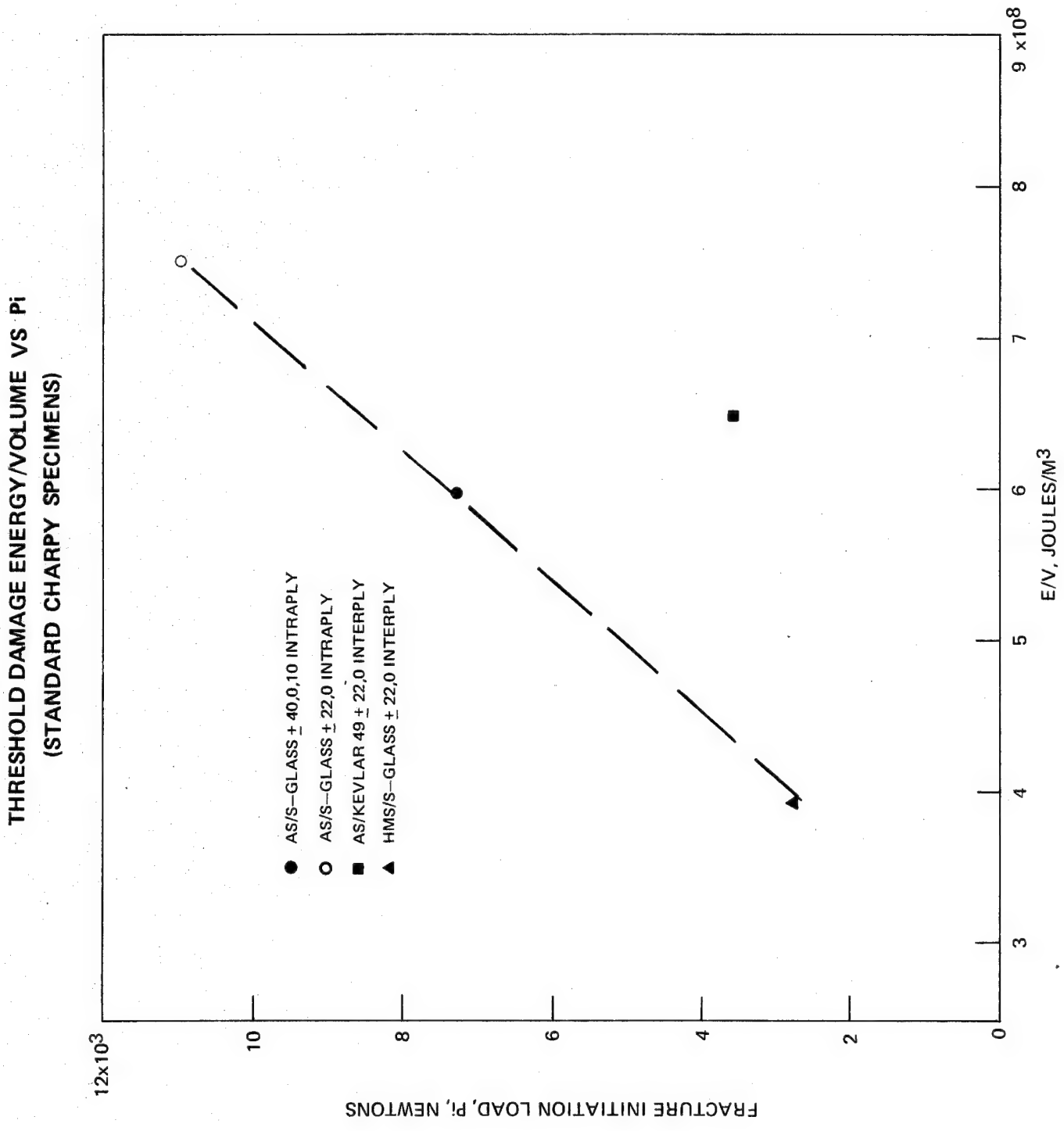

N10–310–5

FIG. 59

STRUCTURAL DAMAGE ENERGY/VOLUME VS TOTAL PENDULUM IMPACT ENERGY (THIN CHARPY SPECIMEN)

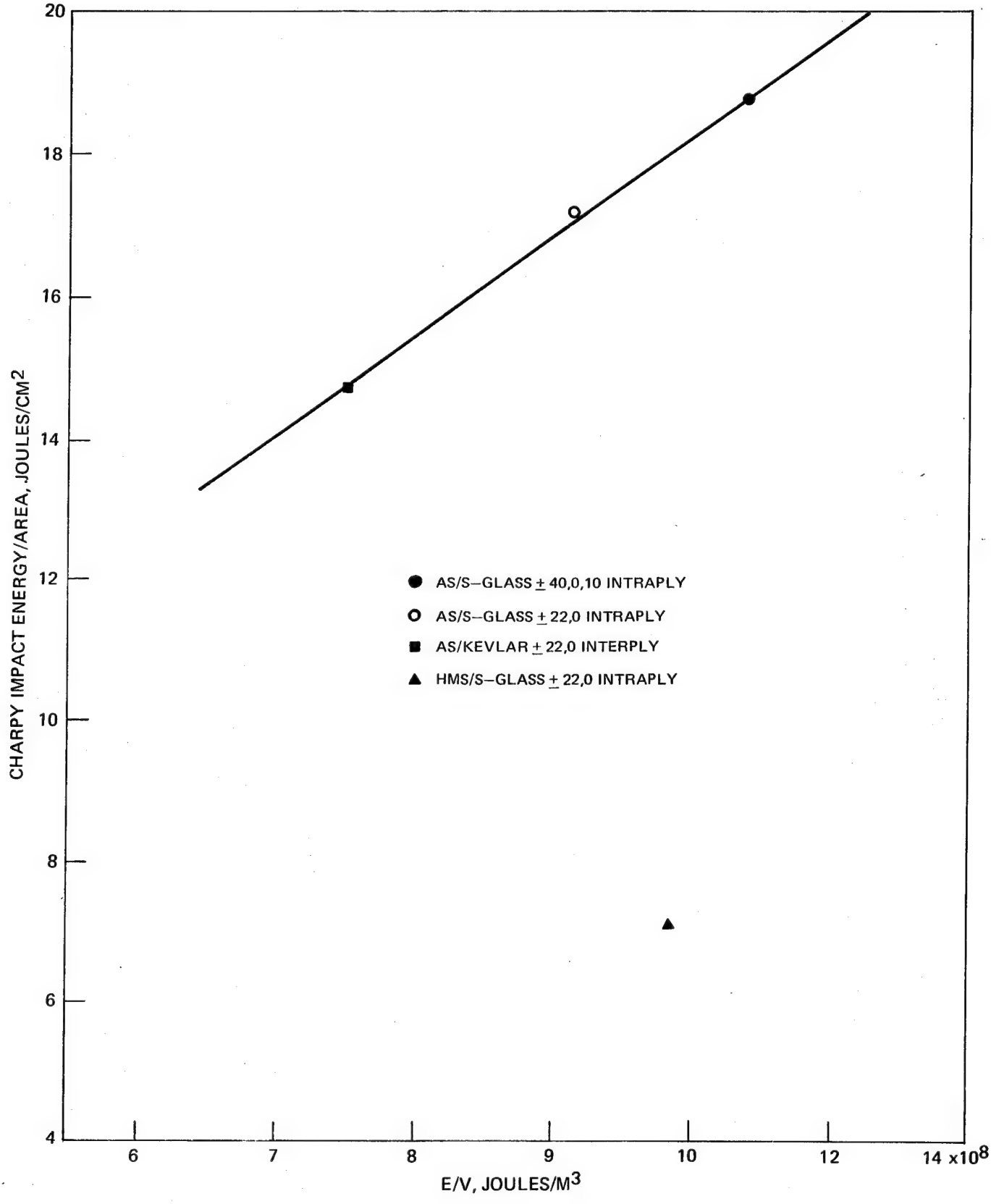

N10–310–4

Thus, the E/V parameter appears to have merit in correlating ballistic and pendulum impact results both for relating initial fracture levels or total destruction levels. The scope and value of the parameter as it relates to composite structure, angle-ply and fiber composition cannot be definitely defined until further study has been carried out. It can be concluded, however, that use of the E/V parameter appears to be the best method developed to date for correlating ballistic and pendulum impact results and merits further study.

3.3 Thin Unidirectional Hybrid Composites

In order to make a judicious selection of the final composite laminates to be more fully evaluated in Tasks III and IV, a series of Task I unidirectional, multi-fiber composites was refabricated for evaluation in the thin pendulum impact test.

Based on the angle-ply ballistic and multi-thickness Charpy impact results, a thickness level of approximately 0.254 cm (0.100 in.) was selected for the series of thin unidirectional composites (having greater than 19 x 10^6 psi modulus) to be tested by instrumented Charpy impact. The laminates consisted of nine HMS/S-glass, three HMS/Kevlar 49, two AS/S-glass and two AS/Kevlar 49 systems. In addition, the homogeneous graphites, S-glass and Kevlar 49 composites were also impacted at the same thickness level. The flexural and shear strengths of the sixteen hybrid composites were also determined. The physical properties of the hybrid laminates are listed in Table XXXII. For convenience in identification the same composite number used in Task I has been employed. Previous results may be found in Table IV. With few exceptions, reproducibility was good. Minor shifts in S-glass content will be noted due to a change from 20-end to 12-end S-glass roving. Composite flexural and shear strengths are listed in Table XXXIII. (For comparison see Tables V-VIII.)

3.3.1 Static Properties

All of the laminates gave modulus values above the 19 x 10^6 psi minimum with one exception. This was the tow-by-tow AS/S-glass, NAS-76II, laminate which has consistently given the highest impact response of any of the laminate types tested. All the composites, except two, gave slightly higher flexural strengths than previously obtained while shear strengths varied in a haphazard manner. Failure modes were the same as previously encountered. Some of the differences are undoubtedly due to use of different lots of AS and HMS graphite fiber.

3.3.2 Dynamic Properties

The impact properties of the composites are listed in Tables XXXIII and XXXIV. The results correlate well with the angle-ply ballistic data in that the intra-ply AS/S-glass (NAS-76 II) and interply AS/Kevlar (NAS-13 II) laminates gave nearly

Table XXXII

Physical Properties of Task II Unidirectional Hybrid Fiber Epoxy Composites

UARL No.	Composition Type	Density (g/cc)	v/o Total Fiber	v/o Resin	v/o Void	v/o Fiber Ratio (actual)
NAS-9II	13	1.86	HMS-36.5 S-28.8	33.8	0.6	HMS-56 S-44
-10II	13	1.75	HMS-51.1 S-13.2	33.3	2.4	HMS-78.2 S-21.8
-15A-II	13	1.71	HMS-60.7 S-5.5	30.8	3.1	HMS-91.5 S-8.5
-24II	17	1.69	HMS-58.1 S-5.7	32.7	3.7	HMS-91.2 S-8.8
-36II	2-UARL	1.73	HMS-43.4 S-16.1	38.3	2.3	HMS-73 S-27
-55II	20_{a-1}	1.70	HMS-52.2 S-10.3	33.5	4.2	HMS-83.7 S-16.3
-54II	20_{a-2}	1.70	HMS-62.8 S-4.3	28.8	4.1	HMS-93.5 S-6.5
-47D	2-Heltra	1.84	HMS-45.4 S-24.6	30.8	1.3	HMS-64 S-36
-6II	11	1.66	AS-58.9 S-5.5	35.6	0	AS-91.5 S-8.5
-76II	1-UARL	1.75	AS-51.0 S-17.3	30.8	0.9	AS-74.6 S-25.4
-12A-II	14	1.61	HMS-56.9 K-7.1	31.2	4.7	HMS-89 K-11
-11A-II	14	1.53	HMS-35.8 K-37.0	23.6	3.6	HMS-49.2 K-50.8

Table XXXII (Cont'd)

UARL No.	Composition Type	Density (g/cc)	v/o Total Fiber	v/o Resin	v/o Void	v/o Fiber Ratio (actual)
NAS-28II	18	1.60	HMS-56.9 K-4.8	32.8	5.4	HMS-92 K-8.0
-13II	12	1.57	AS-54.2 K-6.4	38.6	0.8	AS-89.4 K-10.6
-78II	3-UARL	1.60	AS-56.1 K-11.1	31.5	1.3	AS-83.6 K-16.4

Table XXXIII

Flexural, Shear and Pendulum Impact Energies of Thin Unidirectional Hybrid Fiber Epoxy Resin Composites[a]

UARL No.	Composition Type	v/o Fiber Ratio (actual)	Short Beam Shear[b] MN/m^2	(psi)	Flexural Strength[c] GN/m^2	(ksi)	Flexural Modulus[c] GN/m^2	($psi \times 10^6$)	Charpy Impact Strength Joules/cm^2	(ft-lbs/in^2)
NAS-9II	13	HMS-56 S-44	45.0	(6535)	1.345	(195.5)	146	(21.2)	17	(78.2)
-10II	13	HMS-38.2 S-21.8	50.7	(7350)	1.37	(199)	188	(27.25)	12.8	(59.4)
-15AII	13	HMS-91.5 S-8.5	41.3	(5985)	1.55	(224.5)	207	(30.1)	9.24	(44.8)
-24II	17	HMS-91.2 S-8.8	44.6	(6470)	1.31	(190.5)	166	(24.1)	10.9	(50.4)
-36II	2-UARL	HMS-73 S-27	41.1	(5970)	1.26	(183)	159	(23.0)	12.9	(59.3)
-55II	20_{a-1}	HMS-33.7 S-16.3	40.1	(5810)	1.68	(243.5)	145.5	(21.1)	13.2	(60.8)
-54II	20_{a-2}	HMS-93.5 S-6.5	40.2	(5825)	1.30	(189)	162	(23.5)	9.55	(44.0)
-72II	9	HMS-85.2 S-14.8	43.2	(6270)	1.37	(198.5)	184	(26.7)	10.3	(47.4)
-47D	2-Heltra	HMS-64 S-36	36.7	(5300)	1.25	(181.5)	158	(22.95)	10.8	(54.5)

Table XXXIII (Cont'd)

UARL No.	Composition Type	v/o Fiber Ratio (actual)	Short Beam Shear[b] MN/m^2	(psi)	Flexural Strength[c] GN/m^2	(ksi)	Flexural Modulus[c] GN/m^2	($psi \times 10^6$)	Charpy Impact Strength Joules/cm^2	(ft-lbs/in^2)
NAS-6II	11	AS-91.5 S-8.5	125.5	(18,200)	2.39	(346.5)	148	(21.55)	16.5	(76.5)
-76II	1-UARL	AS-74.6 S-25.4	118	(17,100)	1.98	(285.5) (270.8)	122	(17.7)	23.2	(107)
-12AII	14	HMS-89 K-11	46.6	(6760)	1.58	(229)	202	(29.2)	9.04	(41.6)
-11AII	14	HMS-49.2 K-50.8	50.2	(7288)	1.25	(181)	138.5	(20.1)	12.7	(58.6)
-28II	18	HMS-92 K-80	44.0	(6380)	1.42	(206)	148	(21.5)	10.1	(46.5)
-13II	12	AS-89.4 K-10.6	100	(14,450)	1.96	(285) (237)	138	(19.9)	19.6	(90.4)
-78II	3-UARL	AS-83.6 K-16.4	80	(11,650)	1.875	(272) (293)	132	(19.15)	19.3	(89.0)
-1AII	AS	AS-59	124	(17,980)	1.90	(275)	125	(18.1)	15.1	(69.7)
-3AII	S-glass	S-66	109	(15,870)	1.90	(275)	56	(8.1)	56.3	(259.5)
-5AII	Kevlar	K-66.9	41.6	(6030)	0.68	(98.4)	75.8	(11)	15.7	(72.6)
-61II	HMS	HMS-63	49	(7100)	1.185	(172)	190	(27.5)	8.72	(40.2)

[a]Average of two tests
[b]Span-to-depth = 4/1
[c]3-point flex, 32/1

Table XXXIV

Impact Data for Thin Unidirectional Hybrid Fiber Epoxy Composites

UARL No.	Composition Type	Fiber	$P_i = P_{max}$ Newtons	(lbs)	Charpy Impact Strength[a] Joules	(ft-lbs)
NAS-9II	13	HMS/S-glass	534	(120)	2.76	(1.97)
-10II	13	"	534	(120)	1.96	(1.40)
-15AII	13	"	534	(120)	1.93	(1.38)
-24II	17	"	623	(140)	2.2	(1.57)
-36II	2-UARL	"	710	(160)	3.05	(2.18)
-55II	20_{a-1}	"	890	(200)	2.74	(1.96)
-54II	20_{a-2}	"	1110	(250)	2.58	(1.84)
-72II	9	"	712	(160)	2.07	(1.48)
-47D	2-Heltra	"	391	(88)	1.3	(0.93)
-6II	11	AS/S-glass	624	(140)	3.36	(2.40)
-76II	1-UARL	"	1200	(270)	4.57	(3.27)
-12AII	14	HMS/Kevlar	712	(160)	1.85	(1.32)
-11AII	14	"	624	(140)	2.31	(1.65)
-28II	18	"	756=P_i= (170) 935=P_{max}=(210)		2.26	(1.61)
-13II	12	AS/Kevlar	1065=P_i= (240) 1690=P_{max}=(380)		4.48	(3.20)
-78II	3-UARL	"	710=P_i= (160) 1242=P_{max}=(280)		4.17	(2.98)
-1AII	-	AS	1420	(320)	2.44	(1.74)
-3AII	-	S-glass	1020=P_i= (230) 1420+=P_{max}= (320+)		8.34	(5.95)
-5AII	-	Kevlar	232=P_i= (52) 334=P_{max}=(75)		1.88	(1.34)
-61II	-	HMS	666	(150)	1.16	(0.83)

[a]average of two tests

the same impact response, 107 and 90.4 ft-lb/in.^{2} respectively, while the intraply HMS/S-glass laminate (NAS-36 II) was lower, 59.4 ft-lb/in.^{2}. It should also be noted that the fracture initiation energy, P_i, of the hybrid composites is similar to or less than the P_i obtained for the respective homogeneous graphite laminates. These data indicate that hybridization while improving total energy adsorption capability may not result in marked improvements in threshold damage levels as measured ballistically.

A plot of flexural modulus vs impact energy shown in Fig. 60 identifies the six laminate types which meet the criteria for further evaluation in Tasks III and IV. These are:

a. NAS-9 II - HMS/S-glass (50 v/o) interply
b. NAS-10 II - HMS/S-glass (25 v/o) interply
c. NAS-36 II - HMS/S-glass (25 v/o) intraply
d. NAS 6 II - AS/S-glass (10 v/o) interply
e. NAS 13 II - AS/Kevlar 49 (10 v/o) interply
f. NAS 78 II - AS/Kevlar 49 (15 v/o) intraply.

The selection of these six composites will be discussed in more detail below.

To provide added emphasis for the use of the thin Charpy impact specimen to correlate with ballistic data it was of interest to compare the standard specimen (thick specimens) in the same manner to determine any differences in selection which would have resulted if the selection were made at the end of Task I. Figure 61 illustrates the differences obtained with the thick specimens using data from Task I for the same sixteen unidirectional composites. Based on these results only three of the above composites, b, c and e, would have been chosen for study in Tasks III and IV. In addition, a large difference in the relative impact response of AS graphite, Kevlar 49 and HMS graphite homogeneous laminates was found. With thin specimens AS and Kevlar 49 gave essentially the same impact energy with HMS approximately 40 percent lower, while with the standard sized specimens Kevlar 49 > AS > HMS.

The core-shell HMS/S-glass and Kevlar 49 laminates as well as the interply HMS/Kevlar 49 laminates show the same relative response of modulus to impact energy in both the standard and thin Charpy specimens. These results indicate the impact response of the various hybrid laminates to thickness changes is different depending upon the primary as well as secondary fibers employed as well as the type of ply layup. Additional investigation of the thickness effect must be carried out before any definite conclusions can be made.

3.4 Analysis of Thickness Effects

As previously discussed in Section 2.2.3 shear stress and flexural stress interaction diagrams were constructed for a unidirectional hybrid fiber composite to determine the maximum L/h value at which failure should occur in interlaminar shear. Above that point failure should be controlled by flexural properties.

FLEXURAL MODULUS – PENDULUM IMPACT ENERGY/UNIT AREA THIN UNDIRECTIONAL HYBRID FIBER EPOXY COMPOSITES

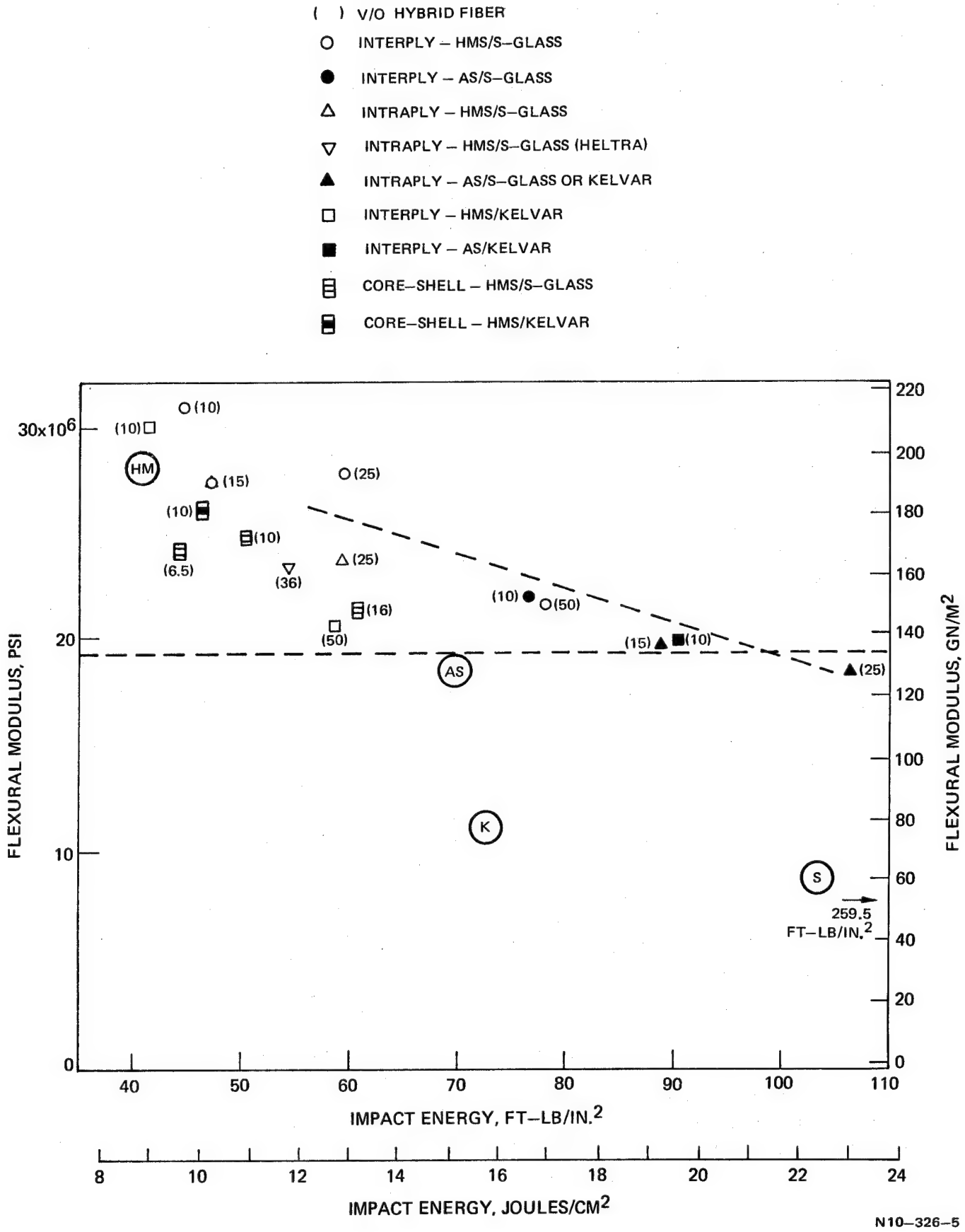

FLEXURAL MODULUS–PENDULUM IMPACT ENERGY/UNIT AREA UNDIRECTIONAL HYBRID FIBER EPOXY COMPOSITES

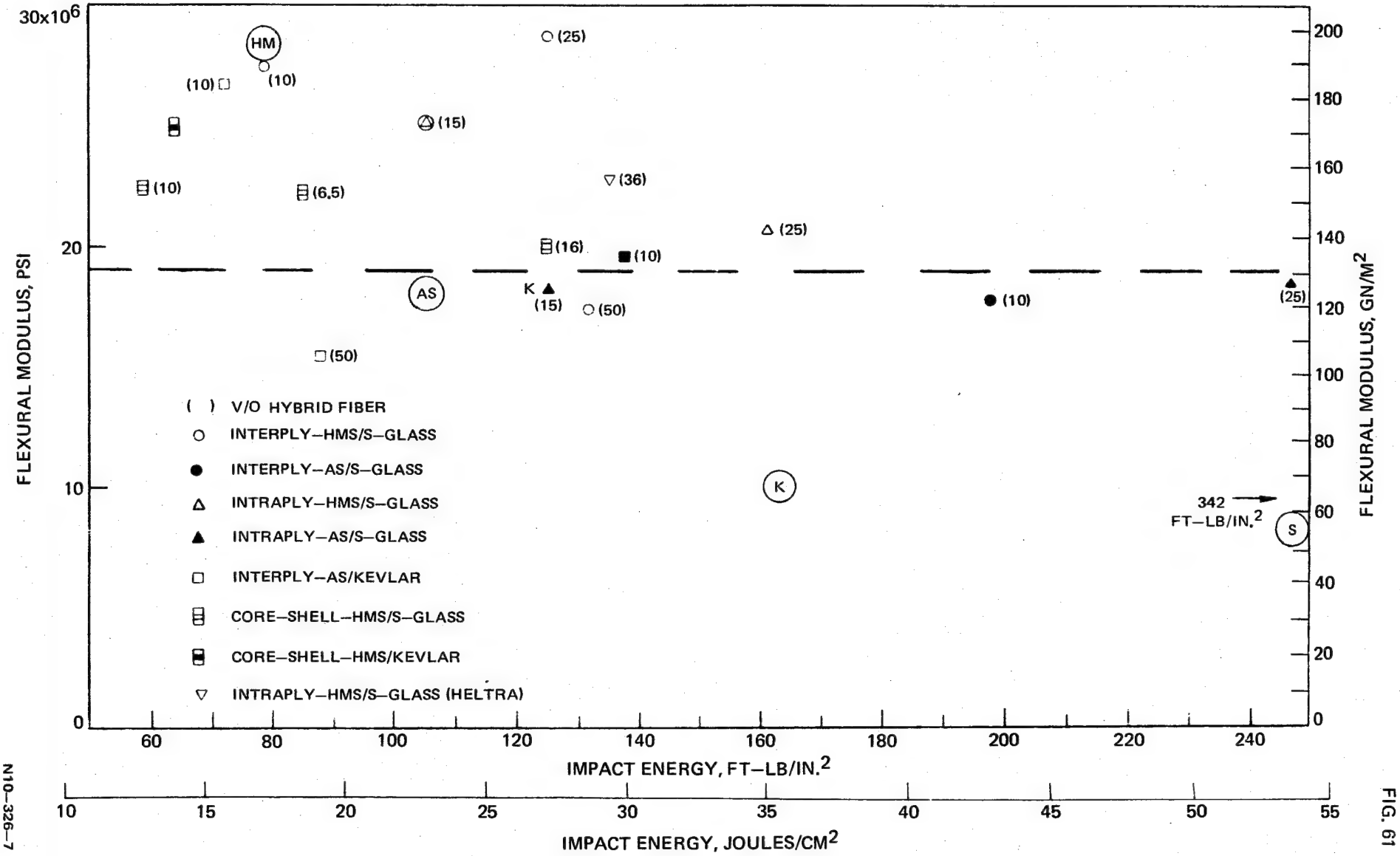

N10–326–7

FIG. 61

Similar calculations were carried out using the angle-ply data for two of the four angle-ply composites evaluated. These were HMS/S-glass $[\pm 22,0,+22,0,-22]_s$ NASX-12 and AS/S-glass $[\pm 40,0,+10,0,-10]_s$ NASX-5. The shear stress interaction diagrams are shown in Figs. 62 and 63. In both instances it is apparent that the theoretical beam equations employed do not relate to angle-ply systems but are only applicable for unidirectional laminates. Reasonable agreement between theory and results obtained from pendulum impact and slow bend tests was found at high L/h values, i.e. in the flexural failure mode area, but at low L/h, approaching the shear failure mode area, deviation from the theoretical curve was evident. Similar effects were found in the flexure stress interaction diagram for the two composites, Figs. 64 and 65.

The type of analysis required to develop new beam equations for shear and flexure stresses in angle-ply composites is beyond the scope of this program. Therefore, no further effort to determine thickness effects as they relate to failure modes in these composites was carried out.

3.5 Conclusions from Task II Results

The $[\pm 40,0,+10,0,-10]_s$ angle-ply configuration is superior to $[\pm 22,0,+22,0,-22]_s$ configuration in pendulum impact resistance while the reverse is true in terms of composite modulus for AS/S-glass and HMS/S-glass intraply and AS/Kevlar 49 interply laminates. The $[\pm 45,0,+45,0,-45]_s$ configuration is inferior to the other angle-plys in both modulus and impact resistance.

For each angle-ply tested the AS/S-glass intraply laminate offered the best combination of modulus and pendulum impact energy.

A definitive change in impact energy levels and presumably fracture mechanism occurs near the 0.508 cm (0.200 in.) thickness range when decreasing the angle-ply composite thickness from that of a standard Charpy specimen. This is apparent in total impact energy obtained, load-time trace curves and comparison of static and dynamic shear and bending stresses calculated from slow bend and impact tests.

In ballistic impact the intraply AS/S-glass and interply AS/Kevlar 49 laminates attain similar threshold damage levels using the $[\pm 22,0,+22,0,-22]_s$ and $[\pm 40,0,+10,0,-10]_s$ angle-ply construction. The Kevlar-hybrid is slightly superior in both instances. The HMS/S-glass intraply laminate in all three angle ply configurations was considerably poorer. This was true when correlating percent shear modulus retention with projectile velocity or total pendulum impact energy.

A ballistic impact parameter (E/V) which relates projectile energy and impact affected volume of the specimen has been shown to provide improved correlation between the ballistic impact data and pendulum impact data, resulting in the same ranking order for laminates impacted in the two tests. The E/V parameter accounts for thickness variations in the present study.

FIG. 62

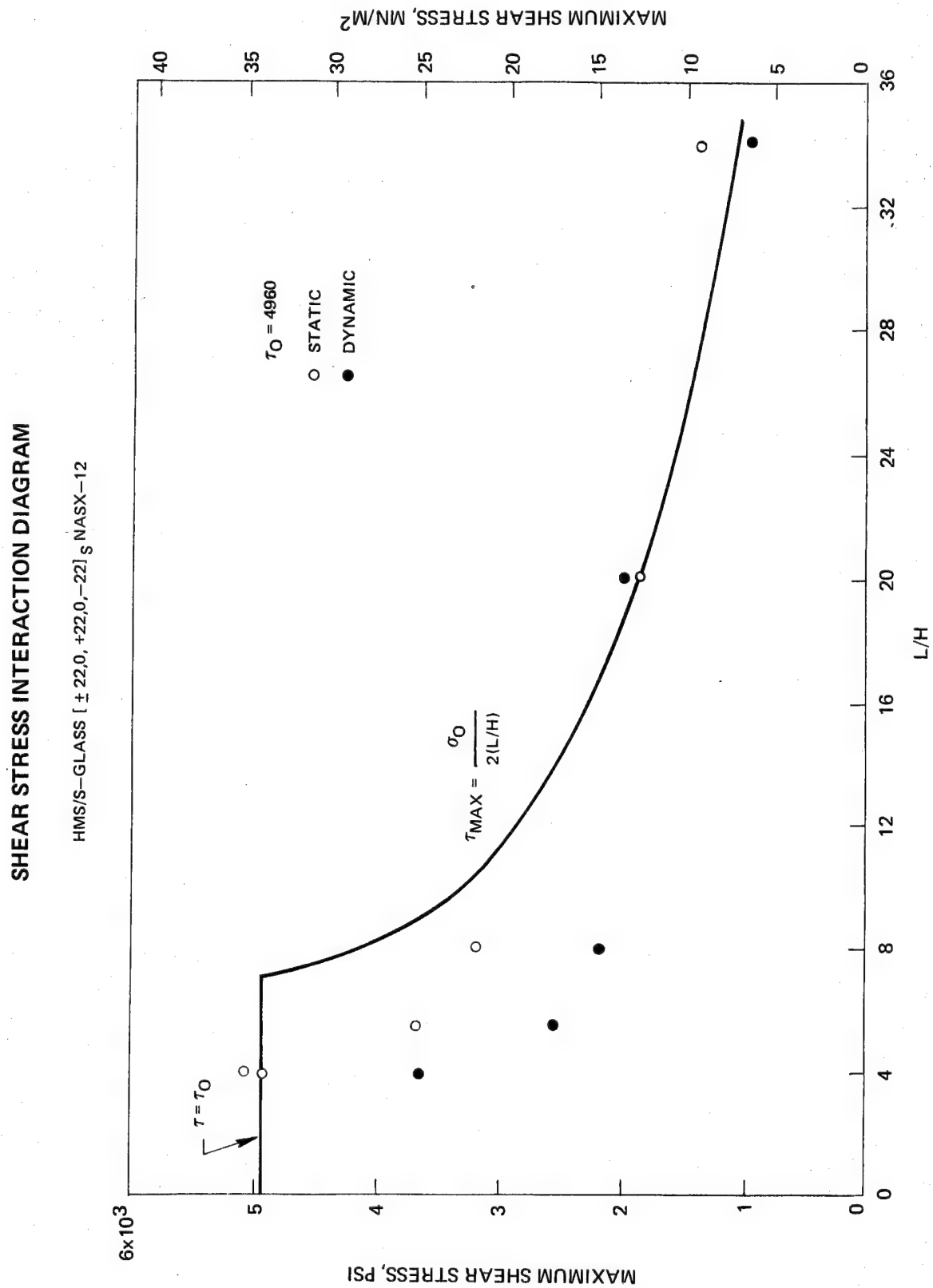

N10–259–3

FIG. 63

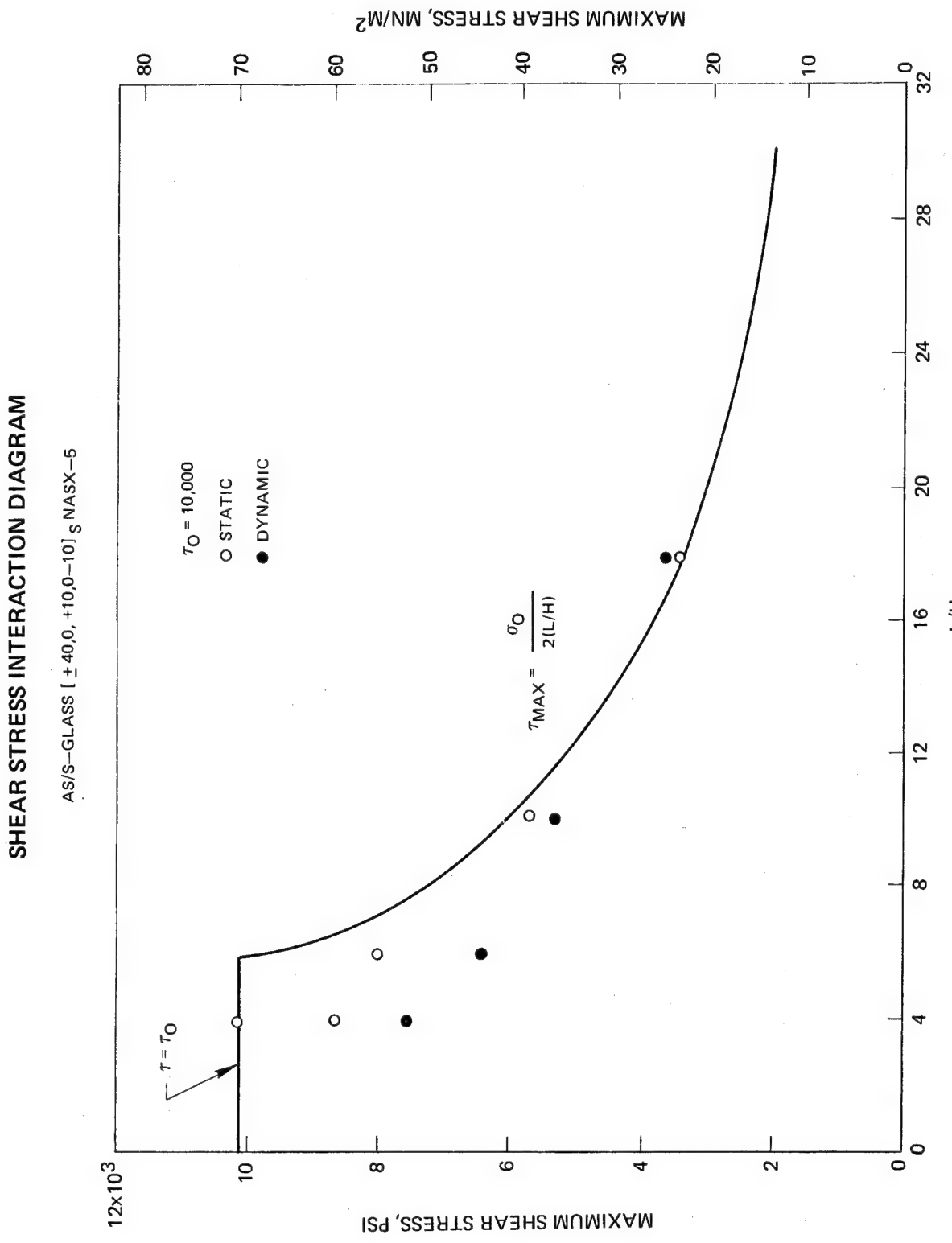

N10–259–2

FIG. 64

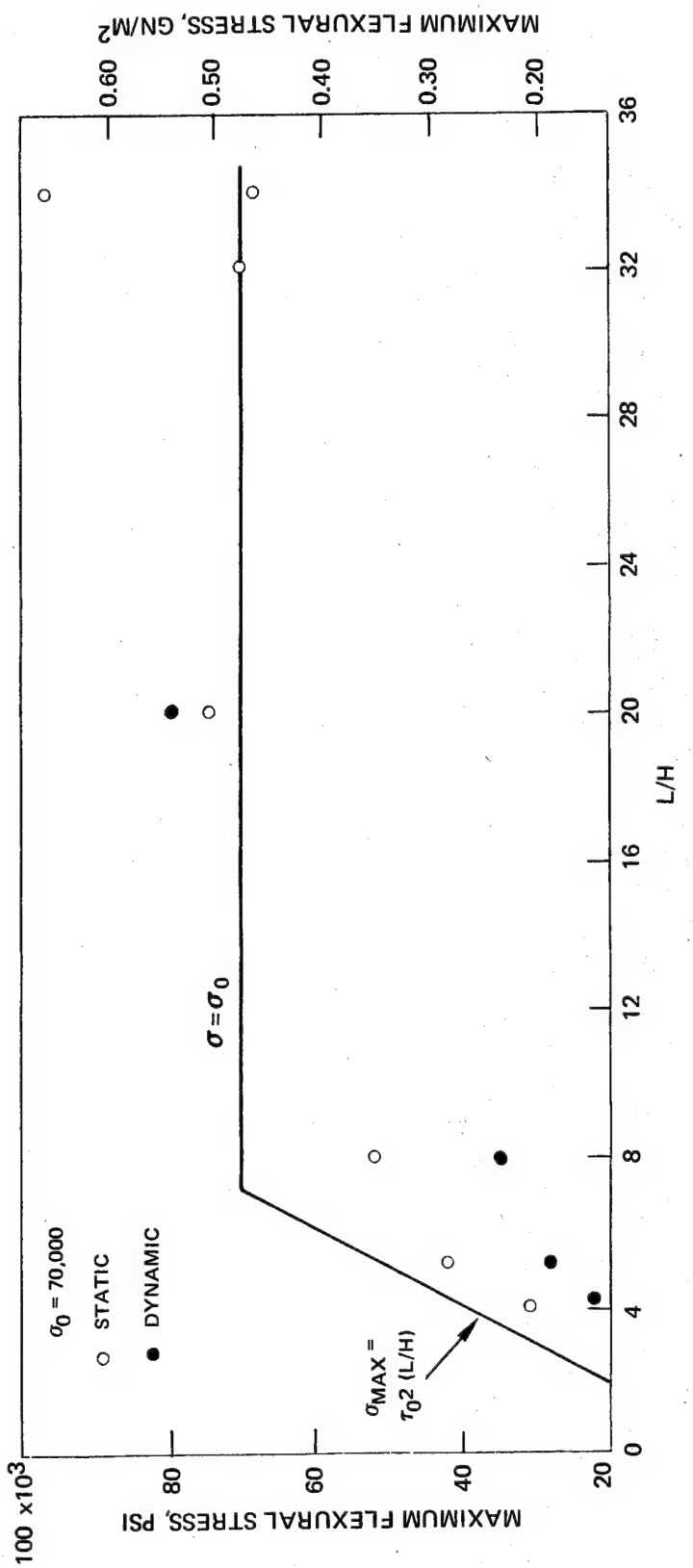

N10–259–4

FIG. 65

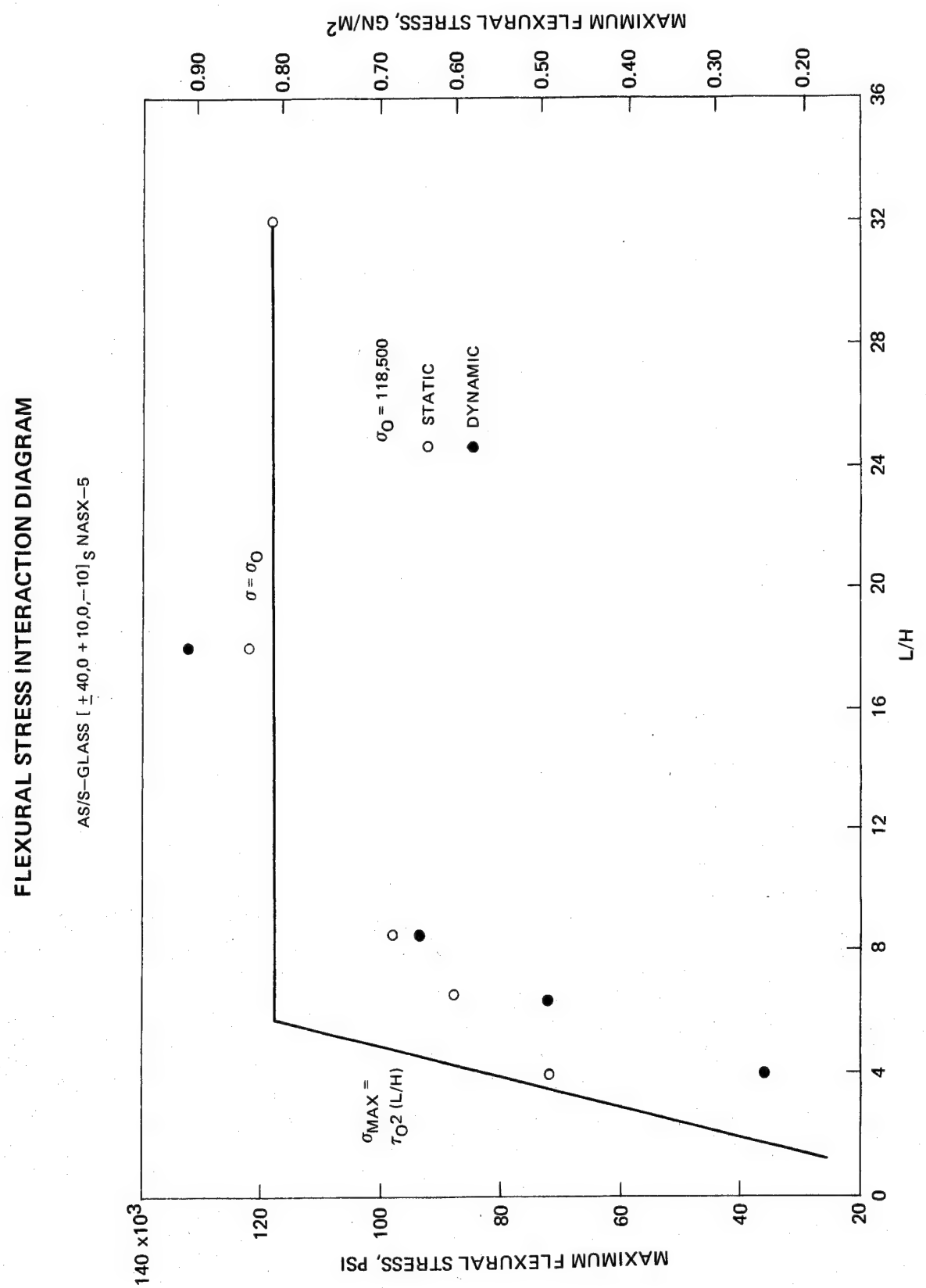

N10–259–1

With the intraply construction it was shown that fracture initiation load (from pendulum impact) correlates with the ballistic threshold damage parameter, E/V regardless of ply-angle or primary graphite fiber. The E/V value near the point of total destruction under ballistic impact correlates with the total impact energy obtained in thin Charpy specimens regardless of angle-ply or hybrid construction but differentiates between primary graphite fibers.

Damage threshold levels as measured in thin Charpy hybrid specimens were lower than those measured with homogeneous graphite specimens. Thus, it appears that hybridization did not increase the resistance to initial fracture. However, total energy absorption or resistance to catastrophic failure was increased.

3.6 Selection of Laminates for Evaluation in Tasks III and IV

As indicated in Section 3.3 above, the six selected laminates for further evaluation in Tasks III and IV provide the best combination of impact level together with other mechanical properties. This conclusion is based on the test results from all fabricated laminates in Tasks I and II. The criteria used for selection was as follows: (1) impact level; (2) When compared with the mechanical properties of unidirectional homogeneous composites made from primary fibers, the candidate laminates shall have (a) flexural and short beam shear strengths not less than 80 percent and 70 percent, respectively of the strengths of the homogeneous composites, and (b) composite flexural modulus not less than 19×10^6 psi. The selections were submitted to and approved by the NASA-LeRC Project Manager.

Because the tow-by-tow AS/S-glass system (NAS-76) had consistently given high impact response, it was included in the group for Tasks III and IV to give a total of seven laminate types rather than six. As shown in Fig. 61, this system does not meet the modulus requirement. However, it does give the same modulus level as obtained with the homogeneous AS graphite system.

The mechanical properties of the seven selected hybrid fiber composites are listed in Table XXXV. They include three HMS/S-glass (one tow-by-tow and two interply), two AS/S-glass (tow-by-tow and interply), and two AS/Kevlar 49 III (tow-by-tow and interply) laminate types. The AS/S-glass and AS/Kevlar 49 interply composites could also be considered as core/shell since they consist of one hybrid fiber layer inserted between eight AS graphite layers.

The order in terms of impact response is different based upon standard sized Charpy and thin Charpy specimens which reflects the difference in primary failure mode between the two thickness levels. This difference is most apparent in the HMS/S-glass composites which by standard Charpy shows the tow-by-tow construction (NAS-36) to be superior to the interply type (NAS-9 and 10). This is due, as previously discussed, to the out of plane shear failure of the tow-by-tow construction. In the thin Charpy laminates the level of S-glass content appears to control impact energy. NAS-9 (50 v/o glass) had a higher impact energy than

Table XXXV

Mechanical Properties of Hybrid Fiber Composites for Task III and IV Evaluation

	HMS/S-glass 2-UARL NAS-36	HMS/S-glass Type 13 NAS-9	HMS/S-glass Type 13 NAS-10	AS/S-glass 1-UARL NAS-76	AS/S-glass Type 11 NAS-6	AS/Kevlar 3-UARL NAS-78	AS/Kevlar Type 12 NAS-13
Flexural[a] Strength, ksi	177	198	195	278	295	283	261
Modulus[a], psi x 10^6	21.8	19.4	27.9	18.1	19.7	19.15[c]	19.7
Shear[a], psi	7085	7200	7725	17,675	16,660	12,880	12,125
Impact[b] Standard Charpy, ft-lbs	24.5	20	18	37.5	30	19	21
Thin Charpy[c] ft-lb/in.	59.3	78.2	59.4	107	76.5	89	90.4

[a]average of five tests
[b]average of three tests
[c]average of two tests

either NAS-10 (22 v/o glass-interply) and NAS-36 (27 v/o glass-intraply) which gave the same impact response. This indicates that shear failure is of minor importance in the thin Charpy, and presumably in ballistic impact at the L/h ratios used.

Comparison of the AS/S-glass and AS/Kevlar composites also shows the effect of specimen thickness. With standard Charpy specimens the two AS/S-glass laminates were considerably higher in impact response than the Kevlar hybrids. In the thin impact specimens the AS/Kevlar laminates are intermediate between the AS/S-glass intraply (tow-by-tow) and interply constructions.

IV. MECHANICAL PROPERTY CHARACTERIZATION OF UNIDIRECTIONAL COMPOSITE LAMINATES - TASK III

In order to gain a more complete understanding of the effects of hybrid fiber reinforcement and ply construction on the mechanical properties of epoxy resin matrix composites, a more comprehensive evaluation of the seven laminates selected at the end of Task II (Table XXXV) was undertaken. The seven selected laminates were fabricated as before using unidirectional ply configuration in 11.4 cm (4.5 in.) x 2.67 cm (10.5 in.) panels from which were cut specimens for longitudinal tension and compression, transverse tension and compression and shear strength ($S_{\ell 11T}$, $S_{\ell 11c}$, $S_{\ell 22t}$, $S_{\ell 22c}$, and $S_{\ell 12s}$) tests. The physical properties of the resulting laminates are listed in Table XXXVI. For convenience, the composites are identified using the same numbers as used in Tasks I and II. All testing was carried out in triplicate.

4.1 Interlaminar Shear Strength

The room temperature shear strengths obtained (S/D = 4/1) are listed in Table XXXVII together with the results previously recorded in Tasks I and II. With two exceptions, the Task III shear strengths fell between the averages of the two previous tests. The two HMS/S-glass interply laminates gave higher shear levels than were previously noted. These laminates were made using a different lot of HMS fiber and as was previously mentioned variations in fiber lots have been noted. This undoubtedly accounts for the results obtained.

All composite test specimens were characterized by shear failure as was previously found in Tasks I and II. These shear results are used in Task IV to correlate with the high and low temperature shear test data.

4.2 Tensile Strength and Modulus

The room temperature transverse and longitudinal tensile strengths and moduli of the seven selected composites are listed in Table XXXVIII.

The transverse tensile strengths of the AS/S-glass inter and intraply laminates are far superior to any of the other combinations with the latter type (tow-by-tow) having the highest strength (10,700 psi) as well as modulus. With the three HMS/S-glass composites the strength increased as the glass content increased in the interply type with the intraply (tow-by-tow) giving the lowest strength but the highest transverse modulus. A similar effect was found with the two AS/Kevlar laminates. The intraply configuration had the lower strength but higher modulus compared to the interply. These results reflect the differences in the two types of construction in that in the interply only the fiber layers which have the highest transverse tensile properties are involved in load transfer while in the intraply type the combined fiber transverse properties are involved.

Table XXXVI

Physical Properties of Task III Hybrid Composites

Composite No.	Composition Type	Density (g/cc)	v/o Total Fiber	v/o Resin	v/o Void	v/o Fiber Ratio (actual)
NAS-78 III	Intraply	1.55	AS-51.2 Kevlar-9.6	38.0	1.2	AS-84.1 Kevlar-15.8
NAS-13 III	Interply	1.59	AS-61.1 Kevlar-6.2	31.3	1.4	AS-90.8 Kevlar-9.2
NAS-9 III	Interply	1.65	HMS-33.9 S-14.6	49.1	2.4	HMS-70 S-30
NAS-10 III	Interply	1.65	HMS-44.5 S-8.0	44.6	2.9	HMS-85.0 S-15.0
NAS-36 III	Intraply	1.72	HMS-40.6 S-16.9	40.3	2.2	HMS-70.8 S-29.2
NAS-6 III	Interply	1.63	AS-50.7 S-4.4	41.7	3.2	AS-90.8 S-9.2
NAS-76 III	Intraply	1.68	AS-46.5 S-13.5	41.3	3.7	AS-77.5 S-22.5

Table XXXVII

Room Temperature Interlaminar Shear Strength of
Hybrid Fiber Epoxy Composites

Composite No.	Fiber	Construction Type	Interlaminar Shear Strength[a]			
			MN/m^2	(psi)	Task I (psi)	Task II (psi)
NAS-78 III	AS/Kevlar	Intraply	90.5	(13,130)	(14,120)	(11,650)
NAS-13 III	AS/Kevlar	Interply	83.8	(12,165)	(10,800)	(14,450)
NAS-9 III	HMS/S-glass	Interply	70.4	(10,207)	(7,940)	(6,535)
NAS-10 III	HMS/S-glass	Interply	72.5	(10,560)	(8,100)	(7,350)
NAS-36 III	HMS/S-glass	Intraply	43.2	(6,270)	(5,970)	(8,200)
NAS-6 III	AS/S-glass	Interply	116.5	(16,930)	(18,200)	(15,125)
NAS-76 III	AS/S-glass	Intraply	112.0	(16,280)	(18,250)	(17,100)

[a] S/D = 4/1; values are average of three tests

Table XXXVIII

Transverse and Longitudinal Tensile Strength and Modulus of Hybrid Fiber Epoxy Composites[a]

Composite No.	Fiber	Construction Type	Transverse Strength MN/m^2	(psi)	Transverse Modulus GN/m^2	($psix10^6$)	Longitudinal Strength GN/m^2	(ksi)	Longitudinal Modulus GN/m^2	($psix10^6$)
NAS-78 III	AS/Kevlar	Intraply	16.4	(2380)	14.8	(2.14)	1.68	(244)	122	(17.7)
NAS-13 III	AS/Kevlar	Interply	26.2	(3790)	12.6	(1.83)	1.78	(257.9)	143.5	(20.8)
NAS-9 III	HMS/S-glass	Interply	32.8	(4750)	13.0	(1.88)	1.035	(150.25)	136	(19.7)
NAS-10 III	HMS/S-glass	Interply	25.7	(3725)	11.1	(1.61)	1.14	(165.4)	143.5	(20.8)
NAS-36 III	HMS/S-glass	Intraply	15.9	(2300)	13.6	(1.98)	1.12	(162)	168	(24.35)
NAS-6 III	AS/S-glass	Interply	54.5	(7915)	11.7	(1.7)	1.63	(237.6)	115.5	(16.76)
NAS-76 III	AS/S-glass	Intraply	73.8	(10,700)	15.9	(2.3)	1.59	(231)	114	(16.5)

[a]All data average of three tests at room temperature

In contrast, longitudinal tensile strengths and modulus are relatively insensitive to the ply construction type. The differences which do occur appear to be related to the ratio of the two hybrid fibers employed in each composite system.

4.3 Compressive Strength and Modulus

The room temperature transverse and longitudinal strengths and moduli of the seven selected composites are listed in Table XXXIX.

The transverse compressive strength and modulus of the AS/S-glass and HMS/S-glass intraply composites were higher than those of the corresponding interply types in each case. In contrast, the AS/Kevlar intraply composite had a lower transverse compressive strength and modulus compared to the corresponding interply laminate (NAS-9). This, as discussed above, reflects the use of the combined fibers in load transfer in the intraply systems as well as the poorer compressive properties of Kevlar 49 compared to S-glass.

The longitudinal compressive strengths, as were the longitudinal tensile properties, appear to be relatively insensitive to ply construction and reflect more the ratio of the two fibers involved in each laminate.

Table XXXIX

Transverse and Longitudinal Compressive Strength and Modulus of Hybrid Fiber Epoxy Composites[a]

Composite No.	Fiber	Construction Type	Transverse Strength MN/m^2	(ksi)	Transverse Modulus GN/m^2	($psix10^6$)	Longitudinal Strength GN/m^2	(ksi)	Longitudinal Modulus GN/m^2	($psix10^6$)
NAS-78 III	AS/Kevlar	Intraply	193	(28.0)[b]	12.4	(1.8)	1.32	(191.8)	124	(18.0)
NAS-13 III	AS/Kevlar	Interply	246	(35.7)	13.8	(2.0)	1.41	(205.2)	166	(24.1)
NAS-9 III	HMS/S-glass	Interply	163	(23.6)	13.4	(1.94)	0.755	(109.4)	136	(19.7)
NAS-10 III	HMS/S-glass	Interply	173	(25.1)	11.5	(1.67)	0.905	(131.7)	154	(22.3)
NAS-36 III	HMS/S-glass	Intraply	162	(23.5)[b]	21.4	(3.1)	0.815	(118.5)	154.5	(22.4)
NAS-6 III	AS/S-glass	Interply	225	(32.6)	13.9	(2.02)	1.29	(188.1)	138	(20.0)
NAS-76 III	AS/S-glass	Intraply	265	(38.4)	16.5	(2.4)	1.26	(183.5)	118	(17.1)

[a]All strength data average of three tests except where indicated.

[b]One test only

V. FINAL COMPOSITE LAMINATE CONFIGURATION SCREENING - TASK IV

The objective of this task was to perform more extensive properties studies on the seven selected laminates. In particular the effect of temperature and resin matrix on shear, flexural, and thin Charpy impact strengths as well as coefficient of thermal expansion has been determined. The three resin matrices used were ERLA-4617 epoxy, PMR-15 polyimide (Ref. 10) and polyphenylquinoxaline prepared from monomeric reactants (Ref. 11). Fabrication procedures for each type are described in the Appendix. The seven laminates were divided between the three resin types as follows:

Composite No.	Type	Fiber	Resin
NAS-9 IV	Interply	HMS/S-glass	Epoxy 4617
-13 IV	Interply	AS/Kevlar	Epoxy 4617
-78 IV	Intraply	AS/Kevlar	Epoxy 4617
NAS-36 IV	Intraply	HMS/S-glass	PMR-15 polyimide
-76 IV	Intraply	AS/S-glass	PMR-15 polyimide
NAS-6 IV	Interply	AS/S-glass	PPQ
-10 IV	Interply	HMS/S-glass	PPQ

The physical properties of the fabricated composites are listed in Table XL. All testing was carried out in triplicate. For convenience the composites are identified using the same numbers as used in Tasks I, II and III. The two polyimide laminates had a lower total fiber content (~50 v/o) than the average fiber volume (~60-65 v/o) which the majority of composites contained throughout the program. The results are discussed without normalizing the polyimide data to the average fiber volume.

5.1 Interlaminar Shear Strengths

Shear strengths determined at -74.6°C (-100°F), 149°C (300°F) and 315°C (600°F) for the seven laminates are listed in Table XLI and shown graphically in Fig. 66.

In general, shear strength increased with decreasing temperature. The magnitude of the increase when cooling from room temperature to -74.6°C varied depending upon the resin matrix and ply construction. AS/S-glass/polyimide-intraply, AS/Kevlar/epoxy-interply and AS/S-glass/PPQ-interply showed significant increases in shear with drop in temperature while AS/Kevlar/epoxy-intraply, HMS/S-glass/epoxy-interply and HMS/S-glass/polyimide-intraply gave only minor increases. The HMS/S-glass/PPQ-interply laminate had a lower shear strength at -74.6°C than at room temperature. This latter type of behavior has been reported in other PPQ laminates with HMS reinforcement (Ref. 12).

Table XL

Physical Properties of Task IV Hybrid Composites

Composite No.	Composition Type	Resin	Density g/cc	v/o Total Fiber	v/o Resin	v/o Void	v/o Fiber Ratio (actual)
NAS-78 IV	Intraply	Epoxy	1.55	AS-51.2 Kevlar-9.6	38.0	1.2	AS-84.2 Kevlar-15.8
NAS-13 IV	Interply	Epoxy	1.59	AS-61.1 Kevlar-6.2	31.0	1.4	AS-90.8 Kevlar-9.2
NAS-9 IV	Interply	Epoxy	1.65	HMS-33.9 S-14.6	49.1	2.4	HMS-70 S-30
NAS-76 IV	Intraply	PI	1.63	AS-38.1 S-14.7	42.7	4.5	AS-72.3 S-27.7
NAS-36 IV	Intraply	PI	1.64	HMS-35.0 S-14.0	45.2	5.7	HMS-71.5 S-28.5
NAS-6 IV	Interply	PPQ	1.62	AS-55.1 S-3.8	41.1	0	AS-93.55 S-6.45
NAS-10 IV	Interply	PPQ	1.66	HMS-55.1 S-8.0	32.2	4.7	HMS-87.3 S-12.7

Table XLI

Interlaminar Shear Strength of Hybrid Fiber Composites
Temperature Effects

Composite No.	Composition	Construction Type	Interlaminar Shear Strength,[a] MN/m^2 (psi) -74.6°C		149°C		315°C	
NAS-78 IV	AS/Kevlar/Epoxy	Intraply	85.0	(13,550)	58.8	(8543)	-	
NAS-13 IV	AS/Kevlar/Epoxy	Interply	118.5	(17,201)	50.0	(7260)	-	
NAS-9 IV	HMS/S-glass/Epoxy	Interply	70.5	(10,230)	25.8	(3750)	-	
NAS-76 IV	AS/S-glass/PI	Intraply	124.8	(18,100)	62.6	(9100)	37.8	(5485)
NAS-36 IV	HMS/S-glass/PI	Intraply	54.5	(7910)	44.7	(6490)	29.2	(4230)
NAS-6 IV[b]	AS/S-glass/PPQ	Interply	105.5	(15,310)	65.5	(9500)	40.9	(5940)
NAS-10 IV[c]	HMS/S-glass/PPQ	Interply	37.7	(5473)	41.8	(6063)	14.1	(2040)

[a]S/D = 4/1, average of three tests
[b]Shear strength at RT = 11,900 psi
[c]Shear strength at RT = 6800 psi

INTERLAMINAR SHEAR STRENGTH VARIATION WITH TEMPERATURE HYBRID COMPOSITES

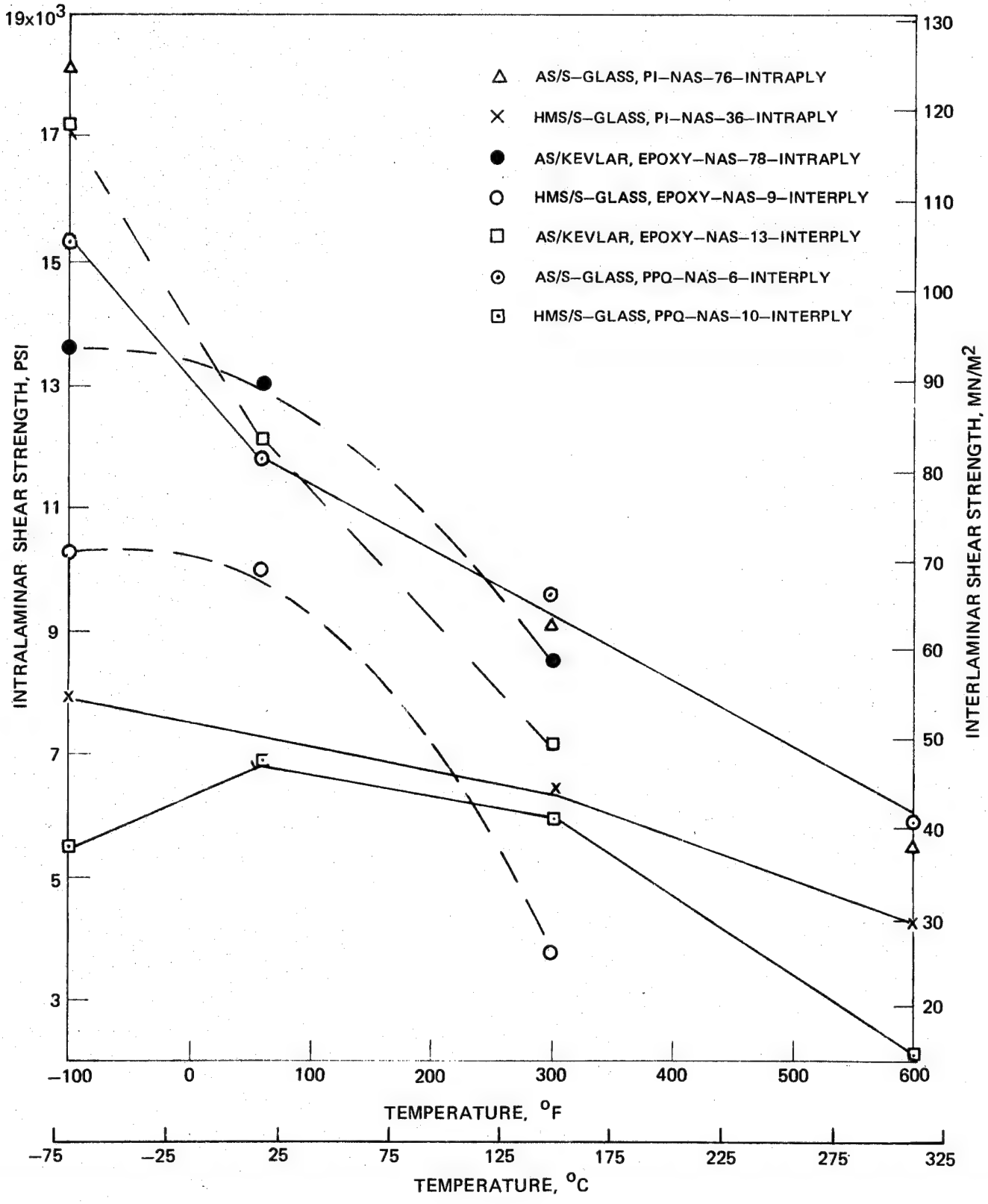

The change in shear strength with increasing temperature (above RT) was also varied with the epoxy laminates showing more rapid strength losses than the PPQ or PI systems. At 315°C the high temperature resin matrix laminates with AS/S-glass reinforcement gave nearly the same shear strength regardless of ply construction (inter or intraply) or matrix resin, PI or PPQ. With the HMS/S-glass laminates the PI intraply laminate had a significantly higher strength than the PPQ interply system.

In the epoxy systems the effect of ply construction on 149°C (300°F) shear strength was also apparent. AS/Kevlar reinforcement with the intraply configuration showed significant improvement in strength retention over the interply construction even though the latter has a higher total fiber content (67%) with a lower Kevlar 49 content (6%). Evidence of the out-of-plane shear fracture, typical of the tow-by-tow construction, was found in the tested intraply laminate which would account for the superior strength retention.

5.2 Flexural Strength and Modulus

The flexural properties of the seven composites measured at -74.6°C, 149°C, and 315°C are listed in Tables XLII and XLIII.

Variations in flexural strengths were minor in the two PPQ laminates each having essentially some strength at -74.6° and 149°C. Strength decreased rapidly, however, from 149° to 315°C. The two polyimide composites behaved similarly in that both had lower strengths at 149°C than at -74.6°C. The decrease in strength from -74.6 to 315°C is linear with the AS/S-glass laminate having the greater strength at all temperatures. The three epoxy laminates all gave rapid strength losses from room temperature to 149°C. Two of the composites decreased in strength on cooling from room temperature to -74.6°C while the third, AS/Kevlar interply showed a slight increase in strength from RT to the low temperature.

The differences in composite failure mode appeared to depend mainly upon the resin matrix rather than construction. The two interply PPQ laminates both failed in shear at -76.4°C and 149°C and in compression at 315°C. The two intraply PI composites failed in tension at -76.4°C, in tension and compression at 149°C and in compression only at 315°C. The three epoxy composites interply and intraply each failed in tension at -76.4°C and in compression at 149°C. Thus, at elevated temperatures, in particular, the softening or thermoplastic nature of the matrix appears to have an effect on the failure modes.

The change in flexural modulus with temperature was also different with the various matrix resins used. The polyimide systems showed only slight modulus change from 149°C to 315°C. The AS/S-glass laminate had the same modulus at all temperatures while the HMS/S-glass laminate gave a somewhat higher modulus at -74.6°C than at 315°C. The PPQ composites gave slight variations in modulus

Table XLII

Flexural Strength of Hybrid Fiber Composites
Temperature Effects[a]

Composite No.	Composition	Construction Type	Flexural Strength, (psi x 10^3) GN/m^2					
			-74.6°C		149°C		315°C	
NAS-78 IV	AS/Kevlar/Epoxy	Intraply	(240)	1.66	(125)	0.86	-	
NAS-13 IV	AS/Kevlar/Epoxy	Interply	(293)	2.02	(117)	0.806	-	
NAS-9 IV	HMS/S/Epoxy	Interply	(163)	1.12	(94)	0.648	-	
NAS-76 IV	AS/S/PI	Intraply	(195)	1.34	(138)	0.95	(63.6)	0.44
NAS-36 IV	HMS/S/PI	Intraply	(144)	0.99	(92.9)	0.64	(57.66)	0.398
NAS-6 IV	AS/S/PPQ	Interply	(115.5)	0.77	(91.9)	0.634	(36.7)	0.253
NAS-10 IV	HMS/S/PPQ	Interply	(160)	1.11	(152)	1.05	(29.85)	0.206

[a]All data average of three tests. S/D = 32/1 three point loading.

Table XLIII

Flexural Modulus of Hybrid Fiber Composites
Temperature Effects[a]

Composite No.	Composition	Construction Type	Flexural Modulus (psi x 10^6) GN/m^2					
			-74.6°C		149°C		315°C	
NAS-78 IV	AS/Kevlar/Epoxy	Intraply	(12.43)	85.5	(15.5)	107	-	
NAS-13 IV	AS/Kevlar/Epoxy	Interply	(17.5)	121	(19.55)	135	-	
NAS-9 IV	HMS/S/Epoxy	Interply	(16.9)	111.65	(14.2)	98	-	
NAS-76 IV	AS/S/PI	Intraply	(11.22)	77.4	(11.33)	77.5	(9.7)	67
NAS-36 IV	HMS/S/PI	Intraply	(17.7)	122	(13.03)	90	(12.3)	85
NAS-6 IV	AS/S/PPQ	Interply	(15.5)	107	(17.4)	120	(7.15)	49.2
NAS-10 IV	HMS/S/PPQ	Interply	(28.4)	196	(26.3)	181.5	(9.65)	66.5

[a]All data average of three tests, S/D = 32/1 three point loading

between -76.4° and 149°C with sharp decreases occurring up to 315°C. The three epoxy laminates each peaked at room temperature with only the AS/Kevlar interply laminate showing no modulus reduction from RT to the 149°C level.

5.3 Pendulum Impact Strength (Thin Specimens)

The results of the Charpy impact test at the three test temperatures, -76.4°, 149°, and 315°C, as well as room temperature are listed for each of the seven selected laminates in Table XLIV in terms of P_i, P_{max} and total impact energy.

In all cases except for one, the P_i and P_{max} loads were the same. The exception was the AS/S-glass/PPQ interply laminate which showed fracture initiation slightly below the highest load capability prior to catastrophic failure. The load-time traces of the AS/S/PI intraply (NAS-76 IV) are shown in Fig. 67 to illustrate the effect of temperature on impact load.

The measured total impact energy variation of the seven laminates with temperature is illustrated graphically in Fig. 68. The three epoxy laminates each peak at room temperature with a slightly lower impact energy at 149°C than at -74.6°C. The AS/Kevlar interply composite resulted in the highest impact strength at room temperature but the HMS/S-glass interply was the best system at -74.6 and 149°C of the three epoxy matrix laminates.

The two PPQ laminates behaved similarly in that little change in impact strength occurred from -74.6 to 149°C followed by a more marked decrease up to 315°C. As would be expected the AS/S-glass laminate had double the impact energy of the HMS/S-glass up to 149°C and was 1.5 times greater at 315°C. The two polyimide systems proved to be the most interesting of the seven laminates. The HMS/S-glass intraply composite gave a substantial decrease in impact resistance from -74.6 to 149°C (approximately 50% loss). At 315°C, however, the impact strength was higher than the value measured at room temperature. This increase in strength at the elevated temperature may be due to thermoplasticity or plastic flow in the resin matrix although there was no visual evidence in the fractured specimens which would indicate this to be the case. Further testing will be required to validate the present data.

The AS/S/PI intraply system proved to have the best overall impact resistance over the temperature range investigated. The impact strength decreased uniformly from -74.6 to 315°C. The high temperature impact strength was 75% of the strength found at -74.6°C and 85% of the room temperature strength. It should be noted that the total fiber content of the laminate was only 52 v/o and that if normalized

Table XLIV

Pendulum Impact Energy Variation with Temperature
Hybrid Fiber Composites[a]

Composite	Impact Load $P_i = P_{max}$ Newtons	(lbs)	Energy Joules	(ft-lbs)	Energy/Area Joules/cm^2	(ft-lb/in^2)
HMS/S/Epoxy-Interply NAS-9 IV						
RT	-	-	3.36	(2.4)	17.9	(83.2)
-100	5,600	(127)	2.78	(1.99)	15.3	(71.0)
300°F	6,660	(150)	2.54	(1.81)	13.9	(64.5)
AS/Kevlar/Epoxy-Intraply NAS-78 IV						
RT	14,900	(335)	3.52	(2.52)	15.2	(70.5)
-100	11,700	(263)	2.48	(1.77)	11.2	(52.0)
300°F	12,000	(270)	2.39	(1.71)	10.35	(48.0)
AS/Kevlar/Epoxy-Interply NAS-13 IV						
RT	12,600	(283)	4.34	(3.1)	22.6	(105)
-100	11,000	(247)	2.73	(1.95)	14.0	(64.8)
300°F	11,000	(247)	2.16	(1.54)	10.8	(50.0)
AS/S/PI-Intraply NAS-76 IV						
RT	14,500	(327)	4.0	(2.95)	17.1	(79.2)
-100	16,000	(360)	4.63	(3.33)	19.45	(90.2)
300°F	14,200	(320)	3.7	(2.64)	15.75	(73.0)
600°F	9,200	(207)	3.4	(2.43)	14.5	(67.1)
HMS/S/PI-Intraply NAS-36 IV						
RT	7,770	(175)	2.84	(2.03)	12.8	(59.2)
-100	6,900	(155)	3.96	(2.83)	19.4	(89.8)
300°F	6,980	(157)	2.46	(1.76)	10.8	(50.0)
600°F	6,230	(140)	2.72	(1.94)	13.9	(64.2)

Table XLIV (Cont'd)

Composite	Impact Load $P_i = P_{max}$ Newtons	(lbs)	Energy Joules	(ft-lbs)	Energy/Area Joules/cm^2	(ft-lb/in^2)
HMS/S/PPQ-Interply						
NAS-10 IV						
RT	5,480	(123)	1.25	(0.89)	7.0	(32.4)
-100	6,000	(135)	1.25	(0.89)	7.0	(32.4)
300°F	6,900	(155)	1.11	(0.79)	6.26	(29.0)
600°F	5,350	(120)	0.825	(0.57)	4.5	(20.9)
AS/S/PPQ-Interply						
NAS-6 IV						
RT	7,340	(165)	3.22	(2.3)	14.05	(65)
-100	6,800	(153)	3.3	(2.36)	14.07	(65.2)
300°F	6,100	(137)	2.98	(2.13)	13.1	(60.6)
600°F	6,800	(153)	1.69	(1.21)	7.46	(34.6)

[a]All data average of three tests at each temperature

FIG. 67

PENDULUM IMPACT ENERGY VARIATION WITH TEMPERATURE HYBRID FIBER COMPOSITES

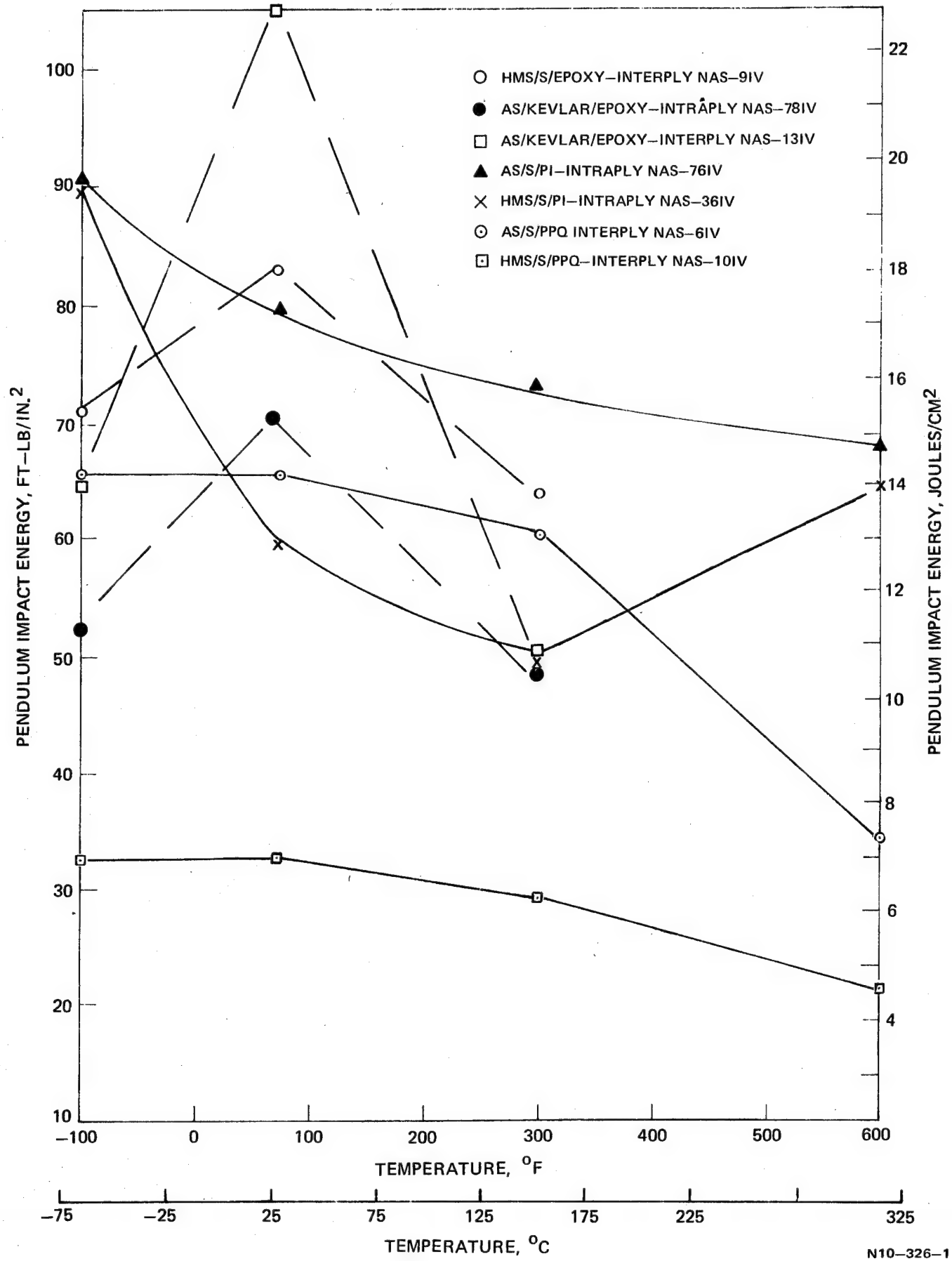

N10–326–1

FIG. 68

EFFECT OF TEMPERATURE ON AS/S–GLASS/POLYIMIDE (NAS–76 IV)
COMPOSITE LOAD–TIME TRACE

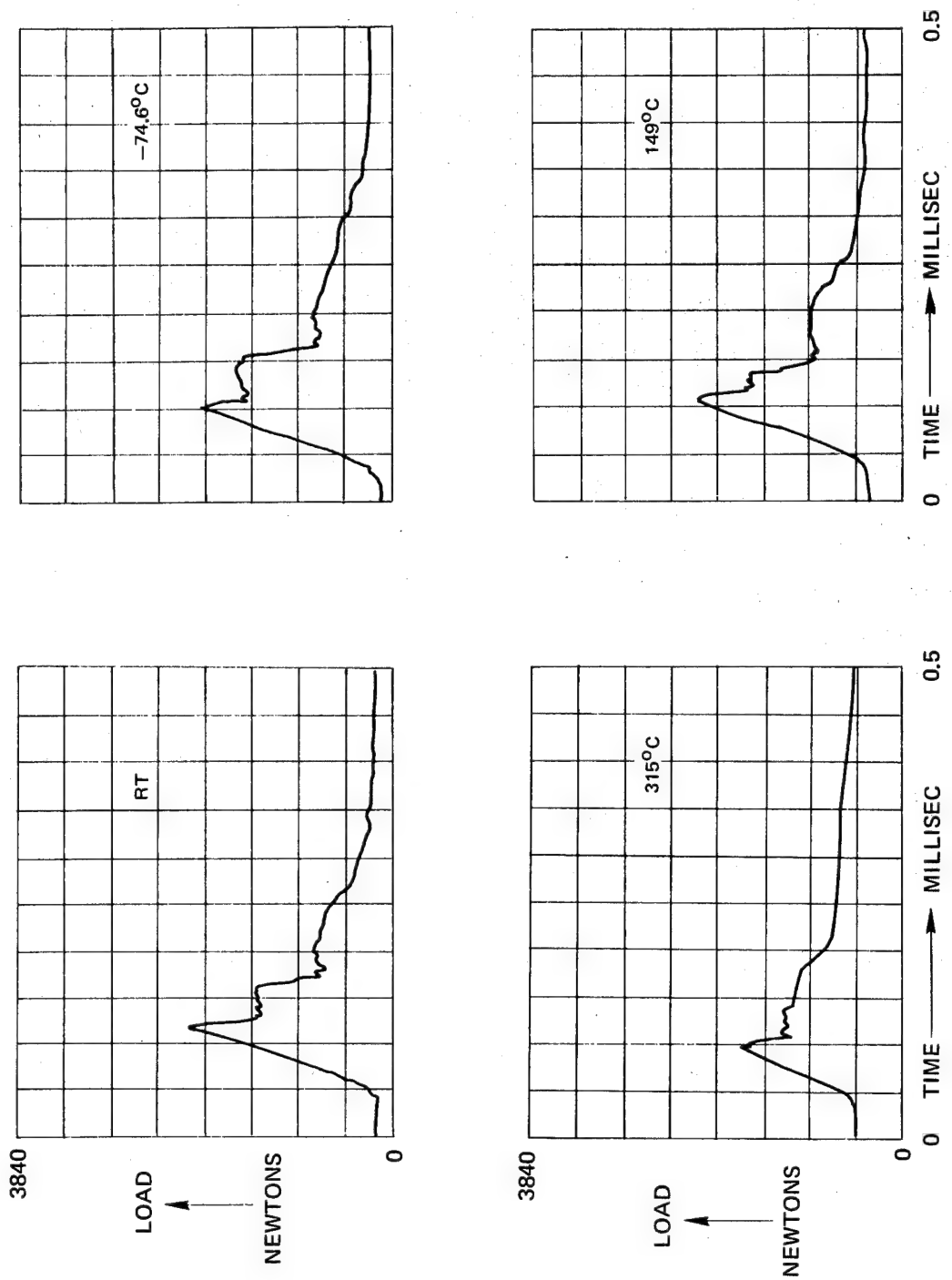

N10–259–5

to a fiber content of 65 v/o, used throughout the program, would result in higher overall impact resistance values. If this extrapolation proves valid, once again the AS/S-glass tow-by-tow configuration appears to be the best configuration evaluated in terms of mechanical properties and impact strengths both in terms of strength retention with increased hybrid fiber (glass) content, temperature, and resin matrix variation.

5.4 Coefficient of Thermal Expansion

Expansion coefficients were measured for the seven laminates in both the longitudinal and transverse directions. Temperatures ranged from -73.4°C (-100°F) to 149°C (300°F) for the three epoxy laminates and from -73.4°C (-100°F) to 315°C (600°F) for the polyimide and polyphenylquinoxaline composites.

As would be expected in the longitudinal direction the thermal expansion was reflected by the fiber reinforcement. The laminates containing AS graphite fiber showed a slightly positive expansion coefficient, from zero to less than +1 in./in. x 10^{-6} while the laminates reinforced with HMS graphite had a slightly negative coefficient of the same order of magnitude.

The transverse thermal expansion coefficients for the seven laminates are listed in Table XLV. Also listed are the Tg temperatures or inflection points obtained during the tests. All laminates showed a low temperature inflection in the -24° to -40°C range. This has been found previously in several different types of epoxy laminates. The upper temperature Tg values reflected the type of resin matrix with the polyimide and PPQ composites showing inflection points between 301 and 315°C while the three epoxy laminates were between 55° and 65°C. With one exception the expansion coefficients of the epoxy laminates were nearly twice those of the polyimide and PPQ composites. The one exception was the NAS-13IV laminate AS/Kevlar/epoxy with interply construction which gave an expansion value similar to NAS-76IV AS/S-glass/PI intraply composite. No reason for this one exception is apparent at the present time. Duplicate runs on different specimens gave the same results.

Table XLV

Transverse Thermal Expansion Coefficient of Hybrid Fiber Composites

Composite No.	Composition	Construction Type	Transverse Therm. Exp. Coeff. $\alpha \times 10^{-6}$ [a] cm/cm/°K	(in./in./°F)	Tg °C	(°F)
NAS-78 IV	AS/Kevlar/Epoxy	Intraply	124	27	-35.5, 57.2	-32, 135
-13 IV	AS/Kevlar/Epoxy	Interply	81.5	17.7	-34.4, 65	-30, 149
-9 IV	HMS/S/Epoxy	Interply	143.5	31.2	-43.3, 54.4	(-39, 130)
-76 IV	AS/S/PI	Intraply	80	17.4	-41, 315	(-37, 600)
-36 IV	HMS/S/PI	Intraply	53	11.5	-24.4, 301	-22, 572
-6 IV	AS/S/PPQ	Interply	70.5	15.33	- , 302	(- , 576)
-10 IV	HMS/S/PPQ	Interply	65.8	14.3	-24.4, 301.5	(-22, 575)

[a]Temperature range -73.4°C to 149°C for epoxy and -73.4° to 315°C for polyimide and PPQ

VI. GENERAL CONCLUSIONS AND RECOMMENDATIONS

1. S-glass is, in general, a better hybrid fiber reinforcement than Kevlar 49 for mechanical strength/impact property correlations in graphite reinforced resin matrix composites.

2. Additions of Kevlar 49 to HMS graphite do not provide significant improvements in impact properties regardless of ply construction.

3. With the intraply composites the tow-by-tow configuration is superior to the dispersed fiber type in pendulum impact behavior. This is primarily due to the out-of-plane shear fracture mode of the former configuration.

4. The standard pendulum impact test is shear limited. With thinner specimens the influence of shear failure on total impact decreases. A definitive change in fracture mechanism occurs near the 0.508 cm (0.200 in.) thickness range.

5. Shear and flexural stress interaction diagrams were constructed which demonstrate the importance of span-to-depth ratio in the pendulum impact test. It was shown that standard Charpy impact data should not be used for comparing materials if the intended application is to involve loading at high L/h values.

6. The ballistic impact parameter (E/V) which relates projectile energy and impact affected volume of the specimen provides improved correlation between ballistic impact and pendulum impact (thin specimen) data. The scope and value of the parameter as it relates to composite structure, angle-ply, fiber composition and specimen thickness requires further study and it is recommended that such an investigation be carried out.

7. Damage threshold levels as measured in thin Charpy hybrid specimens were lower than those measured with homogeneous graphite specimens. Thus, it appears that hybridization did not increase the resistance to initial fracture. However, total energy absorption or resistance to catastrophic failure was increased.

8. The best over-all laminate type in terms of performance was the AS/S-glass intraply (tow-by-tow) system. In terms of fiber material costs the composite is 25% less than homogeneous AS while maintaining the same flexural and shear strengths and flexural modulus with at least a 134% improvement in impact strength. This fiber combination performs equally well with both epoxy and polyimide (PMR-15) matrix resins and shows only a 25% decrease in impact resistance over a temperature range of -74.6° to 315°C.

It is recommended that further investigation of the tow-by-tow AS/S-glass composition be carried out to determine (1) the level of hybrid fiber which can be added before a decrease in flexural strength and modulus occurs, (2) the effect of fiber tow spacing on composite properties, (3) the optimum impact level which can be obtained, and (4) the influence of this fiber type on the thermal fatigue characteristics of reinforced resin matrix composites.

9. It is also recommended that ballistic impact studies be extended to include diamond shaped specimens and angle projectiles. This work should be carried out using a minimum of three of the best hybrid fiber combinations tested in Tasks III and IV of this program.

VII. REFERENCES

1. R. C. Novak and M. A. DeCrescente, "Impact Behavior of Unidirectional Resin Matrix Composites Tested in the Fiber Direction", Composite Materials: Testing and Design 2nd Conference, Anaheim, Calif., April 1971, ASTM, Philadelphia, Pa., 1972, p 311.

2. L. A. Friedrich, "Studies of Impact Resistance of Fiber Composite Blades Used in Aircraft Turbine Engines", 4th Quarterly Report NASA Contract NAS3-15568, July 1972.

3. C. C. Chamis, M. P. Hanson, and T. T. Serafini, "Impact Resistance of Unidirectional Fiber Composites", Composite Materials: Testing and Design, ASTM, STP 497, 1972, p 324.
   C. C. Chamis, M. P. Hanson, and T. T. Serafini, "Designing for Impact Resistance with Unidirectional Fiber Composites", NASA TN D-6463, May 1971.

4. R. A. Simon, "Impact Strengths of Carbon Fiber Composites", 28th Ann. Tech. Conf. Reinforced Plastics/Composites Institute, SPI, Feb. 1973, Sec. 17C.

5. J. V. Mullin and A. C. Knoell, "Basic Concepts in Composite Beam Testing", Materials Research and Standards, MTRSA, Vol. 10, No. 12, p 16.

6. M. P. Hanson and C. C. Chamis, "Experimental and Theoretical Investigation of HTS/PMR-PI Composites for Application to Advanced Aircraft Engines", 29th Ann. Tech. Conf. Reinforced Plastics/Composites Institute, SPI, 1974, Sec. 16-C.

7. NASA Contract NAS3-17789.

8. L. Friedrich and L. Preston, "Impact Resistance of Fiber Composite Blades Used in Aircraft Turbine Engines", NASA CR-134502, 1973.

9. G. E. Hasman, J. M. Whitney and J. C. Halpin, "Residual Strength Characterization of Laminated Composites Subjected to Impact Loading", Tech. Report AFML-TR-73-309, Feb. 1974.

10. P. Delvigs, T. T. Serafini, and G. R. Lightsey, "Addition-Type Polyimide from Solutions of Monomeric Reactants", NASA TN D-6877, Aug. 1972.

11. T. T. Serafini, P. Delvigs, and R. D. Vannucci, "In Situ Polymerization of Monomers for Polyphenylquinoxaline/Graphite Fiber Composites", 29th Ann. Tech. Conf. Reinforced Plastics/Composites Institute, SPI, Inc., Sec. 16-A, 1974.

12. J. T. Hoggatt, S. G. Hill, and J. G. Shdo, "Development of Polyphenylquinoxaline Graphite Composites", NASA-CR-134674, July 1974.

13. A. C. Soldatos, et al, "High Performance Epoxy/Graphite Fiber Composites", Modern Plastics, 48 (12) 62 (1971).

VIII. APPENDIX

8.1 Fabrication of Epoxy Matrix Composites

All epoxy resin used in the program was Union Carbide ERLA-4617 with Furan hardener 9245. The fabrication procedure, based on a slightly modified published procedure (Ref. 13) was as follows:

a. A mixture of ERLA-4617 and Furan hardener 9245, 100/24 wt ratio; was prepolymerized at 85°C (184.5°F) for 2 hrs, cooled, and diluted to 50 w/o solids with methyl ethyl ketone (MEK) solvent.

b. Prepregs of the graphite, glass and Kevlar 49 III were drum wound by drawing the fiber through the resin solution. Prepregs not used immediately were stored at -17.8°C (0°F) in sealed bags.

c. Prepregs were "B" staged 45 min at 80°C (176°F), prior to cutting, in a forced draft oven.

d. The cut prepreg was layed up in the desired mold, inserted into a press at room temperature and molded as follows:

   . Raise temperature at contact pressure to 93.3°C (200°F) and hold one hour. The mold may be inserted into a preheated press at 200°F if convenient.

   . Increase temperature to 121°C (250°F) at contact pressure and hold 40-60 min or until gelation occurs.

   . Pressure to 6.89×10^5 N/m^2 (100 psi) at 121°C (250°F for 10-15 min.

   . Increase pressure to 17.2×10^5 N/m^2 (250 psi) and temperature to 176.7°C (350°F) and hold 2 hrs.

   . Release pressure, transfer hot mold to a 176.7°C (350°F) air oven and postcure 19 hrs.

   . Cool, remove composite and cut into desired test specimens.

8.2 Fabrication of PMR-15 Polyimide Matrix Composites

The PMR-15 resin was prepared at 50% solids in methanol as described in Ref. 9 from the dimethyl ester of 3,3',4,4'-benzophenone tetracarboxylic acid (BTDE) 4,4'-methylenedianiline (MDA) and the monomethyl ester of 5-norbornene-2,3-dicarboxylic acid. Prepregs were prepared by drum winding as described above. After winding the wet tape was dried 1 hr with a hot air dryer prior to removal from the drum. The required plys were cut to fit the mold and the layup was "B" staged in the mold at 204°C (400°F) for three hrs. Stops were inserted in the mold ends during this time to prevent any pressure on the plys. The mold was then inserted into a preheated press at 315°C (600°F) under contact pressure for 10 min. The pressure was then increased to 6.895×10^6 N/m^2 (1000 psi) and held for one-half hour. The mold was allowed to cool slowly to 93.3°C (200°F) before removal from the press.

8.3 Fabrication of Polyphenylquinoxaline, PPQ, Matrix Composites

The PPQ resin was prepared from stoichiometric quantities of 3,3',4,4'-tetra-aminobenzophenone (TABP) and 4,4'-oxydibenzil dissolved separately at 30% solids in N-methylpyrrolidone. After combining the warm solutions, prepregs were prepared by drum winding as described above for the epoxy system. After winding the wet tapes were dried 2 hrs with a hot air dryer prior to removal from the drum. The volatile contents of the tapes prepared ranged from 16 to 24 wt percent.

The cut prepreg plys were stacked in the mold and the composites fabricated as follows:

- Insert mold into 329°C (625°F) preheated press.
- Hold 5 min at contact pressure.
- At 329°C increase pressure to 6.2×10^6 N/m^2 (900 psi) over a 5 min period, "bumping" the press join times.
- Hold for 1 hr at 6.2×10^6 N/m^2 and 329°C.
- Raise temperature to 370.7°C (700°F) at the same pressure and hold for 1 hr.
- Cool press to 204°C (400°F) before removing mold.
- Remove composite from mold and cut into desired specimens.

8.4 Intraply (Tow-by-Tow) Laminates

The UARL tow-by-tow drum winding technique for producing prepreg to be used in making the intraply construction did not involve an ironing step to flatten the wound tows. Consequently the number of fiber bundles per inch of width was greater than with the commercially available tow-by-tow construction. The UARL prepreg contained on the average of 6 tows S-glass or Kevlar 49 and 6 tows of graphite per inch of width. A tow-by-tow prepreg purchased from 3M Co. made of AS graphite and S-glass contains only three tows each of graphite and glass per two inches of width. Figure 69 illustrates the difference in tow width of the prepregs. The effect of the tow width on mechanical properties remains to be determined.

8.5 Testing Procedures

8.5.1 Flexural and Interlaminar Shear Strengths

Flexural and shear specimens were molded in a 3.8 cm x 12.7 cm (1.5 in. x 5 in.) mold except for one laminate which required a 20.32 cm (8 in.) length. Initially, flexural tests were carried out at S/D = 32/1 using a 4 point bend test. However, all specimens failed in a shear mode rather than bending. The shear failure initiated in the region of the supports. Thus, the resulting flexural strengths were lower than anticipated. To eliminate shear failure, flexural testing was changed to S/D = 32/1 three point loading. The resulting flexural strengths were in the expected range and the failure occurred in the bending mode. In addition, this type of bending test more closely approaches the type of bending associated with the 3-point Charpy impact test used for determining the impact strength of the fabricated composites. A crosshead speed of 0.05 in.-min^{-1} was used in all tests.

Interlaminar shear strengths were in the anticipated range (S/D = 4/1) with the exception of the AS graphite composite NAS-1 which is being retested, and all composites failed in a shear mode. All flexural and shear tests were carried out in triplicate.

8.5.2 Tensile Strength

For longitudinal tensile the specimen configuration shown in Fig. 70 was used. The small cross sectional width was necessary to maximize the bond length to cross sectional area ratio for the specimen.

Transverse tensile specimens were 12.8 cm (5 in.) long and 1.28 cm (0.5 in.) wide with 2.54 cm (1.0 in.) gage length. Fiber glass doublers were used for both types of specimens.

INTRAPLY (TOW–BY–TOW) HYBRID FIBER PREPREG AS GRAPHITE/S–GLASS

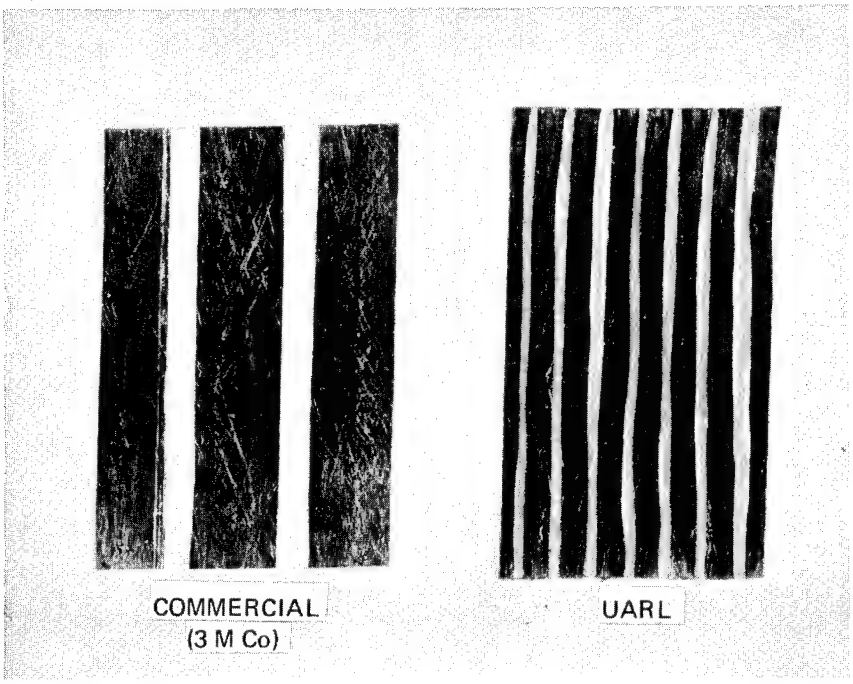

N10–310–1

FIG. 70

TENSILE SPECIMENS FOR FILAMENT REINFORCED COMPOSITES

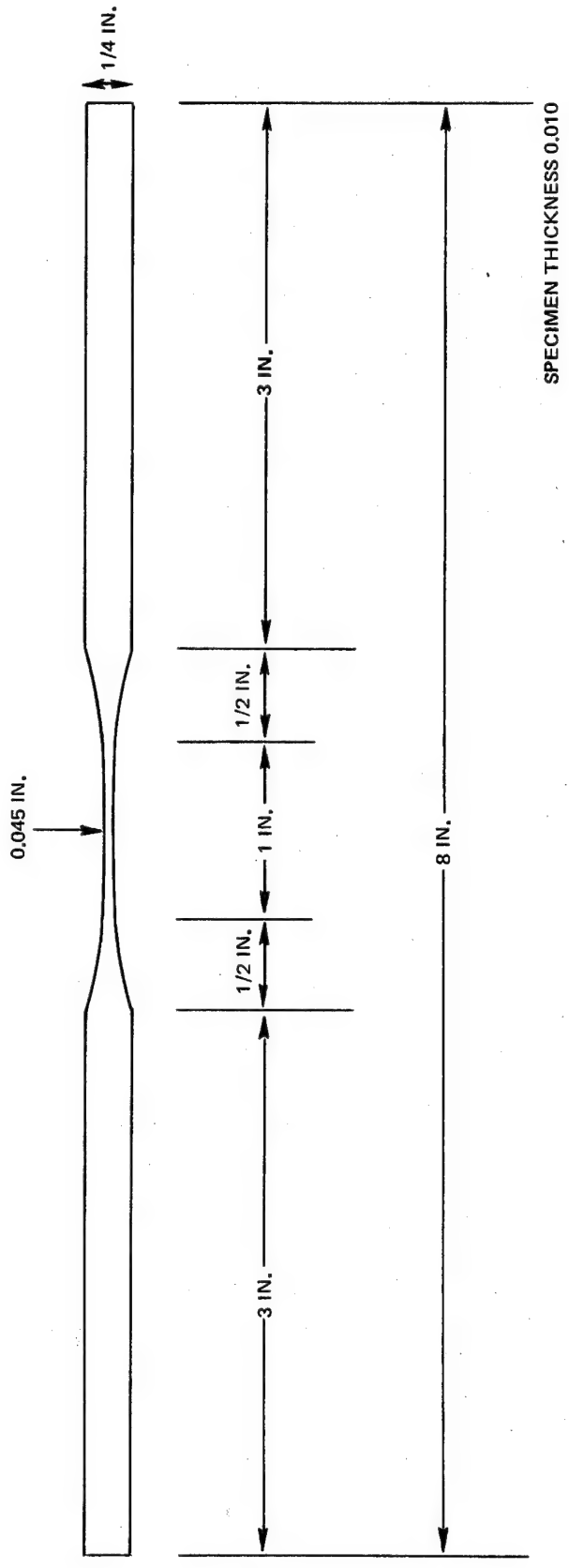

N10–259–7

All tensile testing was carried out using a Tinius-Olsen test machine and K type grips. Crosshead speed was 0.01 in./min. Specimen alignment was provided by the loading extension rods which have spherical bearing surfaces at the upper and lower heads of the testing machine. For room temperature tests, strains were measured by strain gages bonded to the front and back of the specimen to eliminate bending effects or a deflectometer. The data reported for each test includes the following: elastic modulus, yield strength, ultimate strength, and total strain to failure. In addition, the complete stress-strain curve for each test is kept on record.

8.5.3 Compressive Strengths

The Celanese Corporation designed compression jig which allows the compressive forces to be induced by shear stresses on bonded tabs in a collet type grip which does not come in contact with the test specimen which was used for low compression testing. The special design specimen is shown in Fig. 71. The jig was inserted in a Tinius-Olsen four screw universal testing machine and the specimen tested at a constant crosshead speed of 0.05 in./min.

8.5.4 Thermal Expansion

The thermal expansion apparatus consists of a 5/8 in. diameter vertical quartz tube housed in a Haskins tube furnace 13 in. long. The lower end of the quartz tube is sealed with a solid quartz rod about 1 in. long. The sample is placed on the lower rod, and a second rod centered in the tube connector. The sample is a water cooled linear variable differential transformer (LVDT). The LVDT reads out on the y-axis of a Mosely 703A-X-Y recorder, and temperature of the sample which is sensed by a chromel-alumel thermocouple reads out on the x-axis. The system is frequently calibrated against a single crystal MgO standard. Composite specimens were tested over a temperature range of -73.4°C (-100°F) to 315°C (600°F).

8.5.5 Instrumented Pendulum Impact (Charpy)

Impact specimens were fabricated in a 3.8 cm x 6.1 cm (1.5 in. x 2.4 in.) mold. Three test specimens, 5.5 cm x 1 cm x 1 cm (2.165 in. x 0.394 in. x 0.394 in.) were cut from each composite. Testing was carried out at room temperature using a 370 Joule (264 ft-lb) Charpy impact machine. The striker was instrumented with a strain gage to provide a load vs time trace of each impact. The thin Charpy specimens were fabricated in the same mold to provide three specimens per molding. The thin specimens were tested using a Physmet Corp. Impact Tester. The range of this instrument is 0-33.6 Joules (0-24 ft-lbs). Load-time traces were also obtained for each thickness range on this instrument.

TEST SAMPLE FOR SPECIAL CELANESE CORPORATION COMPRESSION JIG

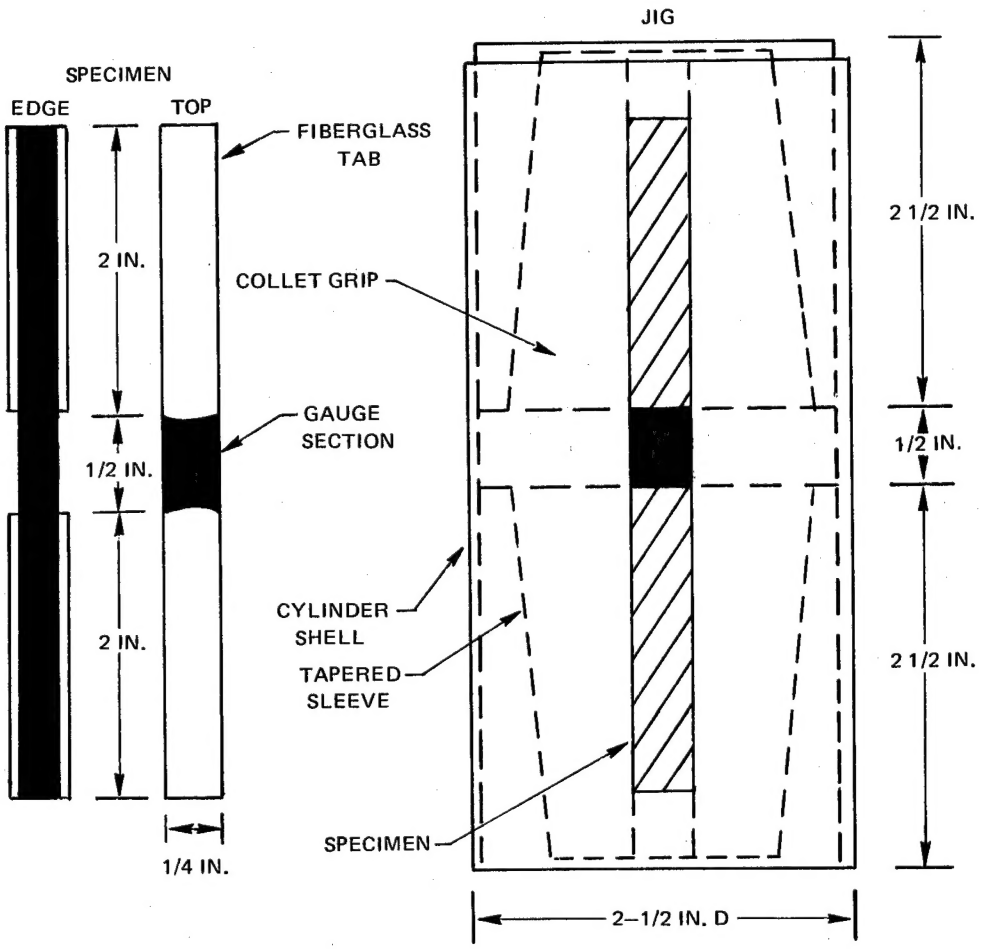

N10–259–6

8.5.6 Ballistic Impact

A high pressure air carrier was used for firing gelatin spheres. Projectile velocity just prior to impact was determined by using a trip-wire system to measure the time for the projectile to cover a fixed distance of 45.6 cm (18 in.). The General Radio Model 1192 timer is accurate to within 3 microseconds and is traceable to the U.S. Bureau of Standards. The approximate projectile velocities were selected by varying tank pressures to the air gun according to a predetermined calibration curve. The projectile gun was capable of firing 1.27 cm (0.5 in.) diameter projectiles with a reproducible velocity range from 30.4 m/sec (100 fps) to over 273.6 m/sec (900 fps).

The ballistic impact specimen was a rectangular parallelepiped 22.86 cm (9 in.) long, 5.08 cm (2 in.) wide and approximately 0.254 cm (0.100 in.) thick. All specimens were cantilevered and impacted normal to the specimen surface at the center of the sample. The center point was located 11.3 cm (4.5 in.) from the supported end of the specimen at mid width.

Cantilevering was accomplished using a pair of compliant fiber glass doublers 5.08 cm (2 in.) wide and 3.81 cm (1.5 in.) long. The doublers were held in place against the specimen with a vise. The specimen with doublers was inserted 2.54 cm (1 in.) into the vise. The 1.27 cm (0.5 in.) length of the doublers which extended beyond the vise was uniformly tapered in thickness to minimize the possibility of specimen breakage at the gripped end.

Gelatin, the projectiles used to simulate birds were fabricated from a solution of gelatin and water. The use of this material has been shown to be a most satisfactory substitute for birds in impact tests of jet engine components.

Advantages of using this material are: ease of fabrication to any shape and mass, repeatability, sufficient toughness to withstand acceleration to velocities approaching the speed of sound, and damage to turbojet structures similar to that caused by actual bird carcusses.

Acid-processed pigskin gelatin is dissolved in hot tap water to make a 20% solution by weight. After standing to allow bubbles to surface, it is poured into any suitable mold and allowed to set. There is virtually no volume change when cold. The density is approximately 1.02 g/cc.

Modulus retention measurements were conducted in conjunction with the impact tests in order to measure the amount of damage which occurred.

Cantilever bending and shear moduli of the test specimens were measured before and after the impact test using dead weight loading. Care was taken to insure that the specimens were clamped in the same manner as in the impact test.

8.6 Materials

The materials used during the program were obtained from the following vendors:

Resins and Intermediates	Source
Methylenedianiline (MDA)	Aldrich Chem. Co.
Tetracarboxylic Benzophenone Dianhydride	Eastman
Nadic anhydride	Eastman
3,3',4,4'-tetraamino-benzophenone	Burdick & Jackson
p,p'-oxybis(benzil)	Whittaker R&D
ERLA-4617 epoxy	Union Carbide Corp.
Furan 9245 hardener	Furan Inc.
Fibers	
AS and HMS graphite	Hercules Inc.
Kevlar 49 III	DuPont
S-glass (20 end)	Ferro Inc.
S-glass (12 end)	Owens-Corning